IDENTIFICATION AND CHARACTERISATION OF GENE REGULATION BY THE POU4F3 (BRN-3C) TRANSCRIPTION FACTOR IN THE INNER EAR

Chrysostomos Tornari

Submitted for the degree of PhD

University College London

2009

DECLARATION

I, Chrysostomos Tornari, confirm that the work presented in this thesis is my own. Where information has been derived from other sources, I confirm that this has been indicated in the thesis. Where work has been conducted by other members of our laboratory, this has been indicated by their initials or an appropriate reference:

SD	Dr Sally Dawson
ET	Dr Emily Towers
VG	Dr Valentina Gburcik Lazovic
JK	Mr John Kelly

ABSTRACT

Hair cells are the mechanosensory cells of the inner ear whose loss causes irreversible hearing loss in mammals. POU4F3, a POU-domain transcription factor, is only expressed in hair cells in the inner ear and is essential for hair cell terminal maturation in mice. In humans, it is essential for hair cell survival as all three identified families with a POU4F3 mutation show autosomal dominant adult-onset progressive hearing loss. The pathways by which POU4F3 has this effect are unknown as little is known about its target genes (only four such genes are known: *Bdnf*, *Ntf3*, *Gfi1* and *Lhx3*). Therefore, identification of unknown POU4F3 target genes would aid the understanding of hair cell maturation and survival.

Prior to starting my doctoral work, a subtractive hybridization was carried out in an inner ear cell line (UB/OC-2) which was manipulated to either over- or under-express POU4F3 to identify unknown POU4F3 target genes. The clones produced by this screen were first matched to their corresponding gene; the presence of these genes in POU4F3-expressing UB/OC-2 cells was then confirmed by western blot and/or reverse transcriptase PCR. Where possible, expression was also confirmed in cochlear hair cells by immunofluorescence microscopy.

Subsequently, the interaction of POU4F3 with these genes was characterised. Bioinformatics software was used to identify putative POU4F3 recognition elements in target gene promoters, and these sequences were then synthesised and used in a DNA binding assay (EMSA) to assess POU4F3 binding. The ability of POU4F3 to regulate putative gene promoters was also tested using luciferase assays.

By these methods, one gene (*Nr2f2*) was shown to be a direct target of POU4F3 *in vitro* and two other genes were shown to be likely POU4F3 targets. The identification of these genes improves our understanding of the mechanism of POU4F3 function and further investigation of these networks may yield therapies for deafness caused by hair cell loss.

TABLE OF CONTENTS

ABBREVIATIONS **11**

NOTES TO READER **13**

1 GENERAL INTRODUCTION **14**

1.1 Normal hearing and balance 15
1.2 Inner ear development 26
1.3 Hair cells 34
1.4 Abnormal hearing 46
1.5 Transcription factors and regulation of gene expression by POU4F3 61
1.6 Investigation of inner ear biology 77
1.7 Project aims 78

2 MATERIALS AND METHODS **80**

2.1 Safety 80
2.2 General equipment 80
2.3 Stock solutions 81
2.4 BLAST analysis of subtractive hybridization clones 81
2.5 Cell culture 82
2.6 General DNA manipulation 83
2.7 Reverse Transcriptase Polymerase Chain Reaction (RT-PCR) 85
2.8 Western blotting 86
2.9 Immunofluorescence immunohistochemistry 89
2.10 Electrophoretic Mobility Shift Assay (EMSA) 91
2.11 Cell transfection and reporter gene assay 95
2.12 Site-directed mutagenesis (SDM) of the *Nr2f2* promoter 100
2.13 Allele specific hybridization of plasmid DNA with EMSA oligonucleotides 104
2.14 Sequencing of NR2F2p4kbmut-BS1&2 clones 105

3 CANDIDATE *POU4F3* TARGET GENE IDENTIFICATION AND PRIORITISATION 106

3.1 Previous work in the identification of POU4F3 target genes 107
3.2 Subtractive hybridization in UB/OC-2 cells 108
3.3 Follow-up of subtractive hybridization screen results 109
3.4 Reverse transcriptase PCR in UB/OC-2 cells 113
3.5 Prediction of POU4F3 transcription factor binding sites 114
3.6 Candidate gene expression in the inner ear 118
3.7 Refinement of candidate genes for further investigation 119
3.8 Summary 121

4 CHARACTERISATION OF THE INTERACTION OF POU4F3 WITH THE *NR2F2* PROMOTER 122

4.1 Identification of *Nr2f2* as a potential POU4F3 target gene 122
4.2 Introduction to *Nr2f2* 125
4.3 Steroid/thyroid hormone nuclear receptors 125
4.4 NR2F2 function and expression 128
4.5 Initial selection of *Nr2f2* as a candidate gene for investigation 131
4.6 Verification of NR2F2 expression in UB/OC-2 cells 134
4.7 Immunohistochemistry for NR2F2 in rat and mouse inner ear tissue 137
4.8 Does POU4F3 directly activate the *Nr2f2* promoter? 143
4.9 Transcriptional regulation of the *Nr2f2* 5' flanking region by POU4F3 152
4.10 Site-directed mutagenesis of POU4F3 binding sites in the *Nr2f2* promoter 161
4.11 Discussion of *Nr2f2* activation by POU4F3 173

5 INVESTIGATION OF PUTATIVE *LUZP1*, *RBMS1* AND *ZRANB2* REGULATION BY POU4F3 176

5.1 Introduction to *Luzp1*, *Rbms1* and *Zranb2* 176
5.2 Identification of *Luzp1*, *Rbms1* and *Zranb2* as potential POU4F3 targets 182
5.3 Initial prioritisation of *Luzp1*, *Rbms1* and *Zranb2* for investigation 186
5.4 Investigation of the inner ear expression patterns of selected genes 188
5.5 Design of oligonucleotides for EMSA analysis of *Luzp1*, *Rbms1* and *Zranb2* 193
5.6 EMSA analysis of POU4F3 binding sites in candidate gene 5' flanking regions 201
5.7 Activation of candidate gene 5' flanking regions by POU4F3 210
5.8 Summary and discussion of candidate gene activation by POU4F3 217

6 GENERAL DISCUSSION 220

6.1 Conclusions 225

APPENDIX: REVERSE TRANSCRIPTASE PCR PRIMERS 227

BIBLIOGRAPHY 229

TABLE OF FIGURES

Figure 1.1. Gross anatomy of the ear. 16
Figure 1.2. Cochlear anatomy. 21
Figure 1.3. Anatomy of the membranous labyrinth. 25
Figure 1.4. Inner ear morphogenesis. 28
Figure 1.5. Development of the organ of Corti. 35
Figure 1.6. Stereocilial links and structure. 40
Figure 1.7. Cochlear expression of factors involved in hereditary hearing loss. 51
Figure 1.8. Interaction of transcription factors to initiate transcription. 62
Figure 1.9. The role of POU4F3 in hair cell development. 66
Figure 1.10. DFNA15 caused by *POU4F3* mutation. 69
Figure 1.11. POU4F3 protein composition. 74
Figure 2.1. pDrive cloning vector. 95
Figure 2.2. pGL4.10[*luc2*] vector. 96
Figure 2.3. pGL4.23[*luc2*/minP] vector. 97
Figure 2.4. pSi mammalian expression vector. 98
Figure 3.1. Candidate gene mRNA in UB/OC-2 cells. 114
Figure 4.1. Clone D8 of the subtractive hybridization screen matches the *Nr2f2* gene. 123
Figure 4.2. Expression of NR2F2 in UB/OC-1 and UB/OC-2 cells. 135
Figure 4.3. NR2F2 expression in undifferentiated (proliferating) UB/OC-2 cells. 136
Figure 4.4. NR2F2 expression in the E18 rat cochlea. 138
Figure 4.5. NR2F2 expression in the postnatal rat cochlea. 139
Figure 4.6. NR2F2 expression in the postnatal mouse cochlear apex. 140
Figure 4.7. NR2F2 expression in the P0 mouse crista. 141
Figure 4.8. Schematic representation of *Nr2f2* regulation. 143
Figure 4.9. Identification of putative POU4F3 binding sites in the *Nr2f2* promoter. 145
Figure 4.10. Binding of *in vitro* translated POU4F3 to transcription factor binding sites. 148
Figure 4.11. Binding of POU4F3 to *Nr2f2* promoter binding sites. 150
Figure 4.12. Schematic of *Nr2f2* 5' flanking region reporter constructs. 153
Figure 4.13. *Nr2f2* promoter regulation by POU4F3 in BHK and ND7 cells. 154
Figure 4.14. NR2F2p4kb dose response to cotransfected POU4F3 expression construct. 156
Figure 4.15. Upregulation of pGL4.23-NR2F2BS1 by POU4F3 in ND7 cells. 158
Figure 4.16. Upregulation of pGL4.23-NR2F2BS2 by POU4F3 in ND7 cells. 159
Figure 4.17. Design of mutant POU4F3 binding sites. 162
Figure 4.18. Effect of binding site mutation on transcription factor binding. 164
Figure 4.19. Site-directed mutagenesis (SDM) of NR2F2p4kb by overlapping PCR. 166
Figure 4.20. Screening of SDM colonies for incorporation of mutation. 167
Figure 4.21. POU4F3 binding site mutation reduces *Nr2f2* promoter upregulation. 170
Figure 4.22. Alignment of mouse NR2F2BS1 with equivalent human and rat sequences. 172
Figure 4.23. Alignment of mouse NR2F2BS2 with equivalent human and rat sequences. 172
Figure 5.1. Clone D3 of the subtractive hybridization screen matches *Luzp1*. 183
Figure 5.2. Clone FB5 of the subtractive hybridization screen matches *Rbms1*. 184
Figure 5.3. Clone FA8 of the subtractive hybridization screen matches *Zranb2*. 185
Figure 5.4. RBMS1 and ZRANB2 expression in UB/OC-1 and UB/OC-2 cells. 190
Figure 5.5. ZRANB2 expression in the P0 rat cochlea. 192
Figure 5.6. Prediction of potential POU4F3 binding sites in the *Luzp1* promoter. 194
Figure 5.7. Prediction of potential POU4F3 binding sites in the *RBMS1* promoter. 196
Figure 5.8. Prediction of potential POU4F3 binding sites in the *Zranb2* promoter. 199

Figure 5.9. Binding of *in vitro* translated POU4F3 to predicted binding sites. 202
Figure 5.10. Binding of *in vitro* translated POU4F3 to RBMS1BS1-3. 203
Figure 5.11. Binding of UB/OC-2 cell nuclear protein extract to LUZP1BS1 & 2. 207
Figure 5.12. Binding of UB/OC-2 cell nuclear protein extract to RBMS1BS1-3. 208
Figure 5.13. Binding of UB/OC-2 cell nuclear protein extract to ZRANB2BS1 & 2. 209
Figure 5.14. Response of LUZP1p2.8kb to POU4F3. 212
Figure 5.15. Regulation of RBMS1p1.3kb by POU4F3. 214
Figure 5.16. Regulation of RBMS1p5.1kb by POU4F3. 215
Figure 5.17. ZRANB2p3.2kb is not regulated by POU4F3. 216

TABLE OF TABLES

Table 1.1. Sensory organs of the inner ear. 19
Table 1.2. Classification of hearing loss. 47
Table 1.3. Types and onset of SNHL. 49
Table 1.4. Causes of hereditary hearing loss. 53
Table 1.5. Global prevention strategies for SNHL. 56
Table 1.6. Functions of the original POU family genes. 64
Table 2.1. PCR primer oligonucleotide design parameters. 85
Table 2.2. Primers for attempted QuikChange® II XL kit site-directed mutagenesis. 100
Table 2.3. NR2F2BS1 and NR2F2BS2 mutagenesis primers. 102
Table 3.1. Genes corresponding to clones produced by subtractive hybridization screen. 111
Table 3.2. Categorisation of POU4F3 candidate target genes for follow up. 112
Table 3.3. MatInspector and ModelInspector analysis of candidate genes. 116
Table 4.1. *Nr2f2* GO units. 132
Table 4.2. Oligonucleotides for *Nr2f2* EMSA analysis. 145
Table 5.1. *Luzp1* GO units. 186
Table 5.2. *Rbms1* GO units. 187
Table 5.3. *Zranb2* GO units. 188
Table 5.4. *Luzp1* EMSA oligonucleotides. 195
Table 5.5. *RBMS1* EMSA oligonucleotides. 198
Table 5.6. *Zranb2* EMSA oligonucleotides. 201
Table 5.7. Consensus sequence oligonucleotides for competition assays. 206

DEDICATION

In loving memory of

Dr Kyriacos Chrysostomou Tornari

1935 - 2003

ACKNOWLEDGEMENTS

I would like to thank the people who provided the opportunity for me to carry out the work reported in this thesis and who supported me throughout. Firstly, I would like to thank Stefano for giving me the opportunity to explore my interest in hearing and later supervising my BSc project. I would also like to thank the UCL MB PhD programme for funding this research; Professor Gordon Stewart for his willingness to sign anything and Sue Beesley for being a rock of good sense and organisation in a sea of confusion.

The support that I have received at the UCL Ear Institute has been outstanding and I would like to thank the staff and students that have influenced my development over the time I have spent in the department. Many thanks to Nico, Elena and Andy for the patient hours of teaching and discussion that were beyond their responsibilities and, most importantly, the members of the Dawson-Gale laboratory: Jonathan (B), Manuela, Zoë, John (K), Valentina, Lisa and, especially, Emily. This work would truly not have been possible without their help and their friendship has been a great source of strength and happiness through some testing times. Outside of UCL I would like to thank my friends who have put up with me over the last few years and who I have not been able to see as much of as I would have liked. To my former housemates, Doug and Bhairavi, thanks for putting up with me the many nights I would be locked in my room working and not being much fun! Thanks to Nicola, Theo and Sofronis for their help and advice and many thanks to Chad for his endless technical expertise, assistance and even equipment!

To Sally, thank you for your endless patience and professionalism, sorry for not being able find the words with which to fully express my gratitude. To Jonathan (G), thank you for your insight that always gives me a new angle on a problem.

Most importantly, I would like to thank my mother Maria, my sister Katerina and my partner Natalia for helping me keep my perspective over the last few years.

Nat, thank you for not letting me forget the things that are most important to me and always challenging me.

ABBREVIATIONS

ABR	**auditory brainstem response**
AF	**activation function**
ARHL	**age-related hearing loss**
BLAST	**basic local alignment search tool**
BM	**basilar membrane**
bp	**base-pair(s)**
cDNA	**complementary DNA**
CVG	**cochleovestibular ganglion**
DTT	**dithiothreitol**
EMSA	**electrophoretic mobility shift assay**
ENU	**N-ethyl-N-nitrosourea**
GER	**greater epithelial ridge**
GO	**gene ontology**
HAT	**histone acetyl-transferase**
HBS	**Hank's buffered saline**
HDAC	**histone deacetylase**
IHC	**inner hair cell**
kb	**kilobase(s)**
LBD	**ligand binding domain**
LER	**lesser epithelial ridge**
LTLD	**lower tip-link density**
MET	**mechanoelectrical transduction**
MGI	**Mouse Genome Informatics**
NHS	**National Health Service**
NIHL	**noise-induced hearing loss**
NLS	**nuclear localization signal**
OHC	**outer hair cell**
PAGE	**polyacrylamide gel electrophoresis**
PBS	**phosphate buffered saline**
PCR	**polymerase chain reaction**
PVDF	**polyvinylidene fluoride**

RNA	**ribonucleic acid**
ROS	**reactive oxygen species**
RT-PCR	**reverse transcriptase polymerase chain reaction**
SDM	**site-directed mutagenesis**
SDS	**sodium dodecyl sulphate**
Shh	**sonic hedgehog**
SNHL	**sensorineural hearing loss**
TEMED	**tetramethylethylenediamine**
TM	**tectorial membrane**
TSS	**transcriptional start site**
UTLD	**upper tip-link density**
UTR	**untranslated region**
WHO	**World Health Organization**
λ	**wavelength**

NOTES TO READER

- Human gene names are in upper case and italicised
- Non-human gene names are italicised with capitalised first letters only
- Non-human gene names are used if referring to both human and non-human genes
- All protein names are fully upper case and not italicised.

1

GENERAL INTRODUCTION

Being able to perceive, interpret and appreciate sound is an important part of human life. Our sense of hearing is essential to our ability to respond to changes in our environment, communicate with others and appreciate music. Though the loss of this ability can be compensated for through various means (sign languages, hearing dogs, appliances with visual alerts etc.), such methods are often only used by people who lose their hearing early in life (RNID 2009). For the increasing number of people who have to manage hearing loss later in life, the adjustment can pose a very different and difficult challenge (Van Laer *et al.* 2007). Across the age range, hearing loss can have a wide personal and social effect. In children, it has been shown to adversely affect confidence, behaviour and acceptance by peers (Moeller 2007), whilst quality of life is reported to be significantly affected in older people with age-related hearing loss (ARHL) (Howarth *et al.* 2006).

Worldwide, approximately 278 million people have a moderate to profound hearing loss in both ears (World Health Organization 2006). Though more is being done to identify children with hearing loss and reduce risk factors for hearing loss at all ages, ARHL – which affects approximately 40% of people by age 65 – will become an increasing problem due to our ageing society (Ohlemiller 2004). Furthermore, greater voluntary noise exposure – e.g. due to increased use of personal music players – is predicted to contribute to the incidence of noise-related hearing loss despite reductions in occupational noise exposure (Daniel 2007). Therefore, research into the anatomically and molecularly complex systems that underlie hearing is required to improve our understanding of this process and to identify new strategies by which to prevent and treat hearing loss.

This thesis addresses the lack of knowledge regarding gene regulatory networks in hair cells, the primary sensory cells of the inner ear. The POU4F3 transcription factor is uniquely expressed in these mechanosensory cells in the inner ear (Erkman *et al.* 1996;Xiang *et al.* 1998) where it has been shown to be essential for their terminal differentiation in mice (Xiang *et al.* 1998) and for their survival in humans (Collin *et al.* 2008;Vahava *et al.* 1998). However, the mechanism of its function is poorly understood. Therefore, we attempted to identify POU4F3 target genes to explain how this transcription

factor generates and maintains the hair cell phenotype and, thereby, identify proteins that are involved in the terminal differentiation and survival of hair cells.

1.1 Normal hearing and balance

Sound is mechanical energy travelling through a medium in a longitudinal wave at frequencies audible to humans (i.e. in the range of approximately 20Hz to 20kHz) (Kingsley 1999b). Prior to its transduction into electrical energy by the ear, it undergoes multiple complex steps of modification in order to optimise the useful information that can be extracted from the original signal.

The first step in this modification occurs prior to sound reaching the ear. The torso, neck and head give a modest boost to sound below 1kHz (less than 5dB) (Ballachanda 1997). The head is also an important factor in the determination of sound localization on the horizontal axis as the difference in sound pressure and timing between ears is influenced by head size and shape (Pickles 1988).

1.1.1 The outer ear

The ear itself is divided into three sections: the outer, middle and inner ear. Sound first arrives at the outer ear which, in turn, is divided into the pinna and the ear canal (see Figure 1.1). These structures do not simply pass sound into the skull unmodified. They are designed to gather sound, aid in its localization and boost its pressure in the speech frequencies.

The first two of these functions are carried out by the pinna (also called the auricle). Due to its larger surface area, more sound arrives here than would arrive at the ear canal alone and the folds of the pinna direct this additional sound into the ear canal. As well as directing the sound, the pinna modifies sounds that do not enter the ear canal directly in order to aid in localization. Sound therefore takes two paths to the ear canal: the direct path (into the ear canal) and the reflected path (via the pinna). Sound from the reflected path undergoes spectral modification that is variable depending on its horizontal and vertical localization i.e. the location of a sound source determines which part of the pinna the sound arrives at first which determines its spectral modification. This modified sound combines with sound from the direct path, and the signature of the combined signal allows identification of the sound's location following transduction and neural processing (Middlebrooks *et al.* 1991). This processing takes place in the brainstem where the timing, phase, pressure and spectral differences between sounds arriving at each ear are compared. This large area of hearing research is beyond the scope of this thesis and is not discussed further. Though the pinna is essential for vertical localization, its role in horizontal localization is not essential and its most important role in this task is in distinguishing front/back ambiguity (Pickles 1988).

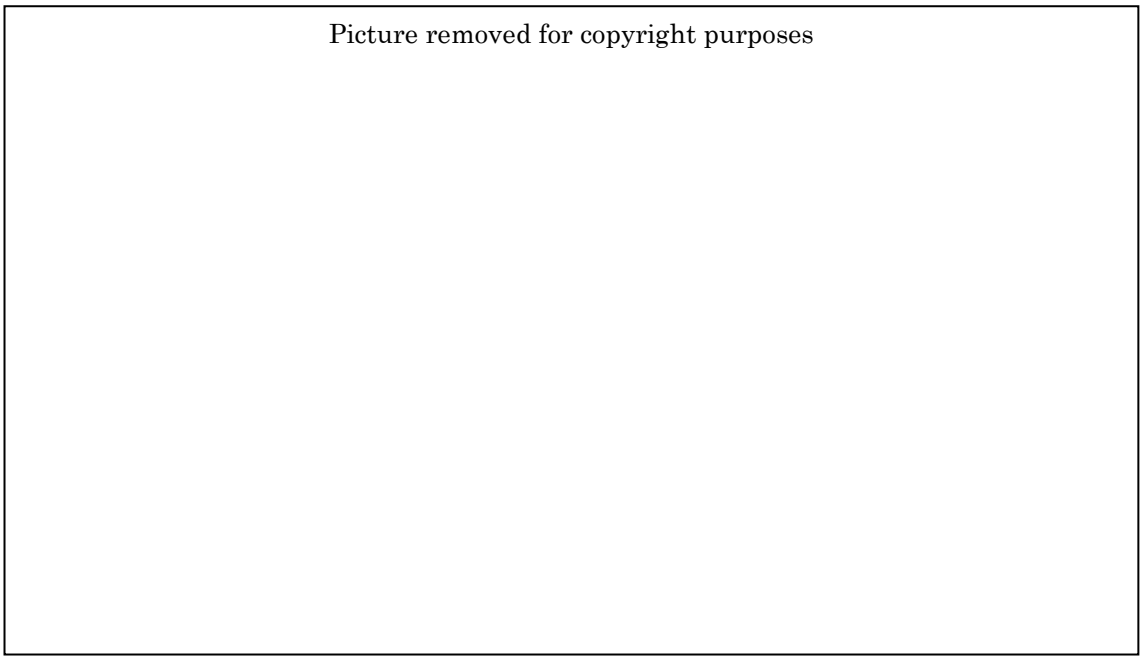

Figure 1.1. Gross anatomy of the ear.
The ear is divided into the outer ear, middle ear and inner ear. The outer ear comprises the pinna and external auditory meatus and is divided from the middle ear by the tympanic membrane. The middle ear transmits movement of the tympanic membrane to the inner ear via the three ossicles: the *malleus*, the *incus* and the *stapes*. The movements of the *stapes* are transduced to electrical energy in the hair cells of the cochlea and transmitted to the brain via the cochlear division of the vestibulocochlear nerve. The remaining sensory organs of the inner ear transduce head acceleration and position information which is passed to the higher brain centres via the vestibular portion of the vestibulocochlear nerve (adapted from Kelley 2006).

The final role of the external ear – amplification of speech frequencies – is primarily performed by the ear canal. This canal starts in the pinna and ends at the tympanic membrane (also called the eardrum) i.e. it is a cylinder that is closed at one end (see Figure 1.1). The length of such a cylinder is ¼λ of its resonant frequency and, as the adult ear canal is approximately 25mm long, its resonant frequency is approximately 3.4kHz. Frequencies at and around this frequency are therefore amplified and the ear canal provides most of the 15 to 20dB amplification that is applied to sounds from 1.5 to 7.0kHz (see Ballachanda 1997 for review). The range of this amplification and the fundamental frequency of the canal therefore lie within the important frequency range for speech (250Hz to 4kHz) (Sataloff *et al.* 1993).

1.1.2 The middle ear

The middle ear translates vibration of the tympanic membrane into vibration of the liquid that fills the cochlea. It not only passes sound from the outer ear to the inner ear but also matches the impedance from air to liquid – to optimise the efficiency of energy transfer – and alters the spectral response of the incoming sound to enhance important frequencies (Pickles 1988). Encased in the temporal bone, it is a space that contains small bones, nerves and muscles that either aid in the above functions or, in the case of the facial and glossopharyngeal nerves, pass through the middle ear (Dean *et al.* 1996).

Sound that has passed through the ear canal reaches the tympanic membrane, which separates the outer and middle ear. This sound causes variation in pressure in the ear canal, creating a pressure difference between the outer ear and the middle ear (which contains air at atmospheric pressure). High pressure on the lateral tympanic membrane – caused by compression of air particles during a sound wave – causes it to move medially i.e. towards the middle ear. Conversely, rarefactions create low pressure, causing the tympanic membrane to move laterally, towards its resting position. The maintenance of atmospheric pressure in the middle ear is necessary for this to occur and it is achieved by the connection of the middle ear to the pharynx via the Eustachian tube which, though closed at rest, is easily opened by pharyngeal muscle movements (see Figure 1.1) (Vander *et al.* 2001).

The functions of the middle ear are primarily achieved by the ossicles – the smallest bones in the human body – without which only a small proportion of sound that is transmitted by the tympanic membrane would reach the inner ear (Kurokawa *et al.* 1995). In each middle ear, there are three ossicles. The first of this chain is the *malleus* (hammer) which has a long arm that is attached to the tympanic membrane, a neck, and a head which articulates with the second ossicle, the *incus* (anvil), via a synovial joint. The *incus* is also divisible into three parts: the head, which is attached to the *malleus*; the short process which connects this bone to the posterior wall of the middle ear; and the long process which articulates, via another synovial joint, to the *stapes* (stirrup). This final ossicle is divided into the head, which articulates with the *incus*, followed by two processes which join the head to the footplate. It is the footplate that delivers the vibration of the ossicles to the cochlea via an opening in the bony capsule of the inner ear called the oval window (*fenestra vestibuli*). In reptiles, the tympanic membrane is joined directly to the oval window by the *stapes*. However, bones from the reptilian jaw evolved to form the *malleus* and *incus* which improve the impedance matching and spectral response of the middle ear, allowing more accuracy in hearing (Clack *et al.* 2004).

The middle ear transfer function

Impedance matching by the middle ear is achieved as follows:

1) A greater pressure is applied at the oval window than at the tympanic membrane because the surface area of the footplate of the *stapes* is smaller than that of the tympanic membrane (see Equation 1.1).

Equation 1.1. Pressure-area relationship between tympanic membrane and oval window. TympM = tympanic membrane, OW = oval window, P = pressure, A = area.

$$P_{TympM} \times A_{TympM} = P_{OW} \times A_{OW}$$

2) The lever action of the middle ear bones modify the movement of the *stapes*, increasing its force and decreasing its velocity to provide a small benefit in impedance matching.
3) The conical shape of the tympanic membrane allows it to buckle so that the *malleus* moves less than the surface of the membrane providing another small benefit to the impedance match (Pickles 1988).

These factors contribute to what is known as the transfer function of the middle ear which increases the pressure at the footplate of the *stapes* whilst decreasing velocity. Differences in the efficiency of this function at different frequencies are the result of the physical properties of the middle ear which optimise transmission of the most important frequencies. In humans, the greatest pressure gain peaks near 0.9kHz (26.6dB) with fairly flat gain at low frequencies and steadily falls off above 0.9kHz to zero pressure gain at 7.0kHz. Therefore, the middle ear can be described as a bandpass filter as it transmits sounds at different frequencies with differing efficiency (Kurokawa *et al.* 1995). Consequently, middle ear dysfunction, e.g. due to abnormal bone remodelling in the middle ear (otosclerosis), causes hearing loss as sound is no longer efficiently transmitted to the cochlea (Cureoglu *et al.* 2009).

Middle ear muscles

Ossicular function is determined both by the constant effect of their anatomy and also by the variable effect of two muscles – *tensor tympani* and *stapedius* – which attach to the *malleus* and *stapes* respectively to control their stiffness. Contraction of these muscles influences both the amount and spectrum of sound that is transmitted from the outer ear to the inner ear. The *tensor tympani* arises from a bony canal in the middle ear wall and attaches to the long arm of the *malleus*. Similarly, the *stapedius* muscle arises from a bony canal and attaches to the neck of the *stapes* (Moore *et al.* 1999). *Tensor tympani* has a modest function, contracting in response to high intensity sound and in response to head and pharyngeal muscle movement and causing almost no attenuation in sound transmission (Kingsley 1999b). The *stapedius* muscle has a larger effect, causing an approximately 10dB attenuation in response to the sound of more than approximately 70dB or muscle movements (Kingsley 1999b;Sataloff *et al.* 1993). The combined effect of these muscles protect the inner ear from damage by sustained sound of high intensity. However, the latency of this reaction renders it insufficient to protect the inner ear from sudden loud noises (Vander *et al.* 2001).

1.1.3 The anatomy and function of the inner ear

The inner ear is responsible for the detection of sound, head acceleration and head position. Encased in the petrosal temporal bone – the hardest bone in the human body – it is a liquid-filled cavity (the bony labyrinth) with extremely complex anatomy that can be divided into the bulla, three semicircular canals (with their associated ampullae) and the cochlea. The bony labyrinth contains the membranous labyrinth and its six sensory organs that convert sensory information to action potentials via their sensory epithelia (see Table 1.1). The ampullae of the semicircular canals house their respective cristae, the bulla contains the utricle and saccule (each of which contains a sensory macula) and the cochlea houses the cochlear duct, within which the organ of Corti transduces sound. Action potentials generated by the sensory hair cells in these epithelia travel through afferent neurons in the vestibulocochlear nerve to the brain where the signal is processed and perceived (Vander *et al.* 2001).

Table 1.1. Sensory organs of the inner ear.
(adapted from Kingsley 1999b).

Organ	*Sensory Epithelium*	*Function*
Cochlea	Organ of Corti	Sound transduction
Saccule	Saccular macula	Linear vertical head acceleration and orientation
Utricle	Utricular macula	Linear horizontal head acceleration and orientation
Superior semicircular canal	Superior crista ampullaris	Head rotation around rostro-caudal axis
Posterior semicircular canal	Posterior crista ampullaris	Head rotation around horizontal axis
Horizontal semicircular canal	Horizontal crista ampullaris	Head rotation around vertical axis

Cochlear anatomy

Sound is delivered to the inner ear either by the movements of the footplate of the *stapes* in the oval window due to sound that has passed through the outer and middle ear, or by conduction through bone. The cochlea extracts frequency and amplitude information from this sound and passes this information to higher centres via the vestibulocochlear nerve. Both cellular and acellular cochlear components are required for this process.

The cochlea – which is, perhaps, the most anatomically complex sensory organ – is composed of three liquid-filled spaces which spiral around a central bony projection called the modiolus for little under 2.75 turns in humans to give the organ its characteristic shape

(Kingsley 1999b). These three spaces are named the scala vestibuli, scala media and scala tympani. The superior edge of the scala vestibuli and the inferior edge of the scala tympani are bordered by the bony labyrinth. The scala vestibuli starts near the oval window and coils up the cochlea on top of the other two compartments to the apex of the cochlea where it is continuous with the scala tympani at an opening called the helicotrema. The scala tympani then coils down the cochlea to end at a membrane called the secondary tympanic membrane that covers the round window of the bony labyrinth. The scala tympani and scala vestibuli are filled with extracellular fluid known as perilymph – a sodium-rich liquid with similar composition to cerebro-spinal fluid that is continuous with the cerebro-spinal fluid via the cochlear duct (see Figure 1.2*a*) (Kingsley 1999b).

Sandwiched in-between these two compartments lies the roughly-triangular scala media. This is separated from the scala vestibuli at its superior border by the Reissner's membrane, which is composed of mesothelial cells superiorly and epithelial cells inferiorly with a basement membrane in between these two layers (see Figure 1.2*b*). The epithelial cells are connected by tight junctions and adherens junctions to maintain fluid separation between the scala media and scala vestibuli (Slepecky 1996;Wangemann *et al.* 1996). The lateral border is formed by the lateral wall which comprises the stria vascularis and spiral limbus; regions important in setting up and maintaining potassium concentration of the liquid that fills the scala media, the endolymph. This liquid also fills the remainder of the membranous labyrinth via the ductus reuniens. On the inner aspect of the inferior border of the scala media lies the organ of Corti and associated support cells. This is the sensory epithelium of the cochlea that contains the hair cells – the sensory transductory cells of the cochlea. Hair cells are organised into one row of inner hair cells (IHCs) and – in humans – three to four rows of outer hair cells (OHCs). The IHCs are the 'true' sensory cells of the inner ear and are mainly innervated by afferent neurons that transmit transduced signals to the brain. OHCs, on the other hand, have a mainly efferent innervation and act to sensitize and modulate IHC function (see below). The nerve fibres travel medially to the spiral lamina, through the habenula perforata and into Rosenthal's canal in the modiolus where their cell bodies form the spiral ganglion. Axons of both bipolar and pseudounipolar neurons continue from here to the vestibulocochlear nerve (Kingsley 1999b). Pillar cells separate IHCs from OHCs, forming the perilymph-filled tunnel of Corti and, along with the other supporting cells of the organ of Corti (Deiters and Hensen cells) contribute to a reticular lamina at the surface of the sensory epithelium. The remaining cells of the floor of the scala media (inner sulcus cells, inner phalangeal cells, Claudius cells and Boettcher cells) have less well-characterised function and are involved in processes such as ion transport rather than mechanical support. The organ of Corti and the cells that populate the distance between the Hensen cells and lateral wall lie on the basilar membrane (BM) which is a specialised basement membrane that is mainly composed of homogeneous ground substance with fibres embedded in its matrix (see Figure 1.2*b*) (Slepecky 1996).

Picture removed for copyright purposes

Picture removed for copyright purposes

Picture removed for copyright purposes

Figure 1.2. Cochlear anatomy.
a) mid-modiolar section of the mature cochlea showing the pathways up the scala vestibuli (*red arrows*) and down the scala tympani (*blue arrows*). *Green*, perilymph; *yellow*, endolymph; *red*, structures required for transduction and establishment of endolymphatic potential (adapted from Boley 2008). *b*) detailed anatomy of the cochlear duct (taken from Figure 1 in Gates *et al.* 2005). *c*) Fluid boundaries in the cochlea. *Green*, perilymph; *yellow*, endolymph; *SL*, spiral ligament; *BM*, basilar membrane (adapted from Slepecky 1996).

Morphologically the BM forms the inferior border of the scala media. However, liquid separation between the scala media and scala tympani is achieved by the reticular lamina which connects hair cell and support cell apices across the sensory epithelium, maintaining cell apices in the potassium-rich endolymph and cell bodies in the sodium-rich perilymph (Slepecky 1996). The location of this boundary is important because the differential ion concentrations across the reticular lamina set up an electrical potential (the endocochlear potential) of +80mV (Wangemann 2006). This potential difference, combined with basal conductances in hair cells, establishes the hair cell resting membrane potential which is required for transduction (see Figure 1.2*c*) (Housley *et al.* 2006;Kros 1996).

Highly organised finger-like projections called stereocilia arise from the hair cell apices into the endolymph of the scala media towards a structure called the tectorial membrane (TM) which overlies the organ of Corti and arises from a bony prominence of the modiolus called the spiral lamina. The TM is composed of gel-like connective tissue and the tips of the OHC stereocilia are known to be embedded in this matrix. There is still some debate as to whether IHC stereocilia are also embedded in the TM, though it is widely agreed that they are not and that a groove in the TM that overlies the IHC stereocilia (Hensen's stripe) interacts with the inner hair cell stereocilia indirectly (Raphael *et al.* 2003). The mass and movement of the TM are required for normal hair cell mechano-electrical transduction (see below) and mutations in the genes that encode TM proteins are known to cause deafness (see Richardson *et al.* 2008 for review).

Cochlear function

Early inner ear physiologists attempted to discover what function different parts of the cochlea played in converting sound – which was itself poorly understood – into hearing. Helmholtz theorised that the BM acts as a string of resonators tuned to different frequencies that conduct a Fourier analysis of incoming sounds. Georg von Békésy provided empirical evidence to support this by showing that the cadaveric BM vibrates in different places for different pure tones depending on frequency and that movement of one part of the BM causes movement in other parts i.e. the BM is not a string of independent resonators. Importantly, he observed that the basal BM resonates to high frequencies at its thin, narrow base and low frequencies at its thick, wide apex (Patuzzi 1996). This ability to separate sounds into their component frequencies underlies the tonotopy of the inner ear: the observation that different frequencies are represented at different locations on the BM and, consequently, that different hair cells correspond to specific frequencies.

In this model, sound that is delivered to the scala vestibuli by movement of the footplate of the *stapes* causes a pressure difference between the scala vestibuli and scala tympani. This pressure difference causes movement of the BM. The movement in a given region is dependent on the resonant frequency of that region and, therefore, only certain parts of the

BM resonate in response to a given frequency with the amplitude of the movement being proportional to the amplitude of the incoming sound. When the organ of Corti moves upwards, towards the TM, hair cell stereocilia are bent in the direction of the longest row, causing a mechanoelectrical transduction (MET) channel to be opened and allowing the non-selective influx of sufficiently small positively charged ions – primarily potassium due to the high endolymphatic potassium concentration – causing transduction currents within the cells. Conversely, when the BM is pushed downwards, hair cell stereocilia are bent towards the shortest row, causing MET channels to close and reducing the likelihood of transduction currents in the cell (Hudspeth 2000). Transduction currents are transmitted to afferent neurons by the release of neurotransmitters from the hair cell base and these signals are then received and processed by higher brain centres (Kingsley 1999b).

However, the observed frequency selectivity of the cadaveric BM described by von Békésy is not sufficient to explain the observed frequency selectivity of the human ear. Applying concepts from radio engineering to this problem, Gold used a mathematical model to show that the input of an appropriate amount of energy to the BM would counteract the viscous damping by the liquid in the cochlea and would sharpen its frequency tuning to better explain observed frequency selectivity (Gold 1948). Gold was not able to identify the site of the required sensation and feedback of signal, though it has since been found that this function is carried out by OHCs. The required sharpening of the BM response is achieved by the opposite process of mechanoelectrical transduction: electromechanical transduction. In this process, OHCs, having converted kinetic energy into depolarising electrical energy (in the form of a transduction current) convert the electrical energy back into mechanical energy by the 'motor protein' called prestin (*Slc26a5*) that causes the OHCs to contract (Zheng *et al.* 2002). The energy provided by this movement is sufficient to overcome much of the viscous damping of BM movement by the cochlear liquids and allows sharpening of the frequency response of the BM to allow more frequency-specific activation of IHCs, accounting for the observed frequency-selectivity of hearing (Gold 1948;Robles *et al.* 2001). Furthermore, loss of prestin function due to its mutation, such as that seen in two human families, results in a recessive non-syndromic hearing loss (Liu *et al.* 2003).

Though the precise biomechanical mechanism through which OHC electromechanical transduction sharpens frequency selection is still being debated, the effect of BM movement induced by cellular movement in the inner ear has been exploited for diagnostic purposes. The sound created by this BM movement is detectable in the ear canal and is known as an otoacoustic emission (OAE), as predicted by Gold and proven by Kemp in his 1978 paper which first identified evoked OAEs (Kemp 1978). OAEs now serve as a clinical measure of cochlear function that does not require the cooperation of the subject. This method is now widely used to detect hearing loss e.g. in the UK National Health Service's neonatal hearing screening programme (MRC Hearing & Communication Group 2008).

Vestibular anatomy and function

As for cochlear hair cells, vestibular hair cells in all five vestibular sensory epithelia transduce sound by the movement of stereocilia that lead to transduction currents. The differences in vestibular stimuli transduced by the different epithelia are due to the location and overlying structures of each sensory epithelium (see Figure 1.3).

The saccule and utricle transduce the same type of stimuli as they have the same overlying otoconia which provide the necessary mass for the underlying hair cells to respond to gravity. When the head is moved, the inertia of the heavy otoconia causes them to slide back over the underlying sensory epithelium. This causes displacement of the stereocilia which results in depolarisation or hyperpolarisation of the hair cells depending on the direction of the displacement. Though both the saccule and utricle interpret linear acceleration and head position, the differences in the direction of travel sensed is dependent on the placement of the epithelium i.e. the saccular macula lies in the vertical plane whereas the utricular macula is horizontal (see Figure 1.3*a*&*b*) (Kingsley 1999b).

Similarly, the three cristae of each inner ear transduce rotational acceleration by the movement of endolymph against a gelatinous matrix (the cupula) which overlies the hair cells in the sensory epithelia. The relative movement of the cupula against the sensory epithelium causes displacement of the hair cell stereocilia, resulting in transduction currents. The type of rotation detected by the different cristae is dependent on the orientation of the semicircular canal to which it is attached (see Figure 1.3*c*). Higher centres compare contralateral inputs and integrate the signals from the different cristae to determine the net rotation of the head in three dimensions. Signals from the vestibular organs are also integrated with ocular cues in brainstem nuclei to maintain balance. As in the cochlea, vestibular epithelia are connected to their higher brain centres by both afferent and efferent neurons which travel in the vestibulocochlear nerve (Kingsley 1999b).

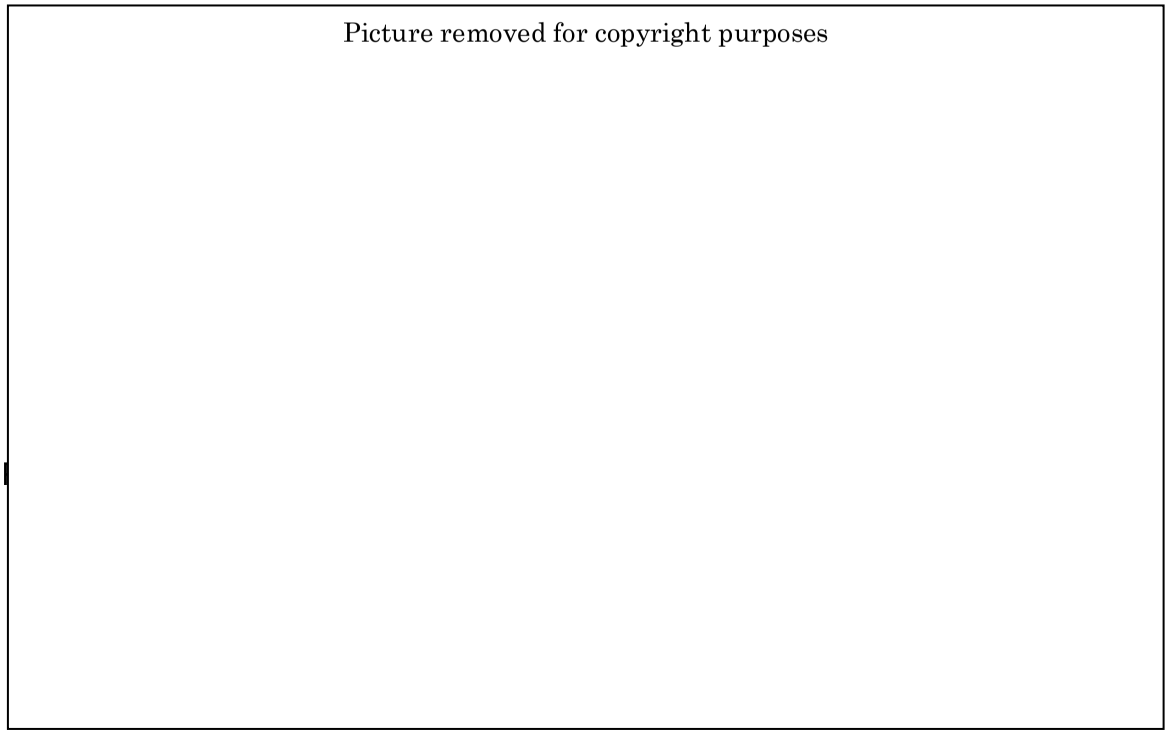

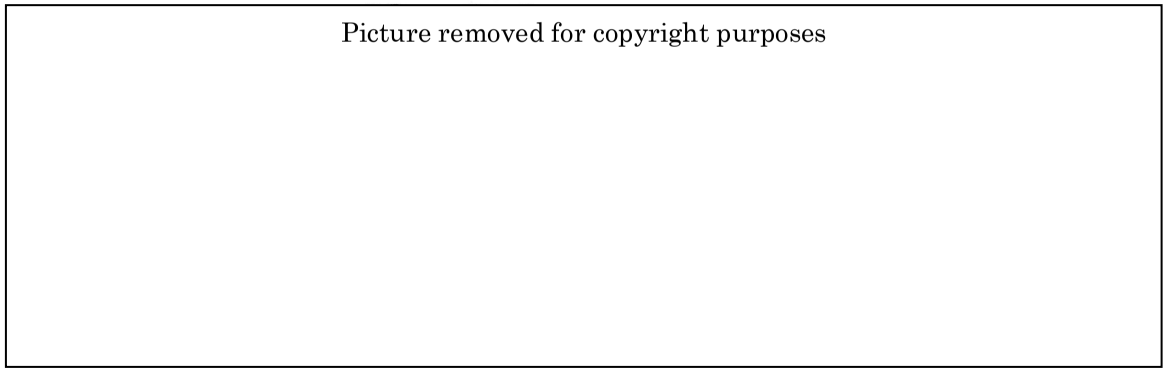

Figure 1.3. Anatomy of the membranous labyrinth. *a*) The position of the membranous labyrinth in the temporal bone and the locations of the vestibular sensory epithelia within it. The utricular macula is oriented horizontally and the saccular macula is positioned vertically (adapted from Kingsley 1999a). *b*) cellular anatomy of the utricular and saccular maculae showing the two types of hair cell within these epithelia that transduce linear acceleration and head position. The hair cells are overlaid with a gelatinous layer (adapted from Kingsley 1999a). *c*) anatomy of the crista, showing the sensory epithelium with the overlying cupula which is displaced by endolymphatic movements in the semicircular canals causing movement of the hair cell stereocilia (taken from Kingsley 1999a).

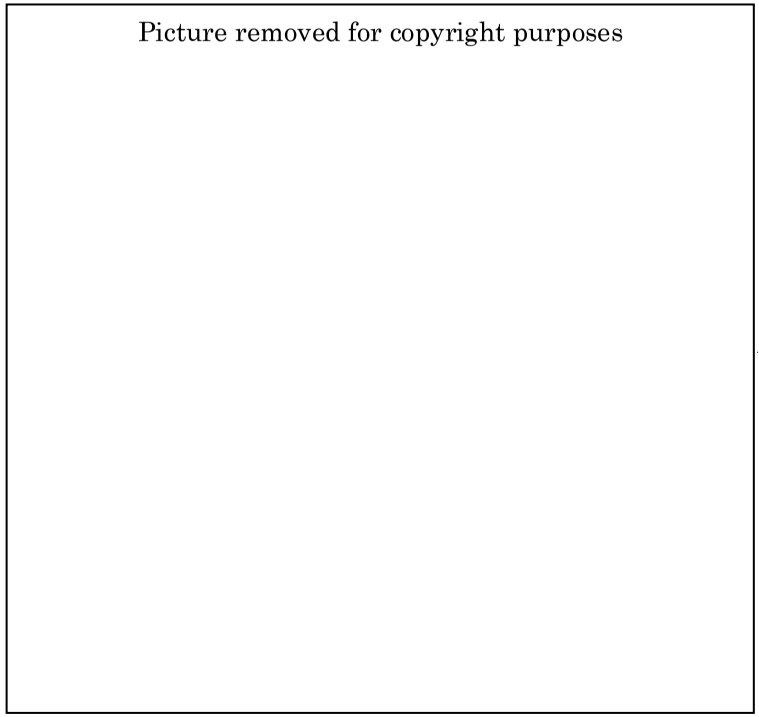

1.2 Inner ear development

With the advent of molecular biological techniques that are sufficiently sensitive to allow the study of inner ear development, there has been an explosion in the understanding of this process in the last decade (Kelley *et al.* 2005). From a patch of thickened ectoderm through to the elaborate structure of the labyrinth, many signalling networks have been shown to be involved in inner ear morphogenesis. These signals direct a combination of proliferation, differentiation, growth, migration and programmed cell death which result in the formation of the mature inner ear (Bok *et al.* 2007).

In brief, the inner ear is formed as follows: a patch of thickened ectoderm called the otic placode is formed on the anterolateral surface of the embryo and invaginates to form the otic cup. The cup then deepens and the surface epithelium begins to close off its roof. Once the cup has pinched off from the surface of the embryo, it is known as the otocyst (also known as otic cyst / otic vesicle). The otocyst undergoes a series of complex remodelling processes which lead to the mature anatomy of the labyrinth. This section describes the above processes in the order in which they occur and the signalling mechanisms on which they are known to rely.

1.2.1 Early inner ear morphogenesis

The first sign of inner ear development is the thickening of the surface ectoderm adjacent to the developing hindbrain to form the otic placode. Though it is known that cells from a wide area converge to form this structure, little is known of the mechanisms by which this is achieved. Therefore, much work is being done to identify the important factors in this process from the bewildering array of signalling molecules – primarily of the FGF family – that are likely to be involved (Groves 2005) and recent work is beginning to unravel this extremely complicated signalling network (Zelarayan *et al.* 2007).

Subsequently, the cup invaginates and a large number of apoptotic cells are detectable at its edges. As the cup begins to close off from the surface epithelium, the diminishing opening between the developing otic cup and the surface becomes known as the otic pore. Apoptotic cells continue to line this pore and are thought to be required to break down its lumen, the obliteration of which results in the otic cup pinching off from the surface ectoderm. The developing inner ear is now known as the otocyst, which is a roughly spherical space that is lined by a pseudo-stratified epithelium (Kelley 2007;Leon *et al.* 2004).

Throughout otic cup and otocyst development, specific proteins demarcate different functional domains which are anatomically indistinguishable. These protein domains define the axes of the developing labyrinth and some proteins are required to establish the axes whilst others are expressed as a result of axis specification. The three axes that are

established by this process are the anteroposterior axis, dorsoventral axis and mediolateral axis (see Figure 1.4*a*) (Bok *et al.* 2007).

Protein expression at this stage and beyond is better understood than that of placode induction. The anteroposterior axis is the first to be established and is first identifiable in the invaginating otic cup though cells in the anterior and posterior domains are unlikely to have become committed to their fate until the cup is half-closed. The signals responsible for the establishment of this axis are unknown; it was thought that signals from the hindbrain were responsible though recent experiments in the chick have cast doubt on this hypothesis. The axis itself, however, is quite clear with multiple genes being selectively expressed in the anterior region (*Fgf10, Lfng, Delta1, Ngn1 and NeuroD*) from which neuroblasts delaminate soon after otic cup closure to form the cochleovestibular ganglion (CVG, initially known as the statoacoustic ganglion (Fritzsch *et al.* 1998)) (Bok *et al.* 2007;Kelley 2006). These neuroblasts migrate into the mesenchymal space ventromedial to the otocyst. They subsequently return axons to innervate the sensory epithelia that develop near to where they were generated (Abello *et al.* 2007). The expression of a different group of genes (*Tbx1, Otx1, Otx2 and Goosecoid*) becomes detectable in the posterior otic cup at the same time as the known anterior markers. *Tbx1* – which is among the best studied of these markers – is thought to be responsible for maintaining the posterior domain by preventing anteriorly expressed genes from extending their expression into more posterior regions (see section 1.2.2 for *Tbx1* function in the developing sensory epithelium) (Bok *et al.* 2007;Mansour *et al.* 2005). Consistent with a role in limiting the anterior neurosensory fate, *Tbx1* deletion results in a 1.83-fold increase in the size of the CVG (Raft *et al.* 2004).

Like the anteroposterior axis, markers of the dorsoventral axis are identifiable at the otic cup stage though the cells in these domains are thought to commit to their fate later than those in the anteroposterior axis. It has been shown that the dorsoventral axis is required for the specification of the cochlea and saccule from the ventral otocyst (*pars inferior*), and of the semicircular canals and utricle from the dorsal otocyst (*pars superior*) (Bok *et al.* 2007;Leon *et al.* 2004). Unlike the anteroposterior and mediolateral axes, the inductive signals for the dorsoventral axis are known. The developing hindbrain secretes Wnt factors that induce the dorsal otic markers (*Dlx5, Dlx6, Hmx2, Hmx3* and *Gbx2*) and sonic hedgehog (Shh)/Gli signals that define the ventral domain (marked by *Lfng, Ngn1, NeuroD1, Sox2* and *Six1*). Furthermore, Shh signalling restricts Wnt expression to the dorsal region though it is unknown how Shh signalling is regulated. Other ventrally expressed proteins (*Six1* and *Eya1*) have also been shown to be involved in this process as Wnt and Shh knockout animals do not completely lose their dorsoventral patterning. However, it is unclear how these signals are regulated and, as their function does not fully explain the observed morphogenesis, it is thought that at least one other hindbrain signal is required for ventral patterning (Bok *et al.* 2007;Mansour *et al.* 2005).

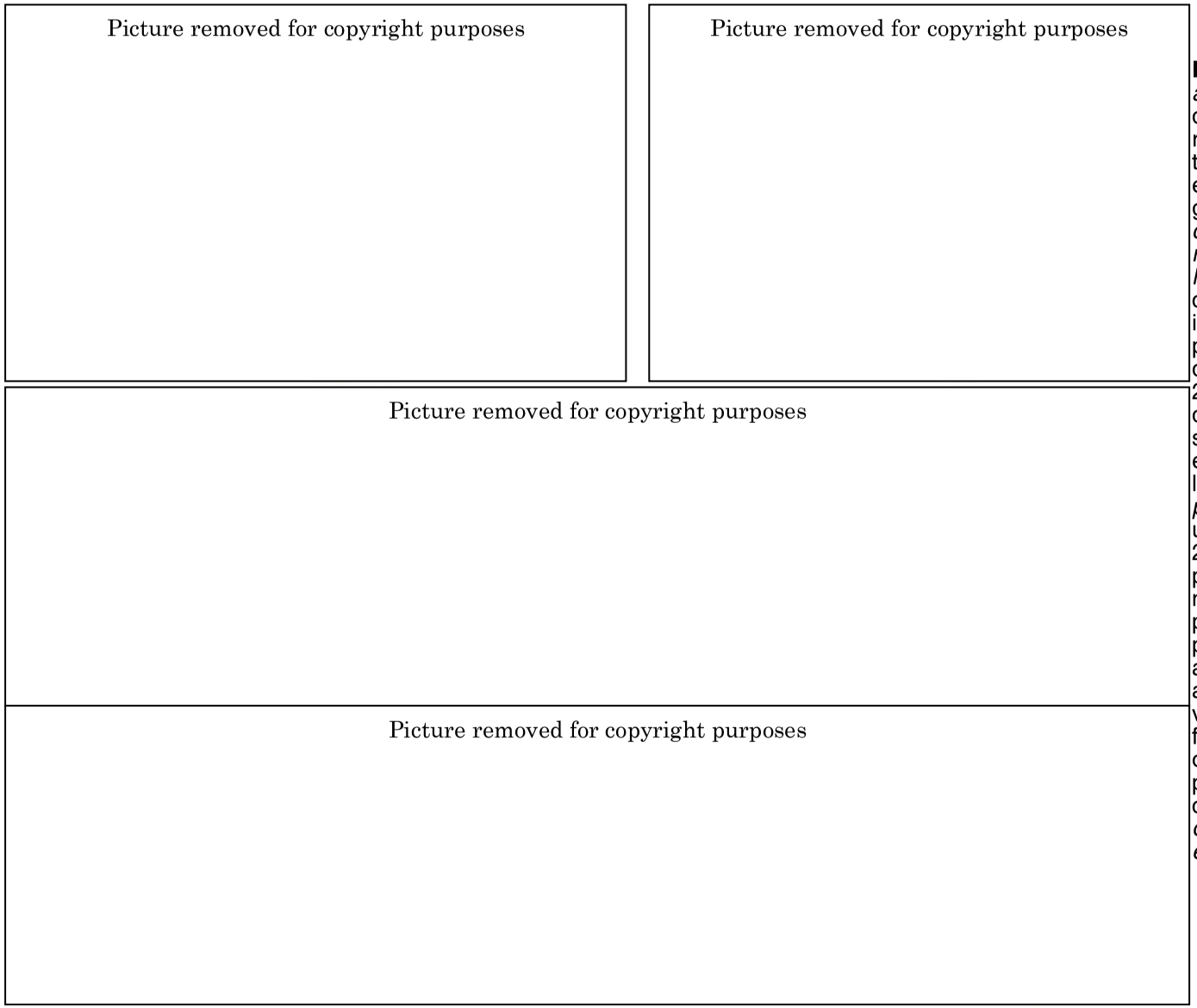

Figure 1.4. Inner ear morphogenesis.
a) Schematic representation of the three-dimensional axes of the inner ear. *b*) Schematic representation of the otocyst with its relations to the spatial origins of the sensory epithelia, endolymphatic duct and cochleovestibular ganglion indicated. *ED*, endolymphatic duct; *CS*, *crista superioris*; *MS*, *macula sacculi*; *MU*, *macula utriculi*; *CP*, *crista posterioris*; *CL*, *crista lateralis*; *OC*, organ of Corti; *CVG*, cochleovestibular ganglion (based on Figure 6 in Rinkwitz *et al.* 2001). *c*) lateral views of paint-filled membranous labyrinths from developing mouse inner ears. *Scale bar*, 200μm. *ed*, endolymphatic duct; *co*, cochlear duct; *aa*, anterior ampulla; *asc*, anterior semicircular canal; *cc*, common crus; *es*, endolymphatic sac; *la*, lateral ampulla; *lsc*, lateral semicircular canal; *pa*, posterior ampulla; *psc*, posterior semicircular canal; *s*, saccule; *u*, utricle (adapted from Figure 1 in Bok *et al.* 2007). *c*) the development of the prosensory patches of the membranous labyrinth and the markers that divide these domains. The posterior prosensory patch (which forms the posterior crista) and the dorsal part of the anteroventral stripe (which forms the lateral and anterior cristae) express *Sox2* and *Bmp4*. The ventral part of the anteroventral stripe (which forms the utricular macula, saccular macula and organ of Corti) expresses *Sox2* and *Lfng*. *pc*, posterior crista; *lc*, lateral crista; *ac*, anterior crista; *mu*, *macula utriculi*; *ms*, *macula sacculi*; *oc*, organ of Corti (adapted from Figure 3 in Bok *et al.* 2007).

The final axis to become identifiable – though it is likely to be specified much earlier than it becomes visible – is the mediolateral axis. Current evidence suggests that medial domain identity is acquired due to Wnt and Fgf signals from the hindbrain and that the specification of the lateral domain is also guided by signals from the hindbrain. However, the latter process is poorly understood and the roles of midline structures (i.e. the notochord and floorplate) require further characterisation, as does the role of hedgehog signalling (Whitfield *et al.* 2007).

Shortly after its appearance, and following the establishment of its axes, the otocyst is largely capable of completing its development independent of signals from its surrounding mesenchyme (approximately E11.5 in mice) (Fritzsch *et al.* 1998). From this point on, cellular proliferation, differentiation and survival – both in the otocyst and CVG – are essential for otocyst growth and development. These processes are initially dependent on insulin-related growth factor signalling that is balanced by apoptotic hotspots (Leon *et al.* 2004).

1.2.2 Late inner ear and sensory epithelial development

The first structures to emerge from the ellipsoid otocyst are the endolymphatic and cochlear ducts. The endolymphatic duct arises from the dorsomedial aspect of the otocyst (Kelley 2006;Rinkwitz *et al.* 2001) and a group of apoptotic cells are visible at the junction of the developing endolymphatic duct with the otocyst; this process may aid duct formation by limiting epithelial proliferation (Fekete *et al.* 1997;Leon *et al.* 2004). Similarly – both temporally and morphologically – the cochlear duct extends from the ventral otocyst and an apoptotic hotspot is visible on the ventromedial otocyst. This spot is located where the cochlear duct joins the saccule and persists for much of cochlear duct extension where it may direct differentiation between these two regions (see Figure 1.4*c*) (Leon *et al.* 2004). As these structures extend, the prosensory regions of the developing otic vesicle (regions that will give rise to the three cristae, utricular macula, saccular macula and organ of Corti) become identifiable as thickened epithelial plaques containing nascent CVG neurites (Kelley 2006).

Prosensory domain development

Initially, two prosensory domains are identifiable: a posterior spot that goes on to form the posterior crista and the anteroventral stripe that forms the rest of the sensory epithelia (see Figure 1.4*d*) (Bok *et al.* 2007). It is currently unclear whether the posterior region separates from the remainder of the developing prosensory domain or if the two regions arise separately (Kelley 2006). These prosensory regions are marked by SRY-box containing gene 2 (*Sox2*) which is expressed in both of the initial prosensory domains and, in mice, has been

shown to be required for the normal development of the sensory epithelia (Dabdoub *et al.* 2008;Kiernan *et al.* 2005b).

The earliest known network that is involved in the specification of these regions is the Notch signalling network. Experiments in chicks, zebrafish and mice have shown that the Notch receptor (*Notch1*) is expressed early in development, before the development of the otic placode. Its expression is maintained throughout the remaining development of the otocyst and inner ear and its function is thought to be in the regulation of the size of the initial sensory patch through regulation of the placement of sensory/non-sensory boundaries. However, it is not thought to be required for sensory patch specification (Daudet *et al.* 2007;Kelley 2006).

Consistent with a role for Notch receptors in prosensory domain patterning, the Notch-related genes lunatic fringe (*Lfng*) and jagged 1 (*Jag1*) are expressed in patterns consistent with the development of the prosensory domain. LFNG is a modulator of Notch glycosylation (Panin *et al.* 2002) that is expressed in the anteroventral prosensory domain; the region that gives rise to the utricular macula, saccular macula and organ of Corti. In non-mammalian vertebrates, the modification of Notch glycosylation by LFNG has been shown to inhibit the sensitivity of Notch 1 to one of its ligands: serrate. The mammalian homologue of serrate is *Jag1*, which is expressed in a pattern that abuts the prosensory domain during its specification. Though it has been suggested that *Jag1* and Notch signalling are involved in the specification of sensory patches, experiments in chick and zebrafish seem to contradict this hypothesis. However, redundancy in mammalian Notch signalling may explain the conflicting data in this field. Therefore, elucidating the role of each of the above genes in prosensory specification and development is likely to determine which factors are necessary for prosensory domain specification (Daudet *et al.* 2007;Kelley 2006).

Another gene that is implicated in prosensory domain development is *Tbx1* As previously mentioned *Tbx1* is expressed posteroventrally and is responsible for restricting neuroblast development from the anterior (CVG-forming) domain (Bok *et al.* 2007). It is therefore protective of the cells of the posterior domain which overlaps with the prosensory domain from which the non-neuronal sensory cells arise (Bok *et al.* 2007;Kelley 2006). Consistent with this model, over-expression of *Tbx1* leads to an enlarged sensory epithelium and *Tbx1* mutation in humans results in a syndrome which includes sensorineural hearing loss amongst its signs (Di George syndrome) (Bok *et al.* 2007;Kelley 2006).

Tbx1 expression overlaps with that of bone morphogenetic protein 4 (*Bmp4*) – a member of the transforming growth factor beta superfamily – in the posteroventral region of the otocyst. Though expression of *Bmp4* is initially diffuse and located in the posteroventral otic

cup, its expression is later refined to the nascent cristae i.e. the non-*Lfng*-expressing prosensory regions (see Figure 1.4*d*) (Cole *et al.* 2000;Pujades *et al.* 2006). As for Notch, BMP4 signalling was thought to be involved in specification of prosensory patches and experiments designed to test this hypothesis yielded unclear results. However, a consistent theme has emerged from these experiments suggesting that BMP4 is involved in cellular patterning of the developing sensory domains; consequently, manipulation of BMP4 signalling results in abnormal hair cell numbers in a chick model (Pujades *et al.* 2006).

A number of other markers, e.g. *Islet1*, prospero-related homeobox 1 (*Prox1*) and fibroblast growth factor 16 (*Fgf16*), have also been shown to be expressed in patterns that are consistent with that of the developing prosensory region and their function is currently being studied (Bermingham-McDonogh *et al.* 2006;Radde-Gallwitz *et al.* 2004;Wright *et al.* 2003). The characterisation of these factors, along with the factors described above, has significantly improved our understanding of prosensory domain establishment and development. This is allowing a shift in focus in this research area from the identification of regional markers to the full understanding of the mechanisms of prosensory specification and development.

Semicircular canal development

The semicircular canals are required for delivering rotational acceleration forces to the cristae for transduction. These canals develop alongside their respective cristae though they arise from the dorsolateral otocyst rather than the posterior or anteroventral otocyst from which the cristae originate (Rinkwitz *et al.* 2001). The nascent semicircular canals evaginate from the otocyst to form the anterior and posterior canal genesis zones prior to that of the lateral semicircular canal. In higher vertebrates, the epithelia of the opposing walls of the pouch come into contact during pouch extension to form a 'fusion plate' at the centre of the pouch. Apoptotic cells appear within these fusion plates at the time of epithelial contact which occurs in the order of semicircular canal development (anterior first, then posterior and, finally, lateral). The clearance of epithelial cells from the centre of the canal that results from these apoptotic foci gives rise to the anatomy of the mature semicircular canal. Consequently, inhibition of apoptosis leads to defects in the clearing of the centres of the semicircular canals in chick experiments (Fekete *et al.* 1997). Alongside central clearing, each canal develops an ampulla at one end that houses its respective crista (i.e. the anterior end of the anterior canal, the posterior end of the posterior canal and the anterior end of the lateral canal) (see Figure 1.4*c* & *d*) (Bok *et al.* 2007;Leon *et al.* 2004).

Utricle and saccule formation

As the *Lfng*-expressing region of the anteroventral prosensory domain develops, it eventually segregates into the utricular macula, saccular macula and organ of Corti. The first of these three to separate is the utricular macula, which is known to become

independent of the anteroventral stripe by E12 in the mouse. The Ngn1 and Notch pathways are then thought to regulate the maturation of this epithelium by guiding cell fate determination i.e. differentiating hair cells, support cells and neural cells. The saccular macula separates from the anteroventral stripe in a similar manner to the utricular macula at E13. As with the utricular macula, members of the Ngn1 and Notch signalling pathways are thought to be involved in guiding its terminal development (see Figure 1.4*d*) (Bok *et al.* 2007).

The processes before and after separation of these epithelia are being elucidated and little is known about the process by which these epithelia become distinct from the anteroventral stripe and each other. A number of genes (*Hmx2*, *Hmx3*, *Otx1*, and *Otx2*) are thought to be active in influencing this process from the non-sensory tissues that surround the prosensory domain and only one protein, GATA3, is known to be differentially expressed between the utricle and saccule at this stage (Bok *et al.* 2007;Karis *et al.* 2001). Also, a conserved region of apoptotic cells is consistently observed at the junction of the cochlea and saccule in a site that goes on to form the ductus reuniens (the duct that joins the scala media to the saccule) which is likely to be required for the separation of these organs (Fekete *et al.* 1997;Leon *et al.* 2004;Nishikori *et al.* 1999).

As prosensory development proceeds, additional apoptotic hotspots are observed within and around the sensory epithelia and within the CVG (including the cristae and organ of Corti). These are thought to be required to allow axons that have been extended from the CVG to penetrate the sensory epithelium and contact sensory cells, as well as aiding in CVG maturation (Bok *et al.* 2007;Fekete *et al.* 1997;Leon *et al.* 2004).

Cochlear extension and maturation

As the cochlear duct extends from the otocyst, it begins to take on its mature (coiled) appearance at around E12 in the mouse (Kelley 2007). The prosensory domain continues to be marked by SOX2 and LFNG whilst a non-sensory stripe of BMP4 expression becomes visible on the opposite wall of the extending cochlear duct after prosensory plaque specification (see Figure 1.4) (Bok *et al.* 2007).

Between E12 and E14, cells in the nascent organ of Corti exit the cell cycle in an apical to basal wave and, from this point on, there is minimal cell proliferation and apoptosis in this developing sensory epithelium (Jones *et al.* 2007;Ruben 1967). The cochlear duct continues to transform after this terminal mitosis in a basal to apical direction and does not complete its coiling until approximately E19-P0 (see Figure 1.4*d*) (Jones *et al.* 2007;Kelley 2007). This elongation process changes the cochlear duct from a short, thick structure (the dorsal cochlear floor is four to six cells deep when the cochlear duct first appears) to a much longer

and thinner structure that is only two cell layers deep in the mature organ of Corti (see Figure 1.5) (Kelley 2007).

The proposed model by which cochlear growth is achieved in the absence of cellular proliferation is known as convergent extension. This model is based on the process by which many axial structures develop across phyla (Zajac *et al.* 2000) and by which the body axis is elongated in vertebrate gastrulation and neurulation (Jenny *et al.* 2006). In this model, cells in the developing epithelium elongate and subsequently intercalate as they move towards the lumen of the cochlear duct, causing growth along the basal-apical axis. As cells no longer proliferate at this stage, the cochlear duct epithelium becomes thinner as epithelial cells intercalate and as the cochlear duct elongates (Jones *et al.* 2007;Wang *et al.* 2005). This cochlear extension occurs at the same time as the organisation of planar cell polarity (PCP) in the nascent organ of Corti (see section 1.3.3).

Once the inner ear has completed its morphogenesis, the elaborate structures that have been created become encased in bone (the otic capsule). Correct formation of the otic capsule is dependent on signaling between the epithelium of the cochlear duct and the surrounding mesenchyme e.g. the *Shh-Tbx1-Pou3f4* axis in the periotic mesenchyme is required for normal duct patterning (Bok *et al.* 2007;Rinkwitz *et al.* 2001). Once the capsule ossifies around the membranous labyrinth, there is no further growth in the inner ear – a fact that is exploited in paediatric cochlear implantation, as implants do not need to be changed as children grow.

1.2.3 Summary of inner ear development

A large number of dynamically expressed factors are now known to be required to transform the flat otic placode into the complicated three-dimensional labyrinth. The high resolution that is being achieved in the identification and characterisation of expressed factors in this process is aiding in the emerging understanding of the precise contribution of each of these factors. Apart from explaining the causes of a number of human deafnesses – e.g. X-linked deafness seen in DFN3 (*Pou3f4* mutation) (de Kok *et al.* 1995) – these processes precede or coincide with hair cell development (see next section) and, therefore, signalling networks involved in morphogenesis may influence future therapies to prevent or reverse hearing loss.

1.3 Hair cells

There are four different types of hair cell in the mammalian inner ear. Inner hair cells (IHCs) and outer hair cells (OHCs) of the cochlea are required for auditory transduction whilst Type I and Type II vestibular hair cells are found in the remaining inner ear sensory epithelia and are required for balance sensation (Kingsley 1999b;Kingsley 1999a). These functions depend on the specialised anatomy and physiology of the sensory epithelia and require functional hair cells. Consequently, hair cell loss causes loss of hearing and vestibular function that is irreversible in mammals, where hair cells do not regenerate.

1.3.1 Hair cell and support cell specification

Cochlear hair cells arise from a group of mitotically quiescent cells of the prosensory patch in the elongating cochlear duct. In many neuronal systems, excessive progenitor cells are produced and subsequently eliminated to produce mature patterning. However, the cochlear prosensory domain does not follow this model as it appears to have the required number of cells for full development at the time of terminal mitosis as supported by the lack of apoptosis in this region (Kelley 2007). Therefore, the timing of the terminal mitosis requires precise control to ensure correct development. Though the signals that control the timing of terminal mitosis are unknown, one of the first identifiable effectors of this timing mechanism is the cyclin kinase inhibitor $p27^{Kip1}$ (Kelley 2007).

Most progenitor cells in the nascent organ of Corti of the mouse cochlear duct have long been known to exit the cell cycle between E13 and E14 beginning in the apex and progressing to the base (Ruben 1967). This wave of terminal mitosis creates an apical-to-basal line of mitotically quiescent cells along the middle of the developing sensory epithelium that encompasses the full thickness of the epithelium and is called the zone of non-proliferation (ZNP) (Chen *et al.* 1999;Chen *et al.* 2002). Consistent with its known role in cell cycle regulation, $p27^{Kip1}$ expression begins abruptly at the cochlear apex at E12 and extends basally, to become strongly expressed throughout the ZNP by E14 (Chen *et al.* 1999). The temporal and spatial correlation of $p27^{Kip1}$ expression with mitotic quiescence, as shown by BrdU studies, provides evidence for its requirement in preventing mitosis in this region (see Figure 1.5*a*) (Chen *et al.* 2002). Results from $p27^{Kip1}$ knockout mice support this result as they show a delay in terminal mitosis that is associated with supernumerary hair cells and severe hearing loss (Chen *et al.* 1999;Lowenheim *et al.* 1999).

Though mitosing cells are identifiable in the organ of Corti of $p27^{Kip1}$ knockout mice as late as postnatal day six (the latest date investigated) (Chen *et al.* 1999), both hair cells and support cells *are* able to stop mitosing and differentiate. This indicates that another factor or other factors are involved in halting mitosis in the developing organ of Corti and retinoblastoma (*Rb*) has been shown to be one such factor.

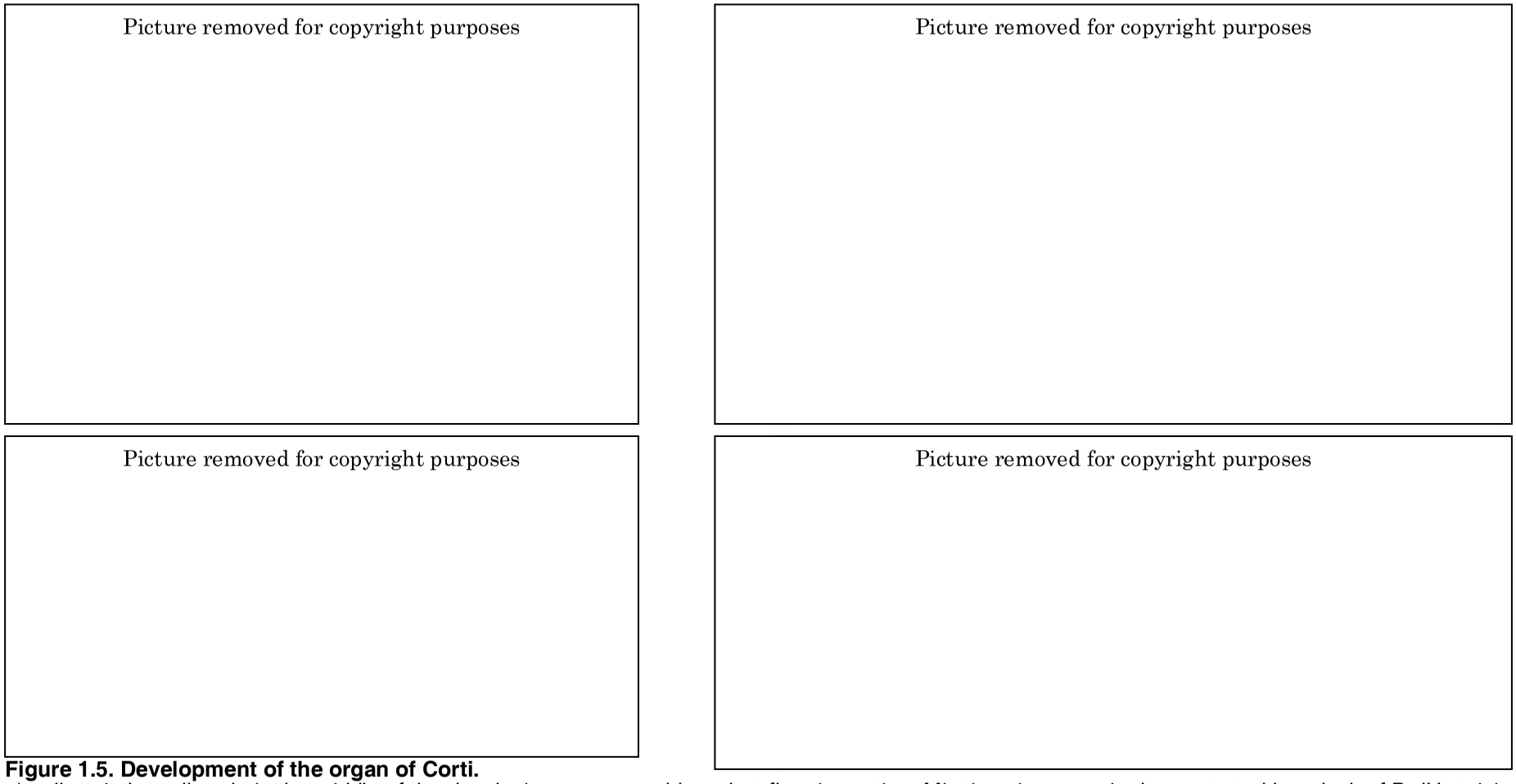

Figure 1.5. Development of the organ of Corti.
a) cells exit the cell cycle in the middle of the developing mouse cochlear duct floor in section. Mitotic quiescence is demonstrated by a lack of BrdU staining and by expression of $p27^{Kip1}$ in the ZNP (taken from Figure 2 in Chen *et al.* 2002). *Atoh1* is expressed in hair cells shortly after terminal mitosis as seen in a cochlear culture (taken from Figure 1 in Chen *et al.* 2002). *b*) a new model of cellular development in the organ of Corti in the rat. *Red*, inner pillar cell; *purple*, inner hair cell; *brown*, support cells. *GER*, greater epithelial ridge; *LER*, lesser epithelial ridge (taken from Figure 11 in Thelen *et al.* 2009). *c*) *Atoh1* expression in an apical section of the E15.5 mouse cochlear duct. ATOH1-expressing nascent hair cells initially form a pillar and are then thought to intercalate in a basal-to-apical direction resulting in convergent extension (CE) of the cochlea (taken from Figure 5 in Chen *et al.* 2002). *d*) model of mouse organ of Corti and hair cell development (taken from Figure 8 in Chen *et al.* 2002).

Rb is upregulated at E15.5 in basal hair cells (i.e. during early hair cell differentiation) and its expression extends from the base to the apex following the wave of hair cell differentiation (see section 1.3.2). It is subsequently expressed throughout the ZNP, and is weakly expressed in other cochlear cells (Liu *et al.* 2008;Mantela *et al.* 2005;Sage *et al.* 2005). Current evidence shows that *Rb* protein is required for the maintenance of mitotic quiescence in the organ of Corti and in the terminal maturation of outer hair cells through an unknown mechanism (Mantela *et al.* 2005;Sage *et al.* 2005;Sage *et al.* 2006). Given its role in prevention of proliferation, *Rb* inhibition is thought to be a potential strategy for hair cell regeneration as hair cells re-enter the cell cycle when *Rb* is inhibited. However, the hair cells produced by this method subsequently die by apoptosis. Therefore, further work on short-term inhibition of *Rb* function is required to clarify whether hair cells can be made to minimally mitose without proceeding to apoptosis or oncogenesis (Sage *et al.* 2006).

Following the induction of mitotic quiescence in the ZNP by $p27^{Kip1}$ and *Rb*, it is thought that the cyclin kinase inhibitors $p19^{Ink4d}$ and $p21^{Cip1}$ are required to prevent hair cells re-entering the cell cycle. Codeletion of these factors results in a sudden loss of cell cycle control at P3 (in mice) and inappropriate S phase entry of hair cells with the production of supernumerary hair cells. This dysregulation leads to p53-mediated apoptosis of mitosing hair cells resulting in a phenotype similar to that of *Rb* knockout mice and supporting the hypothesis that maintenance of hair cells in the postmitotic state is dependent on a network of interacting cyclin kinase inhibitors (Laine *et al.* 2007).

At the time that the ZNP is established, it is thought that its constituent cells have equal potential to become hair cells or support cells and that only cells of the ZNP contribute to the organ of Corti (Kelley 2007). Within the ZNP hair cells and support cells are born simultaneously, suggesting that they share a common lineage, with viral tracing studies in the chick confirming that hair cells and support cells share a common progenitor (Fekete *et al.* 1998). Though it is thought that IHCs are the first cells to become identifiable in the maturing organ of Corti, recent work in developing rats has cast doubt on this as high resolution electron microscopy techniques have revealed cells whose morphology is consistent with that of inner pillar cells *prior* to IHC detection (Thelen *et al.* 2009).

If inner pillar cells are indeed the first cells to differentiate following terminal mitosis in the ZNP, IHCs are the next cell type to become identifiable, followed by the OHCs and support cells (see Figure 1.5*b*) (Thelen *et al.* 2009). The IHCs are located on the modiolar side of the border between the greater and lesser epithelial ridges where inner pillar cells develop. The earliest marker of hair cells is the basic helix-loop-helix (bHLH) transcription factor *Atoh1* (formerly known as *Math1*) which marks a column of nascent inner hair cells that span the distance from the BM to the lumen of the cochlear duct (see Figure 1.5*c*) (Chen *et al.* 2002). Many conflicting results are available regarding when *Atoh1* is first

detectable, though it is accepted that this transcription factor is initially expressed basally in a diffuse group of cells at E12.5 and later refined to be expressed more specifically in nascent HCs once they have adopted their fate (see Figure 1.5*a*) (Kelley 2007). However, it has not been proven whether all of the cells of the *Atoh1*-positive column become hair cells or if only the luminal cells adopt the hair cell fate and it is therefore unclear whether all *Atoh1*-positive cells at this stage are committed to the hair cell fate (Chen *et al.* 2002;Goodyear *et al.* 2006).

Atoh1 is thought to be initially maintained at low levels by the HLH proteins *Ids1*, *Ids2* and *Ids3* until, through an unknown mechanism, *Atoh1* expression is able to rise above a threshold in nascent hair cells. This allows it to regulate its target genes and may allow it to positively autoregulate. Two of the genes that are upregulated in *Atoh1*-expressing cells are the Notch ligands *Jag2* and *Delta-like 1* (*Dll1*). These factors mediate a process of lateral inhibition by acting on the *Notch1* receptor of adjacent cells, thereby initiating the expression of Notch target genes in these cells (*Hes1* and *Hes5*), causing them to differentiate as support cells (Kelley 2007;Kiernan *et al.* 2005a). Consistent with this model, dysregulation of Notch signalling – e.g. by deletion of the *Nr2f1* nuclear receptor – disrupts normal patterning of the sensory epithelial mosaic (Kelley 2007;Tang *et al.* 2006) and alters the expression of the prosensory marker *Sox2*, which is downregulated in *Atoh1*-expressing cells through an unknown mechanism. However, *Sox2* expression is maintained in support cells – most likely due to Notch-mediated upregulation – where it is able to induce the homeodomain transcription factor *Prox1* to suppress the hair cell fate, thereby preventing overproduction of inner hair cells (Dabdoub *et al.* 2008;Kelley 2007).

1.3.2 Hair cell differentiation

Soon after the onset of *Atoh1* expression, a number of hair cell-specific proteins become identifiable. The cells that express these markers subsequently develop morphologically, acquiring the specialised structures required for MET and electromechanical transduction (in OHCs), and gaining functional maturity. Hair cell differentiation proceeds in a basal-to-apical direction (Lim *et al.* 1985).

One of the first known steps in hair cell differentiation is the downregulation of the connexin genes that leads to a loss of gap junctions. In chick studies, this downregulation has been shown to precede morphological changes in hair cells and occurs with a decoupling of developing hair cells from much of the basal extracellular matrix so that only the most basilar of the column of nascent hair cells has contact with the underlying extracellular matrix (similar to the developing mouse organ of Corti) (Bryant *et al.* 2005;Chen *et al.* 2002).

Unlike gap junctions, tight junctions and adherens junctions are retained by developing hair cells (Bryant *et al.* 2005). At the hair cell apices, tight junctions become more complex

as development proceeds with adherens junctions developing beneath them. These apical junctions become mature as the endocochlear potential is generated at P6 in mice. They also define the junction between apical and lateral membranes in the hair cells and this distinction is thought to allow trafficking of different proteins to these different sites (Bryant *et al.* 2005).

Almost immediately after hair cell specification and onset of *Atoh1* expression, hair cells begin to express an array of marker genes. These include the calcium-binding proteins calmodulin, calretinin and parvalbumin; the unconventional myosins VI, VIIa and XVa (see section 1.3.3); and the POU-domain transcription factor, POU4F3 (see section 1.5.3) (Bryant *et al.* 2005;Xiang *et al.* 1998). Calretinin and parvalbumin are also expressed in sensory ganglion neurons making them less specific markers for early differentiating hair cells (Xiang *et al.* 1998). In contrast to this, other factors are downregulated as hair cells differentiate, e.g. the gap junctions and GATA3, the latter of which is first downregulated in hair cells and subsequently downregulated in support cells (Rivolta *et al.* 1998b).

As well as the signalling proteins described, retinoic acid signalling is known to be involved in hair cell development. In the embryonic organ of Corti, it is known to promote differentiation of epithelial cells to hair cells and accompanying support cells. It normally acts through hetero-dimers of its receptors (Goodyear *et al.* 2006) of which retinoic acid receptor (RAR) α, retinoid X receptor (RXR) α and RXRβ are expressed by E13 in the cochlear epithelium, becoming more strongly expressed as hair cells develop (though RAR α expression is rapidly suppressed between E17 and P3) (Raz *et al.* 1999). Treatment of cochlear cultures with a retinoic acid antagonist causes changes in the expression of *Pou4f3* and myosin VIIa but does not affect myosin VI expression, suggesting that retinoic acid signalling is not required for hair cell specification but is responsible for hair cell maturation. The fact that not all markers are eliminated when retinoic acid signalling is suppressed suggests that there is more than one differentiation pathway at work in nascent hair cells (Raz *et al.* 1999).

1.3.3 Morphological maturation of hair cells

As described in section 1.1.3, hair cells display highly specialised apical structures called stereocilia that are grouped together to form a hair bundle that is required for mechanoelectrical transduction (MET). Stereocilia are identifiable early in hair cell differentiation with scanning electron microscopy studies in the developing mouse showing that they are first observable at E12.5 in the utricle and E13.5 in the cristae and saccule (Bryant *et al.* 2005;Goodyear *et al.* 2006). In the cochlea they have been tentatively identified at E15 by transmission electron microscopy (E18 in rat as shown by scanning electron microscopy) (Bryant *et al.* 2005;Goodyear *et al.* 2006;Siemens *et al.* 2004;Zine *et al.* 1996).

A striking feature of the mature organ of Corti is the high regularity and identical orientation of its cells and cellular organelles including hair bundles. This regularity arises because cells must be correctly oriented in the organ of Corti if they are to respond appropriately to movements of the BM. A similarly strict regulation of orientation is exhibited in the vestibular sensory epithelia (Kelly *et al.* 2007). At the hair cell apices, this process of polarisation can be seen in the development of the hair bundles.

Around the time that they are born, hair cells have polygonal apices with many microvilli and a kinocilium (a true cilium) at the centre (Zine *et al.* 1996). Lateralisation of the kinocilium is one of the earliest events in hair bundle development, and this initiates asymmetry in the hair cell apex. The bundle develops centrally in a circular shape but is refined to its adult shape as development proceeds. Mature OHC hair bundles are W-shaped and IHC hair bundles are characteristically straight or slightly curved (see Figure 1.6*a*) (Kelly *et al.* 2007). Consistent with the wave of hair cell differentiation, stereocilia first appear in the basal region of the cochlea and are later detectable apically (Zine *et al.* 1996). As they grow, they undergo extensive remodelling to achieve their mature morphology e.g. tapering at the base and repositioning on the apex. The regular rows of both IHC and OHC hair bundles mature to form a 'staircase' pattern in which adjacent rows of stereocilia increase in height in the modiolar to striolar direction (Bryant *et al.* 2005;Goodyear *et al.* 2006). The staircase arrangement of stereocilia becomes more apparent throughout the P0-P4 age range and, by P4-P6, hair bundles attain their adult shape (Lelli *et al.* 2009;Nishida *et al.* 1998); the kinocilia are also lost at P6 (Lelli *et al.* 2009). By the time of functional hair cell maturation (P10-12), apical hair cell stereocilia are longer than those in the base due to their faster growth rate and due to shortening of basal hair cell stereocilia (see Figure 1.6*b*) (Bryant *et al.* 2005;Goodyear *et al.* 2006;Lelli *et al.* 2009).

Though the kinocilium is initially moved in the same direction in all hair cells, apical cell polarity is not as strictly aligned as it will become as the organ of Corti matures. A microfilament network that runs parallel to the apical membrane – which is associated between hair cells and support cells through adherens junctions – may be involved in signalling this polarization and striated rootlets parallel to the hair cell apices may be involved in positioning the kinocilia. Though the orientation of the bundles is slightly variable early in hair bundle development (e.g. at E17 in the mouse cochlea), by P10, there is very little difference in bundle orientation between hair cells (Goodyear *et al.* 2006). This orientation process is thought to be mediated by a group of genes that control similar cell polarity processes in Drosophila development (*Celsr1*, *Vangl2*, *Frizzled* and members of the Wnt signalling pathway) (Kelly *et al.* 2007).

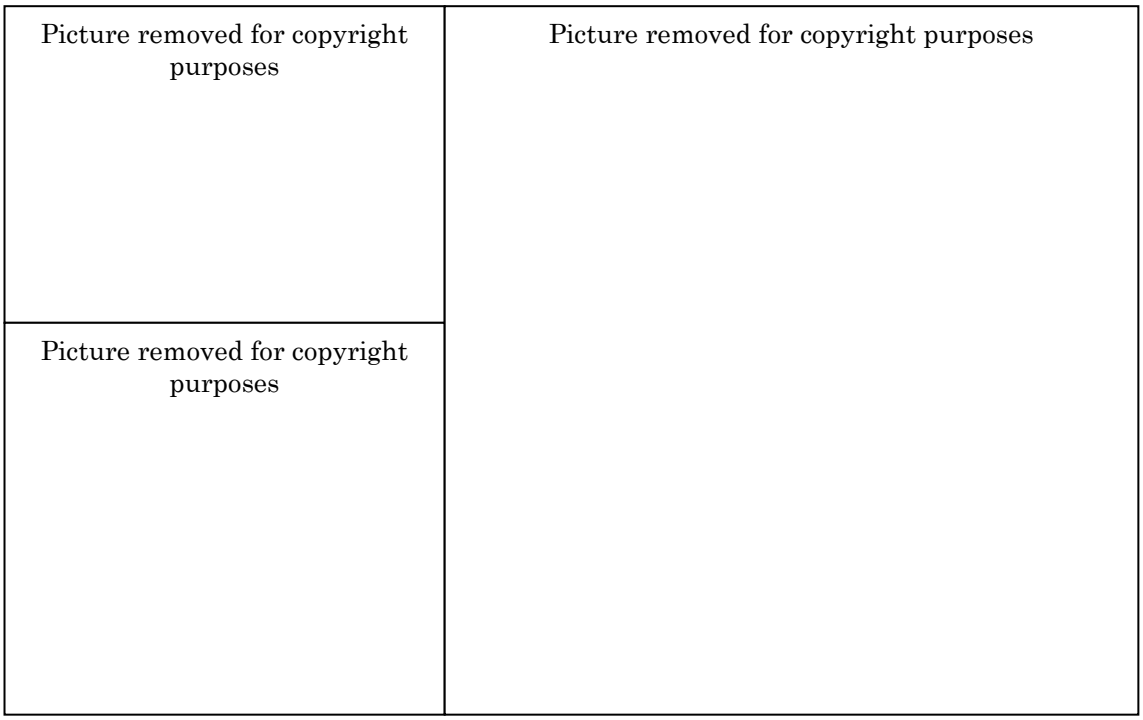

Figure 1.6. Stereocilial links and structure.
a) Scanning electron micrograph of the mid-basal guinea pig organ of Corti showing mature stereocilial morphology. *Red arrow*, IHCs; *blue arrows*, OHCs; *asterisk*, tunnel of Corti; *green arrows*, neurons (adapted from Lenoir 1999). *b*) electron micrographs of the five different types of link seen in the hair bundle (*centre*) (taken from Figure 1 in Nayak *et al.* 2007). *c*) a recent model of MET at the stereocilial apex. In this model, stereocilial movement in the excitatory direction puts tension on the tip-links (composed of CDH23 apically and PCD15 basally), physically opening the MET channel (*mc*), thus allowing small cations to enter. The upper portion of the tip-link is attached by a harmonin isoform and the tip-link is maintained at optimum tensions by a process of adaptation that requires MYO1C (taken from Figure 7 in Grillet *et al.* 2009).

The stereocilia – which more closely resemble enlarged microvilli than true cilia like the kinocilium – are known to be composed of a large number of proteins. Cytoskeletal core proteins Actin, Fimbrin, and Espin form much of the stereocilial structure whilst the unconventional hair cell myosins are required for correct stereocilial development and function. In mice, a myosin VI mutation leads to a circling and deaf phenotype (Snell's waltzer); a myosin VIIa mutation causes vestibular dysfunction and deafness (Shaker1); and a myosin XVa mutation causes deafness and circling behaviour (Shaker2) (Goodyear *et al.* 2006;Liang *et al.* 1998). Though the precise functions of these molecular motors are unknown, the above mutations are known to cause auditory and vestibular defects by disruption of the hair bundle (Bryant *et al.* 2005;Goodyear *et al.* 2006).

As the stereocilia mature, links between them become apparent. These links have been best characterised in the chick basilar papilla where, from hair bundle apex to base, tip-links, horizontal top connectors, shaft connectors and ankle links have been identified (Bryant *et al.* 2005;Goodyear *et al.* 2006). If the kinocilium is still present (i.e. before P6 in the mouse cochlea), then there are also abundant kinocilial links present which join the kinocilium to the immediately adjacent stereocilia in the tallest row of the hair bundle (see Figure 1.6*b*) (Nayak *et al.* 2007). The tip-links grow radially between the stereocilia and are later refined

to remove extraneous links, leaving only those that are in line with the direction of hair bundle displacement (Waguespack *et al.* 2007). These are thought to be involved in the gating of the MET channel (see section 1.3.4) and are formed by an asymmetric complex of the cell adhesion molecules cadherin 23 and protocadherin 15 (Kazmierczak *et al.* 2007). A large and heterogeneous group of mutations in these genes are known to cause deaf-blindness in humans (Reiners *et al.* 2006) but only cause inner ear dysfunction in Ames Waltzer mice due to abnormal stereocilial development; the difference between mice and humans most likely being due to functional redundancy between different isoforms of these cadherins in mice (Ahmed *et al.* 2008). The remaining links are thought to play a purely structural role in co-ordinating hair bundles so that they move as a functional unit, though their precise roles are uncharacterised (Bryant *et al.* 2005). Furthermore, the function of an increasing array of cell membrane proteins (Integrins and Ptprq), PDZ-binding domain proteins (Harmonin b, Whirlin and Sans) and downstream target genes of PCP genes and integrins (Rho-GTPases) are being characterised in developing hair cells (Bryant *et al.* 2005;Goodyear *et al.* 2006) where they are also thought to be involved in hair bundle maturation and function.

As well as the array of proteins described above, microRNAs have also been implicated in normal hair cell development. These molecules bind to target mRNA and repress its translation to produce subtle changes in protein expression (Weston *et al.* 2009). miR-96, which is expressed from a primary transcript that also encodes miR-182 and miR-183, has been shown to be required for normal hair cell development. Mutation in the seed region of this microRNA (the part of the molecule that interacts with target mRNAs) causes hair bundle deformity in heterozygous mice and very few recognisable hair cells in four to six week old homozygotes. Heterozygotes consequently display highly raised hearing thresholds and homozygotes have no detectable hearing at 4 weeks of age (Lewis *et al.* 2009). Furthermore, miR-96 mutation in humans causes a progressive autosomal dominant hearing loss (Mencia *et al.* 2009). These effects are thought to be due to the dysregulation of translation of 96 transcripts identified by microarray analysis (particularly *Slc26a5, Ocm, Gfi1, Ptprq* and *Pitpnm1* which are involved in hair cell development and function) (Lewis *et al.* 2009).

At the hair cell apices, stereocilial roots insert into a dense body of cytoskeletal proteins called the cuticular plate. This structure contains α-actin, spectrin, tropomyosin, myosin Ie and myosin VI and is first identifiable at E14-15 in the mouse cochlea using an antibody that recognises one of its unidentified components i.e. before stereocilia become detectable. During its generation, many uncoated vesicles are present in the apical hair cell cytoplasm, and coated pits suggest extensive endocytotic activity and high membrane turnover at the apical membrane. As this subsides, the cuticular plate thickens and joins the hair cell apex and neck by the formation of a junctional complex (Forge *et al.* 1993; Nishida *et al.* 1998).

1.3.4 Functional maturation of hair cells

To perform their specialised functions properly, hair cells require a hair bundle with MET channels; ion channels in the basolateral membrane (for K^+ and Ca^{2+}) with fast enough kinetics to produce sufficiently sensitive receptor potentials; and adequately developed synapses for the informative release of neurotransmitter. Mice start to hear at about P10-12, at which point all of the above factors are in place. Electromechanical transduction is also in place in OHCs at this stage (see below) (Kros 1996;Marcotti *et al.* 1999;Meyer *et al.* 2009). The development and mature function of these processes is described in this section.

Mechanoelectrical transduction

When hair cell stereocilial bundles are deflected away from the modiolus, it is thought that tip-links are stretched due to the relative rotational movement of stereocilia in neighbouring rows. The tension generated in the tip-links is transmitted to the as-yet unidentified MET channel by an unknown coupling mechanism causing the influx of small cations from the endolymph that results in hair cell depolarisation (Xu *et al.* 2009). These tip-links are maintained at optimal tension by an adaptation process (Holt *et al.* 2000). Gradually, more aspects of these processes are being identified and their development is being characterised (see Figure 1.6*c*).

Morphologically, the transduction apparatus can be divided into the upper tip-link density (UTLD), the tip-link, the lower tip-link density (LTLD) and the MET channel. It is thought that the MET channel is located at the tips of the stereocilia though it is uncertain whether it is located on taller or shorter stereocilia (though it is unlikely to be present at both ends of the tip-link) (Fettiplace *et al.* 2006). The most recent model at the time of writing places the MET channel at the top of the shorter stereocilia in the LTLD where force is transmitted to it by the lower (PCD15) portion of the tip-link via an unknown mechanism (Grillet *et al.* 2009). The upper part of the tip-link is composed of CDH23 and this part inserts into the UTLD. A protein called harmonin has recently been shown to form part of the UTLD and it is thought that harmonin couples CHD23 to the F-actin in the taller stereocilium (see Figure 1.6*c*) (Grillet *et al.* 2009). Though harmonin a and/or b is known to be primarily expressed at the UTLD in adult mice, different isoforms of harmonin are expressed in different parts of the stereocilia and at different levels throughout development (Boeda *et al.* 2002;Grillet *et al.* 2009).

The MET channel is known to be expressed as early as E18.5 in mice as its transducer current (I_T) develops in the basal cochlea at this date. It is thought that this early MET channel expression (well before the onset of hearing) might be required to regulate hair bundle maturation and to facilitate spontaneous action potentials that are generated by developing hair cells (Kros 1996). Though the MET channel current is identifiable from

E18.5 (in inner hair cells), cochlear IHCs and OHCs do not become mechanosensitive until between P0 and P2 (Lelli *et al.* 2009). These hair cells are identifiable in the basal P0 cochlea with the developmental gradient of mechanotransduction moving from base to apex to encompass all cochlear hair cells at P7 as demonstrated by FM1-43 staining (a styryl dye that permeates the open MET channel (Gale *et al.* 2001)) (Lelli *et al.* 2009). Functional, but closed, MET channels have been identified at earlier dates in these regions by deflecting hair bundles and measuring evoked currents. By this method, >80% of OHCs in the mid apical and apical turns are identified as being mechanosensitive at P2. Furthermore, there is a systematic increase in the amplitude of maximal transduction currents (between P0 and P2 in the base and between P2 and P6 in the apex) with similar maturation of the operating range (stabilising at P2-3 basally and P5-6 apically) and adaptation (stabilising at P4 basally and P6 apically) (Lelli *et al.* 2009). It is thought that harmonin is required for maturation of these MET transducer currents as the currents produced by mature harmonin mutant cochlear hair cells resemble those of immature wild type hair cells (Grillet *et al.* 2009).

Hair cell ion channels, currents, innervation and synaptic maturation

A full discussion of the variety of currents that are seen in developing and mature hair cells (including the MET current) is beyond the scope of this work. However, these currents will be briefly discussed along with synaptic maturation due to the requirement of these processes for normal hair cell development.

Following specification, the IHC has a resting potential of approximately -50mV due to the $I_{K,emb}$ current. This resting potential becomes more negative by E16.5 due to the additional K^+ current, I_{K1}. At this stage, Ca^{2+} and Na^+ currents with fast activation kinetics become identifiable and IHCs are therefore likely to be able to release synaptic vesicles by this point (Housley *et al.* 2006). All of these currents rapidly increase in size in the base by E17.5 (E18.5 in the apex) where I_{Ca} is necessary for calcium action potentials and I_{Na} and I_{K1} modulate the frequency and shape of these action potentials which are quite small and slow (Goodyear *et al.* 2006;Kros 1996).

These action potentials are spontaneous and are thought to be important for the correct maturation of synaptic connections i.e. they are necessary for the development and survival of neural connections as well as the development and survival of IHCs themselves. Afferent neurons begin to form synapses with IHCs at about E18 when, in the basal cochlea, the MET transducer current (I_T) is also present (though probably not yet mechanosensitive) (Goodyear *et al.* 2006;Housley *et al.* 2006;Kros 1996;Lelli *et al.* 2009). Therefore, as well as potentially regulating hair bundle maturation, I_T might be required with I_{Ca} to facilitate spontaneous action potentials (Goodyear *et al.* 2006;Kros 1996).

Spontaneous action potentials, both due to intrinsically generated Ca^{2+} spikes and purinergic signalling, continue into the second postnatal week by which time *in vitro* studies have shown that large changes are completed in hair cell innervation and ion channel expression (Housley *et al.* 2006;Tritsch *et al.* 2007). From P3 to P10, temporary efferent synaptic connections are formed with the IHCs that are thought to inhibit afferent firing via the I_{SK2} current, thereby setting up rhythmic firing patterns in immature afferent neurons that are required for coding functional hair cell output. Also in the early postnatal period, the delayed-rectifier K^+ current $I_{K,neo}$ develops (P0), efferent synapses at the OHCs express SK2 currents and OHCs become electromotile (from about P8) (Goodyear *et al.* 2006;Kros 1996).

Final maturation of IHCs occurs towards the end of the second postnatal week when there is a sudden expression – at the onset of hearing – of the fast, non-inactivating outward K+ current $I_{K,f}$ which allows IHCs to respond to hair bundle movement with the fast, graded receptor potentials required for appropriately detailed encoding of sound intensity. A potassium current ($I_{K(Ca)}$) is also found and thought to regulate neurotransmitter release. Finally, $I_{K,f}$ (I_{BK}), a KCNQ4 current ($I_{K,n}$) and $I_{K,s}$ are expressed. $I_{K,f}$ and $I_{K,n}$ take over from I_{K1} in setting the resting potential in the mature IHC and $I_{K,s}$ (a delayed-rectifier K+ current with slow action kinetics) may contribute to the adaptation of IHC receptor potentials to long-duration tone bursts (Goodyear *et al.* 2006;Kros 1996).

Once signals are transmitted from the MET channel to the remainder of the IHC, the signal has to be transmitted to the nervous system. This is accomplished by release of the excitatory amino acid neurotransmitter glutamate from IHCs that acts on AMPA receptors on postsynaptic afferent neurons. Glutamate release is dependent on maturation of IHC presynaptic function and, to facilitate this, there is an increase in I_{Ca} and synaptic vesicle exocytosis in the first postnatal week. Though I_{Ca} subsequently declines, exocytosis remains constant and these changes are accompanied by a large-scale remodelling of the presynaptic IHC that is associated with the development of plates of presynaptic 'ribbons' around the onset of hearing. These changes are thought to be essential for precise control of neurotransmitter release (reviewed in Kros 1996;Meyer *et al.* 2009). In mice, ribbon synapses have been shown to be tuned so that their morphology at mature IHCs is similar throughout the cochlea but with a tonotopic variation in synaptic density (Meyer *et al.* 2009).

Effect of thyroid hormone signalling on inner ear development

The thyroid hormone receptors TRα1 and TRα2 (encoded by *Thra*) are expressed in most of the sensory epithelia of the inner ear whereas TRß1 and TRß2 (encoded by *Thrb*) are only expressed in the cochlear epithelium in both the greater epithelial ridge (GER) and lesser epithelial ridge (LER). Induced hypothyroidism influences the activity of the T3-responsive

thyroid hormone receptors (TRα1, TRß1 and TRß2) and causes a delay in organ of Corti development with additional defects in TM development. Furthermore, knockout of all thyroid receptors leads to defects and delay in hair cell functional maturation as measured by the disruption of normal hair cell ion currents (Goodyear *et al.* 2006).

Outer hair cell mechanoelectrical transduction

The lateral membranes of IHCs and OHCs appear similar at birth. However, the OHC lateral membrane becomes specialised by P8 (when OHCs become electromotile) i.e. prior to the onset of hearing at P10-12 in mice (P15 in the rat) (Bryant *et al.* 2005;Goodyear *et al.* 2006;Jensen-Smith *et al.* 2007;Kros 1996). The support cells disconnect from the lateral membrane, leaving a liquid-filled gap, and endoplasmic cisternae develop parallel to the OHC lateral membrane where prestin (*Slc26a5*), Glut-5, actin and Ca^{2+}-ATPase become localised. The organisation of these proteins and the cisternae continues to develop in a time frame consistent with functional maturation of OHCs (as measured by OAEs) and, therefore, the onset of electromotility at P8 in mouse OHCs (Bryant *et al.* 2005;Marcotti *et al.* 1999).

Following the described processes of prosensory domain specification, hair cell specification and differentiation, mature hair cells are able to detect subatomic deflections of hair bundles (Dallos 1992). This ability underlies the exquisite sensitivity of human hearing and small perturbations of the above processes – including genetic mutations – are sufficient to abolish the function of this sensitive system.

1.4 Abnormal hearing

1.4.1 Epidemiology and classification of hearing loss

278 million people worldwide are estimated to have a moderate to profound hearing loss in both ears (World Health Organization 2006) which can arise from damage at any level of the auditory pathway from the outer ear to higher brain centres. Hearing loss often presents in childhood and 68 million people are thought to have hearing loss that originated in childhood with about 62 million of this population aged less than 15 years. This is due to an estimated neonatal incidence of about 720 000 cases per year worldwide which doubles by age 9 in developed countries such as the UK (Fortnum *et al.* 2001;Olusanya *et al.* 2007).

According to current measures, two thirds of the burden of hearing loss is borne by developing countries. However, it has been argued that the World Health Organization's thresholds for disabling hearing loss are set too high and, therefore, do not take into account less severe hearing losses that can be disabling in noisy environments. Therefore the number of people in both the developed and developing world that are living with a disabling hearing loss is likely to be higher than the above figure (Olusanya *et al.* 2007;Smith *et al.* 2006).

Traditionally, hearing loss is described as being either conductive, sensorineural or mixed in origin. Conductive hearing loss is hearing loss due to abnormality of the outer or middle ear that causes reduced sound conduction to sensory hair cells of the inner ear and sensorineural hearing loss (SNHL) refers to damage to the cochlea, sensory neurons or higher auditory centres (Bull *et al.* 2007) (see Table 1.2).

SNHL is the most common sensory deficit in more developed societies and, based on years of healthy life lost, adult-onset hearing loss from all causes is the third largest cause of disability after depressive disorders and unintentional injuries (Olusanya *et al.* 2007). However, some authors argue that permanent childhood hearing impairment is likely to cause a greater loss of healthy life if properly accounted for (Olusanya *et al.* 2007).

Due to differences in healthcare, living conditions and culture, the causes of hearing loss vary greatly between developed and developing countries. The largest causes of hearing loss in developing countries (infection and medication) now account for only a small amount of hearing loss in the developed world where genetic deafness and age-related hearing loss (ARHL) are responsible for most hearing loss (see Olusanya *et al.* 2007 for review). The problem of ARHL – which is growing due to the ageing population in developed countries such as the UK – is further complicated by increasing rates of dual sensory loss as vision impairment is also associated with age (Heine *et al.* 2002). In recent studies, ARHL has

been shown to have a prevalence of 29-43% in men and 17-20% in women of 60-69 years of age (Agrawal *et al.* 2008;Gopinath *et al.* 2009).

Table 1.2. Classification of hearing loss.
Causes of hearing loss categorised by location of lesion and in approximate order of incidence in the developed world (adapted from Bull *et al.* 2007).

Conductive	*Sensorineural*
Wax	Age-related hearing loss (ARHL)
Otitis media	Noise-induced hearing loss (NIHL)
Barotrauma	Genetic (Congenital, early- or late-onset)
Otosclerosis	Drug- / Poison-induced (including solvents)
Injury of tympanic membrane	Menière's disease
Traumatic ossicular dislocation	Late otosclerosis
Congenital ear canal atresia	Inner ear infections and meningitis
Middle ear agenesis	Hypoxia
Middle ear tumours	Jaundice
	Vestibular Schwannoma
	Head Injury
	CNS disease
	Metabolic

1.4.2 Testing and characterisation of hearing loss

Worldwide, there is a trend towards early detection of childhood hearing impairment. The importance of early identification and characterisation of hearing loss in achieving better outcomes in auditory habilitation has been established, especially regarding childhood development; late (>1 year) detection and management of hearing impairment is associated with substantial developmental deficits in communication and cognition (Olusanya *et al.* 2007). Adequate assessment of adult hearing loss is, likewise, important in determining the cause and, therefore, the appropriate treatment for hearing loss.

Simple clinical tests can be used to identify and categorise hearing loss. The tuning fork tests devised by Weber (to identify unilateral hearing loss) and Rinne (to differentiate conductive and sensorineural hearing losses) still form part of hearing examination though they provide little information on the frequency distribution of hearing losses (Ludman *et al.* 1998). Audiometric tests can also perform the function of identifying hearing loss and aid in the differentiation between conductive and sensorineural hearing loss. However, they serve the further purpose of characterising the frequency distribution and quantifying hearing loss which makes it possible to track its progression (Ludman *et al.* 1998;Prosser *et al.* 2007). Finally, imaging techniques such as MRI and CT are employed to identify gross anatomical causes of hearing loss (Phelps 1998).

Focussing on SNHL, commonly available quantitative tests are pure tone audiometry, speech audiometry, auditory brainstem responses (ABRs) and otoacoustic emissions. In the first two tests, a subject's ability to detect sounds of differing frequency and intensity is tested. Pure tone audiometry presents sinusoidal waveforms for this task whereas speech audiometry uses speech sounds. Subjects report their ability to detect a pure tone or repeat speech sounds to the examiner as appropriate. This results in the production of an audiogram whereby the lowest intensity at which sound of a given frequency can be detected is plotted relative to the expected threshold for a number of frequencies (see Figure 1.10*b* for an example) (Ludman *et al.* 1998;Prosser *et al.* 2007). Of the two tests, speech audiometry is thought to be more relevant to communication and is therefore more useful in monitoring the results of rehabilitative interventions (Prosser *et al.* 2007). However, both pure tone and speech audiometry are restricted by the requirement of communication from the subject. Though most adults and children aged five years and above can undergo pure tone audiometry, younger children require special conditioning procedures and it is difficult and time-consuming to test these children (Prosser *et al.* 2007).

Such co-operation is not required for ABRs and OAEs. ABRs measure the response of the auditory brainstem to auditory stimuli by detecting action potentials at six to seven points between the cochlear nerve and subthalamic nuclei. This test looks for neural abnormalities and is able to localise auditory brainstem deficits as well as detecting cochlear hearing loss. OAEs, on the other hand, look solely at OHC function. Different stimuli are used to measure the cochlear response at different frequencies and intensities (Ludman *et al.* 1998) to identify cochlear causes of hearing loss. Given the ease with which OAEs can be measured (usually in 3-5 minutes per subject), they have become the screening method of choice for the UK NHS neonatal hearing screening programme (MRC Hearing & Communication Group 2008).

The above tests, allied with more specialised tests and a battery of vestibular function tests, currently aid in the assessment and management of patients with hearing loss (Ludman *et al.* 1998;Omahoney *et al.* 1998;Prosser *et al.* 2007). Once an audiogram is obtained, the severity of hearing loss can be quantified, and the type of hearing loss can be categorised (i.e. low-frequency, middle-frequency, high-frequency or flat).

The above tests currently aid in tailoring treatment for hearing loss (see section 1.4.6), though they are likely to play a greater diagnostic role as the audiogram phenotype of different hearing losses becomes better-characterised, as the temporal progression of different hearing losses are better understood and as the audiogram-histological relationship of hair cell-mediated and non-hair cell-mediated hearing loss is elucidated (Prosser *et al.* 2007). Perhaps most importantly, future improvement in the sensitivity of these assessment tools may guide genetic investigations for hearing loss in order to identify

which of the hundreds of chromosomal loci that cause hearing loss are at fault in a given patient with a suspected genetic cause of hearing loss (see sections 1.4.4 and 1.5.4) (Prosser *et al.* 2007).

1.4.3 Sensorineural hearing loss (SNHL)

SNHL can be caused by a diverse group of factors that either cause direct damage to the organ of Corti (e.g. infection and trauma) or cause hair cell dysfunction through other mechanisms which can underlie the differences in onset of different hearing losses (e.g. genetic hearing loss and aminoglycoside antibiotics) (see Table 1.3). Fortunately, in the developed world, the incidence of hearing loss due to preventable causes has been greatly reduced. This change is due to improvements in prenatal and perinatal care (including maternal vaccination against rubella), careful use of aminoglycoside antibiotics (see section 1.4.6), appropriate treatment of infection, reduced exposure to solvents and genetic counselling (Olusanya *et al.* 2007).

Unfortunately, although NIHL caused by occupational exposure to noise is thought to be on the decline, NIHL from other causes seems set to rise. This is thought to be due to increased voluntary exposure to high intensity noise though personal music players and loud concerts as well as the failure to implement a variety of lifestyle factors (of various levels of evidence) which can be preventative, i.e. using hearing protection, smoking cessation, increasing exercise, improving nutrition and reducing other risk factors for diabetes or heart disease. (Daniel 2007).

Table 1.3. Types and onset of SNHL.
The different types of SNHL categorised by onset (data from Bull *et al.* 2007;Daniel 2007;Howarth *et al.* 2006;Olusanya *et al.* 2007;Smith *et al.* 2005).

Onset	*Prenatal*	*Perinatal*	*Postnatal*	*Early-onset*	*Late-onset*
Type	Genetic / Chromosomal				
	Infectious				
	Drugs (e.g. Aminoglycoside antibiotics) / Poisons (e.g. solvents)				
		Noise			
		Trauma			
		Birth Asphyxia			
			Neonatal Jaundice		
			Prematurity		
			Low Birthweight		
					Age

1.4.4 Genetic causes of hearing loss

Many of the critical factors for physiological hearing have been identified as their mutation results in hearing loss (in both humans and mouse models) (Robin *et al.* 2005;Van Camp & Smith 2008). Less than 15 years ago, few genetic causes of hearing loss were known. However, since the advent of new molecular biological experimental techniques, mutations at over 100 loci have been shown to be responsible for hereditary hearing loss and the majority of the mutations at these loci cause SNHL (Prosser *et al.* 2007;Robin *et al.* 2005;Van Camp & Smith 2008). Though mutations causing hearing loss eventually result in similar pathology (i.e. hair cell loss and organ of Corti degeneration), the factors which they affect are active in a range of sites as shown in Figure 1.7 (Friedman *et al.* 2007); this diversity of function and localization is representative of the complexity of the inner ear. The level of disability caused by these hereditary hearing losses is dependent on the severity (mild, moderate or profound) and time of onset (typically described as congenital, prelingual, postlingual or adult) of hearing loss, though these factors can vary greatly (summarised in Table 1.4).

More than half of neonates with SNHL have hereditary hearing loss. Of this number, 30% are syndromic (most commonly due to *SLC26A4* mutation that causes Pendred's syndrome) and approximately 50% are attributed to non-syndromic gap junction mutation (*GJB2 and* GJB6*)*, with the remainder being attributable to other non-syndromic causes, such as *POU4F3* mutation (Robin *et al.* 2005;Smith *et al.* 2005) (see Table 1.4 and sections 1.5.3 and 1.5.4). Consequently, clinical investigation of suspected hereditary hearing loss is usually restricted to *GJB2* and *SLC26A4* analysis (Prosser *et al.* 2007).

Such hearing losses can be inherited by a number of different modes (autosomal dominant, autosomal recessive, X-linked or mitochondrial). Furthermore, both the mode of inheritance and type of hearing loss caused by different mutations in the same gene can vary greatly (see Table 1.4). This is illustrated by *GJB2* mutation that can result in either autosomal recessive nonsyndromic hearing loss or autosomal dominant syndromic hearing loss depending on the mutation present. Looking more closely at these *GJB2* mutant phenotypes, the time of onset of hearing loss is also highly variable, causing either prelingual or postlingual deafness, which will result in a large difference in language acquisition in affected individuals (see Table 1.4).

Although the largest cause of hearing loss (*GJB2* mutation) does not cause hearing loss by a direct effect on hair cells (mature hair cells do not express gap junctions), a large amount of genetic deafness is due to hair cell loss (Smith *et al.* 2005;Van Camp & Smith 2008). This is either due to mutation of genes that are selectively expressed in hair cells (as in Figure 1.7*d,e & f*) or by hair cell death secondary to other cochlear disorders (Friedman *et al.* 2007).

Attempts are currently underway to identify more genes that are required for normal inner ear function through large forward genetics (phenotype-driven) mutagenesis programs. In such programs, random mutations are generated in mice (e.g. by ENU mutagenesis) and the progeny are tested for hearing loss, initially with a simple test (e.g. response to a click) and later by more detailed investigation (e.g. ABR hearing testing) (Acevedo-Arozena *et al.* 2008). It is hoped that these new mutant mice will give us a better understanding of the mechanisms of hearing and deafness.

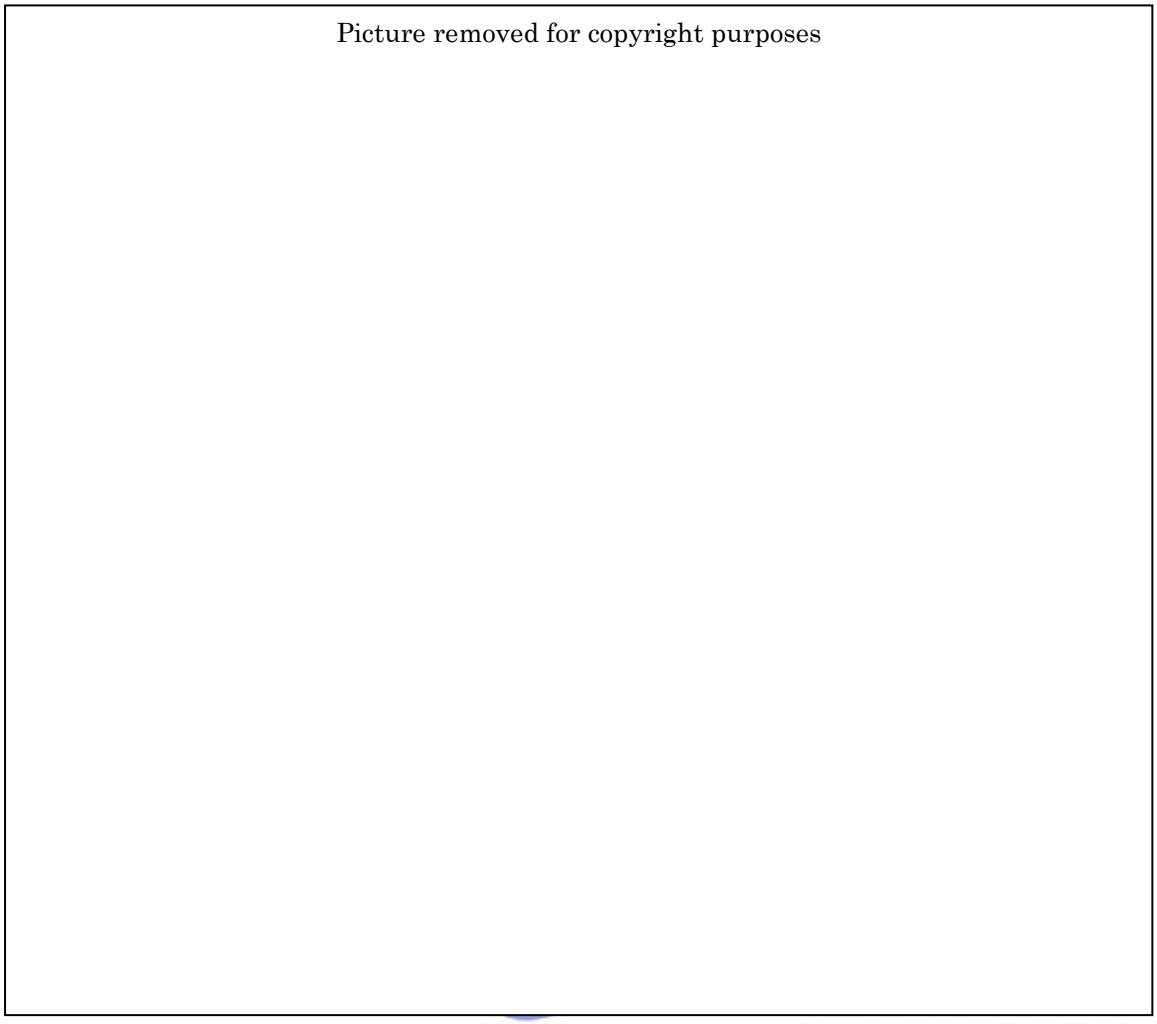

Figure 1.7. Cochlear expression of factors involved in hereditary hearing loss.
Schematic of factors required for normal hearing which are expressed in different parts of the cochlea and whose mutation results in SNHL: *a*) cochlear section (*RM*, Reissner's membrane); *b*) tectorial membrane; *c*) stria vascularis; *d*) hair cell and support cells; *e*) hair cell apex and hair bundle links; *f*) stereocilium (taken from Friedman *et al.* 2007).

Though there is a strong focus on the identification of mutations that cause SNHL in animal models, this sometimes overlooks the complex interaction between genetic and environmental factors that confound human SNHL study. As environmental factors can greatly influence hearing loss, it is difficult to identify genetic factors that can underlie sensitivity to these environmental causes of hearing loss, making it hard to attribute the correct share of causality to each factor. An example of this is the mitochondrial mutation

(A1555G) that underlies a non-syndromic hearing loss and increased sensitivity to aminoglycoside ototoxicity (Zhang *et al.* 2005). However, using novel resources, genetic modifiers of susceptibility to late-onset hearing loss are being identified. Using a large sample of patients with hearing loss, Friedman *et al.* were recently able to identify *GRM7* (a gene that encodes a type of metabotropic glutamate receptor), the mutation of which is thought to underlie susceptibility to ARHL (Friedman *et al.* 2009b). Furthermore, using a different approach (i.e. candidate gene SNPs and the HapMap project), van Laer *et al.* were able to identify a gene that is associated with ARHL (*GRHL2*) due to a mutation in an intronic region that is likely to affect its regulation and, therefore, expression (Van Laer *et al.* 2008).

Given that more deafness-causing genes are now known, it has been suggested that genetic testing is likely to become a more integral part of the evaluation of hearing impairment, particularly in children. This is important for prognosis in terms of disease progression and response to treatment, as well as being valuable for genetic counselling of parents. It is also an appealing prospect for healthcare services as it can be cheaper than the battery of tests that many patients are subjected to, assuming that a mutation is found (Robin *et al.* 2005). However, given the considerable heterogeneity in the genetic causes of hearing loss, the poor genotype-phenotype correlation seen for most forms of deafness (see Table 1.4), and the number of environmental factors that can greatly affect phenotype, the challenges facing the design and implementation of such diagnostic tests are considerable.

Table 1.4. Causes of hereditary hearing loss.
A number of genes that are known to cause hearing loss when mutated are shown below. *DFN*, X-linked; *DFNA*, autosomal dominant; *DFNB*, autosomal recessive (Kharkovets *et al.* 2006;OMIM 2009;Petit *et al.* 2001;Van Camp & Smith 2008).

Gene	*Protein*	*Human deafness*	*Mouse Model*	*Type*	*Onset*
MYO7A	Myosin VIIA	DFNB2 ± retinopathy (Usher 1B); DFNA11	*Shaker-1*	Both	Variable
MYO15	Myosin XV	DFNB3	*Shaker-2*	Non-syndromic	Congenital
MYO6	Myosin VI	DFNA22	*Snell's waltzer*	Non-syndromic	Postlingual-late
USH1C	Harmonin	DFNB18 ± retinopathy (Usher 1C)	*Deaf circler*	Syndromic	Congenital
CHD23	Cadherin-23	DFNB12 ± retinopathy (Usher 1D)	*Waltzer*	Syndromic	Congenital
Espn	Espin	DFNB36	*Jerker*	Non-syndromic	Prelingual
KCNQ4	KCNQ4	DFNA2A	$Kcnq4^{-/-}$; $Kcnq4^{dn/dn}$	Non-syndromic	Postlingual – late 20s
Atp2b2/Pmca2	Ca^{2+}-ATPase 2	Unknown	*Deafwaddler*	Unknown	Unknown
OTOF	Otoferlin	DFNB9	$Otof^{-/-}$	Non-syndromic	Congenital – <2 years
POU4F3	POU4F3	DFNA15	$Pou4f3^{-/-}$; $Pou4f3^{ddl/ddl}$	Non-syndromic	Childhood onwards
CX26/GJB2	Connexin 26	DFNB1; DFNA3 ± keratodermia	$Cx26^{-/-}$	Both	Prelingual – Postlingual
CX30/GJB6	Connexin 30	DFNA3' ± keratodermia; DFNB1	$Cx30^{-/-}$	Syndromic	Prelingual
CX31/GJB3	Connexin 31	DFNA2'; DFNBi ± peripheral neuropathy	$Gjb3^{-/-}$	Non-syndromic	Early – late childhood

Gene	*Protein*	*Human deafness*	*Mouse Model*	*Type*	*Onset*
Slc12a2/ Nkcc1	NKCC1	Unknown	*sy^{ns}; Nkcc1$^{-/-}$*	Unknown	Unknown
PDS	Pendrin	DFNB4 ± thyroid goitre	*Pds$^{-/-}$*	Syndromic	Congenital
CLDN14	Claudin-14	DFNB29	*Cldn14$^{-/-}$*	Non-syndromic	Congenital
COCH	Cochlin	DFNA9	*Coch$^{-/-}$*	Non-syndromic	Postlingual
EYA4	EYA4	DFNA10	*Eya4$^{-/-}$*	Non-syndromic	Late-onset
POU3F4	POU3F4	DFN3	*Pou3f4$^{-/-}$*	Non-syndromic	Unknown
COL11A2	Collagen XI (α2 chain)	DFNA13 ± osteochondrodysplasia	*Col11a2$^{-/-}$*	Syndromic	Postlingual
TECTA	α-tectorin	DFNA8/12; DFNB21	*Tecta$^{-/-}$*	Non-syndromic	Prelingual – postlingual
Otog	Otogelin	Unknown	*Twister; Otog$^{-/-}$*	Non-syndromic	Unknown
TMPRSS3	TMPRSS3	DFNB8/10	*Tmprss1$^{-/-}$*	Non-syndromic	Congenital
PCDH15	Protocadherin-15	DFNB23 ± retinopathy	*Ames waltzer*	Syndromic	Prelingual
HDIA1	Diaphanous-1	DFNA1	*Unknown*	Non-syndromic	Postlingual
DFNA5	DFNA5	DFNA5	*Dfna5$^{-/-}$*	Non-syndromic	Postlingual
MYH9	Myosin IIA	DFNA17 ± giant platelets	*None*	Syndromic	Second decade

1.4.5 Hair cell death

Hair cell loss in humans leads to permanent SNHL and loss of vestibular function because there is no hair cell regeneration in the mammalian cochlea and little regeneration in the vestibular epithelia (Matsui *et al.* 2005). As well as gene mutation, noise, medications (such as aminoglycoside antibiotics and the cytotoxic agent cisplatin), age and other factors can also cause hearing loss via hair cell death (Holley 2005).

Although the mechanisms that trigger hair cell death have not been elucidated, the signalling pathways involved in this process are becoming increasingly well characterised. For example, apoptosis (type 1 programmed cell death), necrosis and necrosis-like programmed cell death (type 2 programmed cell death) have all been implicated in hair cell loss due to noise and cochlear implantation trauma (Eshraghi *et al.* 2006). In noise-induced hearing loss (NIHL), basal cochlear OHCs have been shown to be the most susceptible to damage as these are the first hair cells to be lost following noise exposure (Henderson *et al.* 2006). This may be due to reactive oxygen species (ROS) and toxic free radicals that are known to be produced in the stria vascularis and later appear in OHCs. ROS are also associated with aminoglycoside-induced hair cell loss, cisplatin-induced hair cell loss and, along with reactive nitrogen species, hair cell loss in pneumococcal labyrinthitis (secondary to meningitis) (Cheng *et al.* 2005;Klein *et al.* 2008;Matsui *et al.* 2004a;Rizzi *et al.* 2007;Rybak *et al.* 2007). However, it is not understood whether ROS cause cochlear damage or if they are the products of dying cells (Henderson *et al.* 2006). In NIHL, hair cell death occurs via a mixture of necrosis and apoptosis in the initial phase which later progresses due to apoptosis alone (Henderson *et al.* 2006). Hair cell death is thought to be triggered by JNK and c-jun activation which leads to Bax translocation to the mitochondria and cytochrome c release with associated caspase activation (Cheng *et al.* 2005).

The mechanism of hair cell death due to aminoglycoside antibiotics is thought to share the same upstream component as NIHL (Cheng *et al.* 2005). Approximately 4 hours after neomycin application, the intracellular Ca^{2+} concentration undergoes a sustained increase which is temporally linked to phosphorylation of JNKs (and, subsequently, c-Jun) which, in turn, leads to apoptosis (Cheng *et al.* 2005;Gale *et al.* 2004;Matsui *et al.* 2004b). Though cisplatin-induced apoptosis acts through the same end-effectors as aminoglycosides and produces a similar pattern of hair cell loss, it does not seem to be controlled by the JNK / MAPK pathway, suggesting the presence of more than one apoptotic trigger in hair cells (Cheng *et al.* 2005). One such trigger may be p53, which is upregulated in hair cells in response to cisplatin treatment suggesting that it is an upstream regulator of cisplatin-induced hair cell death (Cheng *et al.* 2005;Rybak *et al.* 2007).

The deeper insight into hair cell death that has been gained in recent years has clarified the disease mechanisms of many different types of hearing loss. This knowledge is now being turned into potential preventative measures against hearing loss (see section 1.4.7).

1.4.6 Current SNHL management strategies

Though a variety of medical and surgical interventions are available for the treatment of conductive hearing losses, there is still only a limited range of treatment options for SNHL (Kulkarni *et al.* 2008). However, for many causes of SNHL, effective preventative measures can be taken from the governmental to the personal level (see Table 1.5).

Table 1.5. Global prevention strategies for SNHL.
(based on Daniel 2007;Fransen *et al.* 2008;Olusanya *et al.* 2007).

Cause	*Interventions*
ARHL	Risk factor reduction e.g. smoking cessation and weight loss for overweight individuals
NIHL	Public health education to avoid exposure to excessive noise. Legislation to reduce noise exposure
Genetic	Genetic counselling and avoidance of consanguineous marriages
Drug- / Poison-induced (including solvents)	Medical and public health education to avoid exposure to ototoxic drugs and solvents
Infection	Immunisation, improved obstetric and neonatal care and prompt treatment
Hypoxia	Improved obstetric and neonatal care
Jaundice	Improved obstetric and neonatal care

SNHL has fallen in developed countries due to the implementation of some of these prevention strategies, especially improvements in neonatal care and vaccination. However, children in less developed countries have not benefited from these advances as they cannot access this care and rates of both acquired and genetic hearing loss (often due to consanguinity) are higher. Vaccination, better healthcare and genetic counselling is required to overcome these problems and, more importantly, prevent serious and potentially fatal infections (Smith *et al.* 2005).

Due to the irreplaceable nature of hair cells, however, such measures provide no benefit once SNHL is established. Therefore, treatment focuses on the development of management strategies such as lip-reading and signing along with amplification of incoming sounds to optimise input to remaining hair cells. Amplification is currently possible through three strategies: increasing the volume of sound reaching the inner ear, electrical stimulation of the cochlea and electrical stimulation of the brainstem (Kulkarni *et al.* 2008).

Amplification of sound to the inner ear is achieved through wearable hearing aids, bone-anchored hearing aids and middle ear implants. These interventions are aimed at patients with mild to severe hearing loss and rely on residual hearing to detect incoming sound. An increasing array of devices are becoming available for this and more digital hearing aids are being produced as these devices are able to perform signal processing to optimise signals in different auditory environments (Kulkarni *et al.* 2008).

Direct electrical stimulation of the cochlea in the form of cochlear implants has become increasingly refined over the last two decades and has greatly improved the treatment of severe to profound hearing loss that was previously treated by high-powered hearing aids (Ramsden *et al.* 2007). Cochlear implants work through an array of electrodes (usually 22) that are inserted into the scala tympani of the affected cochlea and present incoming sounds (received by an external microphone and transmitted transdermally to a speech processor) to the spiral ganglion cells and surviving dendrites by direct, tonotpic electrical stimulation (Kulkarni *et al.* 2008;Ramsden *et al.* 2007). Though originally used in adults, there has been a rapid move to early implantation because of improved neonatal hearing screening. Though it is unclear what the effect of early implantation will be, it is thought that the improvement in hearing provided by cochlear implants will cause hearing-impaired children's development to more closely match that of their peers and that this will not adversely affect family relationships (Moeller 2007;Smith *et al.* 2005). Unfortunately, due to their cost, cochlear implantation only remains a viable therapeutic option for patients in developed countries (Tarabichi *et al.* 2008).

The most recent intervention for the treatment of SNHL is the implantation of the electrode arrays that either stimulate the surface of the brainstem or use penetrating electrodes to stimulate brainstem nuclei. Such implants are used when the normal neural pathway from the cochlea is absent and, though they do not provide the same performance as cochlear implants, they aid in patients' ability to lip-read and recognise sentences (Kulkarni *et al.* 2008;Ramsden *et al.* 2007).

1.4.7 Future strategies in hearing loss

Future strategies will focus on reducing the incidence of hearing loss and on the creation of new treatments for SNHL. The former task will rely, for the most part, on making existing

preventative strategies more widely available whilst the latter is the focus of a large amount of scientific research.

Prevention and treatment of hearing loss in the developing world

Given that the largest cause of acquired SNHL in the developing world is infection, increased vaccination against rubella, *haemophilus influenzae* and *streptococcus pneumoniae* – most likely through the World Health Organization's global programme for vaccines – has the potential to greatly reduce the burden of hearing loss in these countries (Smith *et al.* 2005).

However, existing therapies for infection can also cause SNHL, particularly aminoglycoside antibiotics. Though these effective bactericidal drugs are the mainstay for the treatment of serious (usually gram-negative) infections due to their affordability and efficacy, the morbidity caused by aminoglycoside-induced SNHL is significant, particularly in China. As cheap alternatives for these antibiotics are not available, pharmaceutical hair cell protection by aspirin co-administration is being investigated. This strategy appears promising and the use of aspirin with other ototoxic drugs, such as cisplatin, is also being studied. However, it is uncertain whether the gastric side-effects of aspirin will outweigh any benefit and whether hair cell protection comes at the cost of drug efficacy (Rizzi *et al.* 2007;Rybak *et al.* 2007).

Other prominent causes of hearing loss in industrialised developing countries are noise and solvents. In developed countries, legislation to reduce exposure to noise and solvents in the workplace has shown a marked reduction in occupational hearing loss and the implementation of similar laws in developing countries is likely to have a similar effect (Tarabichi *et al.* 2008). Finally, increased provision of existing SNHL treatments in developing countries through global health strategies will provide benefit to a large population, the main impediment being cost.

New therapies for SNHL

Much work is going into identifying new methods to prevent hair cell loss and regenerate lost hair cells. As well as using existing drugs to protect hair cells from programmed cell death following an insult, new molecules are being trialled for their protective properties. For example, inhibitors of the JNK pathway, such as D-JNKI-1, have shown promise in protecting hair cells against damage due to noise and cochlear implant insertion in animal models (Eshraghi *et al.* 2006). Similarly, infusion of caspase inhibitors has shown promise in protecting against cisplatin ototoxicity (Rybak *et al.* 2007). Finally, antioxidants and free radical scavengers, which are presumed to work by reducing ROS in the cochlea following an insult such as cisplatin administration, have also shown promise in the prevention of SNHL in animal models. These molecules are thought to assist endogenous otoprotective

mechanisms and free radical scavengers to protect hair cells against damage from noise, drugs and age (Darrat *et al.* 2007;Rybak *et al.* 2007).

Though these strategies provide hope for a great reduction in hearing loss in the future, they cannot provide any benefit to those who already have SNHL due to hair cell loss. As avians and lower vertebrates are able to regenerate their hair cells following trauma such as aminoglycoside administration or noise (unlike mammals), there has been a drive to understand the mechanisms that mediate regeneration with a view to manipulating these pathways in mammalian support cells to induce hair cell regeneration (Cotanche 2008). Following hair cell loss in the chick basilar papilla (the chicken equivalent of the cochlea), hair cells are regenerated by two distinct pathways: transdifferentiation and proliferation. Initially transdifferentiation predominates. In this process, support cells upregulate genes involved in hair cell development and become hair cells. Later, support cells re-enter the cell cycle and mitose to form either two new hair cells, one hair cell and one support cell or, later, two support cells (Cotanche 2008;Matsui *et al.* 2005). Though the understanding of this process is progressing, the signals that initiate transdifferentiation and proliferation in the chick basilar papilla have yet to be identified and, therefore, it has not been possible to determine whether these signals can induce regeneration in the mammalian cochlea (Cotanche 2008). Furthermore, attempts to induce support cell differentiation using growth factors (e.g. FGF, IGF, BDNF, EGF and TGF) have had only limited success (Matsui *et al.* 2004a).

Therefore, current efforts to induce hair cell regeneration are focusing on more recent techniques such as gene therapy and transplantation (e.g. of stem cells). Gene therapy relies on the manipulation of gene expression in cochlear cells to correct genetic hearing loss, prevent hair cell loss or replace lost hair cells from residual cochlear cells. The correction of genetic hearing loss would most likely require an understanding of the mechanism of hair cell loss and, potentially, the creation of a specific therapy for each form of genetic deafness. Otoprotection would require the upregulation of protective genes such as *Ntf3* and *Bdnf* (which enhance spiral ganglion cell survival) and antioxidant enzymes such as Mn superoxide dismutase (Kesser *et al.* 2008;Pfister *et al.* 2007). Finally, strategies for regeneration, without knowledge of factors that trigger regeneration in avian and other systems, rely on upregulation of factors involved in hair cell specification such as ATOH1 (Cotanche 2008;Kesser *et al.* 2008;Pfister *et al.* 2007).

As well as there being limited knowledge of which factors to target, gene therapy faces challenges in terms of routes of application and gene transfer vectors. Much progress has been made in solving these problems in recent years. Many routes have been tested for the delivery of reagents to the inner ear (e.g. diffusion through the round window and injection at different sites), with detectable expression of transgenes being identified using many of

these techniques. However, the trauma caused by some of these delivery techniques may mean that they are not viable routes for the treatment of human hearing loss. Different gene transfer methods have also been intensely investigated, with adenovirus and adeno-associated virus showing the most promise. Furthermore, recent experiments have shown that adenoviral vectors are capable of transfecting human vestibular epithelia *in vitro*. However, initially promising *in vivo* results in non-primate laboratory animals have shown that there are still many obstacles to overcome in this field. For example, *Atoh1* overexpression by a viral transfection strategy is capable of inducing hair cell regeneration in the deafened cochlea (Izumikawa *et al.* 2005), however, trauma during delivery, cytotoxicity of transfection, misplacement of regenerated hair cells and degeneration of regenerated hair cells mean that such therapy still appears far from clinical applicability (Edge *et al.* 2008;Izumikawa *et al.* 2005).

The final novel and promising method proposed for the regeneration of hair cells is centred around the transplantation of stem cells to the cochlea. This method has both the potential to replace hair cells and to reform the cochlear microarchitecture which is eventually lost when hair cells die. Ideally, cells for transplantation would come from the patient in order to avoid host-versus-graft disease and the need for immunosuppression. However, xenografting (e.g. using porcine cells) or allografting (e.g. with stem cells derived from human foetal tissue) currently seem more realistic strategies as cells are more readily available for these purposes. The challenges faced in this field are similar to those in gene therapy (e.g. potential oncogenesis). Furthermore, the triggers that can induce full hair cell differentiation have yet to be identified and the targeting of stem cell delivery to desired sites is currently impossible (Chen *et al.* 2007;Rivolta 2007;Ulfendahl 2007).

Though much work remains to be done in order for the above methods to benefit SNHL patients, they remain viable strategies. Recent advances in retinal regeneration aid in the proof of many principals of sensory epithelial regeneration and lessons learned from this, and similar systems should aid the advancement of hair cell regeneration whilst protecting against some of the pitfalls of regenerative therapy (Enzmann *et al.* 2009).

1.5 Transcription factors and regulation of gene expression by POU4F3

The ability of cells to selectively express different genes from an identical genome underlies the large differences in cell type seen in individual organisms and allows cells to respond to external signals at the transcriptional level. This ability is primarily achieved through the interaction of gene regulatory proteins with DNA binding sites and non-DNA binding cofactors (Alberts *et al.* 2002). Both gene regulatory proteins and non-DNA binding cofactors are known as transcription factors as they both influence the rate of gene transcription though this term is usually used with reference to gene regulatory proteins and will be used as such with non-DNA binding proteins referred to as cofactors, coactivators or corepressors as appropriate.

In some cases, the relationship between the binding of transcription factors to DNA binding sites and the initiation of transcription is simple, acting as an on/off switch. However, this is rarely the case in eukaryotic gene promoters, which are DNA regions that are responsible for the control of transcription of a given gene. Promoters act as processors; integrating multiple inputs from regulatory transcription factors to determine the level of expression of the gene they control (Alberts *et al.* 2002). They can be present at a number of locations, though they are usually located 5' to the transcriptional start site (TSS) of the gene they control. Such promoters are classically composed of a core promoter (the minimum part of the promoter that is required for transcriptional initiation), proximal promoter and a distal promoter. These different regions contain binding sites that are recognised and bound by different transcription factors, which recognise them due to their sequence. Such binding sites vary in length though they are usually less than 20bp long (Alberts *et al.* 2002;Heintzman *et al.* 2007).

Epigenetic regulatory mechanisms also influence whether a transcription factor is able to bind the DNA. Various forms of DNA methylation prevent transcription factor binding whilst modification of chromatin packing, e.g. due to the modification of histones, can also inhibit or favour transcription factor binding (Alberts *et al.* 2002;Heintzman *et al.* 2007).

1.5.1 Transcription factor structure and function

Transcription factors typically contain a DNA binding domain and protein-protein interaction domains through which they mediate the regulation of their target genes. Through different forms of DNA binding domain, transcription factors are able to recognise diverse binding sites, usually by binding the major groove of the double helix and reading the outside of the nucleotides in this groove. As well as the individual code of the bases, the overall geometry of the helix can be recognised and other features of the DNA, e.g. the energy required to bend it, can also influence TF binding (Alberts *et al.* 2002).

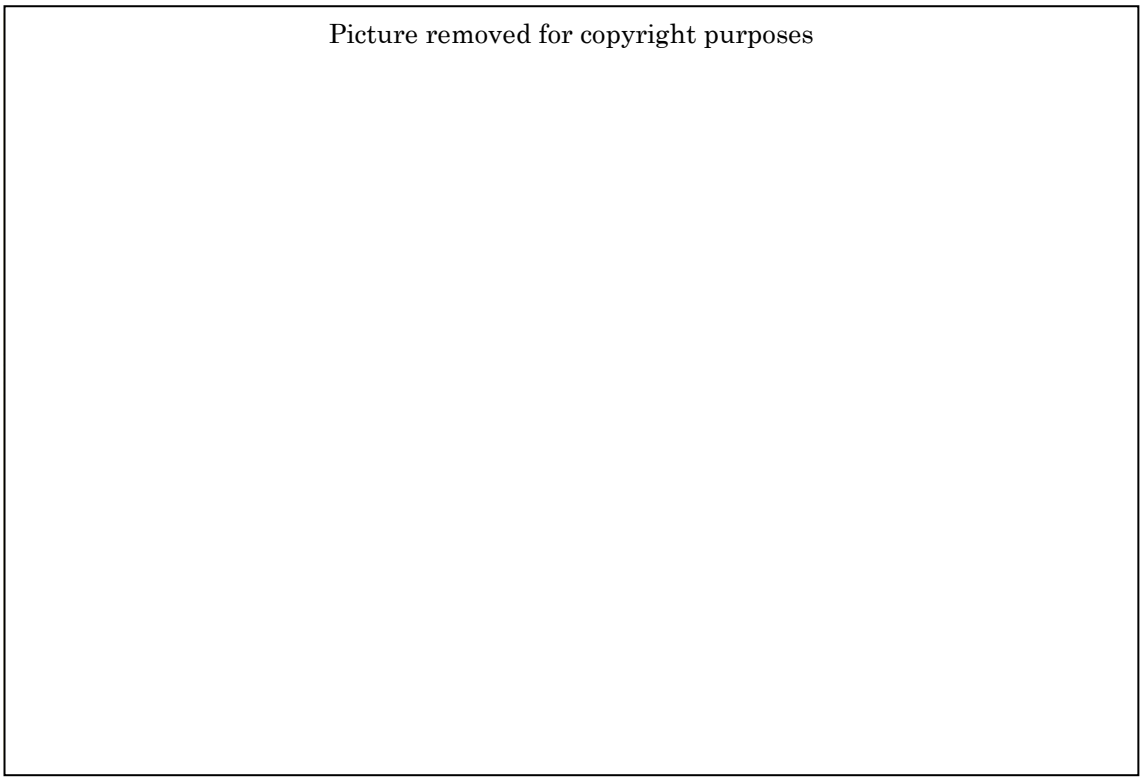

Figure 1.8. Interaction of transcription factors to initiate transcription.
The assembly of the RNApol II preinitiation complex on eukaryotic promoters. Transcription factors act on distal enhancers to increase the probability of assembly of the RNApol II complex on the core promoter via their interaction with general transcription factors (Krishnamurthy *et al.* 2009).

A number of different structures have evolved in order for transcription factors to bind DNA. These are the helix-turn helix, zinc finger, leucine zipper and helix-loop-helix domains. One of the most commonly occurring of these is the helix-turn-helix domain in which there are typically two alpha helices joined by a short amino acid chain (the turn). It is usually the helix nearer the C-terminal which binds DNA in the major groove (Alberts *et al.* 2002).

Once bound to the DNA, transcription factors can upregulate target gene transcription by recruiting cofactors to aid in the assembly of the RNA polymerase II (RNApol II) complex (e.g. coactivators and general transcription factors that form part of the RNApol II preinitiation complex). Transcription factors can also repress the transcription of target genes. In its most simple form, gene transcription can be downregulated by the binding of a transcription factor to a region that causes the binding site of an upregulatory transcription factor to become blocked. However, transcriptional repression is often more complicated and requires the recruitment of corepressors which downregulate target gene transcription by modifying chromatin or inhibiting RNApol II formation. The complexes formed between transcription factors, cofactors and transcriptional protein complexes are extremely large and, due to the ability of DNA to be remodelled to bring distant regions into close contact, enhancer elements can be located far from the core promoter that they influence (Figure 1.8) (Alberts *et al.* 2002;Krishnamurthy *et al.* 2009).

Typically, a group of transcription factors, acting proximal to the TSS, will be responsible for basal gene expression with this transcriptional control being modulated by numerous other transcription factors, acting distally. The effect of distally acting transcription factors may be weaker and these factors might only be expressed in special circumstances e.g. during oxidative stress (Heintzman *et al.* 2007).

1.5.2 The POU family

The POU family is named after the first members of the class to be identified: *Pit-1*, *Oct-1* and *Oct-2* (mammalian); and *Unc-86* (*C. elegans*) (Verrijzer *et al.* 1993). These transcription factors are members of the larger homeodomain family that is defined by the presence of a characteristic 60 amino acid helix-turn-helix DNA-binding domain – the homeodomain (Scott *et al.* 1989). The homeodomain contained in POU transcription factors is called the POU-homeodomain (POU_H) and comprises three alpha helices of which the second and third form a helix-turn-helix motif, and the third contacts the major groove (Verrijzer *et al.* 1993).

The POU_H is preceded by another DNA-binding domain that is 74-82 amino acids long and, as it is unique to POU factors, is called the POU specific (POU_S) domain (Verrijzer *et al.* 1993). The POU_S, which comprises four alpha helices, contacts the DNA with an extended form of the helix-turn-helix motif formed between helices two and three with helix three making contact with the major groove (Assa-Munt 1993). These two domains are joined by a linker that is poorly-conserved between family members and the three components described (POU_S, linker and POU_H) together form a region named the POU-domain (Verrijzer *et al.* 1993). It is thought that the complicated structure of this bipartite DNA-binding domain allows for fine control of DNA binding at binding sites in target gene promoters – typically octamers – which are asymmetrical due to the structure of the POU domain (Alberts *et al.* 2002;Aurora *et al.* 1992;Verrijzer *et al.* 1993). In support of this explanation, it has been shown that all three components of the POU domain contribute to the sequence-specificity of DNA binding (Aurora *et al.* 1992;Verrijzer *et al.* 1993).

Though POU family members tend to exist as monomers in solution, they have been shown to bind DNA both as monomers and dimers. Dimerisation, where it occurs, is thought to take place on the DNA, i.e. once a monomer has bound to a DNA binding site in a target gene promoter, and such interactions are mediated through the POU domain (Andersen *et al.* 2001;Aurora *et al.* 1992;Verrijzer *et al.* 1993). Once bound, POU family transcription factors are able to either upregulate or downregulate target genes. The type of regulation at a particular site is dependent on coregulators which interact with N- and C-terminally located transactivation domains in the POU protein as well as interacting with the homeodomain (Andersen *et al.* 2001).

The functional role of these transcription factors has since been investigated and they have been shown to be important in a variety of developmental and homeostatic functions. The main action of POU domain transcription factors is seen in neural cells of various kinds e.g. pituitary, neocortical and retinal with particular attention being given to their actions in embryonic development (He *et al.* 1989;Robertson 1988;Veenstra *et al.* 1997). In these cells, they regulate terminal cell proliferation, differentiation, migration and survival (Table 1.6) (Andersen *et al.* 2001).

Table 1.6. Functions of the original POU family genes.
(Andersen *et al.* 2001;McGhee *et al.* 1997;Robertson 1988).

Organism	*Transcription Factor*	*Localization*	*Function*
Mammalian	Pit-1	Pituitary Cells	GH, PRL, TSHβ, GHRHR and other pituitary marker activation
	Oct-1	Ubiquitous	Activates small nuclear RNA (snRNA) and histone H2B genes
	Oct-2	B-Lymphocytes, glia & neurons	Activates immunoglobulin genes
C. elegans	Unc-86	Neuroblast Cells	Fate specification of neural cells

A large array of POU family genes have now been identified and divided into subfamilies (POU1 to POU6) based on their homology in the POU domain (Andersen *et al.* 2001;He *et al.* 1989;Verrijzer *et al.* 1993). The POU4 family (POU4F) is one of these subfamilies and the first member of this group to be identified was *Pou4f1* (also known as Brn-3a and Brn-3.0) which is involved in gene regulation in sensory neurons and is required for differentiation and survival of certain sensory and autonomic neurons (Andersen *et al.* 2001;He *et al.* 1989). *Pou4f2* (also known as Brn-3b and Brn-3.2) was identified soon after and shown to be expressed in the central nervous system and retina (Lillycrop *et al.* 1992;Xiang *et al.* 1993). Finally, *Pou4f3* (also known as Brn-3c or Brn-3.1) was identified from a cDNA library and localised to mouse chromosome 18 (Gerrero *et al.* 1993;Ninkina *et al.* 1993;Xia *et al.* 1993). The POU4F factors are highly conserved and the human POU4F proteins share 98% amino acid similarity to their corresponding murine genes (Xiang *et al.* 1995).

Pou4f3 was found to have limited expression in the rat central and peripheral nervous system beginning at around E13. By adulthood, its expression had reduced to undetectable levels in the mouse brain (Gerrero *et al.* 1993;Ninkina *et al.* 1993;Theil *et al.* 1993). In the spinal cord, it was inferred that POU4F3 was present in mechanosensitive sensory neurons due to labelling of cells in lamina 4/5 of rat spinal cord by *in situ* hybridization (the authors could not identify exactly which cell types had been stained). It was also present in the trigeminal and dorsal root ganglia (Erkman *et al.* 1996;Ninkina *et al.* 1993). Finally, it was found to be expressed in retinal ganglion cells and in the inner ear (Erkman *et al.* 1996;Xiang *et al.* 1995). Though the role of *Pou4f3* in the nervous system and retina has received little attention, its expression pattern in the inner ear has prompted much work.

POU4F3 was shown to be uniquely expressed in hair cells of the inner ear, beginning in the basal cochlea and extending to include all the hair cells of both the cochlear and vestibular sensory epithelia (see Figure 1.9*a*) (Erkman *et al.* 1996;Raz *et al.* 1999;Xiang *et al.* 1997). The onset of this expression, in mice, was found to be as early as E12.5 in postmitotic nascent hair cells (Xiang *et al.* 1998) and no other POU4F members are expressed in hair cells (Erkman *et al.* 1996;Ryan 1997). Two knockout mice, one spontaneous *Pou4f3* mutant mouse and three human families with *POU4F3* mutations have since revealed that *Pou4f3* is required for the terminal maturation and survival of hair cells (sections 1.5.3 and 1.5.4 respectively) (Collin *et al.* 2008;de Heer *et al.* 2009;Erkman *et al.* 1996;Hertzano *et al.* 2004;Vahava *et al.* 1998;Xiang *et al.* 1998;Xiang *et al.* 1997).

1.5.3 The role of Pou4f3 in hair cell development in rodents

The expression of POU4F3 in the inner ears of mice and rats has been investigated from embryonic to adult ages. Its expression begins at E12.5 in the otic vesicle, soon after *Atoh1* and before the hair cell specific myosins VI and VIIa at E13.5. It is accepted to be restricted to postmitotic cells. However, interpretation of results showing this and similar results for other proteins is complicated by a lack of consistency and information in reporting the region of the developing inner ear analysed (e.g. Chen *et al.* 2002;Xiang *et al.* 1998).

In the developing cochlea, *Pou4f3* expression begins in the base (see Figure 1.9*a*) (Erkman *et al.* 1996;Raz *et al.* 1999) and extends to include all hair cells of the inner ear by birth, following the wave of hair cell differentiation. Once present, POU4F3 expression is thought to be maintained at a high level in the hair cells of the inner ear throughout adulthood, though direct evidence of this is lacking (Erkman *et al.* 1996;Raz *et al.* 1999;Ryan 1997;Xiang *et al.* 1998;Xiang *et al.* 1997). There has been no report of a basal-to-apical gradient of POU4F3 expression in the late postnatal or adult organ of Corti.

The role of *Pou4f3* in hair cell development and maintenance has been clarified by three *Pou4f3* mutant mice (a fourth mouse was created to investigate the role of *Pou4f3* in retinal ganglion cell axon outgrowth and is therefore beyond the scope of this thesis (Wang *et al.* 2002)). Erkman *et al.* produced the first reported *Pou4f3* knockout mouse by creating a null mutation at the gene locus which removed the entire protein coding region. Heterozygous animals were normal, but homozygous knockout mice (*Pou4f3*$^{-/-}$) had severe deficits in balance, coordination and autonomic response to vestibular stimuli, with hyperactivity (by 5-6) weeks and complete deafness (Erkman *et al.* 1996;Murakami *et al.* 2002). This was shown to be due to a lack of differentiated hair cells in the early postnatal period and was followed by deterioration of the morphology of the organ of Corti and spiral ganglion neurons (Erkman *et al.* 1996).

Picture removed for copyright purposes

Picture removed for copyright purposes

Picture removed for copyright purposes

Picture removed for copyright purposes

Figure 1.9. The role of POU4F3 in hair cell development.
a) *Pou4f3* mRNA in the E18 rat (taken from Figure 3 in Erkman *et al.* 1996) and E12 mouse (taken from Figure 7 in Raz *et al.* 1999) cochlea showing a basal-to-apical wave of expression consistent with the wave of hair cell differentiation. *b*) Though *Pou4f3* heterozygotes display normal hair cell morphology (including hair bundle formation), *Pou4f3*$^{-/-}$ mice display a complete lack of hair cells. *Scale bars*, 10µm (taken from Figure 4 in Xiang *et al.* 1997). Though myosin VIIa-expressing cells are seen in the P2 mouse organ of Corti (*c*), these cells do not properly migrate to the lumen of the sensory epithelium, nor do they develop normal hair cell morphology. *Co*, cochlea (taken from Figure 5 in Xiang *et al.* 1998). *d*) Radial neuron bundle density is reduced in the 6-month-old *Pou4f3*$^{-/-}$ mouse organ of Corti, though there is some retention of innervation (taken from Figure 7 in Xiang *et al.* 2003).

A knockout mouse was also created by Xiang *et al.* in which all of exon one and most of exon two of the *Pou4f3* gene were deleted by homologous recombination. Again, heterozygous mice showed a normal phenotype. Knockout mice, however, showed circling behaviour with reduced weight and fertility when compared to wild type mice. The deficits seen were thought to be due to the increased energy expenditure that arises due to circling behaviour. These knockout mice were also completely deaf and showed a marked balance deficit (Xiang *et al.* 1997). Histological investigation again revealed that the deafness and balance deficits seen are caused by a severe loss of hair cells (see Figure 1.9*b*). Though mature hair cells are not seen, nascent hair cells are produced in the developing organ of Corti of knockout mice (see Figure 1.9*c*). However, these cells (which express the hair cell markers myosin VI and VIIa, calretinin and parvalbumin) never develop mature hair cell morphology and undergo apoptosis in the late embryonic and early postnatal inner ear resulting in near complete loss by P5, supporting a role for POU4F3 in hair cell survival (Xiang *et al.* 2003;Xiang *et al.* 1998;Xiang *et al.* 1997). At P7/8, only 1% of nascent hair cells remain in the cochlea and 20% remain in the vestibular sensory epithelia (Xiang *et al.* 2003). These results support the suggestion of Raz *et al.* that more than one pathway may be involved in hair cell differentiation (Raz *et al.* 1999).

The final *Pou4f3* mutant mouse to be reported is the dreidel mouse (Hertzano *et al.* 2004). This mouse has a spontaneous dinucleotide deletion in the *Pou4f3* coding sequence, upstream of the POU domain (reported as c.388_389delTG). This mutation was predicted to result in a truncated, non-functional protein. Dreidel homozygous mice display a similar phenotype to other *Pou4f3* mutant mice with vertical head tossing, circling and hyper-reactivity combined with a hearing loss (ABR threshold >100dB SPL). As in the other mouse mutants, the phenotype observed is a result of hair cell degeneration and, though hair cell loss in dreidel homozygous mice is severe, it appears less severe than that of the other two *Pou4f3* knockout mice whose inner ear morphology has been reported (Erkman *et al.* 1996;Hertzano *et al.* 2004;Xiang *et al.* 1998;Xiang *et al.* 1997).

As well as hair cell degeneration, neuronal loss has been noted in the inner ears of *Pou4f3* knockout mice. The spiral ganglia of *Pou4f3*$^{-/-}$ mice show minimal neuronal loss at E17.5 and appear normal up to P0. From P1-4 onwards, however, there is a clear reduction in the number of spiral ganglion neurons and, by P14, most spiral ganglion and vestibular ganglion neurons have degenerated with synapses on type I hair cells being markedly reduced (Erkman *et al.* 1996;Xiang *et al.* 2003;Xiang *et al.* 1997). In fact, vestibular ganglion neuron degeneration appears to begin earlier than spiral ganglion neuron degeneration with a significant reduction in vestibular ganglion size by E16.5. The deterioration of spiral and vestibular ganglia was shown to be due to an increased rate of apoptosis in the late embryonic and early postnatal periods (Xiang *et al.* 1998). In the cochlea, there is a consequent disruption in both afferent and efferent innervation with

particular disruption in the outer hair cell region. By six months, very little innervation remains in the inner ear apart from in the cochlear apex where it appears that some fibres can remain despite the lack of mature hair cells (see Figure 1.9*d*) (Xiang *et al.* 2003).

As support cells and neurons do not express *Pou4f3*, it is most likely that their deterioration is secondary to a lack of trophic support from mature hair cells (Erkman *et al.* 1996;Xiang *et al.* 2003;Xiang *et al.* 1998;Xiang *et al.* 1997). However, the pattern of neuronal loss in *Pou4f3*$^{-/-}$ mice does not match that of any single neurotrophic factor knockout mouse (Xiang *et al.* 2003). Nonetheless, POU4F3 has been shown to upregulate the expression of the neurotrophic factors brain-derived neurotrophic factor (*Bdnf*) and neurotrophin 3 (*Ntf3* also known as NT-3) and it is possible that the combined reduction of expression of these two factors contributes to the phenotype seen (Clough *et al.* 2004;Xiang *et al.* 2003) (See section 1.5.5).

1.5.4 The role of POU4F3 in hair cell maintenance

Given that *Pou4f3* was found to be expressed in adult rodent hair cells, it was suggested that it might play a role in maintaining hair cells and promoting their survival (Ryan 1997). Furthermore, given that POU4F3 is able to upregulate the neurotrophins BDNF and NT-3 (Clough *et al.* 2004), it may be required for the maintenance of innervation of hair cells or for the trophic support of neighbouring cells.

Evidence for such a role has been provided by three human families. In these families, individuals who are heterozygous for one of three disease-causing *POU4F3* mutations display a late onset, dominant and progressive non-syndromic hearing loss (DFNA15) (see Figure 1.10*a*) (Collin *et al.* 2008;Vahava *et al.* 1998). The first family to be identified was an Israeli Jewish family (family H) in which hearing loss begins the ages of 18 and 30 years and progresses to a moderate to severe hearing loss by age 50 with complete penetrance in affected individuals by the age of 40. Following linkage analysis, precise identification of the genomic location of *Pou4f3* and sequencing, the investigators identified an eight base-pair deletion in the protein coding region. This deletion causes a frameshift that was shown (*in vitro*) to cause a truncation of the resulting protein due to a premature stop codon. Prior to the stop codon, four amino acid residues are also mutated (Collin *et al.* 2008;Vahava *et al.* 1998).

A detailed audiological evaluation of members of family H revealed bilateral, sensorineural and progressive deafness with variable audiogram configuration (see Figure 1.10*b*). Furthermore, OAE testing of affected individuals confirmed OHC dysfunction and ABR testing revealed a normal central auditory pathway, supporting the hypothesis that hearing loss in this family is due to hair cell loss and that POU4F3 is required for hair cell maintenance (Frydman *et al.* 2000).

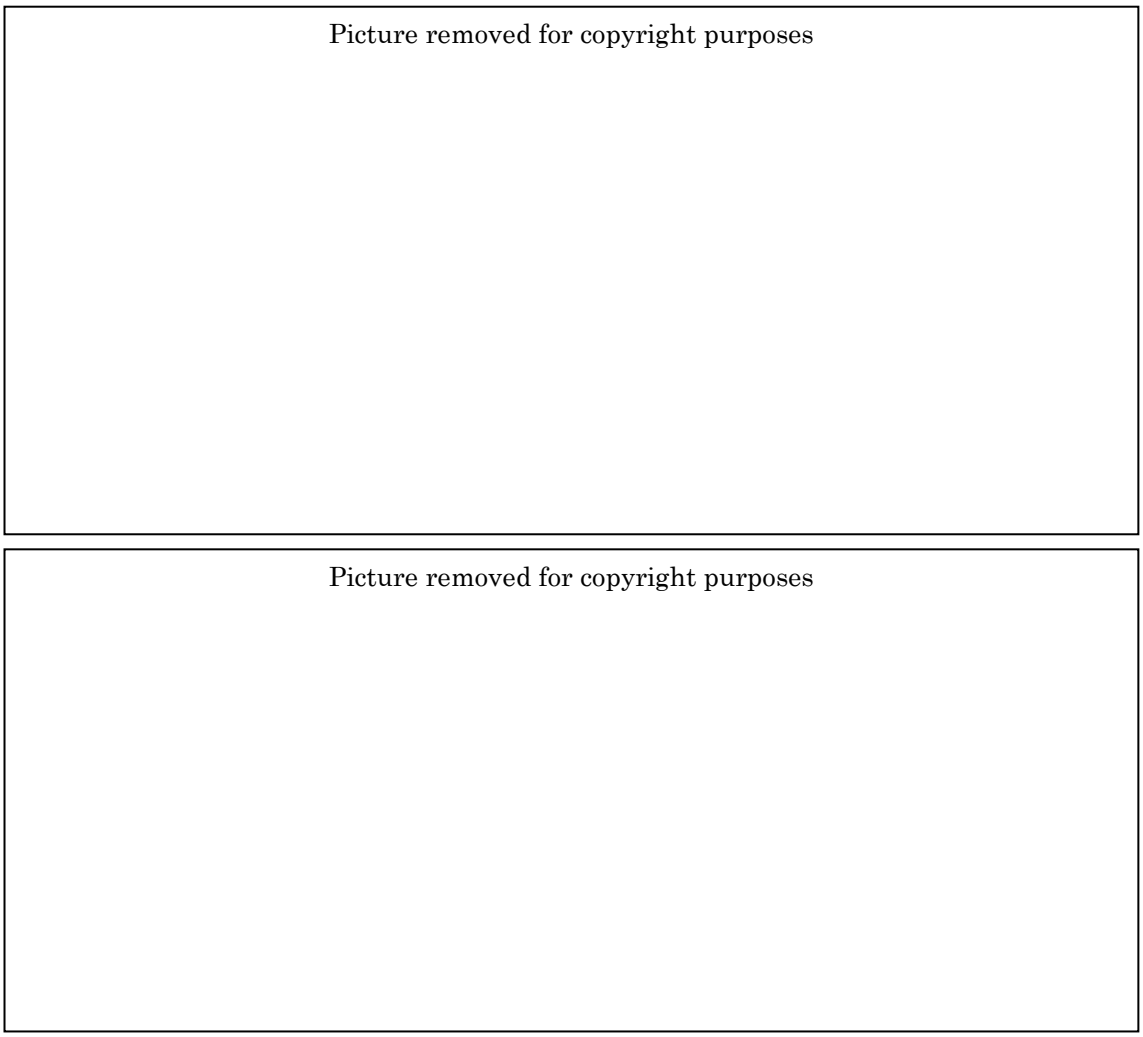

Figure 1.10. DFNA15 caused by *POU4F3* mutation.
POU4F3 mutation has been shown to be the cause of DFNA15 in three human families. The mode of inheritance has been shown to be autosomal dominant (*a*) (taken from Figure 1 in Pauw *et al.* 2008). Though audiograms in affected individuals are not sufficiently characteristic to aid diagnosis, affected individuals typically demonstrate flat or gently downsloping audiograms (*b*) (taken from Figure 1 in Vahava *et al.* 1998).

For a decade, family H was the only known family with hearing loss due to *POU4F3* mutation. However, two Dutch families have recently been identified to have missense *POU4F3* mutations which, like in family H, result in non-syndromic autosomal dominant hearing impairment. In the first of these two families (family W05-549), investigators identified c.865C>T which is predicted to result in L289F (where 1 is the initiator methionine) (Collin *et al.* 2008). Hearing loss in family W05-549 is self-reported to begin from childhood to the age of 60 years (mean age of onset was 35 years) with most patients exhibiting an early adult to midlife onset. Again, the mutation was fully penetrant with most individuals showing flat or gently downsloping audiogram configurations (however, other configurations were also observed). These audiograms were comparable to those seen for family H (see Figure 1.10*b*), though the rate of progression and severity of hearing loss

at different ages was shown to vary between family H and family W05-549 (Pauw 2008). Interestingly, the authors comment that speech recognition in family W05-059 is relatively preserved compared to audiogram severity. This may be due to loss of OHCs with relatively preserved IHC function as is the case for other deafnesses, which show preservation of speech recognition scores compared to pure-tone audiometry (Pauw *et al.* 2008). Furthermore, nearly all members of this family (28 of the 30 living family W05-059 members) display vestibular deficits. These deficits are highly variable and do not correlate to gender, tinnitus or degree of hearing impairment. Vestibular involvement cannot be excluded from family H as it was not tested (van Drunen *et al.* 2009).

Most recently, the audiometric and vestibular characterisation of a family with a c.668T>C mutation in the POU4F3 POUs domain, resulting in L223P, has been carried out (Collin *et al.* 2008;de Heer *et al.* 2009). This family again displays an autosomal dominant late onset hearing loss with onset most often in early adulthood and with a flat or gently downsloping audiogram. Good speech recognition scores were again reported (though these results were not subjected to statistical analysis) (de Heer *et al.* 2009) and the phenotype of this family was reported to be milder than that of the other two families reported (de Heer *et al.* 2009;Frydman *et al.* 2000;Pauw *et al.* 2008). This is likely to correlate with milder impairment of L223P mutant POU4F3 function compared to L289F as reported in molecular studies of the DNA binding and transactivation capability of these mutants (Collin *et al.* 2008).

One of the challenges faced by clinicians in this field is the identification of the cause of hearing loss in their patients. As more therapies become available, this will become increasingly important. Unfortunately, according to the evidence above, there is no clear phenotype-genotype correlation for DFNA15. Though many patients display flat or gently downsloping audiograms with good speech recognition scores relative to pure tone audiometry scores, there are also affected individuals with very different results and vestibular dysfunction appears to vary greatly depending on the disease causing mutation (Collin *et al.* 2008;de Heer *et al.* 2009;Frydman *et al.* 2000;Pauw *et al.* 2008;Vahava *et al.* 1998;van Drunen *et al.* 2009). It is possible that this variation is due to confounding factors, however, no such factors have yet been identified, making the future identification of affected individuals and families difficult. As Collin *et al.* suggest, the recent identification of the two Dutch families with *POU4F3* mutations may reflect a higher prevalence of DFNA15 than previously thought. Therefore, they suggest routine screening of the small *POU4F3* gene as part of a battery of diagnostic tests for deafness in certain populations appears reasonable (Collin *et al.* 2008). However, a more comprehensive study of the prevalence of DFNA15 in different populations would be required before the cost-effectiveness of such a strategy could be determined.

As well as the genotypes and phenotypes of DFNA15 patients, the likely mechanisms of the three disease-causing POU4F3 mutations have also been investigated. All three mutations are predicted to cause amino acid substitution or peptide truncation in the POU domain of POU4F3 (Collin *et al.* 2008;Vahava *et al.* 1998). In family H, the four residue mutation and truncation is found in the POU_H (at the end of the first of three alpha helices that form this subdomain), as is the L289F mutation of family W05-059 (which is in the third alpha helix) (Collin *et al.* 2008;Vahava *et al.* 1998;Weiss *et al.* 2003). L223P, on the other hand, causes its substitution in the POU_S (adjacent to the start of the third of four alpha helices in this subdomain) (Collin *et al.* 2008). The effect of these mutations on DNA binding, transactivation and nuclear localization have since been investigated. As expected for mutations in the POU domain, all three mutations cause deficits in DNA binding and transactivation with L223P appearing to cause the smallest deficit (Collin *et al.* 2008;Weiss *et al.* 2003). Weiss *et al.* investigated the effect of the original mutation on protein localization and identified one bipartite nuclear localization signal (NLS) which is disrupted in the truncated protein and one monopartite NLS. Protein localization has since been investigated for L223P and L289F. Though neither of these mutations are predicted to affect either NLS (as the eight base-pair deletion in family H does), they both cause transfected cells to show a degree of cytoplasmic POU4F3 expression (Collin *et al.* 2008;Vahava *et al.* 1998;Weiss *et al.* 2003), suggesting that they may interfere with the known NLSs or that they disrupt/interfere with unknown NLSs in POU4F3.

Given the impediments to obtaining and manipulating human inner ear tissue (see section 1.6.1), alternative methods have been used to try to elucidate the mechanism by which *POU4F3* heterozygosity causes hearing loss. Four hypotheses may explain deafness in human heterozygous individuals with a mutation in the POU domain of *POU4F3*. The first of these is a dominant negative effect whereby mutant POU4F3 dimerises with wild type POU4F3 or other proteins to inhibit or otherwise alter their function; the second is that the mutation causes a gain of function which results in mutant POU4F3 binding to new DNA sequences; the third is that mutant POU4F3 might somehow trigger cell death; and the fourth is haploinsufficiency.

Following the identification of family H, *Pou4f3*$^{+/-}$ mice (Erkman *et al.* 1996) were aged to 24 months in order to identify which of the above mechanisms might explain DFNA15 (Keithley *et al.* 1999). However, these mice did not show a greater ARHL than wild type controls. Given that the mouse strain used may not be a suitable model for investigating this form of hearing loss – one of the strains of the mixed background mouse used displays ARHL due to hair cell loss which may mask *Pou4f3*-related hearing loss despite wild type controls (Spongr *et al.* 1997), and many humans with *POU4F3* mutations do not display hearing loss until mid-life (Vahava *et al.* 1998) – *in vitro* models have provided more evidence of the mechanisms through which *POU4F3* mutations cause hearing loss. Firstly,

in vitro experiments show that a dominant negative effect is unlikely to underlie DFNA15. Without binding to DNA, the N-terminal domain of POU4F3 does not appear to bind cofactors and, if POU4F3 is capable of dimerisation, this is likely to be through the POU domain which is mutated in all three identified DFNA15-causing mutations (Collin *et al.* 2008;Sud *et al.* 2005;Vahava *et al.* 1998). Furthermore, mutant POU4F3 does not interfere with wild type POU4F3 transactivation *in vitro* (Weiss *et al.* 2003). The second hypothesis described (gain of function) is also unlikely to be correct as it is unlikely that the three different mutations identified could all cause such a similar gain of function (Collin *et al.* 2008;Vahava *et al.* 1998). Thirdly, Weiss *et al.* proposed that cytoplasmic accumulation of mutant POU4F3 may lead to hair cell death, though a potential mechanism by which this might occur has not been suggested (Weiss *et al.* 2003). Therefore, the most probable explanation of deafness due to *POU4F3* mutation currently appears to be haploinsufficiency, though it is difficult to prove this mechanism as *Pou4f3*$^{+/-}$ mice do not appear to be an appropriate model for DFNA15 (Keithley *et al.* 1999).

In summary, the three human families identified with mutations in the POU4F3 coding sequence causing DFNA15 have suggested that POU4F3 mutation causing deafness may not be as rare as first thought (Collin *et al.* 2008;Vahava *et al.* 1998). Furthermore, they support a life-long role for POU4F3 in maintaining hair cells and promoting their survival. Therefore, a greater understanding of the mechanism of POU4F3 function can not only provide potential strategies for prevention of DFNA15, but can also identify hair cell survival mechanisms which could be manipulated to prevent acquired hearing loss.

1.5.5 POU4F3 regulation, structure and function

The function of POU4F3 in hair cell development and maintenance is dependent on its regulation, structure and transcriptional environment. Regulation of *Pou4f3* is important for highly cell-specific expression whilst its structure and environment dictate its subcellular localization, DNA binding capability and target gene regulation. *Pou4f3* has been localized to chromosome 18 in the mouse (Xia *et al.* 1993) and rat and chromosome five in humans (Xiang *et al.* 1995). It is composed of two exons, with a similar structure to *Pou4f1*, and gives rise to only one transcript, which produces a 37kDa protein (Gerrero *et al.* 1993;Xiang *et al.* 1995). This is in contrast to its two family members, each of which has been shown to produce a long and short transcript with different functions (Theil *et al.* 1995;Theil *et al.* 1993).

Little is known of the factors that regulate *Pou4f3* in order to produce hair cell-specific expression in the inner ear. In an *in vivo* preparation of the chicken retina, the products of a number of genes have been associated with increased cBrn3c (Chicken *Pou4f3*) expression (*Cath5* (Chicken *Ath5*), *Math5* (Mouse *Ath5* / *Atoh7*), *Pou4f1*, *Pou4f2* and *Pou4f3*) though a direct mechanism of cBrn3c of upregulation has not been shown for these genes (Liu *et al.*

2001). Similarly, in cochlear cultures, POU4F3 expression has been shown to be dependent on retinoic acid signalling, without evidence for the mechanism of regulation, which may be indirect (Raz *et al.* 1999). Conversely, an NFAT-C/EBP composite element is able to regulate a recognition element in the *POU4F3* promoter (Yang *et al.* 2003) and an analysis of sequence variants at the *POU4F3* locus identified an SP family binding *cis*-regulatory element in the *POU4F3* 5' flanking region which may affect its regulation *in vitro* (Nolan *et al.* 2007). However, the significance of these relationships have not been studied *in vivo*. Further characterisation of these interactions is likely to help clarify the requirement of POU4F3 for hair cell survival and may identify polymorphisms associated with late onset hearing loss, particularly presbyacusis (Nolan *et al.* 2007).

The POU4F3 protein can be separated into two main domains. The first domain is the N-terminal activation domain, which encompasses the POU-IV box – a region of high homology between POU4F members (Gerrero *et al.* 1993). Similar to the N-terminal of POU4F1 (Budhram-Mahadeo *et al.* 1995;Theil *et al.* 1993), this N-terminal domain is involved in transactivation and appears to function following binding of POU4F3 to DNA, presumably through protein-protein interactions (Smith *et al.* 1998;Sud *et al.* 2005). The second domain in POU4F3 is the POU domain described above (see section 1.5.2) which is present in POU4F3 in its normal POU_S-linker-POU_H conformation (see Figure 1.11) (Gerrero *et al.* 1993;Ninkina *et al.* 1993).

The POU domain is highly conserved between POU4F members, showing approximately 95% sequence similarity with the greatest number of mismatches present in the linker region (see Figure 1.11*a*). The third helix of the POU_H (i.e. the helix that makes contact with the major groove (Verrijzer *et al.* 1993)) is fully conserved between mammalian POU4F members (Xiang *et al.* 1995). It was therefore predicted that POU4F members compete for the same DNA sequences when coexpressed (Xiang *et al.* 1995) and this is supported by experiments which show that POU4F3 can upregulate POU4F1 target genes (Budhram-Mahadeo *et al.* 1995;Smith *et al.* 1998). However, this is not the case in the organ of Corti as only POU4F3 is expressed in hair cells and, though POU4F DNA binding sites have been shown to be similar, there are subtle differences in sequence specificity between POU4F members (see Figure 1.11*c*) (Gruber *et al.* 1997;Xiang *et al.* 1995).

Picture removed for copyright purposes

Picture removed for copyright purposes

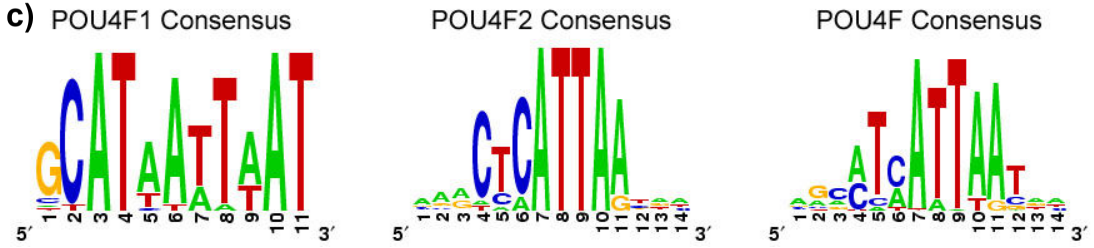

Figure 1.11. POU4F3 protein composition.
a) Alignment of POU4F1 and POU4F3. The amino acid sequences of POU4F1 and POU4F3 are shown with homologous residues *shaded*. The POU-IV box, POU_S and POU_H are *over lined*, indicating the conservation of these functionally important domains. The *arrow* indicates the splice junction that differentiates the long and short POU4F1 transcripts and is located between exons one and two in POU4F1 (adapted from Gerrero *et al.* 1993). *b*) POU4F3 protein domains (taken from Sud 2005). *c*) graphic representation of POU4F1 and POU4F2 consensus sequences from positional weight matrices and a combination of the two consensus sequences with position one of the combined sequence being equivalent to position -1 of the POU4F1 consensus and position 1 of the POU4F2 consensus (adapted from Gruber *et al.* 1997;Xiang *et al.* 1995). Sequences visualised using WebLogo (Crooks *et al.* 2004).

Although transactivation by POU factors, including POU4F1, can be mediated through the POU domain (Andersen *et al.* 2001;Budhram-Mahadeo *et al.* 1995), the isolated POU4F3 POU domain was not able to mediate transactivation when tested in an inner ear cell line (Sud *et al.* 2005) in contrast to its ability to upregulate a herpes simplex virus promoter in neuronal cells (ND7) (Liu *et al.* 2000). It was also thought that POU4F members, unlike other POU factors, were unable to dimerise through their POU domain (Andersen *et al.* 2001;Gruber *et al.* 1997), however, POU4F members are likely to form dimers on appropriate recognition elements as demonstrated by the dimerisation of the POU4F1 POU domain on a Brn-2 (POU3F2) consensus oligonucleotide; though they may also function as monomers (Rhee *et al.* 1998). No structural data are available for POU4F members and it is therefore unknown whether the POU_S and POU_H bind opposite DNA strands like Oct1 (Klemm *et al.* 1994) or the same strand, like Pit-1 (Jacobson *et al.* 1997).

As POU4F3 is only likely to affect target gene transcription when bound to DNA (Sud *et al.* 2005), its regulatory function is dependent on the presence of POU4F3 binding sites in target gene promoters. Furthermore, as shown by experiments with POU4F1 and POU4F2, the structure of the promoter, including the context and spacing of binding sites, can have an effect on transcriptional regulation (Dawson *et al.* 1996;Morris *et al.* 1996). Though no consensus sequence has been independently derived for POU4F3, consensus sequences for both POU4F2 (Xiang *et al.* 1995) and POU4F1 (Gruber *et al.* 1997) have been determined (see Figure 1.11*c*) and shown to be similar to those of Brn-2 (POU3F2) and Brn-5 (POU6F1) (Rhee *et al.* 1998). POU4F3 has been shown to have affinity for similar binding sites to its family members (Xiang *et al.* 1995), however, the affinity and transcriptional activity of POU4F3 at these sites has not been reported (binding affinity being a strong predictor of transcriptional activation for POU4F1 (Trieu *et al.* 1999)). Given the large amount of genomic sequence currently available (in stark contrast to the time that the above work was published), a greater understanding of POU4F3 affinity for these sites and the factors that determine its transcriptional function once bound will greatly aid in the identification and characterisation of POU4F3 target genes. However, targets discovered *in silico* may be biased to the existing consensus sequences. Therefore, unbiased identification of POU4F3 binding sites, e.g. by random oligonucleotide selection or chromatin immunoprecipitation, will greatly aid the accuracy of such experiments, as will feed back on the transcriptional effect of POU4F3 at predicted binding sites.

Though POU4F3 is known to be a transcription factor, few of its targets have been identified. Initially its regulatory function was investigated for known targets of POU4F1 in neuronal cells. POU4F3 was able to transactivate a number of POU4F1 target gene promoters (SNAP-25, α-internexin, synapsin three neurofilament subunits) (Budhram-Mahadeo *et al.* 1995;Morris *et al.* 1996;Smith *et al.* 1998). It was also shown to be capable of repressing one promoter (the α3 nicotinic acetylcholine receptor subunit gene promoter)

(Milton *et al.* 1996). However, the relevance of these interactions to hair cells is unclear as POU4F3 is able to regulate different promoters in different cell types (e.g. neuronal versus non-neuronal) (Clough *et al.* 2004;Smith *et al.* 1998;Sud *et al.* 2005). Though it was suggested that differences in regulation are due to the POU4F3 N-terminal activation domain only being active in neuronal cells (Smith *et al.* 1998), contradictory results were obtained using a more sensitive assay system (Sud *et al.* 2005). Furthermore, regulation by POU4F3, like regulation by other POU4F members, is likely to be influenced by the context of its binding sites (Budhram-Mahadeo *et al.* 1995;Dawson *et al.* 1996).

Since the demonstration of the requirement for POU4F3 in hair cell development and survival (Erkman *et al.* 1996;Vahava *et al.* 1998;Xiang *et al.* 1998;Xiang *et al.* 1997), the identification of POU4F3 target genes has focused on these cells. To date, the only proven directly upregulated targets of POU4F3 are the neurotrophins BDNF and NT-3, as demonstrated by DNAse footprinting, EMSA and luciferase assay (Clough *et al.* 2004) and, for BDNF, supported by microarray results in POU4F3 mutant mice (Hertzano *et al.* 2007). These genes are known to be required for maintenance of normal hair cell innervation by providing trophic support to neurons, and a role for POU4F3 in their expression *in vivo* is supported by the reduced expression of BDNF in immature hair cells in *Pou4f3*$^{-/-}$ mice (NT-3 expression does not appear to be markedly reduced) (Xiang *et al.* 2003). However, it is likely that BDNF expression in the developing inner ear is also influenced by additional factors, e.g. miR15a (Friedman *et al.* 2009a), as its expression does not closely match that of POU4F3 (Hertzano *et al.* 2007).

In addition to the above targets *Gfi* and *Lhx3* are strongly associated with POU4F3 expression. *Calbindin2* may also be associated with POU4F3 expression though very little evidence exists for this possible interaction (Hertzano *et al.* 2004;Hertzano *et al.* 2007). Both *Gfi1* and *Lhx3* were identified based on the microarray comparison of cDNAs present in wild type and *Pou4f3*$^{ddl/ddl}$ (homozygous dreidel mutant) whole inner ears and the expression of both genes seems to mirror that of *Pou4f3*, though *Lhx3* expression declines postnatally despite increased *Pou4f3* transcription (Hertzano *et al.* 2007). Subsequent RNA *in situ* hybridization and immunohistochemistry has revealed that both genes have hair cell-specific expression patterns in the inner ear. Though *Lhx* knockout does not affect hair cell development (Hertzano *et al.* 2007), *Gfi1* knockout results in OHC loss, which proceeds to total disruption of the organ of Corti by P14, demonstrating an important role for this presumed target of POU4F3 in hair cell development and maintenance (Wallis *et al.* 2003). However, the mechanism by which POU4F3 may upregulate these genes has not been reported, and there is, therefore, a lack of evidence to support direct regulation of *Gfi1* or *Lhx3* expression by POU4F3.

In summary, POU4F3 expression in the inner ear is essential for hair cell terminal differentiation and survival (Erkman *et al.* 1996;Xiang *et al.* 1998;Xiang *et al.* 1997) and little is known of the target genes through which it is able to generate and maintain the mature hair cell phenotype. In order to understand the mechanism of POU4F3 function, unknown targets must be identified and characterised. Furthermore, the mechanism through which POU4F3 regulates these genes is likely to be important in the identification of strategies to prevent hair cell loss in patients with *POU4F3* mutations as well as identifying new strategies in preventing hair cell loss in the general population due acquired hearing loss. However, such investigations face unique challenges posed by the complicated biology of the inner ear.

1.6 Investigation of inner ear biology

1.6.1 Difficulties of analysing inner ear biology

The inner ear is one of the most inaccessible organs in the mammalian body and the irreplaceable hair cells are surrounded by a complex and delicate microarchitecture that necessitates removal of the whole inner ear in order to use them for molecular biological investigation. As mammalian hair cells are mitotically quiescent and cannot be cultured, experiments rely on hair cells obtained from inner ears of laboratory animals; commonly mouse, rat or guinea pig. Many inner ears would be required to provide enough tissue for biochemical analyses given the low number of hair cells available per inner ear (approximately 20 000 depending on species (Slepecky 1996)) and many research techniques require the separation of hair cells from other cell types in order to yield meaningful results. Though the latter has been attempted with success (e.g. Zheng *et al.* 2000) in studies similar to the present one (see section 3.1), such techniques present differing challenges which could interfere with the identification of transcription factor target genes. The traditional techniques of enzymatic-, microdissection- and trituration-based hair cell isolation (see references in He *et al.* 2000) can cause damage to hair cells which may alter gene expression (this may be due to direct effects of enzymes, or mechanical damage). The main limitation, however, is the length of time required between sacrificing the animal and using the cells (e.g. the trypsinisation step in He *et al.* 2000 alone takes 15 minutes) which can affect gene expression. The more recent technique of laser capture microdissection for the isolation of inner ear hair cells (Anderson *et al.* 2007;Cristobal *et al.* 2004;Cristobal *et al.* 2005;Gao *et al.* 2007;Wu *et al.* 2008) circumvents the above problems and allows a reduction in the time between animal sacrifice and cell fixation by intracardial PFA infusion (Wu *et al.* 2008). However, as stated by De Preter *et al.* (De Preter *et al.* 2003), only small amounts of nucleic acids are obtained by LCM and the required staining protocols are not beneficial for RNA quality.

1.6.2 Utility of cell lines in inner ear research

Cell lines provide a method with which to circumvent many of the problems outlined above. Many cells can be rapidly generated and their contents are rapidly accessible for use in molecular biological experimentation. However, according to the desired application, the cell line used can be of pivotal importance and cell lines are often not suitable for the study of protein function as they do not express required proteins or are not in their required niche.

In investigating transcriptional regulation, the choice of cell type is particularly important given that the transcriptional environment can vary greatly and is a major determinant of cell phenotype. For example, POU4F3 is able to upregulate the SNAP-25 promoter in a neuronal cell line (ND7), but not in non-neuronal and inner ear sensory epithelial cell lines (BHK, UB/OC-1 and UB/OC-2) (Smith *et al.* 1998;Sud *et al.* 2005). Conversely, it is able to upregulate *Bdnf* and *Ntf3* promoters in UB/OC and BHK cell lines but not in ND7 cells (Clough *et al.* 2004). As these differences are likely to be due to differences present in the native tissue that these cells were derived from, the use of an inner ear cell line is likely to yield more physiologically relevant results in investigations of inner ear transcriptional regulation than other cell types (see section 3.1). However, as cultured cells do not precisely represent the cells of interest, it is possible that artefactual interactions will be discovered in these cells. Therefore, regulatory relationships identified in cell lines require supporting evidence from native tissue, where possible, to confirm and strengthen evidence for any interactions discovered.

1.7 Project aims

Hair cell loss due to different causes remains the principal cause of deafness. In turn, deafness is the most common sensory disability in the western world (Olusanya *et al.* 2007). Therefore, a method to replace hair cells, or prevent their loss, would benefit a large population. Unfortunately, no such methods exist and we remain reliant on prostheses such as hearing aids and cochlear implants to ameliorate hearing without improving and, in some cases, further damaging residual hearing (Kulkarni *et al.* 2008).

Though an increasing number of proteins are being shown to be expressed in hair cells, signalling networks within these cells remain poorly characterised and, until recently, very difficult to investigate. A greater understanding of these networks could potentially aid in a variety of therapeutic measures e.g. gene therapy, drug therapy, stem cell programming and growth factor therapy.

In my project, I took the POU4F3 transcription factor as a start-point from which to investigate the networks that it is likely to control given its essential role in hair cell differentiation and survival (Collin *et al.* 2008;Erkman *et al.* 1996;Vahava *et al.* 1998;Xiang

et al. 1998;Xiang *et al.* 1997). I investigated a pool of potential POU4F3 target genes, previously generated in our laboratory by a subtractive hybridization screen in UB/OC-2 cells, in order to determine whether these genes alter their expression in response to POU4F3 and whether they are directly regulated by POU4F3. I also aimed to investigate the physiological significance of any regulatory relationships *in vivo* by determining the expression patterns of selected newly identified POU4F3 target genes. Particular priority was given to genes that might be important in hair cell survival and might therefore be useful in preventing hair cell loss or promoting hair cell regeneration.

2

MATERIALS AND METHODS

NB *All water used is type III purified water unless otherwise stated.*
All chemicals were supplied by BDH, Invitrogen, Promega or Sigma-Aldrich unless otherwise stated.
Restriction endonucleases were purchased from Promega unless otherwise stated.
Where work has been carried out by other members of the laboratory, it is made clear in the text

2.1 Safety

2.1.1 Unsealed radioactive sources

All procedures using unsealed radioactive sources were conducted according to local regulations. Where possible, radioactive sources were used in a room designated for work with radioactive reagents and appropriate monitoring and personal dosimetry was carried out.

2.1.2 Genetically modified bacteria

Bacteria were manipulated and disposed of according to local regulations.

2.1.3 General

All procedures were carried out according to UCL safety regulations.

2.2 General equipment

Eppendorf

Centrifuges: 5417C, 5417R, 5804R, MiniSpin; Concentrator: 5301; Thermal cyclers: Mastercycler gradient, Mastercycler personal

Jenway

6305 UV/Vis Spectrophotometer

Luckham

R100 rotatest shaker

Millipore

Elix and Milli-Q® water purification system

Nanodrop®

ND-1000 spectrophotometer

New Brunswick Scientific

C2 incubator shaker

Sorvall

RC 5C plus centrifuge

Stuart Scientific

STR6 platform shaker

Techne

Dri-Block® DB-2D heat block

UVP

3UV™ Transilluminator; GelDoc-it imaging system

2.3 Stock solutions

Luria-Bertani broth (LB)

- 1% Tryptone (DUCHEFA)
- 0.5% Yeast extract (DUCHEFA)
- 0.17M NaCl

LB-Agar

- 98.5% LB
- 1.5% Micro Agar (DUCHEFA)

PBS pH 7.4 at 25°C (Sigma-Aldrich)

- 0.01M phosphate buffer
- 0.0027M potassium chloride
- 0.137M sodium chloride

50x TAE

- 2M Tris
- 1M Glacial acetic acid
- 50mM EDTA pH 8.0

2.4 BLAST analysis of subtractive hybridization clones

cDNA clones that had been produced by the subtractive hybridization screen were sent for sequencing by members of the laboratory. The sequences generated from this analysis contained adaptor sequences that had been used to amplify and clone differentially expressed transcripts from the subtractive hybridization screen into the pGEM-T® Easy vector. The sequences of these adaptors were therefore aligned with the sequenced data from the subtractive hybridization clones using the 'pairwise alignment' function of the BioEdit software package (a modified Smith-Waterman alignment algorithm) or manually and then deleted from the sequence data if present (Hall 2007;Hall 1999). This edited sequence data was copied to a text file and annotated in FASTA format for each gene. In order to identify genes corresponding to the cDNA sequences, these files were used to query the Ensembl mouse cDNA database by nucleotide-nucleotide BLASTN analysis using the WU BLAST 2.0 software package through the Ensembl website (Ensembl 2008a;Gish 2004). The algorithm for near-exact matches was used to identify genes that corresponded to the

cDNA sequences in order to minimise type 2 error. If significant alignments were found for a given sequence, the most significantly aligned gene was taken to be the corresponding gene for that sequence. Sequences that had no significant matches ($p < 0.05$) were re-analysed using mouse genomic database and discarded if no significant matches were identified. Subsequent analysis of these matches is described in section 3.2.

2.5 Cell culture

2.5.1 Equipment for cell culture

ALC

PK10 centrifuge

Binder

WTC tissue culture incubator

Kendro

Heraeus HeraSafe KS safety cabinet; Heraeus HeraCell 150 tissue culture incubator

Nikon

Eclipse TS100 microscope

2.5.2 University of Bristol organ of Corti-1 (UB/OC-1) and UB/OC-2 cells

UB/OC-1 and UB/OC-2 cells — developmental inner ear sensory epithelial cell lines — were cultured in Eagle minimum essential medium supplemented with L-Glutamine, 10% heat-inactivated foetal bovine serum and 50U/ml γ-interferon in a 33ºC incubator with 5% carbon dioxide (Rivolta *et al.* 1998a). Cells were passaged by trypsinisation with 1% trypsin in 5mM HEPES-buffered Hanks' balanced salt solution followed by centrifugation at 1000rpm for 3 minutes, resuspension in culture medium (described above) and seeding at approximately 1-2 x 10^5 cells per 75cm^2 flask.

2.5.3 Baby hamster kidney -21 (BHK-21) cells

BHK-21 cells were cultured in Dulbecco's modified Eagle medium supplemented with 10% heat-inactivated foetal bovine serum in a 37ºC incubator with 5% carbon dioxide. Cells were seeded and passaged as for UB/OC-1 & -2 cells.

2.5.4 ND7 cells

ND7 cells — a sensory-neuronal / neuroblastoma hybrid cell line (Wood *et al.* 1990) — were cultured in L-glutamine-containing L-15 media supplemented with 10% heat-inactivated foetal bovine serum, 0.32% sodium bicarbonate, 0.25% glucose and 0.85% penicillin-streptomycin. Cells were incubated at 37ºC, 5% carbon dioxide, seeded at approximately 1-2 x 10^5 cells per 75cm^2 flask and passaged by mechanical dissociation.

2.6 General DNA manipulation

2.6.1 Plasmid DNA purification

Where plasmid DNA has been used, it has been purified using the MiniPrep kit (Qiagen) spin method or the MidiPrep kit (Qiagen) spin method:

MiniPrep

Bacteria (typically XL1-Blue cells (Stratagene) or JM109 cells (Promega)) were cultured in 2ml LB containing 1x ampicillin (100µg/ml) for 8 hours or in 5ml LB + 1x ampicillin (100µg/ml) for 16 hours. 1.5ml of broth was centrifuged in a 1.5ml microcentrifuge tube at 3000rpm for 2 minutes at 4°C. The bacterial pellet was resuspended and DNA was purified according to the manufacturer's instructions. Typically, the column (used to bind and wash the DNA) was dried on a heat block for two minutes at 50°C following the final ethanol ('Buffer PE') wash and DNA was eluted in 50µl water.

MidiPrep

Bacteria (typically XL1-Blue (Stratagene) or JM109 (Promega) cells) were cultured in 50ml LB containing 1x ampicillin (100µg/ml) for 16 hours. The full culture was typically centrifuged at 4000rpm for 20 minutes at 4°C and the pellet was processed according to the manufacturer's protocol apart from the second centrifugation step which was replaced by the filtration of the supernatant from the first centrifugation step through a cloth filter. DNA was typically resuspended in 200µl water and its concentration was determined as explained in section 2.11.4 or using a Nanodrop® ND-1000 spectrophotometer.

2.6.2 Digestion of DNA by restriction endonucleases

Typically, 1µg plasmid DNA was digested with 10 units of restriction endonuclease with the appropriate buffer at 1x concentration in a final volume of 30µl made up with water. 1 hour at 37°C was sufficient to ensure complete digestion.

2.6.3 Agarose gel electrophoresis

Typically, 0.5-1µg DNA was electrophoresed on a 1-1.5% agarose gel containing 0.01% ethidium bromide at approximately 80mA for 45 minutes. The gel was then visualised and electrophoresed further if necessary. Exposure to the ultra-violet light of the visualiser was minimised if the integrity of the DNA sequence needed to be maintained as the UV light is mutagenic.

2.6.4 Extraction of DNA from agarose gel

DNA for extraction was electrophoresed in a low melting point agarose gel of appropriate percentage (typically 1%). The required band was cut out using a scalpel under UV illumination and the DNA from the band was extracted using the MinElute kit (Qiagen)

(for bands of >70bp and <4kb) or using the Gel Extraction kit (Qiagen) according to the manufacturer's instructions.

2.6.5 DNA ligations

DNA ligation was carried out either by the TA method or using T4 DNA ligase.

TA method

PCR amplicons which had been amplified using a polymerase that leaves un-paired adenine residues at the 3' ends (typically GoTaq (Promega)) were ligated into the pDrive cloning vector according to the manufacturer's instructions (PCR Cloning kit (Qiagen)). The ligation typically proceeded for 3 hours at room temperature or 16 hours at 16°C.

T4 DNA ligase method

The following mixture was typically used for DNA ligations for both blunt- and sticky-ended inserts though blunt-ended ligations were usually attempted at more than one vector:insert ratio:

- 1µl T4 DNA ligase (Promega)
- 1µl Linearised Vector
- 3µl Insert
- 5µl 2x T4 DNA ligase buffer (Promega)

Ligations were typically incubated for 16 hours at 16°C.

2.6.6 Transformation of competent bacteria

Chemically competent XL1-Blue (Stratagene) bacteria of transformation efficiency of >1 x 10^5 cfu/µg DNA/100µl competent cells (for subcloning applications) or >1 x 10^5 cfu/µg DNA/100µl (for transformation of purified circular DNA) were thawed on ice and aliquoted into 1.5mL microcentrifuge tubes on ice. To each aliquot, no more than 5µl of ligation mixture was added (typically the maximum amount was used). The reaction was incubated on ice for a minimum of 45 minutes followed by a two minute heat shock at 42°C. 500µl LB was then added and the cells were incubated for 30 minutes in a shaking incubator at 230 rotations per minute prior to being spread onto LB-Agar plates and incubated upside-down at 37°C for 16 hours in an oven. Colonies were picked either the following morning (for MiniPreps from 2mL cultures) or stored at 4°C and picked in the evening (for MiniPreps from 5mL cultures or MidiPreps from 50mL cultures) using a 1-200µl pipette tip and incubated for 8 or 16 hours respectively prior to DNA purification.

2.7 Reverse Transcriptase Polymerase Chain Reaction (RT-PCR)

2.7.1 Equipment for RT-PCR agarose gel electrophoresis

Jencons

Mini-Plus horizontal electrophoresis unit

2.7.2 RT-PCR primer oligonucleotide design.

Table 2.1. PCR primer oligonucleotide design parameters.

Parameter	*Range*
Length	20-35bp
GC content	40-60%
Terminal nucleotide	C or G
Salt-adjusted melting temperature (T_m)	>60ºC
Single nucleotide repetitions	<3bp at 3' end of oligonucleotide
Hairpins	None with Oligocalc
Complementarity	None with Oligocalc
Self-annnealing	None with Oligocalc
Primer Dimers	<5bp match between primers
Amplicon length	>800bp, <1.5kb
Exon specificity	cDNA specific
BLAST results against appropriate genome	Ensured that Tm of non-specific interaction was at least 5ºC below that of the specific reaction

Primers were designed to be as sequence-specific as possible whilst maintaining optimal melting temperatures for PCR to minimise non-specific amplification (Table 2.1). This was done by ensuring that primers were of optimum length and GC content (for optimal melting temperature), checking for secondary structure potential within primer pairs and, finally, checking that the sequences to which the primers were designed were genomically unique. Furthermore, where possible, primer pairs were designed to differing exons in order differentiate – by size – between sequences amplified from cDNA and those amplified due to genomic DNA contamination. The amplicon was designed to be large enough to easily size-separate by agarose gel electrophoresis though small enough to not exceed the optimum range for the GoTaq polymerase (Promega) that was used. Furthermore, where possible, primers were designed to amplify target gene exons whose transcription in UB/OC-2 cells had been suggested by the results of the subtractive hybridization screen and subsequent BLAST analysis (for full details of individual primer sequences and properties, see Appendix).

2.7.3 RNA extraction and reverse transcription from UB/OC-2 cells

The RNeasy Mini kit (Qiagen) was used to extract RNA from a 75cm^2 tissue culture flask of approximately 90% confluent UB/OC-2 cells. The RNA was then reverse transcribed into cDNA using the Omniscript RT kit (Qiagen) according to the manufacturer's instructions.

2.7.4 PCR design and parameters

The following recipe was used for each reaction:

- 13.875µl water
- 5µl GoTaq Green Master Mix, 2X
- 2µl 25mM $MgCl_2$
- 1µl dNTPs (5mM each)
- 1µl sense primer
- 1µl antisense primer
- 1µl UB/OC-2 cell reverse transcribed cDNA (diluted to approx. 5ng/µl)
- 0.125µl GoTaq polymerase

The above samples were used in PCR with the following thermal cycler program:

1. 95°C 1 minute
2. 95°C 30 seconds
3. 64°C 30 seconds
4. 72°C 1 minute 20 seconds
5. REPEAT STEPS 2 TO 4 FOR 34 CYCLES
6. 72°C 10 minutes

Samples were then electrophoresed on a 1.5% agarose gel and visualised (see section 2.6.3).

2.8 Western blotting

2.8.1 Equipment for western blotting

Bio-Rad

Protean IIxI cell for PAGE

2.8.2 Reagents for whole cell protein extraction and western blotting

Lysis buffer

- 50mM Tris-HCl pH 7.9
- 50mM KCl
- 1mM EDTA
- 2mM DTT
- 1 tablet/10ml cOmplete mini protease inhibitor cocktail (Roche)
- 25% glycerol

Lysis buffer was filter sterilised prior to use.

10x TBS

- 1.5M NaCl
- 0.2M Tris (24.2g Tris)

TBS-T

- 1x TBS
- 0.1% Tween

1L 10x SDS PAGE Gel Running Buffer

- 144.2g Glycine
- 100ml 10% SDS
- 30.3g Tris

1L 10x Western Blotting Buffer

- 144g Glycine
- 30.3g Tris

1x Western Blotting Buffer

- 10% 10x Blotting Buffer
- 30% methanol
- 60% H_20

1x SDS Gel Loading Buffer

- 50mM Tris-HCl pH6.8
- 2% SDS
- 10% glycerol
- 0.1% bromophenol blue
- 100mM DTT

2.8.3 Gels for western blotting

Western resolving gel

- 10% acrylamide / bis-acrylamide (37.5:1)
- 375mM Tris pH8.8
- 0.1% SDS
- 0.1% ammonium persulfate
- 0.04% TEMED

Western stacking gel

- 5% acrylamide / bis-acrylamide (37.5:1)
- 0.125M Tris pH6.8
- 0.1% SDS
- 0.1% ammonium persulfate
- 0.1% TEMED

2.8.4 Whole cell protein extraction

UB/OC-1, UB/OC-2, ND7, BHK and HeLa cells (the latter of which were cultured by ET) were grown in 4-6 175cm^2 tissue culture flasks until approximately 90% confluent — generating 8-12 x 10^6 cells respectively. The growth media were then replaced with 12ml PBS and cells were harvested using a cell scraper. The PBS, containing the dissociated cells, was pooled to a 50ml Falcon tube and centrifuged at 1000rpm at 4ºC for 5 minutes. The supernatant was removed from the tube and the pellet was resuspended in 50µl lysis buffer per 10^6 cells. Lysis was carried out using a 100µl homogeniser and the lysate was pelleted by centrifugation at 14000rpm at 4ºC for 10 minutes. The protein concentration was estimated by measurement of the optical density of the solution at A_{280} and A_{260} by spectrophotometry and using the values obtained in Equation 2.1:

Equation 2.1. Protein Concentration.

$$\text{Protein Concentration } (\mu g/\mu l) = (1.55 \times \text{Optical Density}(A_{280})) - (0.76 \times \text{Optical Density}(A_{260}))$$

100µg aliquots were then snap frozen with liquid nitrogen. Tubes were stored at -80ºC.

2.8.5 SDS PAGE of protein

A 10% polyacrylamide western resolving gel was poured in a Protean IIxI cell for PAGE (Bio-Rad), overlaid with water saturated isobutanol and allowed to set. The isobutanol was then removed with paper towel. A 5% western stacking gel was poured, an appropriately sized well comb was inserted and the gel was allowed to set. Once set, the comb was removed and the wells were rinsed with 1x SDS PAGE gel running buffer. Protein samples were made up to 20µl in SDS gel loading buffer (to a final concentration of 1x SDS gel loading buffer), denatured by heating to 95ºC for 2 minutes and loaded into the wells; 15µl of Rainbow™ coloured molecular weight marker (Amersham Biosciences) was run alongside the protein extract for later sizing. The gel was run at 25mA/gel until the dye front entered the resolving gel, the current was then turned up to 35mA/gel until the molecular weight marker of relevant weight had been adequately resolved.

2.8.6 Western blotting

An Immobilon-P (PVDF) transfer membrane (Millipore) which had been cut to the dimensions of the gel was equilibrated in 100% methanol for 15 seconds, followed by equilibration in water for 2 minutes and then 1x blotting buffer for 5 minutes. The glass plates of the gel assembly were carefully separated and the stacking gel was trimmed from the resolving gel. The gel was then transferred onto a dry piece of Whatmann 3MM paper and a sandwich was assembled comprising, from bottom to top: back plate of western blotting tray; sponge; Whatmann 3MM paper sheet; gel (Whatmann 3MM paper side down); equilibrated PVDF membrane; two more pieces of Whatmann 3MM paper; upper sponge; upper plate of western blotting tray. The blot was run at 215mA for 3-4 hours in a Trans-blot™ cell (Bio-Rad). The sandwich was then separated and the membrane carefully removed and inspected to ensure adequate transfer of the molecular marker. The membrane was dried by immersion in 100% methanol for 10 seconds followed by air-drying at room temperature for 15 minutes or until thoroughly dry. It was then cut into appropriate size strips and either stored at -20ºC or immediately used for immunodetection.

2.8.7 Ponceau S staining of PVDF membranes

In order to visualise lanes on a blotted membrane to assist in cutting the membrane into strips prior to immunodetection, the protein on the membranes was stained by 5 minute incubation with Ponceau S solution (Sigma-Aldrich) at room temperature under gentle agitation. Once the strips had been cut, staining was reversed with water washes until protein bands were no longer visible in order to facilitate immunodetection.

2.8.8 Immunolabelling of proteins on Immobilon P membranes

Membranes were either used directly after blotting or removed from storage at -20ºC and allowed to warm to room temperature prior to manipulation. Blocking of non-specific antigenicity was conducted by incubation of the membrane for 1 hour at room temperature

in TBS-T containing 10% Marvel. Following a 5 minute wash in TBS-T, the membrane was incubated for 1 hour in a solution of 1x TBS-T and 5% Marvel which contained an appropriate dilution of primary antibody (1:1000 for anti-NR2F2; 1:2000 for anti-RBMS1; 1:250 for anti-ZRANB2).

The membrane was then twice rinsed with 1x TBS-T and two 5 minute incubations in TBS-T with 5% Marvel were carried out followed by incubation for 1 hour in a solution of 1x TBS-T and 5% Marvel containing an appropriate dilution of a secondary HRP-conjugated antibody raised against the IgG of the animal that the primary antibody was raised in (1:5000 swine anti-rabbit immunoglobulins for anti-NR2F2 and anti-RBMS1; 1:1000 goat anti-mouse immunoglobulins for anti-ZRANB2). Finally, one 15 minute and two 5 minute washes were carried out in TBS-T.

2.8.9 Detection of chemoluminescence

The membrane was removed from the TBS-T wash and any remaining TBS-T was poured off. 5ml Immobilon™ Western chemiluminescent HRP substrate was added to the membrane for 5 minutes. The reagent mix was then poured off and any excess was drained onto paper towel. The blot was covered with plastic wrap, a piece of Hyperfilm™ ECL™ film was placed on top and was left to expose for 5 minutes in an X-ray film cassette.

2.8.10 Equalisation

Equalisation of protein expression by comparison of detected bands with a housekeeping protein was not carried as this was not required in the present study i.e. the experiment was conducted to identify the presence or absence of protein expression in a given cell line, not to compare the levels of expression between cell lines. However, Ponceau staining of the PVDF membrane was carried out to ensure that sufficient protein had been transferred to the membrane for detection. Coomassie staining (a more sensitive assessment of protein loading) of identically loaded gels was also carried out.

2.9 Immunofluorescence immunohistochemistry

2.9.1 Equipment for immunofluorescence immunohistochemistry

Carl Zeiss

LSM 510 META inverted laser scanning confocal microscope and laser module.

Leica

Dissecting microscopes: MZ 12_5 & MZ 7_5 ; CM1850 cryostat

2.9.2 Reagents for immunofluorescence on UB/OC-2 cells

Blocking solution

- 10% Goat serum (Invitrogen)
- 0.2% Triton X solution (Sigma-Aldrich)
- 89.8% PBS solution

2.9.3 UB/OC-2 cell culture and immunohistochemistry

UB/OC-2 cells were seeded at approximately 1 x 10^5 cells/ well in a six-well plate which contained 0 or 1.5 thickness 13mm diameter uncoated glass coverslips (VWR). Cells were grown to approximately 80% confluency and fixed for 20 minutes in 4% PFA in PBS at room temperature. Three 5 minute PBS washes were carried out and coverslips were stored at 4ºC in PBS. Non-specific antibody binding was prevented by the addition of blocking solution to each coverslip for 1 hour at room temperature prior to the addition of optimally diluted primary antibody in blocking solution for a 1 hour incubation at room temperature (1:1000 for anti-NR2F2; 1:500-2000 for anti-RBMS1). The coverslips were then rinsed with PBS three times followed by the application of a 1-5µM DAPI, 1:200 (i.e. 1Unit/ml) Alexa 633-conjugted phalloidin and 2µg/ml Alexa 488-conjugated goat anti-rabbit IgG secondary antibody mix diluted in blocking serum which was incubated for 2 hours at room temperature. Slides were then rinsed with water three times and finally mounted on glass slides using Fluromount G solution (Southern Biotech). Cells were visualised using a Zeiss LSM 510 Meta microscope.

2.9.4 Reagents for immunofluorescence on cryosections

Blocking solution

- 10% Goat serum (Invitrogen)
- 0.1-0.5% Triton X solution (Sigma-Aldrich)
- 89.8% PBS solution

1% low gelling agarose gel

- 1% low gelling agarose
- 18% sucrose
- 0.05% sodium azide
- 80.95% PBS

2.9.5 Preparation of cryosections

Tissue for cryosectioning (from Sprague Dawley rats or CBA/ca mice) was fixed in 4% PFA solution (in PBS) for 1-2hours at room temperature or overnight at 4ºC. Samples were cryoprotected by incubation in 30% sucrose in PBS overnight at 4ºC. The tissue was then mounted in a 1% low gelling agarose gel which had been heated to 140ºC and allowed to cool to 37ºC. Once the agarose had set (typically by incubation at 4ºC overnight) a block was

cut from the agarose, attached to a cryostat chuck with OCT compound and rapidly frozen by immersion in liquid nitrogen prior to cryosectioning at -20 to -25 ºC.

2.9.6 Blocking of non-specific antibody binding sites, immunolabelling and mounting

Slides were allowed to equilibrate to room temperature and the sections were drawn around using a hydrophobic pen. Blocking solution with 0.1-0.5% Triton-X was then added and incubated for 1 hour at room temperature. Slides were drained and optimally diluted primary antibody, diluted in blocking solution, was added to the slides (1:1000 for anti-NR2F2 and 1:250/500 for anti-ZRANB2) which were left to incubate overnight at 4ºC. The following morning, three 5 minute washes were carried out with PBS and, typically, a solution of blocking solution, 2µg/ml secondary antibody (conjugated to Alexa 488 or 633) and 1Unit/ml phalloidin (conjugated to Alexa 488 or 633) was added for 2 hours at room temperature. Slides were again washed for three 5 minute washes with PBS prior to the addition of DAPI at 5µM (in PBS or blocking solution) for 20 minutes. Finally, the tissue was washed for three 5 minute periods in PBS and mounted in Fluromount G (Southern Biotech) under a 0 or 1.5 thickness 22mmx22mm or 22mmx50mm coverslip (VWR) which was sealed with nail varnish (Boots). Slides were visualised using a Zeiss LSM 510 Meta Microscope.

2.10 Electrophoretic Mobility Shift Assay (EMSA)

NB The design of oligonucleotides used in EMSA analysis is described in section 3.5, 4.8.1 and 5.5.

2.10.1 Equipment for EMSA

Bio-Rad

Protean IIxI cell for PAGE (20cm glass plates, 3mm spacers)

Epson

Perfection 1650 scanner

MSE

Centaur 1 centrifuge

Rietschle Thomas

Welch Gel Master™ gel dryer vacuum system

Scie-Plas

Gel Dryer

UMAX

Astra 1200S scanner

2.10.2 Reagents for EMSA

Cytoplasmic Lysis Buffer

- 10mM HEPES pH7.6
- 1mM EDTA
- 0.1mM EGTA
- 10mM KCl
- 1mM DTT
- 1mM sodium pyrophosphate
- 1mg/ml SP1
- 1mM vanidate

Nuclear Lysis Buffer

- 20mM HEPES pH 7.6
- 0.2mM EDTA
- 0.1mM EGTA
- 25% Glycerol
- 0.42M $NaCl_2$
- 1mM DTT
- 1mM sodium pyrophosphate
- 1mg/ml SP1
- 1mM vanidate

3µg/µl Poly(dI-dC)

- 10Units poly(deoxyinosinic-deoxycytidylic) acid sodium salt (15Units/mg)
- 222.2µl H_2O

10x Medium salt buffer

- 0.5M NaCl
- 0.1M Tris-HCl pH7.5
- 0.1M $MgCl_2$
- 0.01M DTT

2x Parker buffer

- 16% Ficoll
- 40mM HEPES pH7.9
- 100mM KCl
- 2mM EDTA pH8.0
- 1mM DTT

10x TBE

- 0.89M Tris-borate
- 20mM EDTA pH 8.0

2.10.3 In vitro protein translation

cDNA for mouse *Pou4f3* and *Barhl1* was cloned into the pGEM®-T Easy vector under the control of the T7 or SP6 promoter in our laboratory. Protein was synthesised according to the manufacturer's instructions using either the TNT®T7 Coupled Reticulocyte Lysate System (Promega) or the TNT®SP6 Quick Coupled Transcription/Translation System (Promega) using the provided SP6/T7 luciferase control DNA vector to synthesise luciferase protein which was used as a negative control in EMSA experiments.

2.10.4 Nuclear protein extraction

UB/OC-2 cells were grown in four 175cm² tissue culture flasks to 90% confluency. The cells were washed once with PBS and placed on ice. 3ml of cytoplasmic lysis buffer was added to each flask and left to incubate on ice for 5 minutes prior to scraping of the cells with a cell scraper. The contents of each flask were then transferred to microcentrifuge tubes on ice (1ml per tube). 60µl of 10% NP-40 was added to the top side of each tube and the tubes were briefly vortexed and spun at 14000rpm at 4ºC for 30 seconds. The supernatant, which contains cytoplasmic proteins, was removed and stored at 4ºC. All traces of supernatant

were removed from the pellet and 60µl nuclear lysis buffer was added. The tube was flicked gently to dislodge the pellet and was then subjected to three freeze thaw cycles between an ethanol-dry ice bath and a 37ºC water bath. The tubes were then centrifuged at 14000rpm at 4ºC for 10 minutes. The supernatants from this step were pooled, their protein concentration estimated as for whole cell protein extracts (Equation 2.1) and the protein aliquoted into 20µg aliquots and snap frozen in liquid nitrogen prior to storage at -80ºC.

2.10.5 EMSA oligonucleotide design and synthesis

Double stranded oligonucleotides were designed as described in section 3.5 (general design) and synthesised by Operon Biotechnologies Inc.

2.10.6 Probe preparation

10µg of sense and antisense oligonucleotide were combined with 1x medium salt buffer in a total volume of 22.2µl. This mixture was heated to 95ºC for 10 minutes and left to slowly cool to room temperature to anneal the single-stranded oligonucleotides to form double stranded EMSA probe. Probe annealing was checked by electrophoresis of annealed probe alongside single-stranded probe on a 3% Agarose gel. Following confirmation of annealing, probes were stored at -20ºC.

2.10.7 Probe labelling

Probes were diluted to 25ng/µl and 50ng of each probe was labelled in a standard T4 kinase reaction:

- 50ng probe
- 2µl 10x Kinase buffer
- 3µl γ^{32}P γ-ATP (10µCi/µl) (GE Healthcare)
- 1µl T4 Kinase (5-10U/µl)
- to 20µl H_2O

The reaction was incubated at 37ºC for 30 minutes. 80µl H_2O was then added and the diluted reaction mixture was loaded onto a Sephadex-G25 column and spun at 1500 rpm for 2 minutes to separate labelled oligonucleotides from free γ^{32}P γ-ATP (GE Healthcare). Radiolabelled probes were stored at -20ºC.

2.10.8 Assay reaction

Assay reactions were set up and incubated on ice for 10 minutes:

- 10µl 2x Parker buffer
- 3µg polydI/dC
- 2-4µl UB/OC-2 Nuclear Protein Extract or *in vitro* translated protein
- 0-1000ng Non-radiolabelled competition probe
- to 20µl H_2O

1ng of labelled probe was then added to each tube and the tubes were incubated at room temperature for 15-30 minutes.

2.10.9 Non-denaturing polyacrylamide gel electrophoresis

A 4% polyacrylamide (29:1), 0.25x TBE gel was poured (dimensions: 200 x 200 x 3mm) and polymerisation was initiated and catalysed by 0.05% ammonium persulfate and 0.2% TEMED respectively. Once set, the wells were washed with 0.25x TBE and the gel was run in this buffer at 200 volts at 4ºC in the Protean IIxI cell until the current had fallen to below 30 mA per gel (typically 30 minutes). The samples were then loaded onto the gel and electrophoresed at 200 volts for 1 to 3 hours at 4ºC.

2.10.10 Gel drying and autoradiography

After electrophoresis, the gel was removed from its cast to a piece of Whatmann 3MM paper, covered with cling film (Terinex) and placed in a gel dryer at 80ºC under vacuum until dry (typically 1-2 hours). Autoradiography was carried out in an X-ray film cassette with X-ray film (SLS) that was exposed at -80ºC for between 1 hour to 5 days. Once exposed, the film was removed from the cassette in a dark room, developed and fixed using Kodak processing chemicals for autoradiography films (GBX developer/replenisher and GBX fixer/replenisher) (Sigma-Aldrich) according to the manufacturer's instructions. Once dry, autoradiographs were scanned using an Epson or Umax scanner.

2.11 Cell transfection and reporter gene assay

2.11.1 Equipment for luciferase assay

Turner

TD-20e luminometer

2.11.2 Reagents for luciferase Assay

10x HEPES-Buffered Saline (HBS)

- 8.18% NaCl (w/v)
- 5.94% HEPES (w/v)
- 0.2% Na_2HPO_4 (w/v)

Filter sterilised with a 0.22µm filter and stored at 4ºC.

2x HBS

- 10ml 10x HBS
- 40ml water

The solution was pH adjusted to 7.12 and filter sterilized with a 0.22µm filter.

2.11.3 Plasmid constructs for luciferase assay

The pGL3-basic-NR2F2 4kb promoter (NR2F2p4kb) luciferase reporter construct was kindly provided by Dr M Vasseur-Cognet. pGL-3-basic-NR2F2 1.6kb promoter (NR2F2p1.6kb) was kindly provided by Dr S Tsai. pGV-Basic-Rbms1 1.3kb promoter (RBMS1p1.3kb) luciferase reporter construct was kindly provided by Dr H Ariga. pGL4.10[*luc*2] was purchased from Promega UK Ltd. pSi-Pou4f3 was cloned in our lab (Nolan *et al.* 2007).

Picture removed for copyright purposes

Figure 2.1. pDrive cloning vector.
Schematic diagram of the pDrive cloning vector which was used in order to clone gene promoters which had been amplified from genomic DNA by PCR. Purified PCR product was ligated into the pDrive vector by TA ligation i.e. by ligation of the Adenine bases at the 3' ends of the amplified promoter to the free uracil bases of the linearised pDrive vector. © Qiagen.

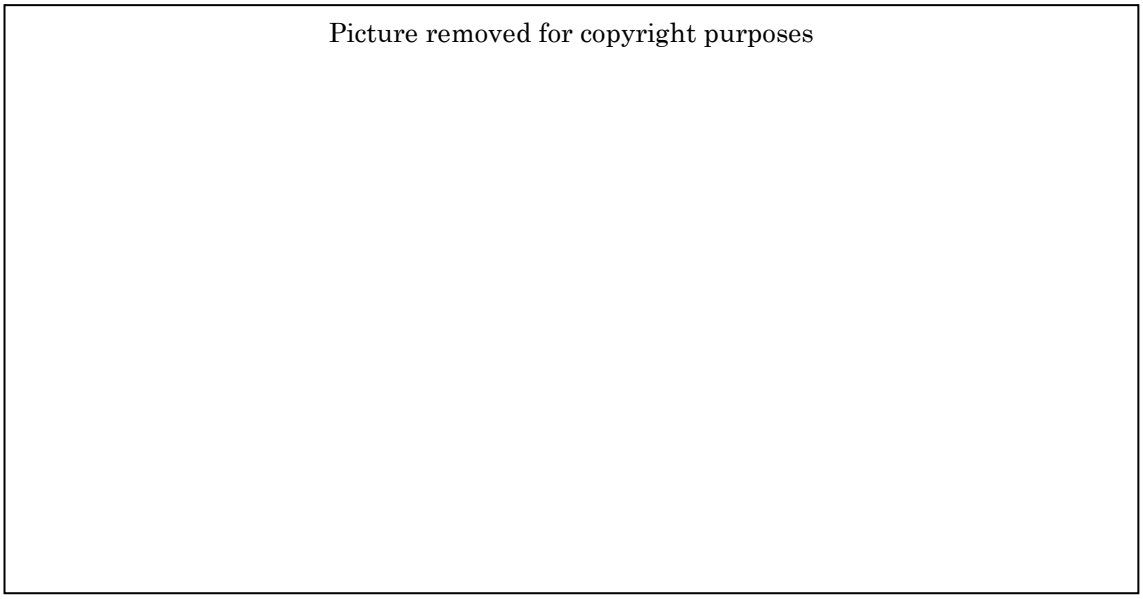

Figure 2.2. pGL4.10[*luc2*] vector.
Schematic diagram of the pGL4.10[*luc2*] luciferase reporter vector which contains a synthetic luciferase gene that has been codon optimised for expression in mammalian cells. Promoters from putative POU4F3 target genes were cloned into this vector for investigation of their regulation by POU4F3. © Promega.

pGL4.10-LUZP1p-2.8kb

The pGL4.10[*luc*2]-LUZP1 2.8kb promoter (LUZP1p2.8kb) luciferase reporter construct was produced as follows: The forward primer 5'-TTCCAGTGTGGTCTTGAACTCCTGTGG-3' and reverse primer 5'-GAGGATCCGGCGCTCCGCTC-3' were used to amplify a 2.8kb fragment of the LUZP1 promoter from mouse genomic DNA (Promega) with GoTaq (Promega) and Pfu (Stratagene) polymerases which was inserted, by TA-based ligation, into the pDrive cloning vector (Qiagen) (see Figure 2.1) according to the manufacturer's instructions. The promoter orientation was checked by restriction digestion with XhoI and the KpnI-NheI fragment of this construct was inserted into the KpnI-NheI site of pGL4.10[*luc*2] (see Figure 2.2). Promoter integrity was checked by DNA sequencing.

pGL4.10-Rbms1p-5.1kb

This construct (abbreviated to RBMS1p5.1kb) was cloned by SD. The BsgI fragment of a plasmid containing 21kb of the *RBMS1* 5' flanking region (kindly provided by Dr H Ariga) was incubated with the DNA polymerase large (Klenow) fragment (Promega) according to the manufacturer's instructions to produce a blunt-ended fragment. This was inserted into the EcoRV site of pGL4.10[*luc2*] (see Figure 2.2). Correct orientation of the insert in pGL4.10[*luc2*] was verified by digestion with PstI.

pGV-B

An empty pGV-B vector (PicaGene) was created by excising the *RBMS1* 5' flanking sequence from RBMS1p1.3kb with XbaI and HindIII. The sticky ends produced were blunted by incubation with Klenow (as above) and re-ligated to produce the final vector.

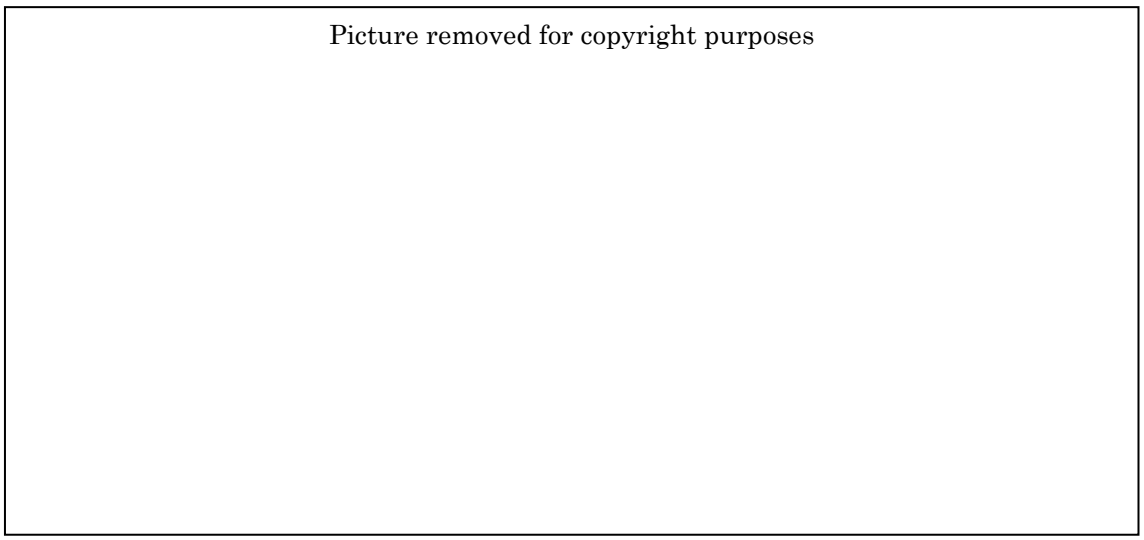

Figure 2.3. pGL4.23[*luc2*/minP] vector.
Schematic of the pGL4.23[*luc2*/minP] luciferase reporter vector which contains the synthetic, codon-optimised *luc2* gene as well as a minimal TATA promoter downstream of POU4F3 binding sites that were inserted into the EcoRV site of the vector. © Promega.

pGL4.10-ZRANB2p-3.2kb

The pGL4.10[*luc*2] 3kb *Zranb2* 5' flanking region luciferase reporter construct (ZRANB2p3.2kb) was produced as follows: The forward primer: 5'-GGTCCTTCACCCTCATGATAGCTCACTG-3' and reverse primer 5'-CGTCACTGACTCGGAAATTCTTGGTCG-3' were used to amplify a 3.2kb fragment of the LUZP1 promoter from mouse genomic DNA (Promega) with long-range enzyme mix (Qiagen) which was inserted, by TA-based ligation, into the pDrive cloning vector (Qiagen) (see Figure 2.1) according to the manufacturer's instructions; the orientation of the promoter was checked by restriction digestion with SacI and the KpnI-XbaI fragment of this construct was inserted into the KpnI-NheI site of pGL4.10[*luc*2] (see Figure 2.2). Promoter integrity was checked by DNA sequencing.

pGL4.23-NR2F2BS1-1,2,3&5x

The minimal promoter constructs pGL4.23-NR2F2BS1-1x, pGL4.23-NR2F2BS1-2x, pGL4.23-NR2F2BS1-3x and pGL4.23-NR2F2BS1-5x were constructed by blunt-ended ligation of T4 kinase-phosphorylated EMSA probe NR2F2BS1 with EcoRV-linearised pGL4.23[*luc2*/minP] (see Figure 2.3). The number of repeats of NR2F2BS1 that had been incorporated into the vector were assessed by NheI-PvuII restriction digestion and size assessment by agarose gel electrophoresis. The "–nx" suffix of the construct name refers to the number of repeats of NR2F2BS1 contained in that construct.

pGL4.23-NR2F2BS2-1-4x

The minimal promoter constructs pGL4.23-NR2F2BS2-1x, pGL4.23-NR2F2BS2-2x, pGL4.23-NR2F2BS2-3x and pGL4.23-NR2F2BS2-4x were constructed as for pGL4.23-NR2F2BS2-1,2,3&5 using NR2F2BS2 instead of NR2F2BS1 (see Figure 2.3).

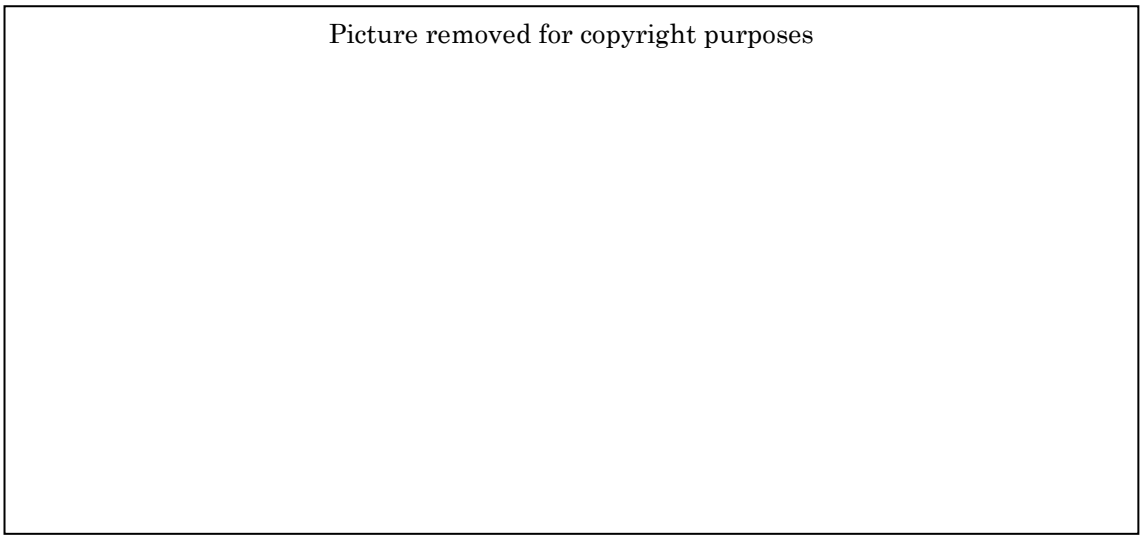

Figure 2.4. pSi mammalian expression vector.
The pSi expression vector, whose SV40 enhancer region induces constitutive expression of inserted DNA in mammalian cells, was used for the expression of proteins. © Promega.

pSi-Dreidel

pHM6-Dreidel, an expression construct for a 2bp missense mutated form of mouse POU4F3, was kindly provided by Prof. Karen Avraham. For compatibility with other expression constructs used in luciferase assays, the dreidel coding sequence was cloned into the pSi expression vector by insertion of the EcoRV-NotI fragment of pHM6-Dreidel into the EcoRV-NotI site of pSi.

2.11.4 Purification of DNA from bacterial culture for transfection

Bacteria were streaked out on an LB-Agar-ampicillin (100µg/ml) plate from glycerol stocks and incubated at 37ºC overnight. The following morning, single colonies were picked using a 200µl pipettor tip into 2ml LB-ampicillin (100µg/ml) and incubated at 37ºC at 220rpm in a shaking incubator for 8 hours. The culture was then decanted into 50ml of LB-ampicillin (100µg/ml) and cultured overnight. The next morning, bacteria were pelleted by centrifugation at 4000rpm for 20 minutes at 4ºC, plasmid DNA was extracted using the MidiPrep kit (Qiagen) and resuspended in 200µl of water. The DNA concentration was estimated by measuring the optical density of the resuspended DNA at A_{260} using a spectrophotometer and using the resultant value in Equation 2.2:

Equation 2.2. DNA Concentration.

$$\text{DNA concentration } (\mu g/\mu l) = \frac{(\text{Optical Density } (A_{260}) \times \text{Dilution Factor} \times 50)}{1000}$$

DNA was diluted to desired concentrations in water and checked by diagnostic restriction enzyme digest followed by electrophoresis on an agarose gel of appropriate concentration.

2.11.5 Preparation of UB/OC-2, BHK and ND7 cells for transfection

Cells were transfected based on a standard calcium precipitation protocol (e.g. Kingston *et al.* 2001). UB/OC-2, BHK or ND7 cells were plated at approximately 2 x 10^5 cells/well in a six-well plate (BD Falcon). The next morning, the culture media were changed to DMEM + 10% FBS and the cells were incubated at 37ºC, 5% CO_2 for at least one hour prior to transfection.

2.11.6 Preparation of precipitate

400µl 2 x HBS was aliquoted into 1.5ml microcentrifuge tubes designated tubes B (one per condition being tested) and allowed to warm to room temperature. In separate tubes, designated tubes A, the following mixture was prepared (one per condition being tested):

- 0.25M $CaCl_2$
- 100-200µg/well Luciferase reporter vector
- 1-3µg/well pSi / pSi-Pou4f3 expression vector
- 10ng/well pRL-null vector
- to 400µl water

The contents of each A tube were added to its corresponding B tube dropwise (total volume 800µl). The precipitate was then allowed to form for 20 minutes at room temperature.

2.11.7 Transfection

Following precipitation, 200µl of precipitate was added to each well and mixed by pipetting up and down three times; experiments were conducted in triplicate. Following addition of precipitate, ND7 cells were incubated at 37ºC, 5% CO_2 for a minimum of 6 hours and UB/OC-2 or BHK cells were incubated under identical conditions for a minimum of 16 hours. After this incubation: The precipitate was removed from UB/OC-2 cells, the cells were shocked with DMEM + 15% glycerol for 2 minutes 30 seconds, washed with HBSS + 10% FBS and then incubated in UB/OC-2 cell culture media; the precipitate was removed from BHK and ND7 cells and replaced with appropriate culture media. All cell types were further incubated for a minimum of 24 hours prior to luciferase assay.

2.11.8 Dual Luciferase assay and analysis

Luciferase assays were carried out with the Dual-Luciferase® kit (Promega) according to the manufacturer's instructions, which were modified by the use of 50µl of LARII reagent instead of 100µl. Samples were assessed in a single-point luminometer (Turner). A reporter construct was deemed to be regulated if significantly activated by pSi-Pou4f3 compared to pSi, promoterless reporter construct, mutant POU4F3 expression construct or a mutant reporter construct ($p<0.05$) as determined by a two-sample two-tailed student's t test i.e. *Nr2f2* and *Rbms1* reporter constructs, but not *Luzp1* or *Zranb2* reporter constructs.

2.12 Site-directed mutagenesis (SDM) of the *Nr2f2* promoter

NB *The mutagenesis for NR2F2BS2 from design of flanking primers and generation of the short insert through to the ligation of the long insert into the pDrive cloning vector was carried out by SD.*

2.12.1 Design of mutant EMSA probes and assessment of abolition of POU4F3 binding

Due to the highly gene-specific nature of this mutagenesis, the design of oligonucleotides with mutations in POU4F3 binding sites that abolish POU4F3 binding is described in section 4.10.1.

2.12.2 Attempted SDM of Nr2f2 promoter by QuikChange® II XL kit

The QuikChange® II XL kit (Stratagene) was used according to the manufacturer's instructions. The mutated EMSA oligonucleotide sequence was submitted with 40bp of its 5' and 3' flanking sequence (from the *Nr2f2* promoter) to the QuikChange® Primer Design Program (Stratagene 2006) in order to automatically generate SDM primers of appropriate physical properties. The results of this analysis are shown in Table 2.2.

Table 2.2. Primers for attempted QuikChange® II XL kit site-directed mutagenesis.
Mutations of the wild type sequence are underlined. *(F)*, forward primer; *(R)*, reverse primer.

SDM primer name	*5' to 3' sequence*
NM1Pri(F)	CCGCGCCCCCCTTTTTAGCCGATTTGATCACTTTGATTCTG
NM1Pri(R)	CAGAATCAAAGTGATCAAATCGGCTAAAAAGGGGGGCGCGG
NM2Pri(F)	GATAAAGTTGAGAGGAATTTATTTTAATTGCAGGGTAACAATGAGGTGAAGTCTGGTGTT
NM2Pri(R)	AACACCAGACTTCACCTCATTGTTACCCTGCAATTAAAATAAATTCCTCTCAACTTTATC

Though multiple attempts were made to mutate the *Nr2f2* promoter by this protocol and despite optimisation, all attempts proved unsuccessful.

2.12.3 Overview of NR2F2p4kb SDM by overlap extension PCR

SDM by overlap extension PCR was carried out on the *Nr2f2* promoter based on a method described by Horton (Horton 1993 and references therein) as this is a more robust means of mutagenesis but involves more subcloning than the QuikChange® method. The overlap extension method exploits the ability of PCR oligonucleotides of standard length (20-30bp) to bind DNA sequences with a 1-3bp mismatch (Ling *et al.* 1997). Such oligonucleotides are designed to both the sense and antisense sequence of the mutagenesis site and are each used with a flanking primer in PCR. The resulting amplicons (named short inserts) incorporate the mutagenesis primer sequence at the 5' end and are designed to contain a restriction endonuclease recognition site 3' to this which is required for later subcloning.

In the second stage of the mutagenesis process, the flanking primers used for both the sense and antisense mutagenesis are used in a PCR with the sense and antisense short inserts as template sequence. In initial cycles of the PCR, the overlapping region of the short inserts (which is equivalent to the mutagenesis primers used in the first PCR) primes polymerisation of a long amplicon (named the long insert) which comprises the two short inserts joined by their overlapping region. Therefore, the long insert contains the mutagenesis site flanked by the desired restriction endonuclease recognition sites. In subsequent cycles of the PCR, the flanking primers prime amplification of the long insert.

This long insert can then be ligated directly into the pDrive cloning vector by TA cloning (when an appropriate polymerase is used) for amplification and subsequent cloning into the wild type NR2F2p4kb vector in order to produce a reporter vector which incorporates the desired mutations. Alternatively, the long insert can be digested by the appropriate restriction endonuclease for direct ligation (by T4 DNA ligase) into wild type NR2F2p4kb which has been similarly digested, phosphatased and purified.

2.12.4 Reagents and methods used for the NR2F2p4kb SDM

The mutant EMSA probes that had been used to verify abolition of POU4F3 binding by EMSA, and the SDM primers that had been used in the attempted QuikChange® SDM were used to introduce the desired mutations into the *Nr2f2* promoter (see Figure 4.19 for schematic of the SDM process).

This strategy minimises the length of amplicons required for the mutagenesis PCR and therefore makes the PCR conditions more favourable. This was particularly important due to the length and high GC content of the *Nr2f2* promoter which were the most likely factors that caused the QuikChange® strategy to be unsuccessful.

Mutagenesis PCR reactions

Primers used for generation of the short fragments are shown in Table 2.3. The primers that had been used for the attempted QuikChange® mutagenesis were used for the mutation of NR2F2BS2 (Table 2.2 & Table 2.3) whilst the mutant oligonucleotides that were used for EMSA analysis of mutations in NR2F2BS1 were used to mutate NR2F2BS1 (Figure 4.17 & Table 2.3). These primers were used in a standard PCR reaction with a mixture of GoTaq (Promega) and Pfu (Roche) polymerases in a 2:1 ratio (see section 2.7.4) and the products of these reactions were electrophoresed on a low melting-point agarose gel of appropriate concentration (typically 1.5%). The band of correct size (see *Short Insert Length*, Table 2.3) was then excised and purified from the gel (see section 2.6.4 for DNA purification method).

Table 2.3. NR2F2BS1 and NR2F2BS2 mutagenesis primers.
Primers used for overlapping extension PCR mutagenesis. Mutated bases of mutagenic primers are underlined.

Insert Name	*Primer Description*	*Primer Name*	*Sequence*	*Short Insert Length*	*Long Insert Length*
NR2F2BS1 mut5'	5'mutagenic primer	NR2F2BS1 mut	CTTTTTAGCCGATTTGATCACTTTGATT	407 bp	786 bp
	3' flanking primer	N1ApaI5'P	AAGCCTCCGGGTCGGGCCCGGAG		
NR2F2BS1 mut3'	5'mutagenic primer	NR2F2BS1 mutRC	AATCAAAGTGATCAAATCGGCTAAAAAG	407 bp	
	3' flanking primer	MVCApaI3'	TCCGCGCTCCGGGGTCCAC		
NR2F2BS2 mut5'	5'mutagenic primer	NM2PriF	GATAAAGTTGAGAGGAATTTATTTTAATTGCAGGGTAACAATGAGGTGAAGTCTGGTGTT	231 bp	804 bp
	3' flanking primer	MVCER3'	GCTTAATGAATTCCCATCACTTGC		
NR2F2BS2 mut3'	5'mutagenic primer	NM2PriR	AACACCAGACTTCACCTCATTGTTACCCTGCAATTAAAATAAATTCCTCTCAACTTTATC	633 bp	
	3' flanking primer	MVCER5'	GGAATTCTCACAATCAACTAGCGG		

Purified short insert DNA was then used as template DNA for generation of the long inserts. Flanking primers that had been used to generate the short inserts for each site were used to amplify the long insert i.e. N1ApaI5'P was used with MVCApaI3' to amplify the long insert containing NR2F2BS1mut and MVCER3' was used with MVCER5' to amplify the long insert containing NR2F2BS2mut (Table 2.3). The same GoTaq (Promega) – Pfu (Roche) mix was used to amplify the long NR2F2BS2mut insert as was used in the short insert PCR whereas Herculase (Stratagene) polymerase was used for NR2F2BS1mut long insert amplification as this insert was GC rich. The NR2F2BS1mut long insert contained the potentially mutated POU4F3 binding site flanked by EcoRI restriction sites and NR2F2BS2mut long insert contained the mutated POU4F3 binding site flanked by ApaI restriction sites. PCR products were electrophoresed on a 1% low melting-point agarose gel and the long insert was extracted from the gel (sections 2.6.3 and 2.6.4).

2.12.5 Cloning of NR2F2BS2mut long insert into the NR2F2p4kb plasmid

Purified insert was ligated into the pDrive cloning vector (section 2.6.5, *TA method*). Colonies incorporating the insert (assessed by blue/white selection) were cultured and plasmid DNA was purified (*Miniprep*, section 2.6.1) and sequenced. NR2F2BS2mut pDrive clones containing the desired insert were digested with EcoRI and electrophoresed on a low melting-point agarose gel. DNA was extracted from the gel as described above. The NR2F2p4kb construct (which contains 4kb of *Nr2f2* 5' flanking region) was similarly digested, electrophoresed and purified prior to being phosphatased using Calf Alkaline Phosphatase (Promega) according to the manufacturer's instructions. The mutant insert was ligated into the prepared vector using T4 DNA ligase (section 2.6.5). The colonies produced were digested with the NheI and PstI restriction endonucleases and subjected to agarose gel electrophoresis (2.6.3) to determine insert orientation within the vector. Clones containing the insert in the correct orientation were subsequently sequenced to verify incorporation of the mutant insert and this vector was named NR2F2p4kb-BS2mut.

2.12.6 Cloning of NR2F2BS1mut long insert into NR2F2p4kb and NR2F2p4kb-BS2mut

NR2F2BS1mut long insert was extracted from pDrive colonies as for NR2F2BS2mut except the ApaI restriction endonuclease was used instead of EcoRI. This insert was ligated into NR2F2p4kb and NR2F2p4kb-BS2mut which had been prepared as NR2F2p4kb was in section 2.12.5 (with ApaI instead of EcoRI) to produce NR2F2p4kb-BS2mut and NR2F2p4kb-BS1&2mut. This ligation mixture was transformed and cultured as above and the purified plasmid DNA of the resultant clones was digested with SacI and electrophoresed in order to identify the orientation of the long insert. As well as selecting clones which incorporated the insert in the desired orientation, incorporation of the desired mutation was verified by allele specific hybridization.

2.13 Allele specific hybridization of plasmid DNA with EMSA oligonucleotides

Prior to costly sequencing of multiple clones, the incorporation of the desired 2bp NR2F2BS1 mutation into pDrive or NR2F2p4kb-BS2mut (to make NR2F2p4kb-BS1&2mut) was verified by allele specific hybridization.

2.13.1 Equipment used for allele specific hybridization

Techne

HB-1D hybridizer

2.13.2 Reagents for allele specific hybridization

Alkali denaturation buffer

- 3.8M NaCl
- 0.5M NaOH

Hybridization solution

- 30ml 20x SSPE
- 5ml SDS
- 5ml 100x Denhardt's solution
- 60ml distilled water

Wash buffer (3x SSPE, 0.1%SDS)

- 15ml 20xSSPE
- 100µl SDS
- 84.9ml distilled water

20x SSPE

- 3M NaCl
- 0.2M NaH_2PO_4
- 20mM EDTA

The solution pH was corrected to 7.4

Denhardt's solution

- 0.1% Ficoll
- 0.1% Bovine serum albumin
- 0.1% polyvinyl-pyrrolidone

2.13.3 Preparation of membrane for hybridization

Amersham Hybond™-N+ membrane (GE Healthcare) was cut to an approximate size of 20cm x 10cm and boxes of approximately 1.5cm x 2.5cm were marked on the membrane in pencil. 1-2µl of Miniprep (Qiagen) DNA from potentially mutated clones was spotted onto individual cells of the membrane with NR2F2p4kb DNA included in one corner cell as a control for estimation of background radioactivity (see section 2.13.5). The DNA spotting pattern was duplicated on another membrane for each experiment and DNA was fixed to the membrane by incubation with alkali denaturation buffer for 20 minutes at room temperature.

2.13.4 Pre-hybridization

The duplicate membranes were placed in separate hybridization tubes (tube A and tube B), and briefly washed in wash buffer (3xSSPE, 0.1%SDS). They were then pre-hybridized by replacement of the denaturation buffer with approximately 50ml hybridization solution

followed by incubation at 58°C (the salt adjusted melting temperature of the wild type NR2F2BS1 EMSA oligonucleotide minus two degrees) for 15 minutes.

2.13.5 Hybridization and washing of membranes

10µg of single stranded sense probes for NR2F2BS1 and NR2F2BS1mut (Figure 4.17) were radiolabelled as described in section 2.10.6 with the volume of the antisense strand omitted and the volume of 1x medium salt buffer reduced to 1.1µl accordingly. The entire volume of each labelled probe (11.1µl) was added to the hybridization solution in a hybridization tube: NR2F2BS1mut was added to tube A and NR2F2BS1 to tube B. Hybridizations were incubated at 58°C for one hour.

The membranes were then washed for 15 minutes periods in pre-warmed wash buffer (3xSSPE, 0.1%SDS) at hybridization temperature and the radioactivity of the control cell (NR2F2p4kb) was estimated using a Geiger counter. Once the control cell had fallen to near-background levels, excess wash buffer was removed from the membrane using paper towel. The membrane was covered in plastic wrap and autoradiographed at -80°C for 16 hours with X-ray film (SLS). Autoradiographs were developed, fixed and scanned as for EMSAs (section 2.10.10).

2.14 Sequencing of NR2F2p4kbmut-BS1&2 clones

Plasmids were sequenced by Geneservice Ltd. Chromatogram and sequence files were returned and the chromatogram was inspected to determine the signal to noise ration of the sequencing reaction. Sequence was aligned against sequenced NR2F2p4kb and the Ensembl *Nr2f2* 5' flanking region. This method was used to identify unintended mutations in clones from the NR2F2p4kb mutagenesis.

3

CANDIDATE *POU4F3* TARGET GENE IDENTIFICATION AND PRIORITISATION

POU4F3 is a transcription factor that is essential to hair cell development and survival. *Pou4f3* knockout and mutant mice have demonstrated that it is required for hair cell terminal maturation (Erkman *et al.* 1996;Hertzano *et al.* 2004;Xiang *et al.* 1998;Xiang *et al.* 1997) and three human families with different *POU4F3* mutations show that it is involved in the maintenance of hearing (Collin *et al.* 2008;Pauw *et al.* 2008;Vahava *et al.* 1998). As a transcription factor, POU4F3 produces the wild-type hair cell phenotype by binding to specific recognition elements in the promoter regions of target genes and recruiting or blocking other transcription factors in order to produce a positive or negative effect on target gene transcription. The phenotype seen in *Pou4f3* knockout hair cells cannot therefore be explained directly by POU4F3 loss e.g. POU4F3 itself is not a component of the stereocilia and therefore cannot be structurally responsible for stereocilial deficits in *Pou4f3* mutant mice. Therefore, the transcriptomal effect produced by the up- or down-regulation of target genes and their subsequent functions in hair cell development and maintenance must be responsible for the production of the hair cell phenotype. Hence, the phenotypes produced by *Pou4f3* mutation in mice and humans are likely to be due to dysregulation of these target genes.

In order to understand how *Pou4f3* produces hair cell terminal differentiation and survival, the regulatory networks from *Pou4f3* through to the hair cell phenotype would have to be traced. A full understanding of these pathways could provide strategies to reverse *Pou4f3*-related hearing loss, prevent hair cell loss from other causes and aid in hair cell regeneration.

In this chapter I report the process by which the candidate target genes of POU4F3 were identified and the difficult – sometimes subjective – process by which a subset of these genes were prioritised for further investigation. Comparative bioinformatic analyses of candidate target genes and preliminary experiments which were used to compare targets in this selection process are reported herein. Detailed bioinformatic investigation of prioritised candidate genes and characterisation of the regulation of individual genes by POU4F3 is reported in subsequent chapters (see chapters 4 & 5).

3.1 Previous work in the identification of POU4F3 target genes

Prior to the start of my doctoral work, experiments were conducted in our laboratory to identify unknown POU4F3 target genes at the transcriptional level using a genetic screen. Historically, hair cell genetic networks have been difficult to investigate by traditional molecular biological methods. This difficulty arises because of challenges in obtaining tissue of appropriate type and sufficient quantity and purity to employ such techniques (see section 1.6.1 for further detail).

In addition to the known difficulties of analysing genetic pathways in the inner ear, analysis of the transcriptional effect of POU4F3 by the common strategy of comparing wild type to mutant tissue could be confounded by secondary abnormalities and deterioration of nascent hair cells in *Pou4f3* mutants. For example, apoptotic genes that are upregulated in cell death in *Pou4f3* mutant mice (Xiang *et al.* 1998) would be more likely to be identified by a genetic screen even if these genes aren't directly regulated by POU4F3. Although investigators have attempted to identify POU4F3 target genes by comparing gene expression in wild type and dreidel *Pou4f3* mutant whole E16.5 cochleas by microarray analysis (Hertzano *et al.* 2004;Hertzano *et al.* 2007), the level of apoptosis in the inner ears of *Pou4f3* mutant mice at this age has not been reliably assessed (Xiang *et al.* 1998). Therefore, though the expression of two genes (*Gfi1* and *Lhx3*) has been shown to be affected by the dreidel *Pou4f3* mutation by this method (Hertzano *et al.* 2004;Hertzano *et al.* 2007), the mechanism by which POU4F3 might regulate these genes is currently unknown. Hence, these genes may be dysregulated due to hair cell death rather than the direct effects of POU4F3 loss.

Identification of target genes by conducting a genetic screen *in vitro* in cell lines circumvents the difficulties in obtaining sufficient tissue of sufficient quality and minimises confounding by abnormal and apoptosing cells. However, a problem posed by cell lines is that the transcriptional environment in which the screen is conducted is potentially different from that in the developing inner ear. As POU4F3 expression is initiated as early as E12.5 in the inner ear (Xiang *et al.* 1998), the UB/OC-2 cell line – which is derived from E13 immortomouse sensory epithelium and constitutively expresses POU4F3, myosin VI

and myosin VIIa – was selected for use in the screen as it is likely to provide as suitable a transcriptional environment as possible compared to other cell lines (Rivolta *et al.* 1998a).

3.1.1 Methods for identification of differential gene regulation

At the time that the subtractive hybridization screen was carried out, many methods were available to identify mRNAs that are differentially expressed between two sources (summarised in Munir *et al.* 2004). Broadly, these techniques can be categorised as differential display, subtractive hybridization and microarray. A subtractive hybridization method was chosen as it is unbiased in its identification of transcripts – unlike non-tiling cDNA microarrays (reviewed in Mockler *et al.* 2005) – it is able to identify lowly expressed transcripts – unlike differential display (Ledakis *et al.* 1998) – and it was cost-effective. Furthermore, at the time of the analysis no microarray chip was available that was tailored to the inner ear transcriptome.

The major limitation of the subtractive hybridization screen is that it is biased towards reporting transcripts that display large differences in mRNA level though slight changes in the expression of some genes can have potent effects on phenotype and such changes are identifiable using oligonucleotide microarrays. It consequently also leaves out the possibility of investigating complex and subtle multi-gene interactions as only the most differentially expressed of the directly regulated genes in a network may be identified. Despite its limitations, this method was appropriate for the identification of POU4F3 target genes.

3.2 Subtractive hybridization in UB/OC-2 cells

In our laboratory, the PCR-Select™ cDNA Subtraction kit (Clontech) was used to identify POU4F3 target genes. UB/OC-2 cells were manipulated to over- or under-express POU4F3 by stable transfection with sense *Pou4f3* cDNA or anti-sense *Pou4f3* N-terminus cDNA respectively. mRNA was extracted from the two cell populations and converted to cDNA which was then separately digested to produce shorter, blunt-ended cDNA molecules to which adaptor oligonucleotides were ligated. These samples were subjected to two rounds of hybridization (to enrich differentially expressed transcripts) and two rounds of PCR amplification (to amplify differentially expressed sequences and reduce background). The above steps were carried out in order to identify both upregulated and downregulated POU4F3 targets that were then subcloned into the pGEM-T Easy vector (Promega). Virtual Northern analysis was carried out (with both upregulated and downregulated transcript pools) in order to confirm the expression pattern of individual clones to minimise the risk of false positives prior to sequencing of differentially expressed clones (Clontech Laboratories 2008).

3.3 Follow-up of subtractive hybridization screen results

As with other methods of identification of differential gene expression, subtractive hybridization screens present the problem of making sense of the substantial amount of data produced. Though not as statistically complicated as the interpretation of microarray data, subtractive hybridization screen results still require thorough verification and further investigation to confirm specific effects of manipulations on target genes. The differentially expressed transcripts produced by the screen were reduced in our laboratory to those that are most differentially expressed based on a series of virtual Northern blots.

From this reduced pool, I began my project with 20 potentially upregulated and one potentially downregulated transcript to investigate. These were provided in 26 sequencing files from 21 cDNA clones that had been generated in our laboratory from the subtractive hybridization screen. All bar one of the clones that I was allocated were from the 'forward' subtractive hybridization screen i.e. these potential targets of POU4F3 were upregulated in the presence of POU4F3 in the subtractive hybridization screen.

3.3.1 Matching cDNA clones from the subtractive hybridization screen to mouse genes

The first step in the analysis of these differentially expressed clones was to identify to which genes they correspond. As the primers used in sequencing these clones flanked the cloned sequence, adaptor oligonucleotides that were used in the subtractive hybridization prior to cloning of differentially expressed cDNAs into the pGEM-T Easy vector (Promega) were included in the sequence returned. These unwanted sequences were identified by alignment of the known adaptor sequence with the sequencing data and manually deleted to leave cDNA sequence alone. The trimmed sequences were then used to identify genes that correspond to the clones from the screen. Each trimmed sequence was individually submitted to the Ensembl nucleotide-nucleotide BLASTN software through the Ensembl website in order to find near-exact matches (Ensembl 2008a;Gish 2004) and the most significant match to a given clone was selected as the corresponding gene. If no statistically significant match was found (i.e. p-value < 0.05), the clone was not followed up.

The BLASTN analysis provides a low false positive rate (it is unlikely to incorrectly report non-matching sequences as matches) however, certain regions of a query sequence will not be aligned with a homologous sequence if that sequence has characteristics that increase the risk of an alignment being due to chance e.g. highly repetitive regions. Therefore, for genes that were selected for further investigation, the trimmed clone sequence was aligned with the Ensembl sequence for its corresponding gene to identify whether intervening regions were false negatives. This analysis also helped to identify which transcripts of a gene (if any) best matched the submitted cDNA sequence.

Of the 21 clones submitted, four did not produce any significant matches – this may have been due to factors such as sequencing error of the clone, short query sequence length, low sequence complexity or deficits in the Ensembl database. The remaining 17 clones matched 14 genes in the mouse genome (see Table 3.1).

3.3.2 Prioritising candidates for further study

The genes identified in Table 3.1 – referred to as candidate genes – perform various functions, are of differing levels of characterisation and consequently had differing numbers of experimental reagents available (e.g. antibody, purified protein etc.). Given the large amount of time and resources required to investigate each interaction, candidates were prioritised for further study based on their known functions in other systems and their potential role in hair cell maturation and maintenance. Gene function data were required to inform this process and formulate hypotheses of candidate gene function which could guide future work.

A rapid method of assessing the available information on the function of a gene product is to examine its Gene Ontology (GO) units. GO units are descriptions of the known functions of wild type gene products. These descriptions are drawn from structured vocabularies that classify the cellular components (i.e. subcellular localization), molecular functions and biological processes in which gene products are involved. Furthermore, the type of evidence on which such functions are based can be identified as the GO database assigns an evidence code to each unit (Gene Ontology Consortium 2008). Therefore, candidate genes' GO units were downloaded from the Ensembl genome browser and compared, with reference to the literature, to assist prioritisation of suitable candidates for further investigation.

As mentioned in section 3.1.1, one of the benefits of the subtractive hybridization screen technique is its potential to identify novel and unknown genes. However – by definition – the literature on such genes is sparse and they have few experimentally verified data. Therefore, the GO units for these genes are few and predominantly computationally predicted (i.e. without experimental verification) making it difficult to hypothesise what their functions could be in the inner ear though these functions could be interesting. Furthermore, there are often few experimental reagents available for the study of novel genes and generation of the required reagents is a lengthy and costly process. These factors make such genes challenging candidates for further study and they were therefore less likely to be prioritised for further investigation when found, as they were much more difficult to pursue immediately despite their potential novelty. Candidate genes whose expression is known to be essential to the function of all mammalian cells were also less likely to be pursued as dysregulation of such genes in hair cells is unlikely to be due to a different mechanism than in other cells.

Table 3.1. Genes corresponding to clones produced by subtractive hybridization screen.
The *E-value* is a measure of the p-value which takes into account the size of the database being searched and, therefore, corrects for the increased likelihood of a match being identified by chance in a large database. E-values of <5 indicate sequences that are likely to be homologous. The lower the E-value, the more significant the score. *+*, potentially upregulated target of POU4F3; -, potentially downregulated target of POU4F3.

Clone Designation	*Potential POU4F3 Effect*	*Mouse Gene Informatics Symbol*	*E-value*	*%ID to matched transcript cDNA*
FA4, B12, C7	+	*Rcn1*	$7x10^{-109}$, $7x10^{-109}$, $5.3x10^{-109}$	89.17, 89.17, 89.17
FA8	+	*Zranb2*	$6.6x10^{-51}$	88.89
FA10, FB3, E4, E12	+	No Significant Match	N/A	N/A
FB5	+	*Rbms1*	$6.7x10^{-99}$	91.37
B9	+	*Hnrnpa2b1*	$7.8x10^{-162}$	94.07
B12R	-	*Actb*	$3.5x10^{-13}$	90.57
FC2	+	*Metap2*	$3.8x10^{-114}$	90.83
FC6	+	*Amd1*	$2.1x10^{-67}$	93.22
FC10	+	*Sertad2*	$1.3x10^{-39}$	93.98
C12, FD1	+	*BC010304*	$1.1x10^{-208}$	95.16
D3	+	*Luzp1*	$3.6x10^{-96}$	87.84
D8	+	*Nr2f2*	$2.7x10^{-224}$	95.07
D10	+	*Anxa5*	$5.4x10^{-44}$	85.37
D12	+	*Slc16a1*	$6.2x10^{-47}$	91.82
E1	+	*Exosc9*	$2.6x10^{-147}$	86.34

Based on these criteria, the genes identified were separated into two groups:

- Genes with known functions which could be relevant to hair cell terminal maturation and maintenance
- Genes with a potentially novel role in the inner ear

Within these groups, genes were ranked according to their potential relevance to hair cell development and maintenance. Though GO units provide an indicator of this, the ranking was also based on scientific judgement of the literature and supporting evidence for those GO units as there is no quantitative method for the analysis of such a small sample of genes' GO units i.e. it was not possible to analyse the GO units common to differentially expressed transcripts as the existing software requires much larger sample sizes to produce significant results. Candidate genes from each group which were judged to have the highest potential relevance to hair cell development and maintenance were then selected for further study. Only *Slc16a1* was not included in this ranking as it was followed up by another member of the laboratory (ET) who had also identified it as a potential target of POU4F3 from a different clone of the subtractive hybridization screen. The results of this analysis are presented in Table 3.2.

Having completed this analysis of the known functions of each gene, I compared the biological processes in which candidate genes are involved to identify whether they function in the same processes. This comparison did not identify a common theme in the functions of the candidate Pou4f3 target genes identified. I therefore continued to investigate high priority genes (Table 3.2) on an individual basis.

Table 3.2. Categorisation of POU4F3 candidate target genes for follow up.
NB: *Slc16a1* is not included as it was investigated by ET.

High priority due to existing evidence	***High priority due to potential novelty***	***Low priority due to existing evidence***	***Low priority due to lack of evidence***
Nr2f2	*Luzp1*	*Actb*	*Amd1*
Metap2	*Sertad2*	*Anxa5*	*BC010304*
Rbms1		*Exosc9*	*Hnrnpa2b1*
Rcn1			
Zranb2			

3.4 Reverse transcriptase PCR in UB/OC-2 cells

Having narrowed down the list of candidate genes, the process of comparing, verifying and characterising POU4F3-candidate gene interactions began. As an initial verification, the correlation of candidate gene expression with POU4F3 expression was investigated. All seven of the high priority candidates for follow-up were from the forward subtractive hybridization screen (i.e. potentially upregulated targets of POU4F3), and may therefore be expressed in POU4F3-expressing cells. A sensitive, rapid and cost-effective way of checking their transcription in such cells is by reverse transcriptase PCR (RT-PCR), which identifies if the candidate gene is being transcribed by detection of mRNA signal.

Ideally, hair cells would be used to identify candidate gene expression as these are the POU4F3-expressing cells of interest and therefore have the most relevant transcriptome. However, as for the subtractive hybridization, this was not practical due to difficulties in isolating sufficient hair cells to obtain RNA for reverse transcription and subsequent PCR. Therefore, in order to verify that the candidate genes are expressed in POU4F3-expressing cells, unmanipulated UB/OC-2 cells, which constitutively express POU4F3, were used as the source of RNA for reverse transcription. As previously explained (section 3.1), these cells provide a transcriptional environment that is more similar to that of the inner ear than many other cell lines (Rivolta *et al.* 1998a).

The UB/OC-2 cDNA was used as the template for PCR reactions to detect candidate gene expression. Genomic DNA (gDNA) was digested using DNAse prior to reverse transcription of UB/OC-2 cell RNA to cDNA and any DNA fragments amplified from gDNA could be size-separated from cDNA bands by agarose gel electrophoresis due to the exon-specificity of the primers designed (see Appendix). Where possible, the primers were designed to amplify the exons that had been detected in the subtractive hybridization screen to ensure identification of relevant transcripts. The BLAST analysis described in section 3.3.1 provided a guide as to which transcripts to design primers against. The exons identified by the BLAST analysis were likely to be at the known 3' end of their gene as transcripts from the subtractive hybridization were amplified using a poly dT primer which primes the amplification of cDNA from the poly(A) tail of an RNA molecule.

Figure 3.1 shows that bands were amplified for all seven of the genes investigated. Though non-specific bands were present for three genes (*Rbms1*, *Sertad2* and *Zranb2*), each gene yielded a band of predicted size without genomic DNA contamination (as determined by size). This result supports subtractive hybridization screen results and is compatible with the potential upregulation of these genes by POU4F3.

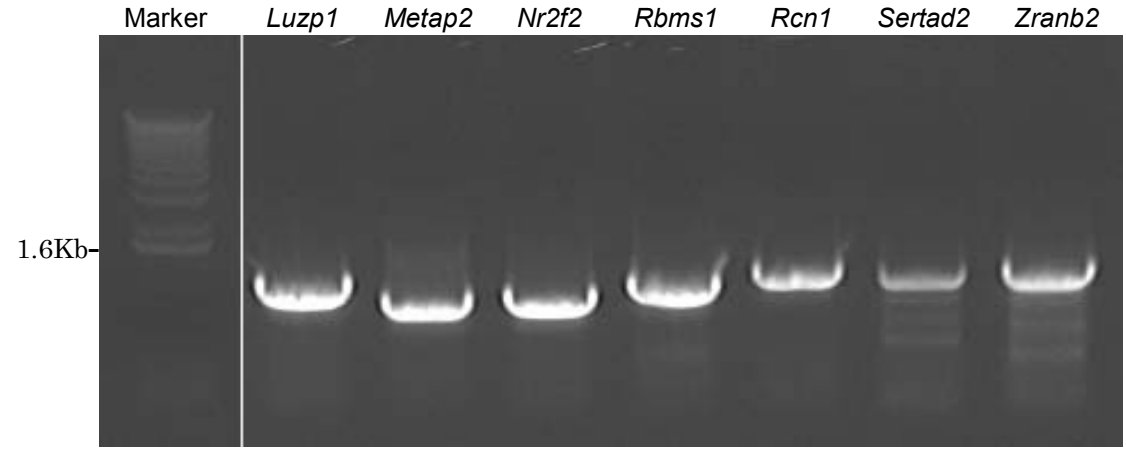

Figure 3.1. Candidate gene mRNA in UB/OC-2 cells.
UB/OC-2 cell cDNA was used as a template in PCR reactions with exon-specific primers against candidate genes identified in the subtractive hybridization screen and prioritised for further study. The most intense band for each gene corresponded to the predicted amplicon length as measured by comparison to the molecular weight marker (see Appendix). NB, the specific production of the above bands from UB/OC-2 cDNA was confirmed by negative controls that did not include cDNA and showed no detectable DNA on agarose gel electrophoresis.

3.5 Prediction of POU4F3 transcription factor binding sites

A bioinformatic analysis was carried out on the promoter regions of the seven candidate genes prioritised for further study (Table 3.2) to identify potential POU4F3 binding sites. The first step in this process is the identification of the promoter regions of candidate genes.

3.5.1 Promoter identification and selection

The Genomatix Gene2Promoter software was the promoter prediction program selected to identify candidate gene promoters. Many programs execute this task with varying success using different methods (Bajic *et al.* 2004), however, the promoter prediction program on which Gene2Promoter is based (PromoterInspector) provides the highest sensitivity available (43%, i.e. 43% of positives can be expected to be true positives) (Scherf *et al.* 2000). This improvement is supplemented with oligo-capping and comparative genomics to verify predictions (Bajic *et al.* 2004;Genomatix 2008;Scherf *et al.* 2000).

In this analysis, more than one promoter per gene was predicted. This selection was narrowed down to the most appropriate promoter prior to transcription factor binding site identification. I based my choice of promoter on the RNA transcript to which it corresponded. The transcript is essential as the transcriptional start site (TSS) of a gene is a useful landmark in promoter prediction by this method (Bajic *et al.* 2004;Heintzman *et al.* 2007). Each transcript is scored by Genomatix based on the completeness of its 5' sequencing by the identification of the known sequence of the oligonucleotide that capped the 5' end of the transcript. If a transcript has experimentally verified full 5' sequencing, it is assigned a gold score; if the 5' end of the transcript was confirmed by PromoterInspector

prediction, its score is silver and a bronze score is assigned if the transcript has no confirmation of 5' completeness. Only promoters with gold transcripts were further analysed. These Genomatix transcripts were compared to the Ensembl transcripts from the BLAST analysis and the promoter of the best-matching transcript was chosen for further analysis. Detailed results for this analysis for genes that were followed-up further are presented in chapters 4 & 5.

3.5.2 Transcription factor binding site identification

The Genomatix MatInspector and ModelInspector programs provided the largest number of publicly available matrices for transcription factor binding sites (including the POU4 family) to assess candidate gene promoters. Therefore, these programs were used to identify binding sites in candidate gene promoters.

MatInspector originally did this by matching promoter sequence to positional weight matrices for transcription factor binding sites based on the TRANSFAC database with positive weighting for experimentally verified sites (Quandt *et al.* 1995). This was improved for the version of the software used in this analysis. The weight matrix library was generated with a new program which extended the original algorithm; multiple positional weight matrices for a transcription factor are grouped into families to reduce redundant matches and matrix thresholds were optimized for each matrix in the library on the basis of length and conservation (Cartharius *et al.* 2005). Unpublished experimental evidence in our laboratory suggest that this version of the MatInspector software has much greater accuracy in predicting transcription factor binding sites than its predecessors.

Though the binding of a transcription factor like POU4F3 to a promoter is essential for its function, the existence of the binding site alone is not sufficient for regulation. Instead, the context of the binding site influences transcriptional regulation subsequent to transcription factor binding. The ModelInspector software takes this into account by adding contextual information (e.g. number of binding site repeats and structural DNA information such as hairpins) to predict binding modules and searches a pre-defined module database for regulatory regions with a similar signature (Frech & Werner 1997). These modules are therefore more likely to be functional than transcription factor binding sites identified in MatInspector and genes with such modules would be more promising candidates for further study than those with transcription factor binding sites alone.

The promoter selected for each gene was subjected to both MatInspector and ModelInspector analysis. ModelInspector modules were selected for further analysis along with the most significant MatInspector predictions. These results were collated (Table 3.3) and the predicted binding sites were compared between candidate genes in order to aid selection of candidate genes for further investigation (see section 3.7).

Table 3.3. MatInspector and ModelInspector analysis of candidate genes.
The *Location* refers to the distance of the MatInspector binding site or ModelInspector module from the candidate gene's TSS. *Matrix Similarity* refers to MatInspector predictions only. For *Software*: *A*, MatInspector; and *B*, ModelInspector. For *Location*: *+*, sense strand; and -, antisense strand. All binding sites were identified in the 5' flanking region of target genes.

Gene	*Promoter*	*Sites identified (sense sequence)*	*Location*	*Family*	*Software*	*Matrix Similarity*	*Comment*
Luzp1	GXP_287887	CACATTTAATTAATCAACT	+ 423-441 - 423-441	V$BRN4.01	A	+ =0.942 - =0.940	On both strands.
		TATTTATTAATTTTTTCAT	+ 975-993	V$BRN3.02	A	0.940	
Metap2	GXP_408241	GATTTATTTATTATATGTA	+ 1025-1043	V$BRN3.01	A	0.786	
		AATCTATTTATTATATGTA	+ 2557-2575	V$BRN3.01	A	0.824	In a cluster of binding sites.
Nr2f2	GXP_158616	TTAGCATATTTGATCACTT	+ 1814-1832	V$BRN5.01	A	0.836	
		GGAATTTATTTTAATTGCATCATAAC AATGAGGTGA	- 919-895	OCT1	B	N/A	High stringency MatInspector Brn-2 sites overlap.
Rbms1	GXP_149594	GATTTTATATCGATGAATGAGCATGA GCTG	- 1600-1553	BRNF	B	N/A	Mouse site presented. Later reanalysed for human. See Chapter 5.
Rcn1	GXP_286271	CTCGATTTGTATCCC	+ 612-693/705	BRNF	B	N/A	Two overlapping modules.
		TGACAAGTTTATTAGTCAGGA	+ 664-705	BRNF	B	N/A	

Gene	*Promoter*	*Sites identified (sense sequence)*	*Location*	*Family*	*Software*	*Matrix Similarity*	*Comment*
Sertad2	GXP_409110	TTATTATAATTATTAGAGA	- 1565-1583	V$BRN3.02	A	0.921	Opposite higher stringency V$BRN2.01 site.
		GCTATTATAATGACTTGCCAGAGAGATATACAATTAG	+ 1368-1446	BRNF	B	N/A	
Zranb2	GXP_430971	GTTTTATACATTATGGTTT	+ 281-316	OCT-PIT1	B	N/A	Probe designed against high-stringency V$BRN3.01 site within module.
		ACAGCACAATTAATAATAA	- 568-586	V$BRN3.01	A	0.811	Opposite high stringency V$BRN5.01 site.

3.6 Candidate gene expression in the inner ear

The decision to continue studying a gene came under iterative review during this investigation. One of the first of these iterations was the identification of the cellular and subcellular expression of candidate genes in the inner ear prior to conducting investigations into potential interactions between these genes' promoters and POU4F3. The literature and a developmental gene expression database (the GENSAT database (Gong *et al.* 2003)) were searched to identify reported expression of candidate genes in the inner ear. The GENSAT database is an online database of the neural expression profiles of a large number of genes. The gene expression profile is made visible by the introduction of a bacterial artificial chromosome containing the *Egfp* gene in place of the gene of interest, the product of which is detectable by fluorescence or immunohistochemical methods (Gong *et al.* 2003). As well as the GENSAT database, the NCBI UniGene database was searched to identify whether target gene mRNA transcripts had been detected in the inner ear (Boguski *et al.* 1995;Wheeler *et al.* 2003). However, the GENSAT and UniGene analyses were found to be poor discriminators of candidate gene inner ear expression at this stage – no inner ear expression of candidate genes was found in GENSAT and the UniGene analysis was positive for all candidate genes. Therefore, only the results of the literature search aided in the further refinement of candidate genes for investigation.

3.6.1 Genes with identified cellular and subcellular inner ear expression profiles

The analysis yielded inner ear expression data for *Nr2f2* only (Tang *et al.* 2005). Tang *et al.* identified *Nr2f2* mRNA expression at E8.75 and demonstrated the cellular and subcellular localization of NR2F2 protein at E15.5 (Tang *et al.* 2005). This evidence is further discussed in section 4.5.2. In brief, the onset of NR2F2 expression in the developing inner ear precedes that of POU4F3. However, at E15.5, NR2F2 was shown to be expressed in regions that were likely to include hair cells which are known to express POU4F3 (Tang *et al.* 2005; Xiang *et al.* 1998). This likely temporospatial colocalisation made NR2F2 a very strong candidate for further study and it was therefore selected for continued investigation.

Expression data found in the above searches yielded two candidate genes – *Rbms1* and *Zranb2* – that are 'ubiquitously' expressed in examined tissues, but whose cellular localization within those tissues is largely unknown (Adams *et al.* 2000;Fujimoto *et al.* 2000;Karginova *et al.* 1997;Nakano *et al.* 1998). *Luzp1*, by contrast, is expressed only in certain organs (Sun *et al.* 1996). The need to understand a gene's cellular localization is highlighted by *Nr2f2* which is known to be expressed in many tissues (e.g. Jonk *et al.* 1994) but shows marked cellular restriction within organs (e.g. Tang *et al.* 2005;Tripodi *et al.* 2004).

3.6.2 Obtaining existing reagents for investigation of candidate genes

With the exception of *Nr2f2*, none of these genes' inner ear expression patterns had been characterised. If these candidate genes are upregulated by POU4F3, they would be predicted to be expressed in hair cells. Furthermore, knowing the timing of the onset of changes in candidate gene expression compared with that of POU4F3 could clarify the putative mechanism of regulation. Identification of expression of these genes in hair cells would therefore confirm the relevance of the potential interactions identified in the subtractive hybridization screen to hair cell development and may provide further clues as to the role of POU4F3 candidate genes in hair cells.

I planned to investigate cochlear expression using antibodies to candidate genes for immunohistochemistry due to the relative rapidity and ease of this method compared to RNA *in situ* hybridization. A search of the literature and company websites was conducted to identify custom made and commercial antibodies respectively. This search identified antibodies for all candidate genes except *Sertad2*. The antibodies identified were verified for differing applications (i.e. not all had been used for immunohistochemistry which was their primary intended use in this study) and were of varying specificities (i.e. some antibodies identified had cross-reactivity to genes homologous to candidate genes).

As this initial screen did not seek to perform a comprehensive characterisation of gene expression or use an antibody-intensive protocol, only a small amount of an antibody that was suitable for immunohistochemistry was required. Therefore, if no suitable commercial antibody was available, I identified and requested a small amount of custom made antibody from the laboratory that had made or commissioned it. If a suitable antibody was available commercially, I contacted a company that would provide a sample of the antibody for assessment.

By this method, I was able to obtain antibodies for RBMS1 (Takai *et al.* 1994) and ZRANB2 (Abnova 2008a) for the identification of their inner ear expression. I was also able to obtain an anti-NR2F2 antibody for further characterisation of NR2F2 expression (Tripodi *et al.* 2004).

3.7 Refinement of candidate genes for further investigation

At this stage of analysis, two genes had been chosen for early study. *Nr2f2* was chosen because it encodes a well-investigated transcription factor which is known to be involved in processes relevant to hair cell development and maintenance (see chapter 4); there are many reagents available for its study; its transcription in UB/OC-2 cells was verified; and it is reported to be expressed in a region of the developing inner ear that gives rise to hair cells. Furthermore, a promoter module for Oct1 – a member of the POU family which,

therefore, binds DNA in a similar way to POU4F3 (e.g. Li *et al.* 1993) – was identified in the *Nr2f2* promoter as well as a high-stringency predicted transcription factor binding site which provided potential sites for direct regulation of *Nr2f2* by POU4F3.

The other gene selected for early study was *Zranb2*. This is a ubiquitously expressed (Adams *et al.* 2000;Nakano *et al.* 1998) regulator of alternative splicing (Adams *et al.* 2001) and therefore, despite being less well characterised than *Nr2f2*, has the potential to regulate developmental and maintenance pathways in the inner ear. An antibody was obtained against ZRANB2, making it easy to rapidly verify its expression profile in the inner ear, provided that the antibody was suitable for immunohistochemistry. It is transcribed in UB/OC-2 cells and, as for *Nr2f2*, one promoter module and one transcription factor binding site were identified in its 5' flanking region making *Zranb2* a good candidate gene for regulation by POU4F3.

Rbms1 encodes a transcription factor which has been implicated in processes relevant to hair cell development and maintenance (e.g. cell cycle (c-*myc*) (Negishi *et al.* 1994) and apoptosis (mitochondrial) (Iida *et al.* 1997)). Like *Nr2f2* and *Zranb2*, it was shown to be transcribed in UB/OC-2 cells by RT-PCR. Furthermore, a BRNF module (i.e. a 'Brn' POU domain factor module (see Andersen *et al.* 2001)) was initially identified in the *mus musculus Rbms1* gene promoter that may have been sufficient for POU4F3 regulation, though the promoter analysis was later redone for the human sequence for compatibility with reagents obtained (see section 5.5.2). *Rbms1* was preferred for follow-up given that we were able to obtain an antibody that was potentially useful for future experiments and promoter reporter and expression constructs were available from collaborators.

Metap2 was not prioritised for further study as the transcription factor binding sites identified in its promoter were of lower quality and stringency than any other candidate gene being followed up at this stage. Although high stringency potential POU4F3 binding sites were identified in the *Rcn1* and *Sertad2* 5' flanking regions, I was unable to obtain an antibody or other reagents for RCN1 and SERTAD2 had no antibody available. Furthermore, very little was known about the functions of either of these genes, making it difficult to assess their potential relevance to hair cell development and maintenance. As there was less reason to continue the investigation of these genes at this stage, they were not prioritised for investigation. However, the decision to continue investigation of prioritised genes came under iterative review throughout this study. Therefore, the literature and online databases of gene expression were monitored for *Metap2*, *Rcn1* and *Sertad2* throughout this investigation, with ongoing attempts being made to identify and obtain reagents for the investigation of these putative POU4F3 target genes.

The final gene selected for follow-up was *Luzp1*. This candidate gene had predicted transcription factor binding sites of comparable quality to those of other genes selected for follow up. Its known expression profile is amongst the most restricted of the candidate genes and it is likely to act as a transcription factor (Lee *et al.* 2001;Sun *et al.* 1996). Therefore, like RBMS1, LUZP1 could potentially regulate a variety of processes in the inner ear. An antibody was available and I attempted (unsuccessfully) to obtain a sample of this whilst I continued to investigate this candidate gene.

3.8 Summary

Having identified candidate POU4F3 target genes from a subtractive hybridization carried out in our laboratory, a small number of candidate genes were selected for further investigation based on measures that indicated the likelihood of POU4F3 regulation i.e. prediction of putative POU4F3 binding sites in predicted candidate gene promoters; the potential role of candidate genes in auditory hair cell maintenance and survival; and the reagents available for experimentation.

The expression patterns of candidate genes in the inner ear and the upregulation of candidate genes by POU4F3 suggested by the subtractive hybridization was subsequently tested to verify any interaction and to elucidate the mechanism by which POU4F3 might affect target gene transcription. Results from these experiments guided the ongoing prioritisation of genes and the allocation of resources for further investigation in order to allow greater focus on genes that were most likely to be involved in the guidance of hair cell terminal differentiation and survival that is mediated by POU4F3.

4

CHARACTERISATION OF THE INTERACTION OF POU4F3 WITH THE *NR2F2* PROMOTER

All candidate genes reported herein were identified as putative targets of the POU4F3 transcription factor from a subtractive hybridization screen that was conducted by members of our laboratory. This screen identified mRNA transcripts that were differentially expressed between cells that had been manipulated to either over- or under-express *Pou4f3*. The transcripts were output from the subtractive hybridization screen in the form of cDNA sequences that had been cloned into the pGEM-T® Easy vector and subsequently sequenced. In order to identify which gene in the mouse genome the transcripts had been produced from (i.e. which gene may be transcriptionally regulated by POU4F3), I used these sequencing files in BLAST analysis against the Ensembl mouse cDNA database.

4.1 Identification of *Nr2f2* as a potential POU4F3 target gene

Nr2f2 was identified as a potential target of POU4F3 from a clone (clone D8) that was produced from the forward (upregulated) subtractive hybridization screen as follows: The sequencing file for clone D8 was analysed to verify full sequencing of the cloned cDNA as a longer, higher quality sequence would provide higher quality matches on BLAST analysis. Sequencing of the whole insert was verified by identification of adaptor oligonucleotide sequences at both the 5' and 3' ends of the sequence. These adaptors had been used to amplify and subsequently clone the differentially expressed *Nr2f2* cDNA from the subtractive hybridization screen into the pGEM-T® Easy vector (Figure 4.1.*a*). Adaptor oligonucleotide sequences were manually trimmed from the cDNA sequence prior to BLAST analysis and this analysis was conducted using the trimmed cDNA sequence against the annotated genes in the Ensembl mouse 'gene build' database (see section 3.3.1) i.e.

sequences that had been annotated as being transcribed from the mouse genome (Curwen *et al.* 2004).

Five significant matches to the *Nr2f2* sequence in the Ensembl database were identified by this method with the most significant match being 343bp long and of 100% sequence identity to *Nr2f2* ($p = 8.6 \times 10^{-273}$) (Figure 4.1.*boxes 1&2*, *b*). However, as an alternative transcript (NP_899084.2) was found to overlap with *Nr2f2* in this region, a match of equal significance to the *Nr2f2* match was identified to this transcript. Therefore, the initial strategy of selecting the most significant match to a given clone as its corresponding gene (section 3.3.1) was not appropriate for clone D8.

In order to verify the match of clone D8 to *Nr2f2*, the genomic locations of all significant matches ($p < 0.05$) that were produced by the BLAST analysis were checked. Though one of these matches was to the other member of the NR2F family (*Nr2f1*) ($p = 3.3 \times 10^{-25}$), this match was much shorter than the other significant matches (116bp, 87% sequence identity), less significant, and near the 3' terminal of the transcript which is the most homologous to *Nr2f2* (Tripodi *et al.* 2004). Therefore, this match to *Nr2f1* was excluded as a match to clone D8.

---

a)

GGGGNGGNNTTCNNNTCCCNNNNNNAAAAAGNGANNANCTTNCCCCGCGGCCGAGGTACAT
AGACACAGGACAATTAATAATTTGGAAAAAAATGACTTACNTTGTCCATTCTGCTAATTTTCT
CCCAATCTCCTTAAATGCACTTTTAGCAATATTTTTCAAAAATTTACCAAAAAGAAAAAAAGA
CTAATTTCCTTTTTATACAAAAATGATAAGTAGCAGGTTGTTCTGCCCAACACAGGAGTTGTTT
TCTTTCTTTTTTTTTAATGCATTCTGTAAAAGTTCATTTGGCAATCTCTCTCTTTCTCTCTCCT
TTTTGAAATTCACAGTCCATTAAATTCTTCCCCTCTCTTCTTTTTAGCAAACTTGTAACATCCTT
TCTTAACAGAAGGAAATTAAGCAAACAAAACCAGTCTTTTGCCTTTTCTTTCTCTGTTTCACTC
CCCCTTATTTTGATTGATTTATTTATTGAATTGCCATATATGGCCAGTTAAAACTGCTGCCGGA
CAGTAACATATCCCGGATGAGGGTTTCGATGGGGGTTTTACCTACCAAACGGACGAAAAACA
ATTGCTCTATGACTGAGGAGGAGACCGTGCGGAGGGAAGGGAGACGAAGCAAGAGCTTTCCG
AACCGTGTTGGCTGGTTGGGGTACCTGCCCGGGCGGCCGCTCGA

b)

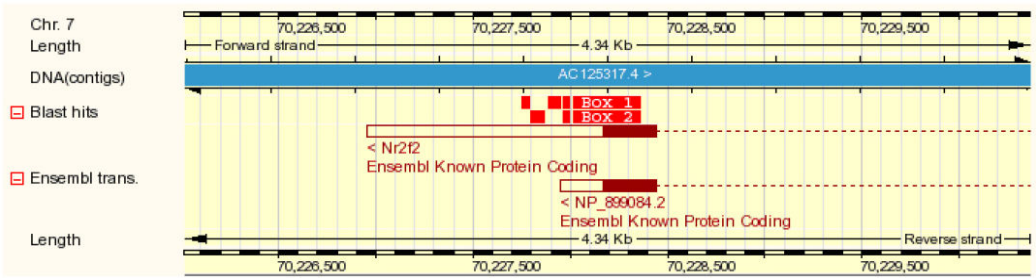

Figure 4.1. Clone D8 of the subtractive hybridization screen matches the *Nr2f2* gene.
(Legend on page 124)

c)

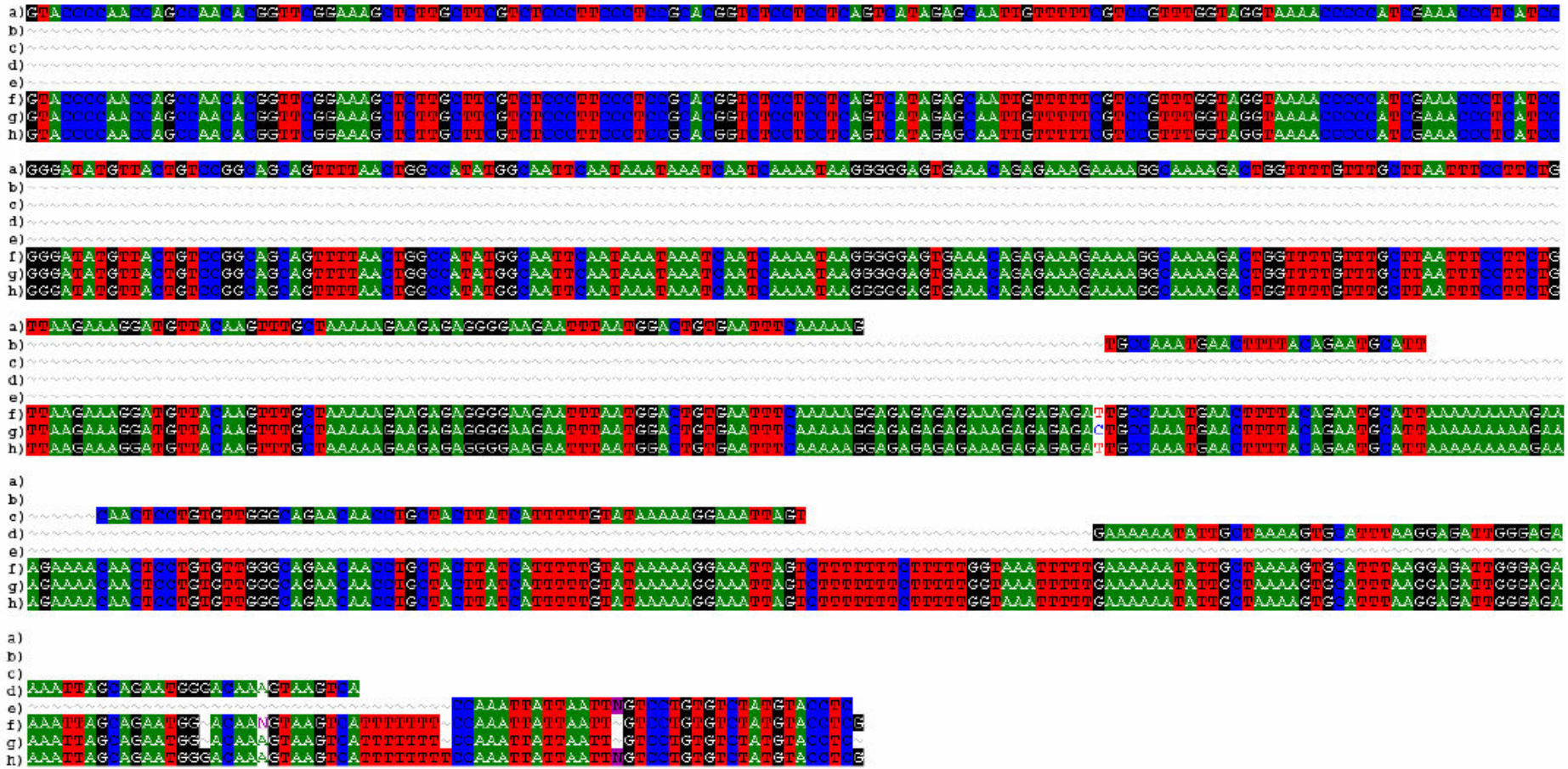

Figure 4.1. Clone D8 of the subtractive hybridization screen matches the *Nr2f2* gene (continued).
a) Adaptor oligonucleotide sequences from the subtractive hybridization screen (*red type*) were identified in the clone sequence in order to verify full sequencing. These sequences were then deleted prior to BLAST analysis, leaving a trimmed sequence (*black type*). *b*) Graphical representation of the sequence match by BLAST analysis from the Ensembl 'ContigView.' The *red boxes* represent clone sequences that match to the two cDNA transcripts represented below in maroon. These transcripts are on the reverse strand of the contig represented above in *blue*. *c*) The alignment of the trimmed forward (*c.f*) and reverse (*c.h*) clone D8 sequence to the *Nr2f2* gene was verified by aligning all of the relevant BLAST matches (*c.a-e*) to the Ensembl sequence for *Nr2f2* (*c.g*).

The remaining matches were found to be in the same genomic region as the most significant match (Figure 4.1.*b*, *red boxes*) and three matched *Nr2f2* but not the overlapping transcript in that region (NP_899084.2). This suggested that *Nr2f2* was the true match to clone D8. However, the BLAST analysis did not report the alignment of regions between matches; as discussed in section 3.3.1, the BLAST software used can fail to identify true homology in low complexity (i.e. repetitive) regions as these regions are filtered out or masked by programs included in the WU-BLAST 2 software package that the Ensembl BLAST tool uses (Gish 2004). Therefore, as a further verification of the match of *Nr2f2* to clone D8, the trimmed clone D8 insert sequence was aligned with the last exon of *Nr2f2* to identify whether the regions between BLAST matches also matched this sequence (Figure 4.1.*c.f*&*h*). All significant BLAST matches to *Nr2f2* were included in the alignment (Figure 4.1.*c.a*-*e*).

This alignment showed that the whole of the clone D8 insert matched the *Nr2f2* transcript in the Ensembl database with high sequence similarity (>99%). Furthermore, homologous regions not identified by BLAST analysis were shown to be of low complexity, as expected. This verified that the clone D8 sequence used in the BLAST analysis matched *Nr2f2* and not NP_899084.2 as the alignment extended beyond the 3' terminal of the latter transcript. Therefore, the clone D8 insert sequence that was reverse transcribed and cloned from an mRNA transcript in the subtractive hybridization screen unequivocally matches the *Nr2f2* transcript in the Ensembl database. As clone D8 was produced from the forwards (upregulated) POU4F3 subtractive hybridization screen, the above match to *Nr2f2* indicates that POU4F3 upregulates *Nr2f2* in UB/OC-2 cells. Therefore, POU4F3 may upregulate *Nr2f2* expression in hair cells.

4.2 Introduction to *Nr2f2*

Nr2f2 was the first gene identified by the POU4F3 subtractive hybridization screen to be investigated. It is a well-characterised member of the steroid/thyroid hormone nuclear receptor superfamily that has commonly been referred to as apoAI regulatory protein-1 (ARP-1) (Ladias *et al.* 1991), COUP-TFII (Ritchie *et al.* 1990) and COUP-TF2 (Wang *et al.* 1991). In this document it is referred to as *Nr2f2* as recommended by the Nuclear Receptors Nomenclature Committee in order to place it in a systematic framework of nuclear receptors based on its phylogeny (Nuclear Receptors Nomenclature Committee. 1999).

4.3 Steroid/thyroid hormone nuclear receptors

The steroid/thyroid hormone nuclear receptor superfamily is a large and well-characterised group of nuclear receptor transcription factors that classically bind steroid/thyroid/vitamin-derived hormone ligands that regulate their function. The binding of the ligand to the nuclear receptor can take place outside the nucleus and induce translocation of the nuclear receptor to the nucleus (reviewed in Benoit *et al.* 2004;DeFranco *et al.* 1998) or, the

typically lipophilic ligand can be transported to the nucleus prior to binding to a nuclearly expressed receptor (e.g. reviewed in Kishimoto *et al.* 2006). Ligand binding classically acts to alter the transcriptional effect of nuclear receptors on their target genes. As the sources of ligands can be systemic, local or exogenous (including xenobiotic compounds), nuclear receptors are involved in both systemic/endocrine signalling (e.g. by steroid hormones) and local/paracrine regulation (e.g. by retinoids), thereby influencing processes from embryonic development to adult homeostasis (reviewed in Beato *et al.* 1995;Benoit *et al.* 2004;Weigel 1996).

4.3.1 Molecular function of steroid/thyroid hormone nuclear receptors

For classical nuclear receptors, ligand binding induces a conformational change in the receptor's ligand-binding domain (LBD) which, in turn, alters the binding of coactivators and corepressors, thus influencing target gene regulation (Beato *et al.* 1995;Weigel 1996). This transcriptional activity is mediated by the two 'activation function' (AF) helices of the nuclear receptor. AF-1 mediates ligand-independent transcriptional activation whilst AF-2 – which is part of the LBD – has ligand-dependent function (Kishimoto *et al.* 2006;Noy 2007;Weigel 1996). When not bound to ligand, the conformation of the AF-2 helix typically facilitates binding of corepressors to the LBD (e.g. HDAC); conversely, the binding of ligand to the LBD induces a conformational change in this protein region that allows binding of coactivators (e.g. HAT) (Gronemeyer *et al.* 2004;Kishimoto *et al.* 2006;Xu *et al.* 1999).

Though co-factors are required for transcriptional regulation of nuclear receptor target genes, their action is often secondary to DNA binding by the nuclear receptor. This DNA-binding function is dependent on the DNA binding domain (DBD) of the protein, which recognises specific response elements in target gene promoters. The canonical hormone response element RGGTCA – in which R is a purine – is modified, extended and duplicated to yield specific response elements for different classes of nuclear receptor (Gronemeyer *et al.* 2004). DNA binding is further modulated by competition for binding sites with other nuclear receptors and by protein-protein interactions. For example, homo- or hetero-dimerisation of nuclear receptors can have both an up and downregulatory effect on transcription and is sometimes required for DNA-binding to palindromic hormone response element half-sites *in vivo* (reviewed in Beato *et al.* 1995;Park *et al.* 2003). Other important protein-protein interactions mediate the shuttling of nuclear receptors between the cytoplasm and nucleus. For example, a 90kDa heat-shock protein (hsp90) is associated with unliganded cytoplasmically-expressed nuclear receptors in order to maintain cytoplasmic expression and dissociates from liganded nuclear receptor, allowing nuclear translocation (DeFranco *et al.* 1998). Though the majority of nuclear receptors are constitutively expressed in nuclei, most steroid-hormone receptors which bind systemically acting ligands shuttle between the cytoplasm and nucleus and this translocation is dependent on associated proteins (reviewed in Benoit *et al.* 2004;Kishimoto *et al.* 2006). Such proteins

might therefore be involved in the controlling the subcellular localization of NR2F2 which is primarily expressed nuclearly, though it has been reported to be expressed cytoplasmically in the rat anterior pituitary gland (Raccurt *et al.* 2006). The final major area of nuclear receptor protein regulation is that of post-translational modification. For example, phosphorylation, ubiquitination and sumoylation of PPARγ (a nuclear receptor involved in development and metabolism) can all affect its function (Burgermeister *et al.* 2007). Therefore, the regulation of nuclear receptor target genes can be controlled at the DNA level (at target gene promoter response elements), by protein-protein interaction (by dimerisation/tetramerisation and nucleo-cytoplasmic shuttling) and by post-translational modification, resulting in complex regulation and function of these genes.

4.3.2 Orphan nuclear receptors

A distinction is drawn between nuclear receptors based on their ligand binding characteristics. Nuclear receptors that display non-classical ligand binding can be described as orphan or promiscuous. Promiscuous nuclear receptors, have affinity for multiple ligands e.g. members of the NR1 receptor subfamily are activated by a number of xenobiotic compounds (reviewed in Noy 2007). At the opposite end of the spectrum, orphan nuclear receptors are those that do or did not have identified ligands; naturally occurring ligands have now been identified for more than half of the human nuclear receptors that were originally termed 'orphan' (reviewed in Willson *et al.* 2002).

Though ligands have now been identified for many 'orphan' nuclear receptors, it has been shown that a number of the remaining orphan receptors are unlikely to utilize ligand signaling. This can be for one of two reasons. Firstly, the ligand binding pocket (LBP) of the receptor can be occupied by a tightly-bound cofactor which is more likely to act as an essential structural component rather than a signaling ligand (e.g. HNF4). Secondly, the LBP of the protein can be blocked by its own bulky amino acid side chains though the receptor can still regulate transcription as the AF-2 helix is folded in an active conformation (e.g. Nurr1) (Benoit *et al.* 2004).

NR2F2 was, until very recently, an orphan steroid/thyroid hormone nuclear receptor that had been categorised as such on the basis of its sequence similarity to Ear-3 (v-erbA-related human receptor-3, also known as COUP-TFI or NR2F1), Ear-2 (NR2F6) and the *Drosophila* gene, Seven-up (Ladias *et al.* 1991;Nuclear Receptors Nomenclature Committee. 1999). Though retinoid acids have now been found to upregulate NR2F2 activity *in vitro*, the ligand for such regulation *in vivo* is unclear as no ligand that is able to bind NR2F2 at physiological concentrations had been identified (Kruse *et al.* 2008). Due to this delay in ligand identification, little is known about NR2F2's endogenous ligand-binding properties whereas its other biological functions are well investigated.

4.4 NR2F2 function and expression

In development, NR2F2 is expressed in a wide range of tissues in a pattern that overlaps with, but is distinct from that of its family member NR2F1 (COUP-TFI) (reviewed in Pereira *et al.* 2000). Its expression was first identified in whole organs by Northern blot (e.g. Ladias *et al.* 1991;Lutz *et al.* 1994), and its localization within organs has since been visualised in skin, brain, spinal cord, salivary gland, oesophagus, thyroid, lung, stomach, intestine, liver, pancreas, kidney, bladder, prostate, testis and ovary primarily by RNA *in situ* hybridization (Lutz *et al.* 1994;Pereira *et al.* 1995;Qiu *et al.* 1994a;Zhang *et al.* 2002). In development, NR2F factors are initially expressed in all three germ layers though their expression becomes more restricted as development progresses. Their level of expression is also modulated throughout organogenesis – NR2F factors are downregulated as organs complete their development (Pereira *et al.* 1995). More recently, knockout and protein expression studies have elucidated many of the suggested roles of NR2F2 and it has been found to be commonly involved in organogenesis.

NR2F2's well-described expression and requirement in organ development is of particular relevance to the present study, as it is known to be expressed in the inner ear in development (see section 4.5.2). Its expression is seen in the otic placode at E8.75 (Tang *et al.* 2005) and subsequently follows a pattern that is comparable to that seen in other organs where it has been shown to be essential for normal patterning (see below). Furthermore, NR2F2 is known to be involved in sensory organ development as its expression in the dorsal retina is thought to mediate dorsal-ventral patterning of this sensory epithelium by interaction with retinoic acid signalling (McCaffery *et al.* 1999) – a signalling pathway that is also important for inner ear development (reviewed in Romand *et al.* 2006).

The most vital developmental function of NR2F2 – in terms of embryonic viability – is in cardiovascular development (Pereira *et al.* 1999). This was demonstrated by *Nr2f2* mutant mice which were generated by disruption of most of exon 1 and the entire exon 2 of the three-exon *Nr2f2* gene. Two-thirds of heterozygous *Nr2f2* mutant mice generated by this method die before weaning and homozygous mutant mice show embryonic lethality at E10 (Pereira *et al.* 1999). This *Nr2f2*$^{-/-}$ phenotype is thought to be due to haemorrhage and oedema in the brain and heart, which is due to defects in angiogenesis, heart development and capillary plexus formation associated with a reduction in Ang1 expression (a gene that is also involved in heart and vascular development) (Pereira *et al.* 1999). Homozygous mutation of *Nr2f2* also caused malformation of the cardinal veins (Pereira *et al.* 1999). This is consistent with observations from a subsequent study in which NR2F2 expression in endothelial cells was ablated, showing that NR2F2 is required for specification of venous identity and is associated with suppression of Notch signalling (You *et al.* 2005a). Like retinoic acid signalling, Notch signalling is required for inner ear development (Fekete *et al.* 2002).

Neurally, NR2F2 is required for normal central nervous system development. It is expressed in the *murine* telencephalon and tectum at day 10.5 p.c. and later shows expression in parts of all three brain compartments (forebrain, midbrain and hindbrain) (Qiu *et al.* 1994a) as is the case in chick development (reviewed in Qiu *et al.* 1994b). In late mouse development, NR2F2 shows highly organised, stripe-like expression in the cerebellum (Yamamoto *et al.* 1999). Functionally, it has been shown to be important for the control of neurogenesis (Park *et al.* 2003), for the guidance of migrating neurons (Tripodi *et al.* 2004) and, with NR2F1, is important in the acquisition of gliogenic competency (the ability to differentiate into glial cells) (Naka *et al.* 2008). Caudally, NR2F2 has been implicated in the development of spinal motor neurons by studies in the developing chick which showed its transient expression in the ventral spinal cord in a region where motor neurons are known to develop (Lutz *et al.* 1994). Furthermore, it is expressed in the substancia gelatinosa of the spinal cord in the chick and mouse, a region known to give rise to sensory neurons. However, by 18.5 days p.c. NR2F2 is expressed in the whole of the mouse spinal cord, suggesting a differing maintenance role following cord development (Qiu *et al.* 1994a;Qiu *et al.* 1994b).

These observations are consistent with NR2F2's developmental theme of organ patterning and cell fate determination, a theme that is continued in other systems. In the stomach, NR2F2 has been shown to be important for radial and anteroposterior patterning by a conditional knockout that showed defects consistent with a model of *Nr2f2* regulation by *Hedgehog* signalling in this system (Takamoto *et al.* 2005b). Conditional *Nr2f2* knockout mice also demonstrated that NR2F2 expression in the developing foregut is required for normal diaphragmatic development: homozygous conditional knockout mice had reduced survival compared to heterozygous littermates due to lung hypoplasia secondary to herniation by the liver and stomach through the diaphragm. This defect is consistent with a human form of congenital diaphragmatic hernia which is likely to be due to heterozygous *Nr2f2* deletion (You *et al.* 2005b).

More peripherally, NR2F2 has been implicated in limb and skeletal muscle development. Chimera analysis and conditional knockout of *Nr2f2* in embryos showed that NR2F2 is required for normal limb bud outgrowth and myogenesis in the developing mouse (Lee *et al.* 2004). Finally, NR2F2 is predicted to be required for lung, liver and pancreatic organogenesis (Kimura *et al.* 2002;Zhang *et al.* 2002). Its role in the latter organ has been investigated by conditional *Nr2f2* knockout in pancreatic beta-cells which resulted in glucose intolerance in heterozygotes and embryonic lethality of unknown mechanism in homozygotes (Bardoux *et al.* 2005). This metabolic involvement is continued postnatally (see below).

The above roles of NR2F2 in organogenesis illustrate that this nuclear receptor is essential for the normal development of a number of systems via differing processes i.e. cell fate determination, regulation of cell cycle and maintenance of cell survival, as supported by data from species other than mouse and chicken, namely *Drosophila, Xenopus and C. elegans*. Furthermore, NR2F2 has been suggested to play a role in mesenchymal-endothelial/epithelial signalling (reviewed in Pereira *et al.* 2000). These functions are consistent with a potential role for NR2F2 in inner ear development.

Though NR2F2 expression displays its greatest variability in development and is reduced on completion of organogenesis (Pereira *et al.* 2000), it is still widely expressed postnatally (see below). In the inner ear, POU4F3 is also expressed postnatally (Erkman *et al.* 1996). If *Nr2f2* is, indeed, upregulated by POU4F3, then its known postnatal functions may aid understanding of POU4F3-dependent postnatal maintenance of hair cell survival (Vahava *et al.* 1998).

NR2F2 is expressed in all postnatal adult human organs examined (primarily in mesenchymal cells) and particular note was taken of its expression in the lung, kidney, gastrointestinal tract, liver, spleen and in the reproductive and endocrine systems (Suzuki *et al.* 2000). This study did not investigate the postnatal expression of NR2F2 in human neuronal tissues though, in the mouse brain, NR2F2 was found to be predominantly expressed in the middle part of the brain, amygdaloid nucleus and arachnoid membranes with lower expression seen in regions neighbouring the hypothalamus and in the choroid plexus (da Silva *et al.* 1995). Subsequent study of NR2F2 in the rat showed that it is also expressed in the pituitary, where it was found to be primarily expressed in lactotropes (prolactin-producing cells) in both the cytoplasm and the nucleus. This study also demonstrated that postnatal NR2F2 expression can be dynamic as both its cytoplasmic and nuclear expression was upregulated in pregnancy (Raccurt *et al.* 2006).

Outside the brain, NR2F2 has been implicated in menstruation (Sato *et al.* 2003), steroidogenesis in the ovary (Murayama *et al.* 2008) and embryo implantation (Takamoto *et al.* 2005a). Its expression varies with the Hedgehog family genes *Indian Hedgehog* and *Desert Hedgehog* (Katayama *et al.* 2006), probably due to regulation by *Sonic Hedgehog* (Shh), which has been shown to directly upregulate transcription at a response element in the *Nr2f2* promoter (Krishnan *et al.* 1997) though a direct interaction has not been shown. As Shh signalling has been shown to be important in inner ear patterning, its interaction with *Nr2f2* provides a potential avenue by which NR2F2 might be involved in inner ear development and function (reviewed in Bok *et al.* 2007).

NR2F2 is also thought to play a role in mesenchymal-epithelial signalling e.g. by mediating epithelial oestrogen receptor expression (Kurihara *et al.* 2007) and this may suggest a

potential role for NR2F2 in hearing maintenance, a function in which the oestrogen receptor has been implicated (Hultcrantz *et al.* 2006). Therefore, NR2F2 appears to be involved at multiple levels of complex biochemical pathways, though its *in vivo* roles require further characterisation. Much work would be required to elucidate whether NR2F2 forms part of such signalling cascades in the inner ear and what effect this may have on hearing. Furthermore, many of these potential interactions have been identified through knockout studies. Though this allows us to see the endpoint of NR2F2 manipulation, it does not establish the mechanism of such interactions that can be elucidated through molecular studies.

4.5 Initial selection of *Nr2f2* as a candidate gene for investigation

4.5.1 Analysis of known function and expression of NR2F2

As many candidate genes were identified by the subtractive hybridization screen (Table 3.1), the known functions of these genes were investigated to identify those with greater potential relevance to hair cell maintenance and development. An efficient method of identifying gene functions and quality of evidence was required and a rapid method of assessing the available information on the function of a protein is to examine its Gene Ontology (GO) units, which are available in the Ensembl genome browser (see section 3.3.2).

NR2F2 had 15 such units assigned to it at the time of this analysis (reproduced in Table 4.1). Ten were based on experimental evidence and five were computationally predicted. This was the largest number of verifiable GO units identified for any candidate gene reflecting both the level of characterisation of this gene and the breadth of functions it has been reported to have.

The GO units in Table 4.1 correctly identified that NR2F2 is a nuclear receptor transcription factor with primarily nuclear expression and that it is involved in metabolism and developmental patterning i.e. the main features of NR2F2 that were known at the time of the analysis. Based on this, *Nr2f2* was selected for further investigation. This was because its ability to act as a transcriptional regulator in development and direct organ patterning (particularly in neuronal systems) could place it at a pivotal point in the genetic pathways of hair cell development and inner ear patterning (e.g. Tripodi *et al.* 2004). Furthermore, though an endogenous ligand has not been identified, the high conservation of its ligand binding domain (LBD) and the ability of retinoids to modulate its function suggest that a ligand does exist (Kruse *et al.* 2008), and this potential for ligand-regulated activity makes NR2F2 a potential drug target (Kruse *et al.* 2008).

Table 4.1. *Nr2f2* GO units.
IDA, inferred from direct assay; *IEA*, inferred from electronic annotation; *TAS*, traceable author statement; *IMP*, inferred from mutant phenotype.

	GO ID	*GO Term*	*Evidence Code*
Cellular component	GO:0005634	Nucleus	TAS
Molecular function	GO:0003700	Transcription factor activity	IEA
	GO:0003706	Ligand-regulated transcription factor activity	TAS
	GO:0003707	Steroid hormone receptor activity	IEA
	GO:0003714	Transcription corepressor activity	TAS
	GO:0008270	Zinc ion binding	IEA
	GO:0046872	Metal ion binding	IEA
Biological process	GO:0001764	Neuronal migration	IDA, IEA
	GO:0006350	Transcription	IEA
	GO:0006357	Regulation of transcription from Pol II promoter	TAS
	GO:0006629	Lipid metabolism	TAS
	GO:0007165	Signal transduction	TAS
	GO:0009952	Anterior/posterior pattern formation	IEA, IMP
	GO:0009956	Radial pattern specification	IEA, IMP
	GO:0030900	Forebrain development	IDA, IEA

4.5.2 Reported expression pattern of NR2F2 in the inner ear

Following initial selection of candidate genes for further study, their known expression and function in the inner ear was investigated in order to help judge their potential relevance to hair cell development and survival. The literature and online databases of gene expression were searched to determine candidate gene expression patterns. *Nr2f2* was the only prioritised gene from the pool described (see Table 3.2) with histologically verified expression in the inner ear. Its expression pattern was described in a single report where RNA *in situ* hybridization and immunohistochemistry were used to identify *Nr2f2* mRNA and protein in the developing mouse cochlea (Tang *et al.* 2005).

Nr2f2 expression has been detected as early as E8.75 in the otic placode by RNA *in situ* hybridization (Tang *et al.* 2005). It is expressed in the ventral-anterior domain and its expression extends posteriorly by E9.75 to include the ventral-posterior domain. Between E10 to E13.5 it was only detected in the distal tip of the extending cochlear duct floor. This changes by E15.5, a stage at which hair cells are maturing at the junction of the greater and lesser epithelial ridges (see Figure 1.5*d*). At this stage NR2F2 expression spanned the greater and lesser epithelial ridges and supero-medial wall of the apical cochlear duct; it is more restricted to the lesser epithelial ridge in the middle turn and only shows faint expression in the lesser epithelial ridge basally (Tang *et al.* 2005). This expression in the organ of Corti is reported to reduce to undetectable levels postnatally, as examined by immunohistochemistry (Tang *et al.* 2005).

Expression of NR2F2 in the developing sensory epithelium at E15.5 in the mouse is consistent with a potential role in hair cell development. Furthermore, its expression is likely to overlap with that of POU4F3, supporting a possible regulatory relationship in developing hair cells and making *Nr2f2* a suitable gene for further investigation. However, a lack of postnatal NR2F2 expression would mean that it is not involved in hair cell survival. Given that the NR2F2 inner ear expression pattern is described in a single report and that the inability to detect its expression postnatally may be due to antibody sensitivity, I investigated NR2F2 expression at late developmental and early postnatal stages. In order to do this, an affinity-purified anti-NR2F2 rabbit polyclonal antibody was obtained from a collaborator (Dr Michelè Studer (Tripodi *et al.* 2004)). This antibody was different to the antibody previously used to investigate the NR2F2 expression pattern in the inner ear though it was raised against the same region in NR2F2 (the N terminal of the protein that is most divergent from NR2F1). The specificity of the antibody had previously been checked by our collaborators by western blotting and immunohistochemistry with immunogen blocking and was found to recognise NR2F2 without cross-reactivity to NR2F1, though the data for this analysis were not shown in the reporting paper (Tripodi *et al.* 2004).

4.6 Verification of NR2F2 expression in UB/OC-2 cells

4.6.1 Immunoblot to examine NR2F2 expression in cell lines

Prior to investigating NR2F2 expression in the inner ear, its expression in UB/OC-2 cells was assessed in order to test antibody specificity and verify translation of *Nr2f2* mRNA detected in UB/OC-2 cells by RT-PCR (see Figure 3.1). Protein expression was first assessed by western immunoblotting to assess antibody specificity by determining the molecular weight of any protein recognised. This method has the additional benefit of being able to identify any alternative NR2F2 isoforms that might be present in this inner ear cell line (though only one *Nr2f2* transcript is known in the mouse (Ensembl 2008b)). Non-POU4F3-expressing undifferentiated UB/OC-1 cells (derived from E13 immortomouse sensory epithelium like UB/OC-2 cells (Rivolta *et al.* 1998a)) were included for comparison.

Undifferentiated UB/OC-1 and UB/OC-2 whole cell protein extract was electrophoresed on a denaturing 10% polyacrylamide gel prior to electroblotting onto a PVDF membrane and immunodetection. The results of this analysis are shown in Figure 4.2. A strong band of approximately 50kDa and a weaker band of approximately 55kDa is seen for both UB/OC-1 and UB/OC-2 protein extract. The predicted size of the NR2F2 protein is 46kDa and two antibody catalogues show the protein size to be reported as 46kDa (Abcam) and 50kDa (Abnova). In these catalogues, both antibodies were tested against human NR2F2 (from HepG2 and 293T cells) which is identical in its peptide sequence to mouse NR2F2. The difference in sizing between the 50kDa band in Figure 4.2, the Abnova data and the Abcam data may be due to differential post-translational modification of the protein, but its molecular weight is within the sensitivity range of the western immunoblot protocol.

The less dense band of approximately 55kDa in Figure 4.2 appears similar to an extra band found in the Abcam western immunoblot and, though the immunogen is unknown, it probably represents a modified protein isoform rather than a non-specific target of the anti-NR2F2 antibody used as it has been identified by two different antibodies (our collaborator's and Abcam's). It is unlikely to be the product of an alternative transcript as only one *Nr2f2* transcript is known (Ensembl 2008b) and it is unlikely to represent cross-reactivity to NR2F1 as any such band would be expected to be of slightly lower molecular weight (45kDa) (Raccurt *et al.* 2006). Furthermore, the antibody used was raised against a divergent NR2F region and has previously been reported not to recognise NR2F1 (Tripodi *et al.* 2004). As this experiment was carried out to determine antibody specificity rather than relative expression levels between cell types, equality of protein loading between lanes was not checked by equalisation with a housekeeping gene. Therefore, though the density of the 55kDa band appears different in UB/OC-1 and UB/OC-2 cells, it is not possible to determine if the antigen is differentially expressed between these two cell types.

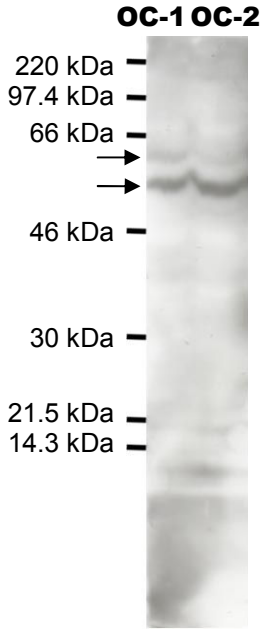

Figure 4.2. Expression of NR2F2 in UB/OC-1 and UB/OC-2 cells.
NR2F2 is detectable in UB/OC1 and UB/OC-2 cells as a strong band of 50kDa and a weaker band of 55kDa (*arrows*). According to two reports, the molecular weight of NR2F2 is 46kDa (Abcam 2008) or 50kDa (Abnova 2008b). A difference of 4kDa is not beyond the limits of error in such an experiment and this immunoblot is therefore consistent with both of these reports.

This western immunoblot therefore shows that the antibody used is able to detect NR2F2 which is expressed in UB/OC-1 and UB/OC-2 cells. Its expression in UB/OC-1 cells is consistent with its reported inner ear expression pattern where NR2F2 is expressed in the developing sensory epithelium from which these cells are derived prior to the onset of POU4F3 expression (Tang *et al.* 2005), demonstrating that POU4F3 is unlikely to be required for its expression. The latter conclusion is not surprising given that NR2F2 is known to be expressed in many non-POU4F3 expressing cells (e.g. Tripodi *et al.* 2004). These possibilities, coupled with the reported work demonstrating the sensitivity of the antibody (Tripodi *et al.* 2004) demonstrate that it specifically recognises NR2F2 and is therefore suitable for the investigation of NR2F2 expression in the inner ear.

4.6.2 Immunohistochemistry to detect NR2F2 in UB/OC-2 cells

Having shown the specificity of the antibody obtained for NR2F2, it was used for immunofluorescence immunohistochemistry in UB/OC-2 cells. This was done to identify if NR2F2 is expressed in all cells in the monolayer and whether its subcellular localization in these cells is nuclear, as is expected – it has only been found to be expressed cytoplasmically in the rat pituitary gland (Raccurt *et al.* 2006). Though the suitability of the antibody for immunofluorescence microscopy had been previously demonstrated (Tripodi *et al.* 2004), this experiment provided the opportunity to optimise the immunofluorescence protocol for later use in the study of rodent inner ear tissue which is harder to obtain and prepare.

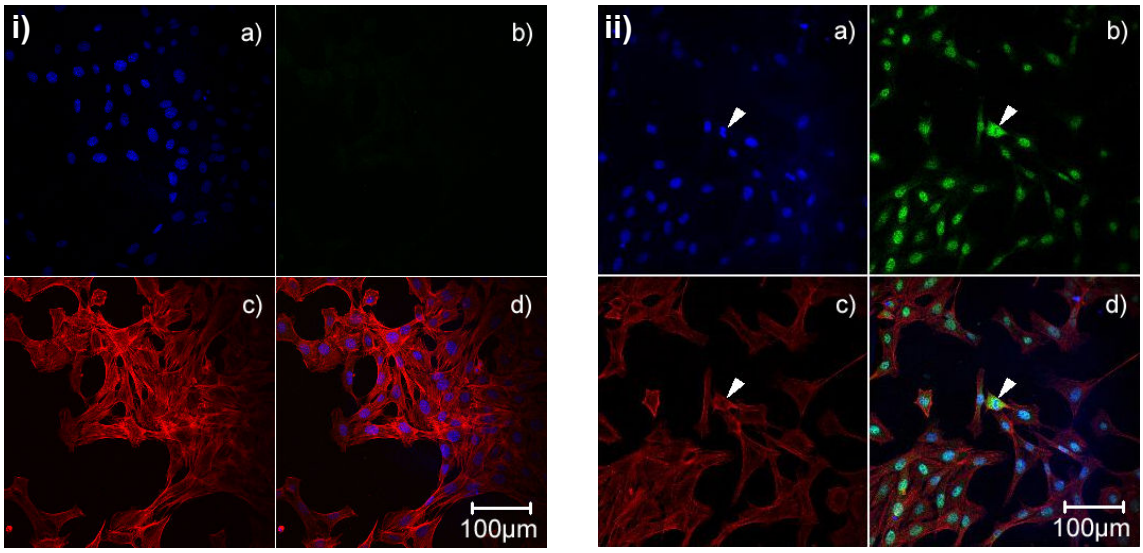

Figure 4.3. NR2F2 expression in undifferentiated (proliferating) UB/OC-2 cells.
NR2F2 is expressed in cell nuclei visualised by immunofluorescence microscopy (*green*, *ii.b* & *ii.d*). Anti-rabbit IgG alone (*i.b*) does not show any signal showing that staining in *ii.b* is specific to the anti-NR2F2 antibody. *i.a & ii.a*) DAPI, a fluorescent stain that binds to DNA and therefore labels cell nuclei; *i.b*) Alexa 488-conjugated anti-rabbit IgG; *ii.b*) anti-NR2F2 (primary antibody) and Alexa 488-conjugated anti-rabbit IgG (secondary antibody); i.*c & ii.c*) Alexa 633-conjugated Phalloidin, a toxin that binds to filamentous actin; i.*d & ii.d*) Merge. Images were taken using identical settings through a 20x objective. *Arrowhead*, mitosing or apoptosing cell.

UB/OC-2 cells were grown to 80% confluence on glass coverslips, fixed and immunolabelled prior to visualisation by fluorescence microscopy with a Zeiss LSM 510 Meta microscope (see Figure 4.3.*ii*). The non-specific (background) labelling pattern of the secondary antibody used (Alexa 488-conjugated anti-rabbit IgG) was also ascertained in these cells in order to verify its specificity and the efficacy of the blocking solution used by omission of anti-NR2F2 antibody from these slides (Figure 4.3.*i*).

Figure 4.3 shows that fluorescent signal is detected for NR2F2 in a pattern that overlaps with that of DAPI and not phalloidin in all but one cell (Figure 4.3.*arrowhead*). These results indicate that NR2F2's subcellular localization in undifferentiated (proliferating) UB/OC-2 cells is nuclear and that NR2F2 is expressed uniformly in UB/OC-2 cells. They also confirm that the antibody used is suitable for immunohistochemistry and that the antibody concentration and blocking solution used are appropriate for this application. I therefore proceeded to use the anti-NR2F2 antibody at the dilution described to investigate NR2F2 expression in the rodent inner ear.

4.7 Immunohistochemistry for NR2F2 in rat and mouse inner ear tissue

As previously described (see section 4.5.2), there is only one report of NR2F2 expression in the inner ear which showed expression in the developing mouse and did not identify postnatal NR2F2 expression in the organ of Corti (Tang *et al.* 2005). I therefore re-examined its expression at late developmental and early postnatal stages in the rat (sections 4.7.1 and 4.7.2) and mouse (section 4.7.3). Particular attention was paid to NR2F2 expression in relation to POU4F3 expression in order to identify any correlation in the expression of the two genes that might indicate whether POU4F3 could modulate *Nr2f2* activation in the inner ear. However, the known expression of NR2F2 in cells that do not express POU4F3 (e.g. Figure 4.2) suggests that such a modulation may be subtle as POU4F3 is unlikely to be required for *Nr2f2* expression.

4.7.1 NR2F2 expression in the embryonic rat inner ear

POU4F3 is known to be expressed in the inner ear at E18.5 in the rat with stronger expression in the base than in the apex (Erkman *et al.* 1996). Therefore, this age was chosen for the investigation of embryonic NR2F2 expression as it provides a gradient of POU4F3 expression to which NR2F2 expression could be compared.

Cryosections were prepared from E18 rat cochleas and immunofluorescence immunohistochemistry was carried out with the antibody described (see section 4.6). Figure 4.4 shows that NR2F2 expression was seen in many cell types in the developing cochlea. Though it was diffusely expressed, strong expression was seen in the cells of the cochlear duct. However, this expression was not uniform throughout the turns of the developing cochlea. In the apical and middle turns, expression is seen in the supero-medial wall, greater epithelial ridge (GER) and lesser epithelial ridge (LER). The supero-medial wall gives rise to the cells of Reissner's membrane whereas the GER and LER both contribute to hair cell development and other cell types of the sensory epithelium (see section 1.3.1). In contrast to widespread NR2F2 expression in the apical and middle turns, basal expression was primarily restricted to the LER.

This expression pattern is consistent with that of the developing mouse (Tang *et al.* 2005). Expression of NR2F2 in the basal E18 cochlea (Figure 4.4*a*, *j*-*m*) is likely to overlap with that of POU4F3 (see Figure 1.9*a*) (Erkman *et al.* 1996), supporting the hypothesis that modulation of *Nr2f2* expression by POU4F3 in hair cells may occur and be relevant to hair cell development. Colocalisation of the two proteins would provide stronger evidence for this; however, I was not able to establish this due to the lack of a suitable anti-POU4F3 antibody. Furthermore, apical cochlear duct NR2F2 expression (Figure 4.4*a*-*e*) and NR2F2 expression outside the developing sensory epithelium suggests a separate (POU4F3-independent) role for NR2F2 in the developing rat cochlea.

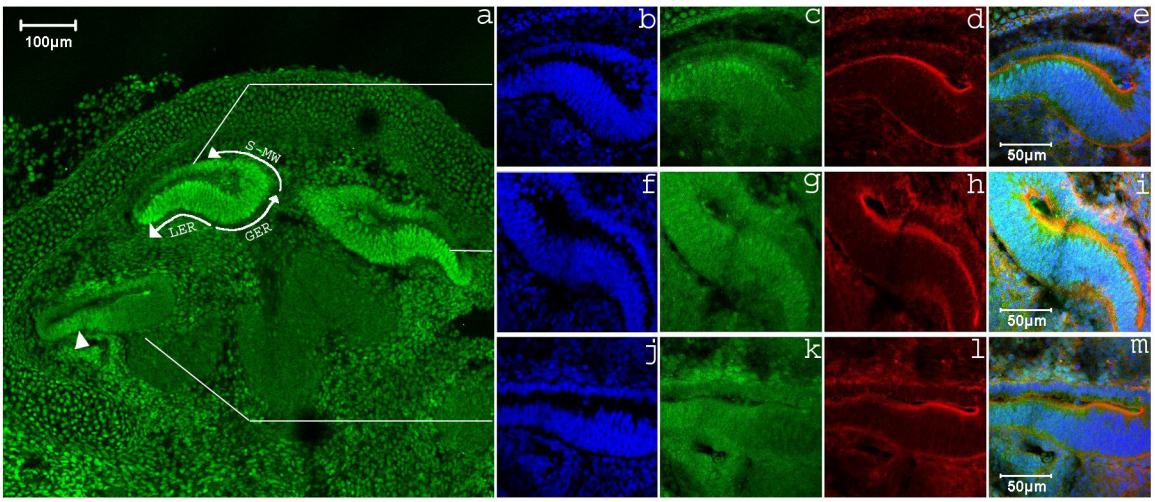

Figure 4.4. NR2F2 expression in the E18 rat cochlea.
a) NR2F2 labelling in E18 rat cochlea is strongest in the apical cochlear duct in the lesser epithelial ridge (*LER*), greater epithelial ridge (*GER*) and supero-medial wall (*S-MW*), where NR2F2 labelling (*green*) overlaps with the nuclear marker, DAPI (*blue*) consistent with nuclear expression (*b-e*). Phalloidin, a marker of filamentous actin, is labelled in *red*. In the middle cochlear turn (*f-i*), NR2F2 labelling is similar to that in the apex whereas in the basal turn (*j-m*), it is restricted to the LER (*arrowhead*).

4.7.2 NR2F2 expression in the postnatal rat inner ear

NR2F2 expression was further characterised by looking at its expression in postnatal rat inner ears. POU4F3 expression has been reported to be maintained into adulthood in rats (Erkman *et al.* 1996) and, therefore, any regulatory relationship between POU4F3 and *Nr2f2* may be relevant beyond the gestational period. P0, P4 and P8 rat cochleas were prepared similarly to E18 tissue and examined. The same antibody was used to immunolabel this tissue as was used for embryonic rat tissue.

This analysis, summarised in Figure 4.5, showed that NR2F2 is expressed postnatally in many cell types of the postnatal rat cochlea up to and including P8 (the latest age examined) with consistent expression in the Hensen cell nuclei. At P0 and P4, NR2F2 is expressed in the nuclei of all cells examined including the POU4F3-expressing hair cells (Erkman *et al.* 1996). This is also true of the P8 apical cochlea though, in the basal turn at P8, there is a shift from nuclear to cytoplasmic NR2F2 expression in hair cells.

This expression pattern suggests that NR2F2 continues to function in the organ of Corti postnatally. As it is expressed in hair cells, which are known to express POU4F3, the suggested modulation of *Nr2f2* expression by POU4F3 could continue beyond gestation. Also, the cytoplasmic expression of NR2F2 in the basal P8 rat cochlear hair cells (Figure 4.5) suggests that NR2F2 may be subject to regulation at the protein level in hair cells. Cytoplasmic NR2F2 expression has only been reported in the rat pituitary, though the significance and mechanism of this change in subcellular localization has not yet been

investigated (Raccurt *et al.* 2006). NR2F2 expression would have to be investigated from P8 to adulthood to identify the duration of its expression in rat hair cells and, therefore, its potential regulation by POU4F3. Such experiments would clarify the timing of the nuclear to cytoplasmic transition in NR2F2 expression, and whether this transition is dynamic or transient.

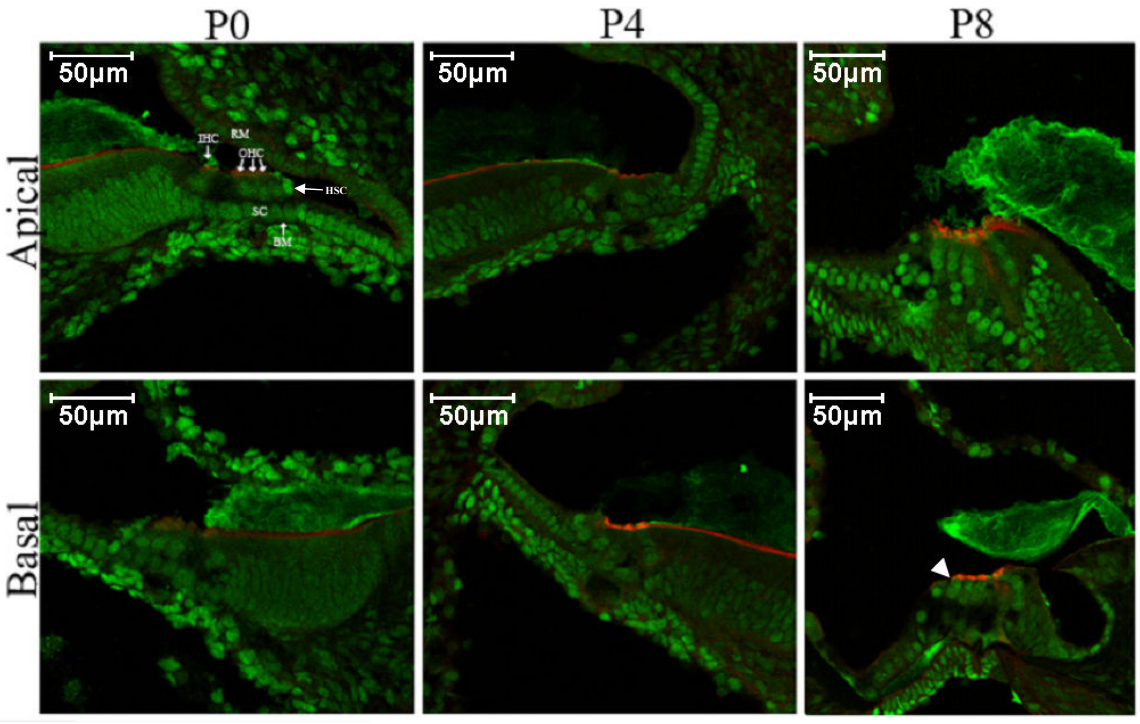

Figure 4.5. NR2F2 expression in the postnatal rat cochlea.
The basal and apical expression profiles of NR2F2 in the organ of Corti were examined at P0, P4 and P8 with two cochleas examined at each age. Representative images of this analysis are shown. *Green*, anti-NR2F2 IgG; *red*, phalloidin. NR2F2 is seen to be expressed in the nuclei of both inner and outer hair cells which are identified by Phalloidin labelling of their stereocilia. Nuclear NR2F2 expression is seen in all areas examined except for the P8 basal region where NR2F2 appears to be expressed in the hair cell cytoplasm (*arrowhead*). Many cells that line the scala media maintain NR2F2 expression, particularly the Hensen cells (*HSC*). *RM*, Reissner's membrane; *IHC*, inner hair cell; *OHC*, outer hair cell; *SC*, support cell; *BM, b*asilar membrane.

4.7.3 NR2F2 expression in the postnatal mouse inner ear

The identified postnatal expression of NR2F2 in the rat cochlea, coupled with its known postnatal functions in other organs (see section 4.4), give NR2F2 the potential to be involved in maintenance functions in the postnatal inner ear. However, it has previously been reported that NR2F2 expression reduces to undetectable levels in the postnatal mouse organ of Corti (Tang *et al.* 2005). Therefore, NR2F2 expression in the postnatal mouse inner ear was examined using the same antibody that was used in the postnatal rat to investigate whether the observed difference in NR2F2 expression was due to variation between species, different antibody/protocol sensitivity or dynamic variation in expression. P0 mouse cochleas were dissected and fixed as for previous immunofluorescence experiments.

However, the organ of Corti and crista ampullaris were immunolabelled as whole mount preparations instead of cryosections. In the organ of Corti, NR2F2 expression was found in the apex (Figure 4.6) where it was most clearly seen in the Hensen cell nuclei. In contrast to the organ of Corti, NR2F2 expression was seen in hair cells in the P0 mouse crista ampullaris as well as other cells in the ampulla (Figure 4.7). This is the first report of NR2F2 expression in vestibular hair cells.

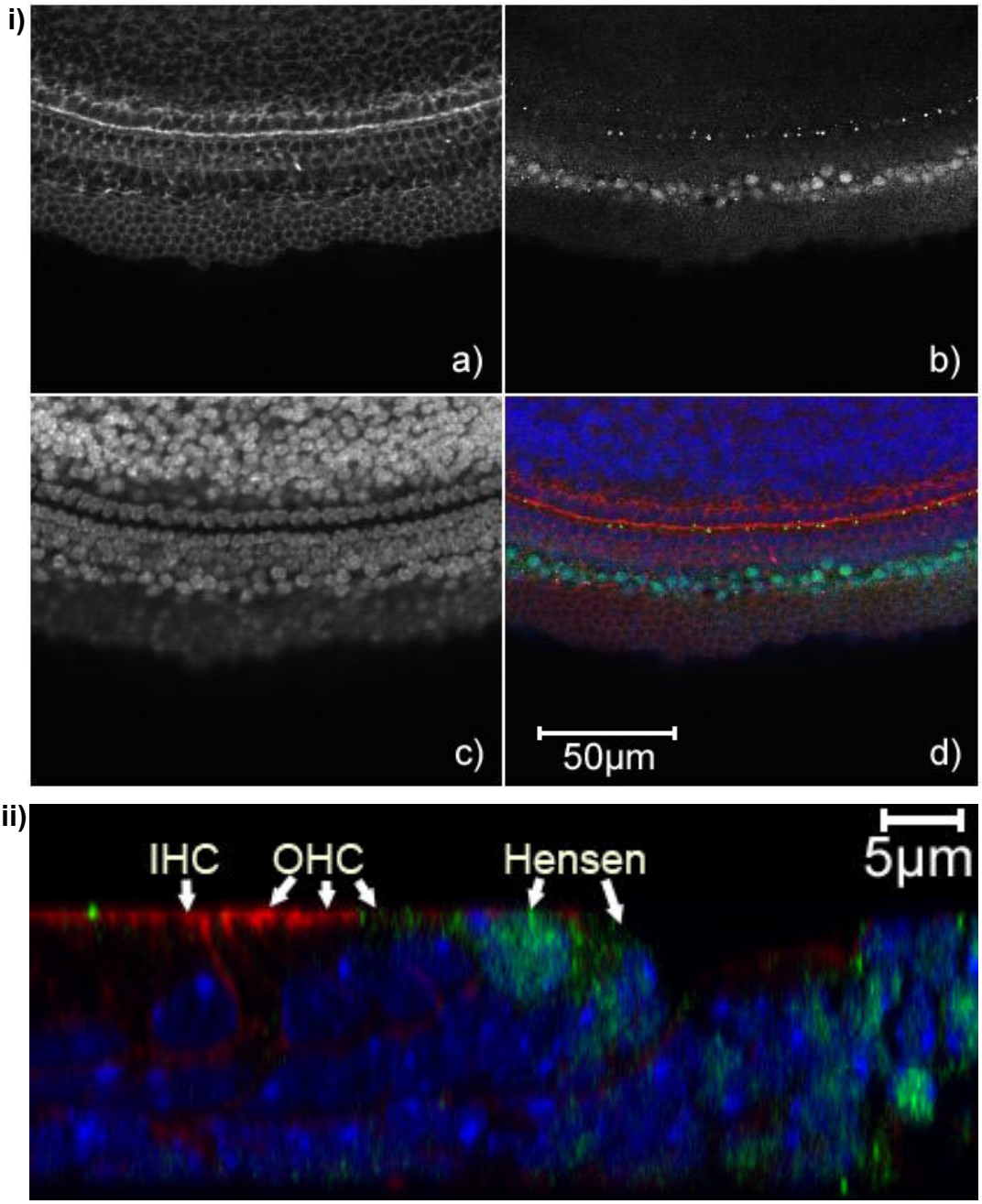

Figure 4.6. NR2F2 expression in the postnatal mouse cochlear apex.
i) An optical section of the whole-mount apical P0 mouse organ of Corti at the level of the hair cell nuclei. NR2F2 was very weakly expressed in the hair cell nuclei, but clearly expressed in the adjacent Hensen cell nuclei in the two animals examined. *a*) Phalloidin, *b*) anti-NR2F2 rabbit IgG, *c*) DAPI, *d*) Merge. *ii*) Orthogonal view. *IHC*, inner hair cell; *OHC*, outer hair cell. *Red*, phalloidin; *green*, anti-NR2F2 rabbit IgG; *blue*, DAPI. NB, hair bundles are flattened due to the coverslip placed on the tissue.

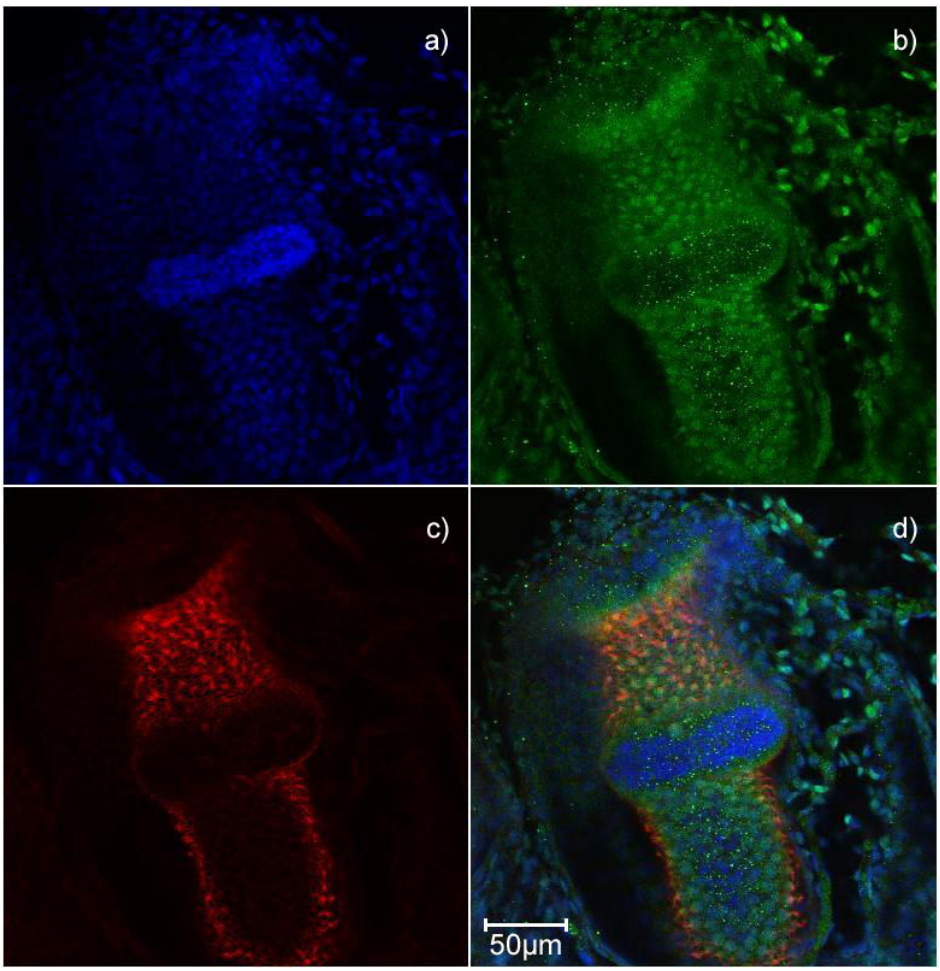

Figure 4.7. NR2F2 expression in the P0 mouse crista.
Widespread NR2F2 expression is seen in the P0 mouse crista. Notably, it is expressed in the sensory hair cells in this sensory epithelium. *a*) DAPI, *b*) anti-NR2F2 rabbit IgG, *c*) Phalloidin, *d*) Merge.

These results contrast both with those previously reported in the mouse organ of Corti (Tang *et al.* 2005) and those found in the postnatal rat inner ear (see Figure 4.5). The discernible differences between this study and the previous report of NR2F2 expression in the postnatal mouse inner ear are the mouse strain and the antibody used. Though different mouse strains show variation in hearing maintenance – there is differing susceptibility to ARHL in commonly used mouse strains (Friedman *et al.* 2007;Spongr *et al.* 1997) – there is no reported difference in the rate of organ of Corti development between mouse strains. Therefore, the differences between the antibodies used are most likely to explain the difference in detection of NR2F2 expression in the postnatal mouse organ of Corti. However, NR2F2 expression may be dynamically regulated or variable at this stage and more animals (from different litters) would have to be examined to clarify the observed NR2F2 expression pattern in the early postnatal mouse inner ear.

The differences between NR2F2 expression in the mouse and rat organ of Corti could be due to differences in antibody sensitivity, interspecies differences in organ of Corti

development or true differences in NR2F2 expression between the two species. Though rat and mouse NR2F2 differ by a single residue that is within the region to which the antibody was raised, this is unlikely to explain the difference in rat and mouse expression patterns (Tang *et al.* 2005). This is because labelling of NR2F2 expression in the developing rat cochlea matches that previously reported in the mouse. Furthermore, the antibody used recognises a single band of identical molecular weight to that found in UB/OC-2 cells when used in western blot analysis of a neuronal cell line which is a hybrid of rat and mouse cells, ND7 (data not shown).

Rat and mouse gestation periods vary (approximately 21 days for mice and up to 24 days for rats), and the inner ears of mice and rats consequently mature at different rates. The difference seen between the mice and rats investigated may therefore be explicable by this developmental difference and NR2F2 expression would have to be investigated with markers of hair cell development (e.g. prestin) to account for these differences (Bryant *et al.* 2005). Also, investigations of rat inner ears at later stages than those reported may help explain if the differences seen are due to slower rat development. Such analyses would help identify whether the differences seen are due to a true difference in the expression of NR2F2 in the developmental organ of Corti between mice and rats.

In summary, it appears that NR2F2 is expressed in developing hair cells and that its expression in hair cell nuclei falls as hair cells mature from base to apex in the late embryonic (mouse) or early postnatal (rat) organ of Corti. NR2F2 expression therefore declines despite reported rises and maintenance of POU4F3 expression in hair cells in the same period (Hertzano *et al.* 2007;Ryan 1997). Furthermore, NR2F2 expression in the hair cells of the crista ampullaris (which also express POU4F3) appears to be maintained to later stages than in cochlear hair cells (Xiang *et al.* 1998). It is, therefore, possible that POU4F3 influences activation of the *Nr2f2* promoter in developing hair cells (when their expression overlaps), as suggested by the subtractive hybridization screen. POU4F3 may be one of a number of transcription factors acting at the *Nr2f2* promoter in developing hair cells whose combined action and interaction determine the rate of *Nr2f2* transcription. Furthermore, the embryonic NR2F2 expression pattern seen combined with the known functions of NR2F2 (see section 4.4) suggest a potential role for NR2F2 in cochlear organogenesis. Therefore, *Nr2f2* was further pursued as a candidate target of POU4F3 and the effect of POU4F3 on the *Nr2f2* promoter was investigated in order to identify whether POU4F3 has a direct effect on *Nr2f2* transcription and in order to verify that *Nr2f2* is upregulated by POU4F3, as suggested by the subtractive hybridization results.

4.8 Does POU4F3 directly activate the *Nr2f2* promoter?

Several *Nr2f2* regulatory elements have been identified, ranging from distal enhancer regions to proximal transcription factor binding sites. Of these sites, a number are responsive to members of signalling cascades with which NR2F2 has been shown to interact i.e. the retinoic acid, notch and hedgehog pathways (see sections 4.4). The schematic diagram in Figure 4.8 shows the regions and factors that have been shown to affect *Nr2f2* regulation. Of these, four have been shown to interact with the *Nr2f2* promoter – Notch (Diez *et al.* 2007), retinoic acid (RA) (Qiu *et al.* 1996), sonic hedgehog (Shh) (Krishnan *et al.* 1997) and the E26 transformation-specific family member, Ets-1 (Petit *et al.* 2004) – though the interaction of POU4F3 with this promoter has not previously been assessed.

As the subtractive hybridization screen suggests that *Nr2f2* is upregulated by POU4F3, the mechanism of this potential interaction was investigated to identify if POU4F3 might produce an increase in *Nr2f2* expression by a direct or indirect mechanism. A direct interaction would require POU4F3 binding to transcription factor binding sites in the *Nr2f2* promoter and mediating an increase in the rate of *Nr2f2* transcription. An indirect mechanism would require POU4F3 to regulate a different target gene that would subsequently interact directly with the *Nr2f2* gene promoter.

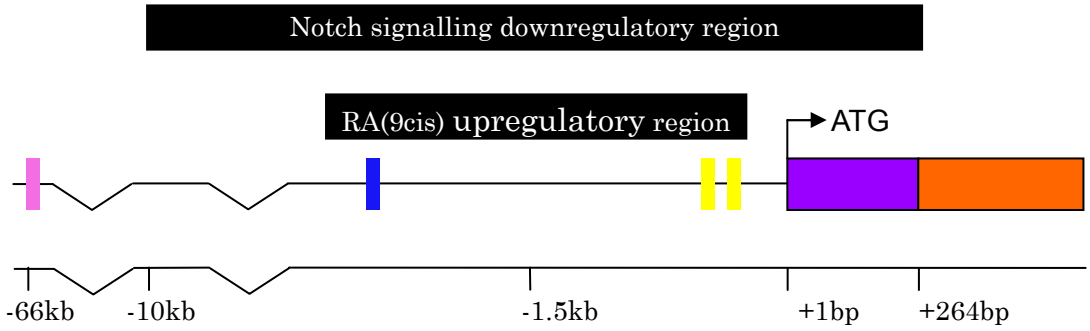

Figure 4.8. Schematic representation of *Nr2f2* regulation.
Schematic of the factors that influence human and mouse *Nr2f2* transcription and the sites at which they act. *RA*, retinoic acid; *pink box*, 571bp liver enhancer region at -66kb to the *Nr2f2* transcriptional start site (TSS); *blue box*, Shh response element (TACATAATGCGCCG) at -1661bp to -1648bp which confers upregulation by Shh on the *Nr2f2* promoter; *yellow boxes*, two inverted Ets protein consensus sequences (TTCC) which confer upregulation by Ets-1; *purple box*, *Nr2f2* 5' UTR; *orange box*, *Nr2f2* exon 1. Inhibition of the MAP kinase pathway represses NR2F2 expression (and vice-versa) whilst treatment with EGF or TGFα increases NR2F2 expression, though the sites of these regulatory actions are unknown (not shown) (Baroukh *et al.* 2005;Diez *et al.* 2007;Krishnan *et al.* 1997;More *et al.* 2003;Petit *et al.* 2004;Qiu *et al.* 1996).

4.8.1 EMSA Oligonucleotide Design

In order to identify whether POU4F3's putative activation of the *Nr2f2* promoter is direct, possible POU4F3 binding sites in this promoter would need to be identified and POU4F3's ability to bind these sites and activate transcription would have to be tested. Bioinformatic software was therefore used to predict potential POU4F3 binding sites in the *Nr2f2* 5'flanking region.

Nr2f2 promoter prediction

Prior to using software to identify potential POU4F3 binding sites, the *Nr2f2* gene promoter region first had to be predicted. The Genomatix Gene2Promoter software was selected for this purpose as explained in section 3.5.1. This analysis was carried out using the mouse database as promoter reporter constructs that I intended to use in subsequent experiments were cloned from this species (see section 4.9 for these experiments).

The software revealed six putative promoters for *Nr2f2*. All six of these promoters corresponded to one or more than one transcript whose 5' region had been fully sequenced i.e. oligo-capping had been used in order to clone the 5' end of transcript, thereby identifying the transcriptional start site and improving the promoter prediction. I selected the most appropriate *Nr2f2* promoter by identifying which Genomatix transcript best corresponded to the *Nr2f2* transcript identified by the BLAST analysis (Figure 4.9*a*). The transcript identified in the BLAST analysis comprised three exons and this gene structure is supported by data in the UniProtKB/Swiss-Prot or RefSeq databases (Ensembl 2009). Figure 4.9*b* shows that two promoters (GXP_158557 and GXP_158616) correspond to a three-exon transcript, however, only the transcript corresponding to GXP_158616 has full 5' region sequencing (i.e. its transcriptional start site had been verified experimentally). This promoter was therefore selected as the most appropriate promoter for further analysis (see section 3.5.1 for more detail on promoter selection criteria).

Prediction of POU4F3 binding sites in the predicted Nr2f2 promoter

The selected predicted *Nr2f2* promoter was analysed using the MatInspector and ModelInspector programs to identify putative POU4F3 binding sites and modules respectively. As the DNA recognition of POU proteins has been shown to be similar (Rhee *et al.* 1998), all predicted binding sites of the 'Brn' sub-class of POU domain factors in the Genomatix software were considered for further analysis (see Andersen *et al.* 2001). Putative binding sites with the highest stringency predictions, i.e. the greatest similarity to known binding sites, were selected for *in vitro* assay of POU4F3's ability to bind them by electrophoretic mobility shift assay (EMSA).

Fourteen POU-family transcription factor binding sites were predicted within the *Nr2f2* promoter at the lowest stringency level (Figure 4.9*c.0.00*). As the stringency is increased, only the transcription factor binding sites that more closely matched their corresponding matrices are displayed. At the highest level of stringency only four POU-family transcription factor binding sites remain (Figure 4.9*c.0.05*). The ModelInspector analysis revealed that the labelled V$BRN2 family site (i.e. POU3 / Brn-2) is contained in an OCT1-SORY module (Figure 4.9*c*,*V$BRN2*), thereby showing that its context as well as its sequence is likely to be suitable for regulation by a POU family member. This site was therefore prioritised for analysis and an oligonucleotide was designed to investigate POU4F3 binding to its sequence by EMSA (Figure 4.9 and Table 4.2, *NR2F2BS2*). Of the remaining sites at this stringency level, the most 3' was selected for analysis due to its proximity to the transcriptional start sites (red arrows) and the presence of lower stringency POU-family binding sites in the same region. The EMSA oligonucleotide designed to investigate this POU6 (BRN-5) site was named NR2F2BS1 (Figure 4.9 and Table 4.2, *NR2F2BS1*). These putative binding sites were then used to design oligonucleotides for EMSA analysis (Table 4.2).

Table 4.2. Oligonucleotides for *Nr2f2* EMSA analysis.
EMSA oligonucleotides (NR2F2BS1 and NR2F2BS2) were designed and synthesised for EMSA analysis of POU4F3 binding to two sites in the *Nr2f2* promoter that had been identified by MatInspector and ModelInspector analyses (Figure 4.9). Bases were included both 5' and 3' to NR2F2BS1 (*underlined*) in order to ensure that POU4F3 binding would not be affected by the ends of the oligonucleotide. NR2F2BS2 was designed to encompass the OCT1 portion of the OCT1-SORY promoter module that had been predicted by the MatInspector program. The part of the high-stringency POU3 site identified in MatInspector that overlaps this promoter module is represented in *bold type*. The POU4F3 and AP4 consensus sequences used in subsequent EMSA analyses are also shown.

Name	*Sequence*	*Length*	*Matrix Similarity*
NR2F2BS1	CTTTTTAGCATATTTGATCACTTTGATT	28	0.836
NR2F2BS2	**GGAATTTATTTTAATTG**CATCATAACAATGAGGTGA	36	N/A
POU4F3 consensus 1	CACGCATAATTAATCGC	17	N/A
AP4 consensus	CTAGCCCAGCTGTGGCAGCCC	21	N/A

a)

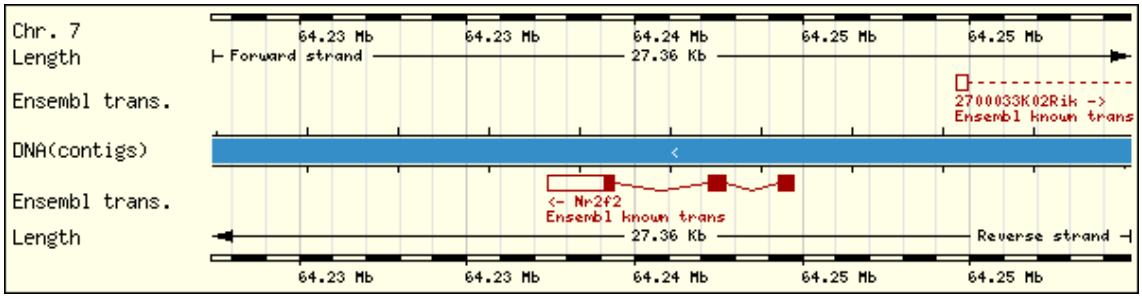

Figure 4.9. Identification of putative POU4F3 binding sites in the *Nr2f2* promoter.
(Legend on page 146)

b)

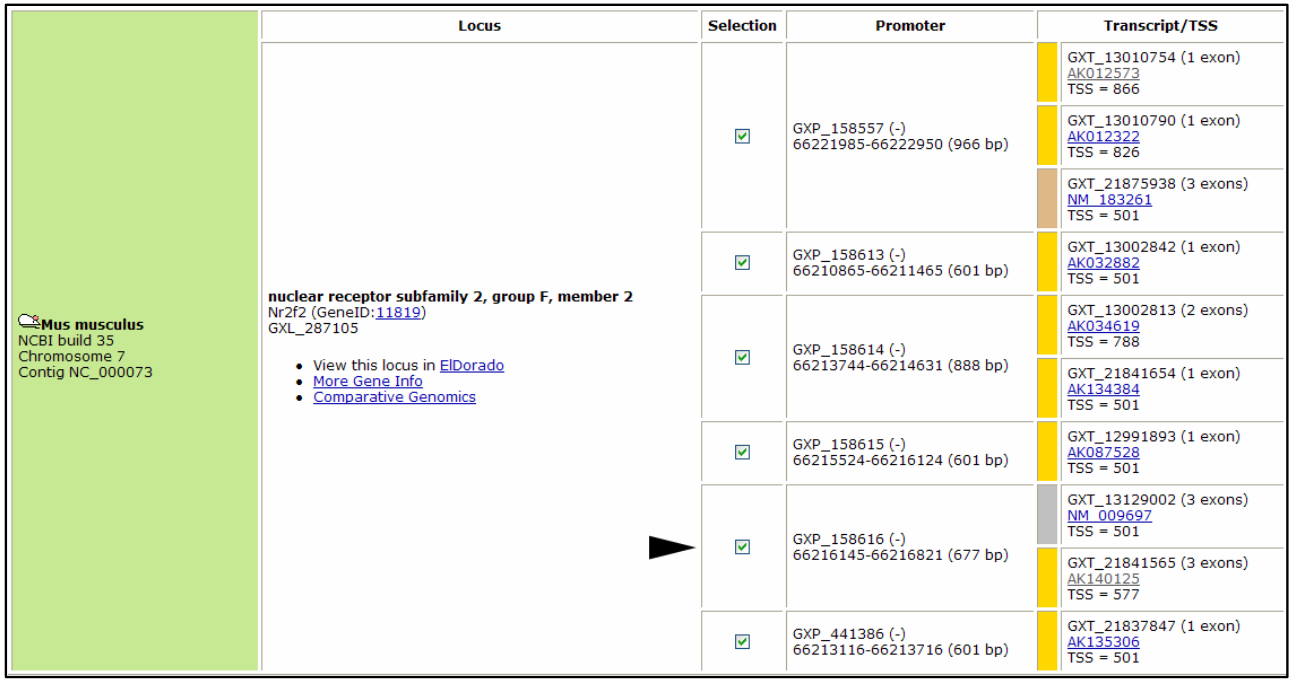

Locus	Selection	Promoter	Transcript/TSS
Mus musculus NCBI build 35 Chromosome 7 Contig NC_000073			
nuclear receptor subfamily 2, group F, member 2 Nr2f2 (GeneID:11819) GXL_287105 • View this locus in ElDorado • More Gene Info • Comparative Genomics	☑	GXP_158557 (-) 66221985-66222950 (966 bp)	GXT_13010754 (1 exon) AK012573 TSS = 866
			GXT_13010790 (1 exon) AK012322 TSS = 826
			GXT_21875938 (3 exons) NM_183261 TSS = 501
	☑	GXP_158613 (-) 66210865-66211465 (601 bp)	GXT_13002842 (1 exon) AK032882 TSS = 501
	☑	GXP_158614 (-) 66213744-66214631 (888 bp)	GXT_13002813 (2 exons) AK034619 TSS = 788
			GXT_21841654 (1 exon) AK134384 TSS = 501
	☑	GXP_158615 (-) 66215524-66216124 (601 bp)	GXT_12991893 (1 exon) AK087528 TSS = 501
	☑	GXP_158616 (-) 66216145-66216821 (677 bp)	GXT_13129002 (3 exons) NM_009697 TSS = 501
			GXT_21841565 (3 exons) AK140125 TSS = 577
	☑	GXP_441386 (-) 66213116-66213716 (601 bp)	GXT_21837847 (1 exon) AK135306 TSS = 501

c)

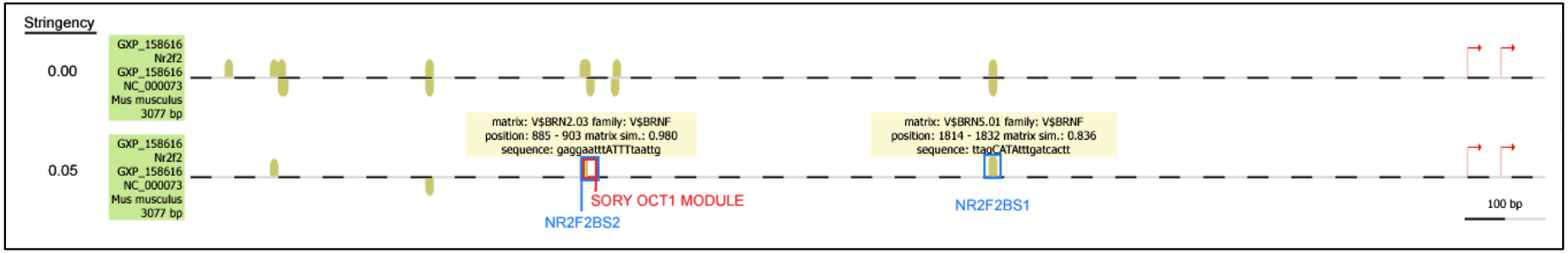

Figure 4.9. Identification of putative POU4F3 binding sites in the *Nr2f2* promoter.
a) Graphical representation of the *Nr2f2* gene in the Ensembl genome browser. This transcript was identified based on experimental data and was therefore used to verifying the accuracy of transcripts annotated in the corresponding Genomatix database. *b*) The predicted *Nr2f2* promoter that corresponded to the transcript that best-matched the Ensembl *Nr2f2* transcript was selected (*arrowhead*) based on both exon number (*three*) and quality of prediction (*gold colour*). *c*) POU-family transcription factor binding sites were predicted in the MatInspector program. *Red box*, SORY-OCT1 module identified by ModelInspector software. *Blue boxes*, POU4 binding sites prioritised for EMSA analysis based on matrix similarity, proximity to the transcriptional start site and supporting evidence from MatInspector and ModelInspector (see section 4.8.1).

4.8.2 *In vitro translated POU4F3 is able to bind to two sites in the Nr2f2 promoter*

In the EMSA, the ability of POU4F3 to bind the two oligonucleotides designed against two sites in a predicted *Nr2f2* promoter was tested. As binding to target gene promoters appears to be a prerequisite step for their activation by POU4F3 (Sud *et al.* 2005), binding of NR2F2BS1 and NR2F2BS2 by POU4F3 would support the hypothesis that POU4F3 directly activates the *Nr2f2* promoter.

1ng of radiolabelled NR2F2BS1 (Figure 4.10*a*) or NR2F2BS2 (Figure 4.10*b*) was either incubated alone or with 5µl *in vitro* translated protein (POU4F3 or luciferase) at room temperature for 30 minutes. The proteins had been *in vitro* translated using the TNT®T7 Coupled Reticulocyte Lysate System (Promega). Samples were then electrophoresed on a 4% non-denaturing polyacrylamide gel at 200 volts at 4ºC for two hours. The gel was dried and autoradiographed at -80ºC for varying exposures (typically 16-24 hours). Protein binding is identifiable as shifted bands (bandshifts) in protein-containing sample lanes. This is due to the protein-oligonucleotide complex having higher molecular weight than oligonucleotide alone and therefore having slowed migration through the gel on electrophoresis.

Figure 4.10 shows binding of *in vitro* translated mouse POU4F3 protein to the putative *Nr2f2* promoter binding sites (NR2F2BS1 and NR2F2BS2). Bandshifts present in both protein-containing lanes were due to non-specific oligonucleotide binding of translated proteins or proteins present in the reticulocyte lysate. However, for both putative binding sites, a bandshift was identified in the *in vitro* translated POU4F3 lane that was not present in the control lanes (*arrowheads*, Figure 4.10). This demonstrates that *in vitro* translated POU4F3 is able to bind to both of the sites identified from the *Nr2f2* promoter. Though these results suggest that POU4F3 is capable of binding the oligonucleotides, the assay does not show whether the binding is sequence-specific and the *in vitro* translated protein (that was produced using a rabbit reticulocyte lysate system) may demonstrate different binding from POU4F3 translated in UB/OC-2 cells due to different post-translational modifications. Therefore, the sequence-specificity of this interaction was further investigated using protein that had been extracted from UB/OC-2 cells.

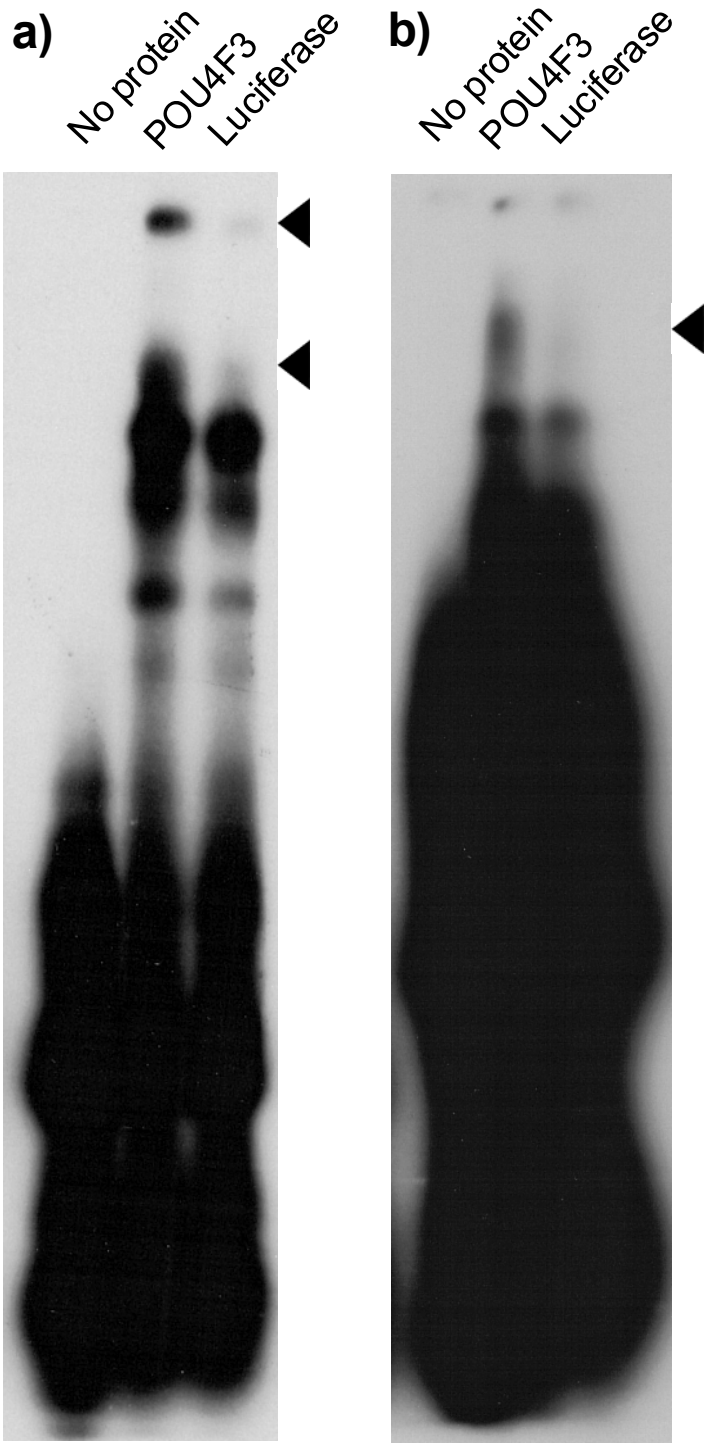

Figure 4.10. Binding of *in vitro* translated POU4F3 to transcription factor binding sites. EMSAs were carried out using [γ-32P]ATP labelled DNA oligonucleotides which corresponded to two predicted POU-family binding sites in the *Nr2f2* gene promoter: NR2F2BS1 (*a*) and NR2F2BS2 (*b*). The binding sites were incubated without protein, with *in vitro* translated POU4F3 or with *in vitro* translated luciferase protein. *Arrowheads* indicate a POU4F3-specific binding pattern.

4.8.3 POU4F3 protein from UB/OC-2 cell nuclear protein extract demonstrates sequence-specific binding to NR2F2BS1 & 2

Nuclear protein extract prepared from UB/OC-2 cells was used to determine whether POU4F3 binding to NR2F2BS1 & 2 is sequence-specific. UB/OC-2 cells were chosen as they express POU4F3 but do not express POU4F1 or POU4F2 (Rivolta *et al.* 1998a). Furthermore, the DNA-binding properties of POU4F3 extracted from these cells should better reflect its physiological function than *in vitro* translated POU4F3 as it is more likely to have appropriate post-translational modifications that may be required for physiological DNA binding. As the nuclear protein extract contains proteins other than POU4F3, some of which will bind DNA, POU4F3-specific bandshifts must be identified amongst bandshifts produced by other proteins. Two methods are commonly used to identify protein-specific bandshifts: supershift analysis and competition analysis. As no suitable anti-POU4F3 antibody is available for supershift analysis, competition analysis was the most appropriate of the available methods for this analysis. Therefore, a competition analysis was conducted in order to identify if any of the bandshifts that are produced by UB/OC-2 cell nuclear extract are due to POU4F3.

In this analysis, an increasing amount of a non-radiolabelled oligonucleotide that is known to be bound by POU4F3 (*cold POU4F3 consensus*, Figure 4.11*a&b*) was added to EMSA reactions. As the unlabelled DNA will compete with the radiolabelled putative *Nr2f2* promoter binding sites for POU4F3 binding, an excess of non-radiolabelled consensus oligonucleotide will ensure that POU4F3 will not bind enough radiolabelled DNA to be visible on autoradiography. Therefore, bandshifts produced by POU4F3 are abolished by sufficient non-radiolabelled consensus oligonucleotide. This also abolishes bandshifts produced by non-sequence-specific DNA-binding proteins; therefore, a negative control was conducted for the competition analysis to identify sequence-specificity of POU4F3 binding. For this control, a 1000-fold excess of unlabelled consensus oligonucleotide for a different transcription factor (AP4) was added to a separate EMSA reaction. Bandshifts caused by non-specific DNA-binding proteins become invisible to autoradiography in this condition as an excess of non-radiolabelled AP4 consensus sequence displaces the radiolabelled oligonucleotides from the non-specific DNA-binding protein. POU4F3, however, does not bind to the AP4 consensus oligonucleotide (as shown by previous experiments in our laboratory), resulting in a persistent bandshift (*cold AP4 consensus* lane, Figure 4.11).

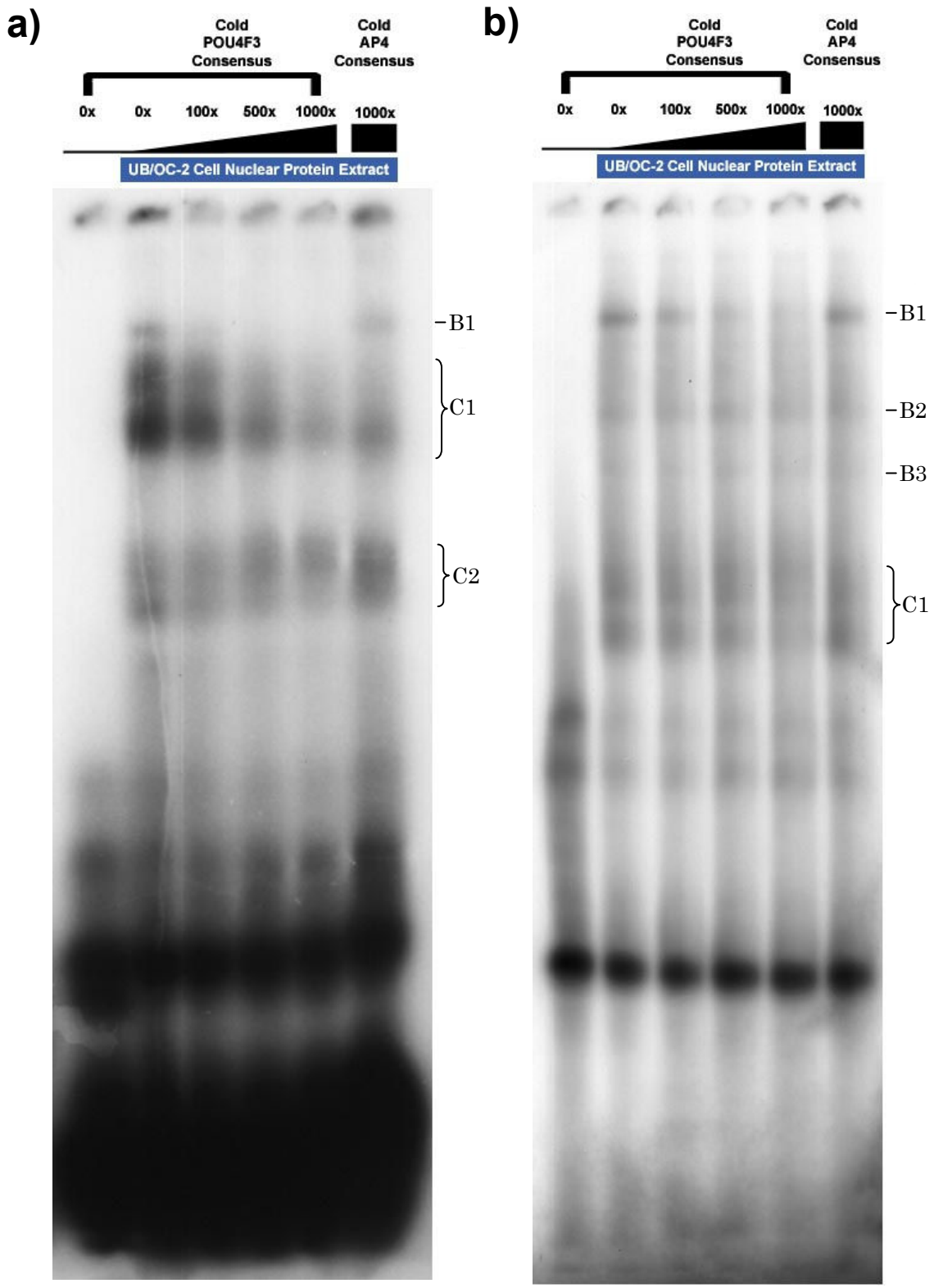

Figure 4.11. Binding of POU4F3 to *Nr2f2* promoter binding sites.
EMSAs were carried out using [γ-32P]ATP labelled NR2F2BS1 and NR2F2BS2. *a*) NR2F2BS1 was incubated with or without UB/OC-2 cell nuclear extract and with varying amounts of non-radiolabelled POU4F3 or AP4 consensus binding site. The same assay was conducted for the second putative binding site, NR2F2BS2 (*b*). For both oligonucleotides, POU4F3-specific banding patterns (i.e. bandshifts that are competed for by specific POU4F3 consensus sequence but not by non-specific AP4 consensus sequence) were identified (*B1* in both cases) along with non-specific bands and complexes. *B*, bandshift; *C*, complex.

On autoradiography, bandshifts were seen for NR2F2BS1 with UB/OC-2 cell nuclear protein extract (Figure 4.11*a*). The banding pattern shows a slow-migrating band (Figure 4.11*a.B1*) and two complexes of faster migration (Figure 4.11*a.C1&C2*). On competition with unlabelled POU4F3 consensus oligonucleotide, *B1* was abolished by 100-fold excess of unlabelled POU4F3 consensus sequence and a 1000-fold excess of this oligonucleotide attenuated *C1* and *C2* density (*cold POU4F3 consensus*, Figure 4.11*a*). In competition with 1000-fold unlabelled AP4 consensus sequence (*cold AP4 consensus*, Figure 4.11*a*), *B1, C1* and *C2* are restored. This pattern shows that the *B1* bandshift is specifically produced by POU4F3 as it is only eliminated by specific competition. It also shows that *C1* and *C2* are likely to be produced by POU4F3 binding, however their competition by unlabelled POU4F3 consensus oligonucleotide is not as clear as that of *B1* (Figure 4.11*a*).

As with NR2F2BS1, bandshifts were seen for NR2F2BS2 on EMSA analysis with UB/OC2 cell nuclear protein extract (Figure 4.11*b*). A slow-migrating band (Figure 4.11*b.B1*), a doublet (Figure 4.11*b.B2&B3*) and a fast-migrating complex were visible on the autoradiograph (Figure 4.11*b.C1*). Of these bandshifts, *B2* and *B3* and were only slightly reduced by maximum unlabelled POU4F3 consensus competition (*cold POU4F3 consensus*, Figure 4.11*b.B2,B3&C1*), indicating that these bandshifts are unlikely to be due to POU4F3. *B1*, however, was markedly reduced by 500-fold POU4F3 consensus competition, abolished by 1000-fold POU4F3 consensus competition and fully restored on 1000-fold AP4 consensus competition. Similarly, *C1* appears to be reduced by 1000-fold POU4F3 consensus competition and restored on 100-fold AP4 consensus competition. This pattern indicates that *B1* and *C1* are produced by POU4F3 (Figure 4.11*b*). On comparison of Figure 4.11*a* and Figure 4.11*b*, POU4F3 appears to have a higher affinity for NR2F2BS2 than NR2F2BS1 as more competition is required to abolish visible binding to this site (1000-fold cold consensus sequence for NR2F2BS2 compared to 500-fold for NR2F2BS1). This is consistent with the similarity of the binding sites to their respective matrices in the bioinformatic analysis (0.980 matrix similarity for NR2F2BS2 to a POU3 matrix and 0.836 matrix similarity for NR2F2BS1 to a POU6 matrix, see section 4.8.1).

The above competition assay shows that *murine* POU4F3 extracted from UB/OC-2 cells is able to bind NR2F2BS1 and NR2F2BS2 oligonucleotides *in vitro*. When considered with the binding of *in vitro* translated POU4F3 to these oligonucleotides (Figure 4.10), this evidence suggests that POU4F3 may be able to bind these sites in the context of the full *Nr2f2* gene promoter *in vivo*. Given this evidence of a direct interaction between POU4F3 and *Nr2f2*, the transcriptional regulation of the *Nr2f2* gene promoter by POU4F3 was investigated to identify whether POU4F3 is able to directly upregulate the *Nr2f2* gene as the subtractive hybridization suggests.

4.9 Transcriptional regulation of the *Nr2f2* 5' flanking region by POU4F3

The ability of POU4F3 to activate the *Nr2f2* promoter was investigated to verify the upregulation suggested by the subtractive hybridization and, if verified, provide evidence for direct interaction between POU4F3 and the *Nr2f2* promoter.

4.9.1 Investigation of Nr2f2 5' flanking sequence response to POU4F3

Plasmids containing *Nr2f2* 5' flanking sequences upstream of the firefly (*photinus pyralis*) luciferase gene were used in cotransfections with varying amounts of *Pou4f3* expression construct (in the pSi expression vector). Empty pSi vector was used to keep the total amount of transfected DNA constant and pRL-null, a promoter-less luciferase construct which produces sea pansy (*renilla reniformis*) luciferase, was included in cotransfections to correct for differing transfection efficiencies between replicates. The Promega Dual Luciferase and DualGlo kits were used to assay firefly and sea pansy luciferase production.

Two *Nr2f2* 5' flanking region constructs were obtained from collaborators. A 4kb luciferase reporter construct containing the sequence from approximately -180bp to the *Nr2f2* transcriptional start site to approximately -4.2kb was received from Dr M Vasseur-Cognet and designated NR2F2p4kb (Figure 4.12*a*). The other construct, designated NR2F2p1.6kb (Figure 4.12*b*), was received from Dr S Tsai and contained 1.6kb of sequence from approximately -234bp to approximately -1.8kb. These constructs are occasionally referred to as promoters for convenience though they have not been shown to act as full length *Nr2f2* promoters. Both constructs were investigated by cotransfections with POU4F3 expression constructs in UB/OC-2, ND7 and BHK cells. Calcium phosphate precipitation was used for these and subsequent transfections as it provided sufficient luciferase expression for this assay and was more cost-effective than liposome-based and related systems (e.g. Lipofectamine (Invitrogen) and FuGENE (Roche)). Though an approximately two-fold activation was seen in UB/OC-2 cells, the presence and magnitude of this response varied between experiments (data not shown). This may have been due to endogenous UB/OC-2 cell POU4F3 expression which leads to increased baseline promoter construct upregulation that masks the effect of the cotransfected POU4F3 expression construct. Alternatively, dynamic POU4F3 expression and post-translational modification or cofactors that regulate the NR2F2p4kb construct in response to different cell states could produce this variability.

Of the three cell types tested, UB/OC-2 cells should, in theory, provide the most appropriate transcriptional environment in which to examine POU4F3 regulation of target genes due to their expression of hair cell markers (Rivolta *et al.* 1998a). However, the variability of NR2F2p4kb response to POU4F3 seen in these cells would make it hard to obtain meaningful results without accounting for this variability, thereby making UB/OC-2 cells unsuitable for further study of this relationship.

In both BHK and ND7 cells, both NR2F2p1.6kb and NR2F2p4kb are activated by POU4F3 (Figure 4.13). In BHK cells (Figure 4.13*a*), NR2F2p1.6kb showed a greater response than NR2F2p4kb: 5.2-fold and 3.2-fold respectively. In ND7 cells, the response was more even, with both promoters responding approximately equally: NR2F2p4kb 3.6-fold and NR2F2p1.6kb 3.3-fold. These results support the hypothesis that POU4F3 activates *Nr2f2* and that this activation is produced by a direct mechanism.

The difference in responses between promoters is attributable to their different lengths and, therefore, the transcription factor binding sites present i.e. the difference in response seen in BHK cells (Figure 4.13*a*) is likely to be due to negative regulatory elements that are present in NR2F2p4kb and not in NR2F2p1.6kb. Differential response between cell types, however, is due to the complex integration of the multiple cell-specific factors that influence POU4F3 transcription, *Nr2f2* promoter upregulation and luciferase translation in the assay.

Though NR2F2p1.6kb showed a greater response than NR2F2p4kb in BHK cells, the latter promoter was selected for further investigation. This was because NR2F2p1.6kb only included NR2F2BS1 in its sequence whereas NR2F2p4kb contained both NR2F2BS1 and NR2F2BS2 (see Figure 4.12), thereby allowing further investigation of these sites. Subsequent transfections used ND7 cells as the selected promoter showed a greater response in these cells than in BHK cells and as variability of the response seen in UB/OC-2 cells could confound future results.

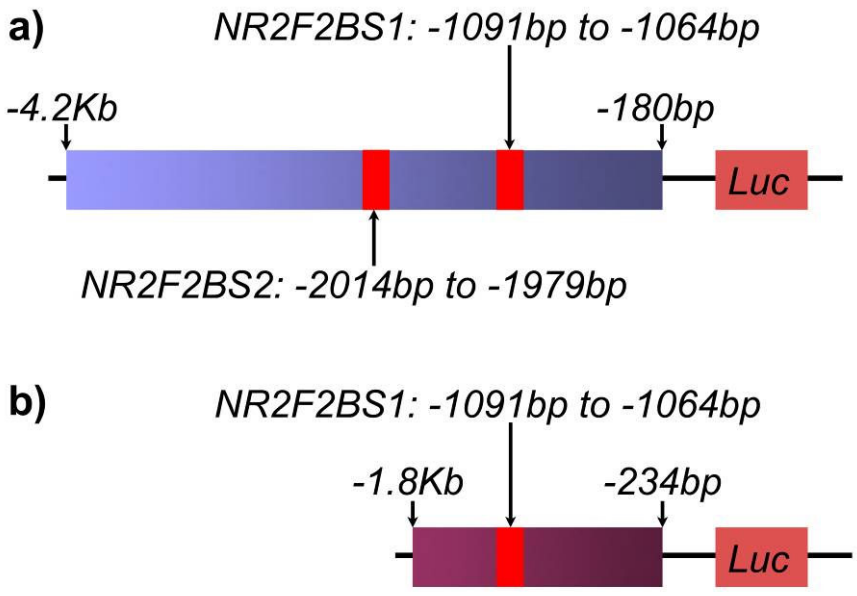

Figure 4.12. Schematic of *Nr2f2* 5' flanking region reporter constructs.
Schematics of NR2F2p4kb (*a*) and NR2F2p1.6kb (*b*) showing the location of NR2F2BS1 and NR2F2BS2. All values are given relative to the *Nr2f2* transcriptional start site in the Ensembl database (Ensembl 2008b).

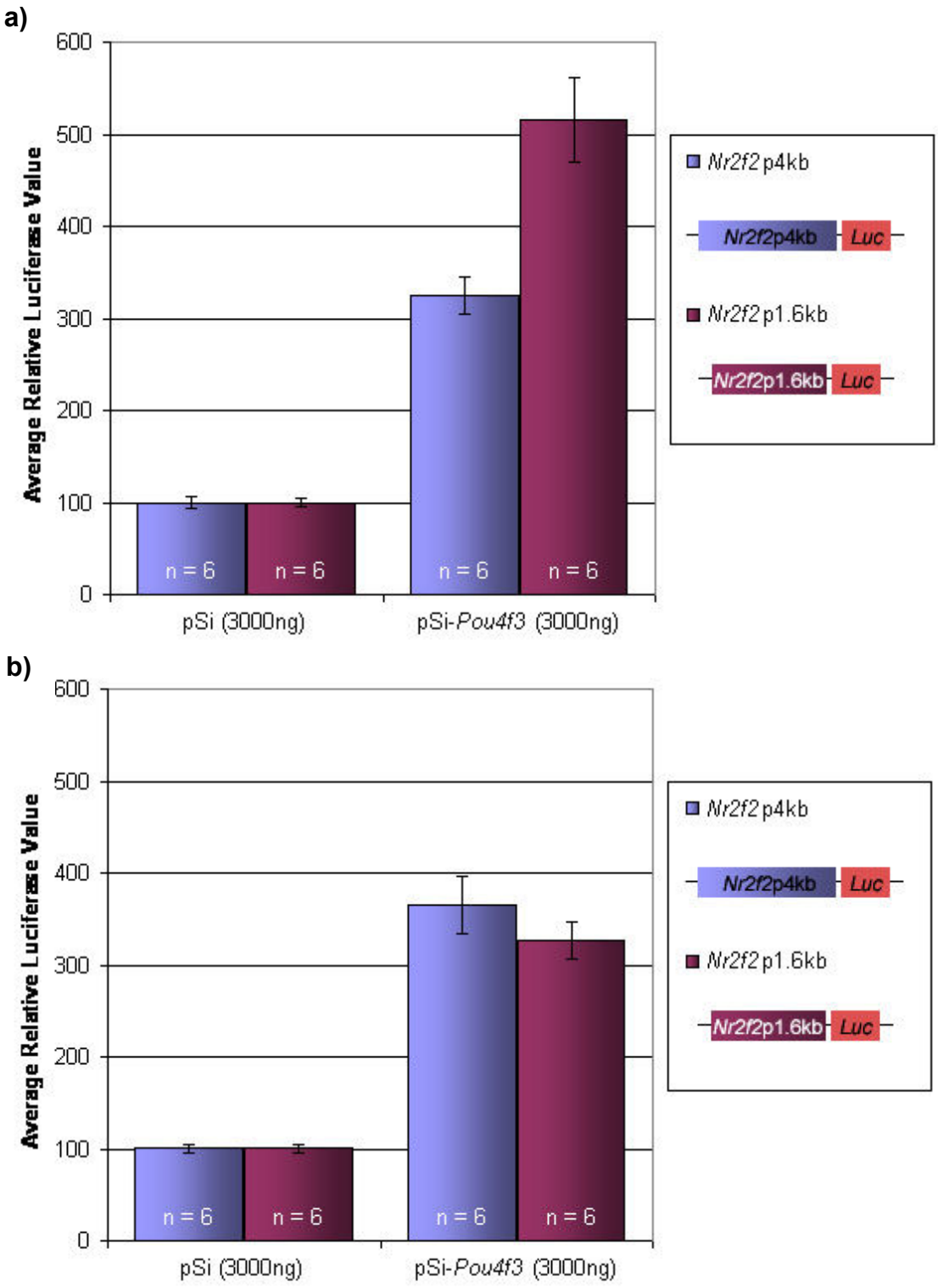

Figure 4.13. *Nr2f2* promoter regulation by POU4F3 in BHK and ND7 cells.
a) In BHK cells NR2F2p4kb shows an approximately three-fold upregulation when cotransfected with a POU4F3 expression construct whereas NR2F2p1.6kb shows an approximately five-fold upregulation. *b*) In ND7 cells, the two promoter constructs show a similar upregulation of greater than three-fold. *Luc*, firefly (*photinus pyralis*) luciferase cDNA.

4.9.2 Characterisation of the POU4F3 activation of NR2F2p4kb

The activation of NR2F2p4kb by POU4F3 was further characterised in order to identify whether this response is dose-dependant (a characteristic of direct interactions between transcription factors and promoters). A control experiment was also carried out to ensure that the POU4F3 response seen was not artefactual and previous experiments in our laboratory showed that the pGl-3 Basic vector into which NR2F2p4kb was cloned does not respond to pSi-Pou4f3.

ND7 cells were transfected with NR2F2p4kb as in previous experiments (section 4.9.1), however, the amount of POU4F3 expression construct was varied (Figure 4.14*a*). In order to verify that any observed upregulation of luciferase production was due to POU4F3 acting through its normal regulatory mechanisms and not due to a non-specific upregulation of NR2F2p4kb caused by increased protein production, a control was performed using a version of the POU4F3 cDNA (named dreidel) that contains a dinucleotide TG deletion (Courtesy of Dr Karen Avraham). The deletion is reported at 388del2 (Hertzano *et al.* 2004), though I located it at c.390_391delTG in the Ensembl sequence. This mutation arose spontaneously in mice and renders the transcription factor non-functional, causing deafness (Hertzano *et al.* 2004). Dreidel cDNA was first cloned from the pHM6 vector in which it was received into the pSi vector for comparability with the pSi-Pou4f3 construct. Subsequently, it was used in transfections as for pSi-Pou4f3 (Figure 4.14*b*).

Figure 4.14*a* shows that increasing the amount of pSi-Pou4f3 that was included in each transfection resulted in an increase in the averaged adjusted relative luciferase values measured, presumably due to the increasing amount of POU4F3 protein acting directly on the *Nr2f2* promoter to increase the rate of luciferase transcription. In the condition containing the largest amount of pSi-Pou4f3 expression construct (Figure 4.14*a 3000ng pSi-Pou4f3*) an upregulation of greater than five-fold was seen. The dreidel protein did not produce such an upregulation (Figure 4.14*b*) as it was only able to produce an approximately 1.5-fold increase in measured relative luciferase values in the condition containing the largest amount of pSi-Dreidel (Figure 4.14*b 3000ng pSi-Dreidel*). These results demonstrate that functional POU4F3 is required in these experiments to upregulate the *Nr2f2* promoter in a dose-dependent fashion, presumably via a direct interaction with the *Nr2f2* promoter, potentially at the binding sites identified in previous EMSA assays (section 4.8).

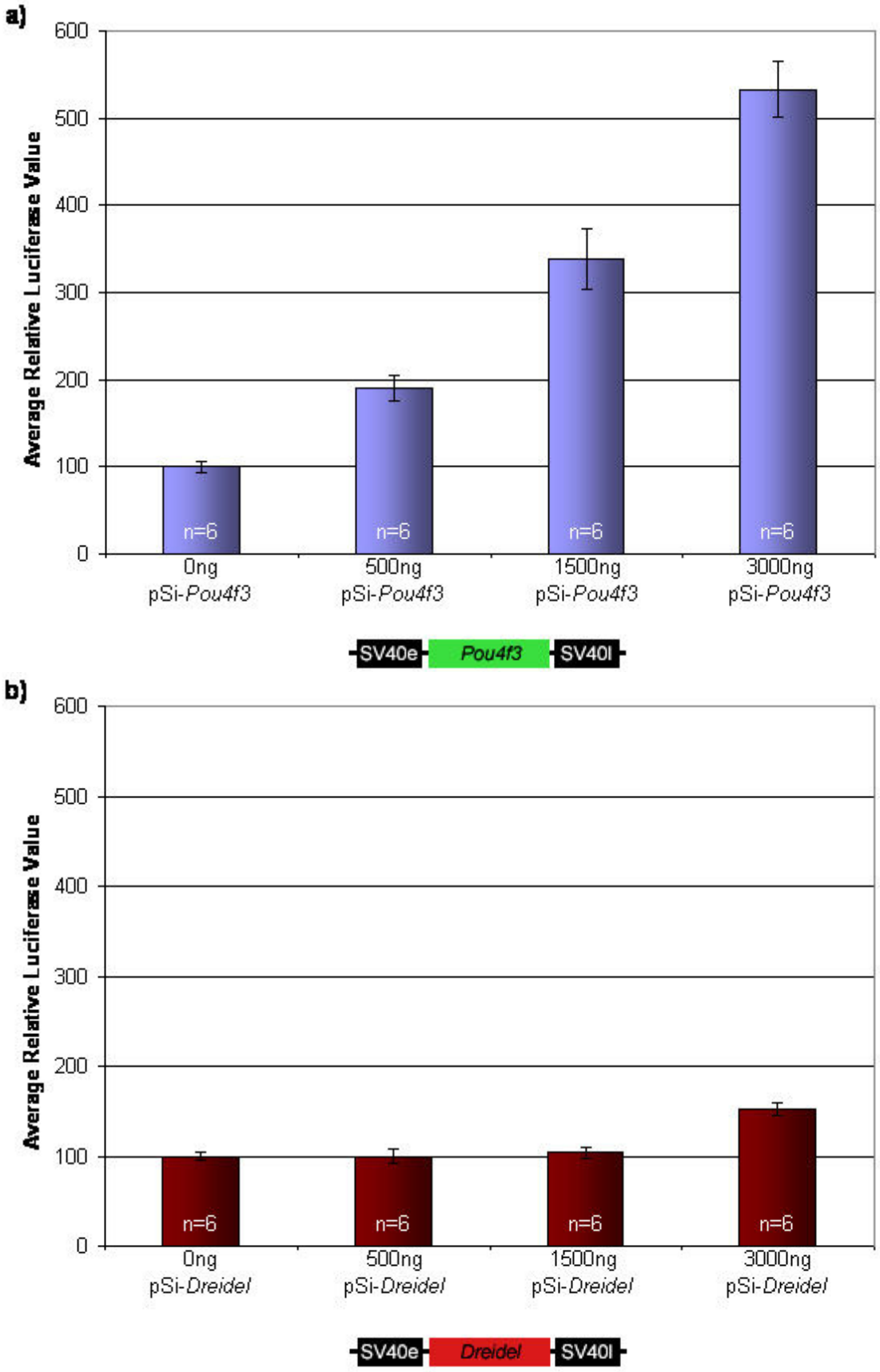

Figure 4.14. NR2F2p4kb dose response to cotransfected POU4F3 expression construct. ND7 cells were transfected with NR2F2p4kb and increasing amounts of expression construct. 10ng pRL-null was included in all conditions and the total amount of DNA was regulated with pSi mammalian expression vector (Promega) (see Figure 2.4). *a*) Increasing amounts of POU4F3 correlate with a dose-dependent increase in luciferase production. POU4F3 expression construct that contains the dreidel dinucleotide deletion (*b*) does not produce such an upregulation. *SV40e*, SV40 enhancer / early promoter; and *SV40l*, SV40 late poly(A) in the pSi mammalian expression vector.

4.9.3 Investigation of the transcriptional effect of POU4F3 on two experimentally verified binding sites in the Nr2f2 promoter

In order to confirm that NR2F2p4kb is directly regulated by POU4F3, the sites at which POU4F3 produces its activation would need to be identified. NR2F2BS1&2 were found to be bound by POU4F3 by EMSA and were, therefore, the most likely sites of POU4F3 regulation of NR2F2p4kb (section 4.8.1). In order to investigate if NR2F2p4kb is regulated by POU4F3 at NR2F2BS1&2, I first investigated the potential of POU4F3 to regulate the EMSA oligonucleotides in isolation i.e. out of the context of their promoter. Regulation of these isolated binding sites by POU4F3 would support the hypothesis that they are the sites of POU4F3 regulation in NR2F2p4kb.

NR2F2BS1 and NR2F2BS2 were cloned upstream of a minimal TATA promoter in the pGL4.23 vector 5' to the sequence for the synthetic *photinus pyralis* luciferase gene, *luc2*. This luciferase coding sequence has been codon-optimised for mammalian expression and, as for the rest of the plasmid, consensus mammalian transcription factor binding sites had been removed where possible in order to reduce background regulation. The number of copies of the binding sites that had been inserted into different clones were assessed by restriction endonuclease digestion followed by size separation of inserts by agarose gel electrophoresis. Plasmids that contained different copy numbers were obtained. NR2F2BS1 clones that contained one, two, three and five copies of the EMSA oligonucleotide were identified. One, two, three and four copy-number plasmids were obtained for NR2F2BS2.

Each site was assayed in cotransfections with pSi or pSi-Pou4f3 and pRL-null in order to assess whether NR2F2BS1&2 confer POU4F3 regulation onto the luciferase gene in the reporter constructs used. This would show whether POU4F3 can upregulate luciferase expression via these sites (as expected based on its action on the *Nr2f2* promoter in NR2F2p4kb (section 4.9.2)) and, if no regulation was seen, might suggest that other sites or non-protein-DNA interactions might produce the observed upregulation of the *Nr2f2* promoter. pSi-Dreidel transfections were also carried out for each plasmid that contained one copy of the binding site in order to demonstrate whether any identified regulatory effect required functional POU4F3. Previous experiments in our laboratory had demonstrated that *luc2* production from the native pGL-4.23 vector is not influenced by POU4F3, thereby ruling out regulation of the base vector.

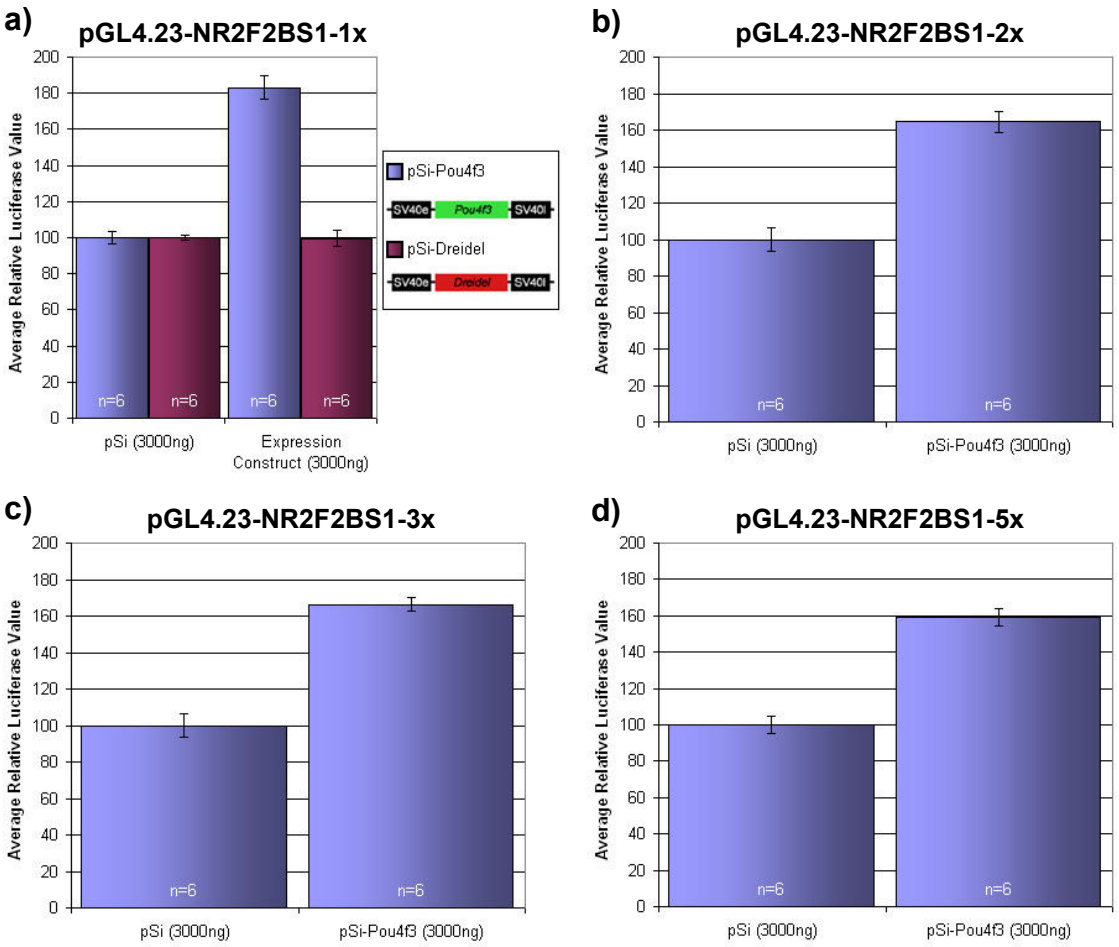

Figure 4.15. Upregulation of pGL4.23-NR2F2BS1 by POU4F3 in ND7 cells.
Reporter constructs were cloned that contained varying copy numbers of NR2F2BS1 or NR2F2BS2 upstream of a synthetic luciferase coding sequence with a minimal TATA promoter. 100ng of each reporter construct was cotransfected with 10ng pRL-null and 3µg of a POU4F3 expression construct in ND7 cells. The plasmid that contained a single copy of the binding site (*a*) was also assayed with dreidel mutant POU4F3 expression construct. All four constructs (*a-d*) showed a 1.6- to 1.8-fold upregulation in the presence of POU4F3. The effect was dependent on functional POU4F3 protein as dreidel mutant POU4F3 did not upregulate luciferase production in pGL4.23-NR2F2BS1-1x. *a*, pGL4.23-NR2F2BS1-1x; *b*, pGL4.23-NR2F2BS1-2x; *c*, pGL4.23-NR2F2BS1-3x; *d*, pGL4.23-NR2F2BS1-5x.

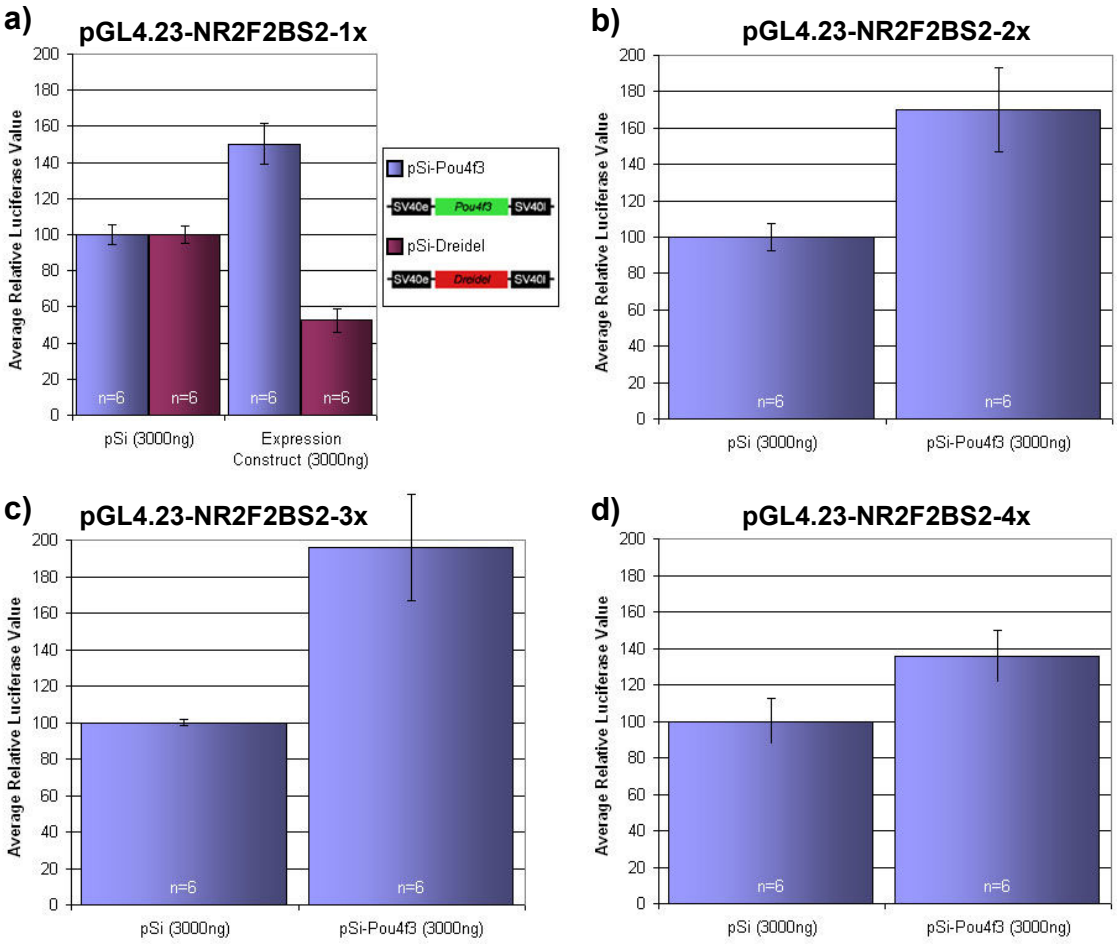

Figure 4.16. Upregulation of pGL4.23-NR2F2BS2 by POU4F3 in ND7 cells.
As for NR2F2BS1, 100ng of plasmid constructs containing a synthetic luciferase coding sequence under the transcriptional regulation of a minimal TATA promoter and a varying copy number of NR2F2BS2 was cotransfected with 10ng pRL-null and a POU4F3 expression construct. All four constructs showed a 1.4- to 2-fold upregulation in the presence of POU4F3. The plasmid that contained a single copy of the binding site was also assayed with dreidel mutant POU4F3 expression construct and this showed that the effect of POU4F3 on this binding site was dependent on functional protein as the mutant POU4F3 did not upregulate luciferase production in pGL4.23-NR2F2BS2-1x (*a*). *a*, pGL4.23-NR2F2BS2-1x; *b*, pGL4.23-NR2F2BS2-2x; *c*, pGL4.23-NR2F2BS2-3x; *d*, pGL4.23-NR2F2BS2-4x.

pGL4.23-NR2F2BS1-1x demonstrated a 1.8-fold upregulation in *luc2* luciferase expression in the presence of POU4F3 protein (Figure 4.15*a*). This effect required functional POU4F3 as dreidel mutant POU4F3 did not demonstrate such an upregulation. Promoter constructs that contained multiple copies of the binding site showed an approximately 1.6-fold upregulation in the presence of POU4F3 (Figure 4.15*b*-*d*). This demonstrates that POU4F3 is not only able to bind to NR2F2BS1, but is also able to confer regulation on a heterologous promoter once bound to this site. The effect is not increased by multiple repeats of the binding site (Figure 4.15*b*-*d*), suggesting either: (i) the spacing or orientation of these sites does not allow more than one copy of POU4F3 to bind; (ii) once bound, multiple POU4F3 copies are not all able to access cofactors to influence transcription or; (iii) that the context of the binding sites limit the activation that POU4F3 is able to produce e.g. due to a limited availability of cofactors.

The NR2F2BS2-containing promoters were also activated by POU4F3 (approximately 1.5- to 2-fold), though they showed a more varied response. As for pGL4.23-NR2F2BS1-1x, the effect of POU4F3 on pGL4.23-NR2F2BS2-1x was found to require functional POU4F3 protein (Figure 4.16). Though increasing copies of the binding site appear to result in a small increase in response for one to three copies, the plasmid that contained four copies of the binding site showed a reduced response (Figure 4.16*b*-*d*). This difference between NR2F2BS1 copy number variants may be due to the orientation of the sites in this plasmid or secondary regulatory factors discussed above. Furthermore, the difference in response for promoters containing different copy numbers of NR2F2BS2 may be sequence-specific or due to the spacing between binding sites in these different constructs (NR2F2BS2 is longer than NR2F2BS1).

As these results show that POU4F3 is capable of binding and upregulating the identified binding sites in the *Nr2f2* promoter, they suggest that the upregulation of NR2F2p4kb seen in luciferase assays (Figure 4.14) occurs at these two binding sites. These results also suggest that POU4F3 may be able to upregulate *Nr2f2* in genomic DNA at these binding sites. Given that these sites were selected as the two most likely sites to be bound by POU4F3 in bioinformatic analysis (section 4.8.1), it is likely that a significant proportion of the upregulation of NR2F2p4kb by POU4F3 is due to upregulation at these sites. Though the above results demonstrate the ability of POU4F3 to bind to and upregulate the two binding sites, they do so in conditions that are quite different to those found in the normal cell. The cloned binding sites are removed from the transcriptional influence of other binding sites that surround them in the full *Nr2f2* promoter and a heterologous promoter confers a basal upregulation of reporter gene expression that is not present in the full promoter. This is also likely to be the reason that the activation of the binding sites in the above experiments is not as large as that of NR2F2p4kb (1.5-fold compared to 5-fold). Furthermore, experimental factors such as the amount of DNA transfected can affect the

assay and confound results e.g. by causing cytotoxicity. I therefore proceeded to identify whether the upregulation of NR2F2p4kb by POU4F3 required NR2F2BS1 and NR2F2BS2 in order to verify the function of these sites in the more physiological context of the *Nr2f2* 5' flanking region.

4.10 Site-directed mutagenesis of POU4F3 binding sites in the *Nr2f2* promoter

In order to identify the contribution of NR2F2BS1 and NR2F2BS2 to the upregulation of NR2F2p4kb, I attempted to mutate these sites in order to abolish POU4F3 binding. The purpose of this site-directed mutagenesis (SDM) was to demonstrate whether the isolated abolition of the two binding sites was sufficient to affect the observed upregulation of the *Nr2f2* promoter in NR2F2p4kb seen in section 4.9.2, thus clarifying their action in the more physiological context of their promoter. The ability of POU4F3 to bind to the mutated sites designed was first assessed by EMSA analysis and these mutations were subsequently introduced to the NR2F2p4kb plasmid in order to quantify their effect on POU4F3 upregulation of this *Nr2f2* promoter construct.

4.10.1 Design of NR2F2BS1 and NR2F2BS2 mutations to abolish POU4F3 binding

The sequences of NR2F2BS1 and NR2F2BS2 were compared to published POU4F3 binding sites to predict: (i) where exactly POU4F3 might bind within these oligonucleotides; (ii) which bases are expected to be essential for binding; and (iii) what changes could be made to these sites to abolish POU4F3 binding (Figure 4.17). Five studies that report binding sites (Gruber *et al.* 1997;Li *et al.* 1993;Trieu *et al.* 1999;Xiang *et al.* 1995), effects of binding site organisation (Gruber *et al.* 1997;Li *et al.* 1993;Rhee *et al.* 1998) and effects of sequence variation (Gruber *et al.* 1997;Trieu *et al.* 1999;Xiang *et al.* 1995) on POU4F DNA-binding were used to identify the regions within NR2F2BS1 and NR2F2BS2 that are likely to be required for POU4F3 binding. This information also aided the choice of mutations to apply to NR2F2BS1 and NR2F2BS2 in order to abolish POU4F3 binding (Figure 4.17). After having predicted POU4F3 binding sites within EMSA oligonucleotides based on the original Genomatix analysis (section 4.8.1) and their sequence similarity to published POU4F3 consensus sequences (particularly the CATAATTAAT sequence identified in Gruber *et al.* 1997), reported effective mutations of POU4F3 binding sites were used to aid in the prediction of mutations of the *Nr2f2* promoter binding sites that would abolish their binding and upregulation by POU4F3 (Xiang *et al.* 1995). In particular, the CAT sequence identified as being important for upregulation by Xiang *et al.* was targeted and AT was replaced with CG to maximise any effect on POU4F3 binding (Xiang *et al.* 1995). For NR2F2BS1 (Figure 4.17*a*) a two base-pair mutation was sufficient however, for NR2F2BS2 (Figure 4.17*b*) a three base-pair was required to disrupt two neighbouring CAT motifs.

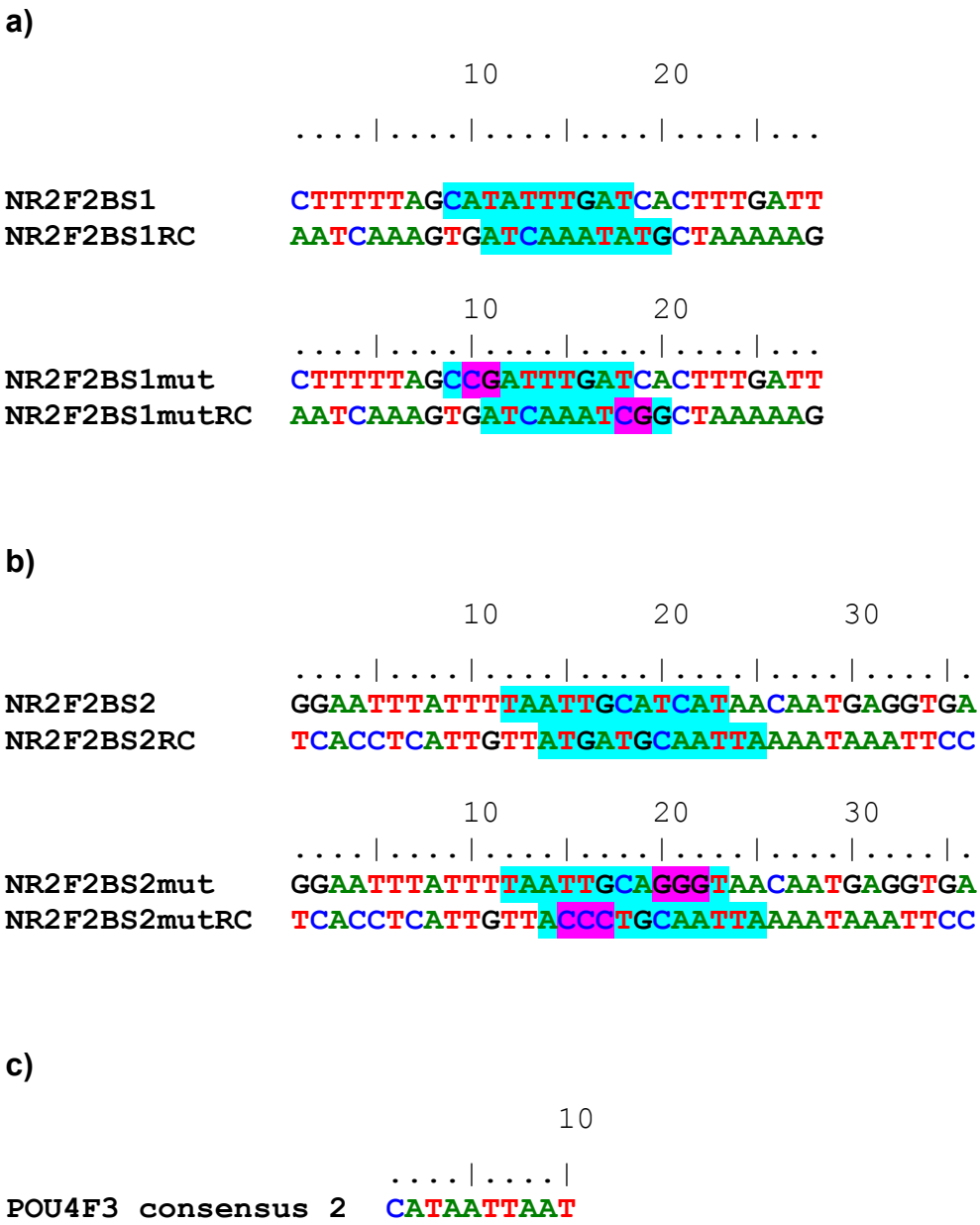

Figure 4.17. Design of mutant POU4F3 binding sites.
The EMSA oligonucleotide sequences are shown with the identified regions of likely POU4F3 binding highlighted in *blue*. These sites were mutated in order to abolish POU4F3 binding (mutations highlighted in *pink*). The reverse complement (*RC*) sequences of unmutated and mutated (*mut*) NR2F2BS1 (*a*) and NR2F2BS2 (*b*) are shown for easy identification of antisense putative POU4F3 binding sites compared to a POU4F binding site consensus sequence (*c*) (Gruber *et al.* 1997).

4.10.2 Effect of mutated EMSA oligonucleotides on in vitro translated POU4F3 binding

Prior to assessing the effect of the mutations shown in Figure 4.17 on POU4F3 regulation in luciferase assays (in the context of the *Nr2f2* promoter), the mutant sequences were synthesised and the oligonucleotides were used in EMSA analysis with *in vitro* translated POU4F3 in order to assess the effect of the mutations on POU4F3 binding. The analysis was carried out as described in section 4.8.2, except that the protein was translated using a new wheat germ quick-coupled transcription/translation system rather than rabbit reticulocyte lysate, and *in vitro* translated Barhl1 transcription factor was used instead of luciferase protein to test non-specific binding background.

Figure 4.18*a&b* shows that the two base-pair mutation of NR2F2BS1 resulted in a substantial decrease in POU4F3 binding (indicated by *opaque arrowheads*). Unexpectedly, the mutation also resulted in an increase in Barhl1 binding to the sequence. Barhl1 and POU4F3 binding sites have since been observed to overlap at some loci in our laboratory (by VG). Mutation of NR2F2BS2 (Figure 4.18*c&d*) resulted in a reduction in the amount of oligonucleotide bound by POU4F3 (Figure 4.18, *hollow arrowhead*). In contrast to NR2F2BS1, the Barhl1 binding pattern was similar for both the wild type and mutant oligonucleotide.

These results demonstrate that the mutations designed for the two POU4F3 binding sites in the *Nr2f2* promoter reduce POU4F3 binding to these sites. In the context of a promoter, this reduction in POU4F3 binding should result in a reduction of POU4F3-mediated upregulation of these promoters if these sites are required for POU4F3 regulation. In order to verify that these binding sites are necessary for POU4F3 regulation of *Nr2f2*, I attempted to reproduce the above mutations in the NR2F2p4kb reporter construct. A reduction in upregulation of this promoter due to these mutations would demonstrate whether the changes in POU4F3 binding shown in Figure 4.18 have an effect on transcriptional activation in the context of the NR2F2p4kb promoter and how much the two binding sites contribute to the upregulation of the *Nr2f2* promoter seen in Figure 4.14.

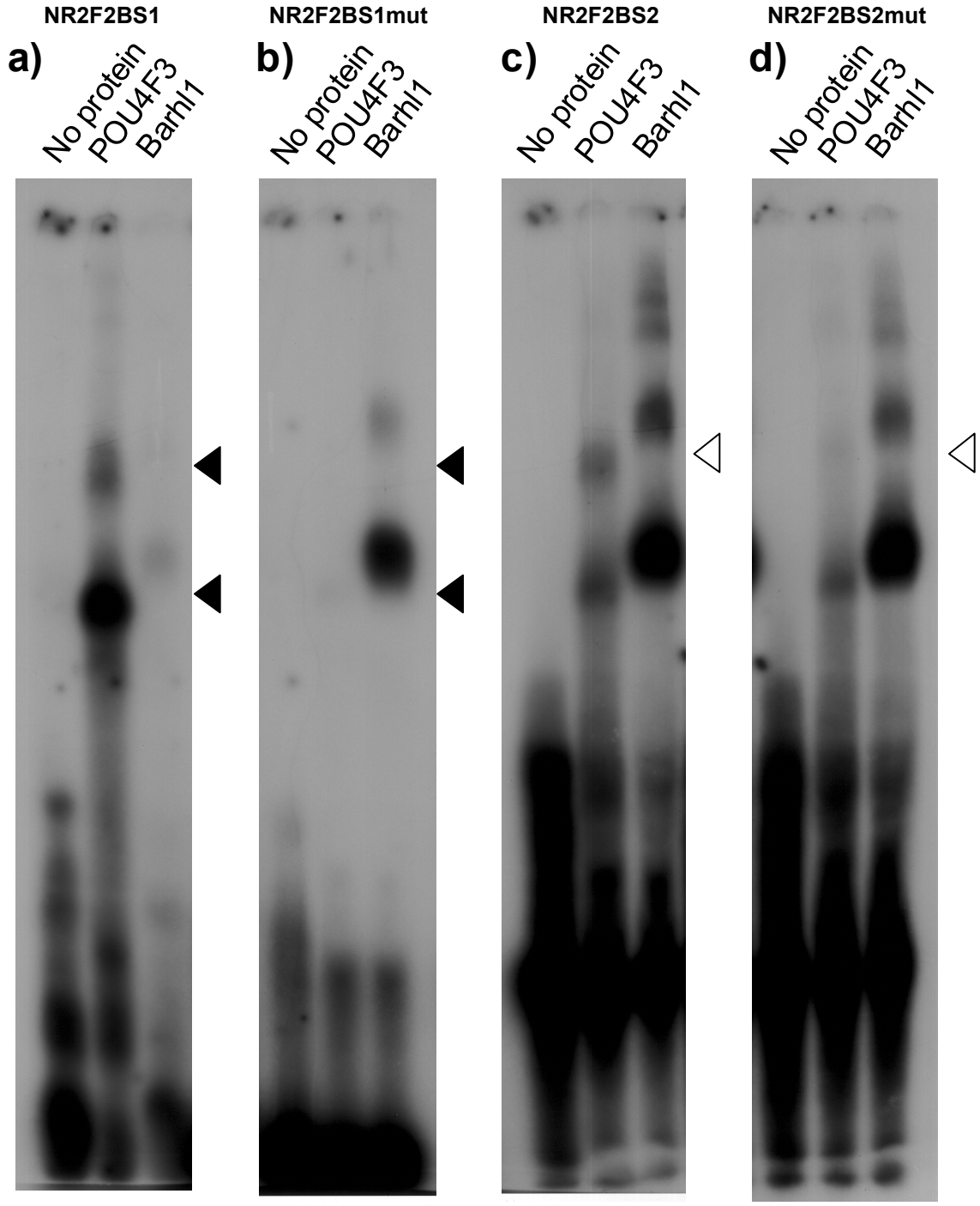

Figure 4.18. Effect of binding site mutation on transcription factor binding.
a) NR2F2BS1 is bound by POU4F3 but not by Barhl1. *b*) The mutated base-pairs in NR2F2BS1mut strongly reduce POU4F3 binding (*filled arrowheads*) and facilitate Barhl1 binding. In contrast, both wild type (*c*) and mutant (*d*) NR2F2BS2 are bound by Barhl1, but POU4F3 binding is reduced by mutation of NR2F2BS2 (*hollow arrowheads*).

4.10.3 Site-directed mutagenesis using the QuikChangeII XL kit

In order to introduce the desired mutations into the POU4F3 binding sites in NR2F2p4kb, site-directed mutagenesis (SDM) was attempted for both binding sites using the Stratagene QuikChangeII XL kit. This kit offers rapid SDM by hybridization of mutant primer to the target site, polymerisation of the remaining plasmid sequence and subsequent digestion of parent DNA to yield mutant plasmid alone. The QuikChange XL kit was selected as it is designed to work for large and difficult plasmids (>8kb) and NR2F2p4kb is approximately 9kb long. Primers were designed using the QuikChange primer design program (Stratagene 2006) and subsequently manufactured and purified commercially.

Though multiple attempts were made using this technique, and the troubleshooting optimisations suggested in the manufacturer's manual were implemented, this strategy was unsuccessful. The *Nr2f2* promoter contains GC-rich regions that are likely to have interfered with polymerase activity even though the QuikSolution™ reagent contained in the kit was used in an attempt to overcome this problem. I therefore used an overlapping PCR method in order to produce the required mutations in NR2F2p4kb.

4.10.4 SDM of NR2F2p4kb by overlapping PCR for NR2F2BS2

NR2F2BS2 lies in a less GC rich and repetitive region of the *Nr2f2* promoter than NR2F2BS1 and therefore presented less challenges in its mutagenesis. This site was mutated by an overlapping PCR strategy that is summarised in Figure 4.19 (initial SDM PCR conducted by SD). Briefly, NR2F2p4kb was used as template DNA in two initial PCR reactions. In the first reaction, (5' reaction) MVCER5' and NR2F2BS2RC or its equivalent SDM primer were used to amplify a region from -621 to the most 3' nucleotide of NR2F2BS2 to produce fragment a. The second reaction (3' reaction) used NR2F2BS2 and MVCER3' and amplified up to +182bp from the most 3' nucleotide of NR2F2BS2 to produce fragment b (Figure 4.19). The DNA amplified in these two reactions was then used as the template for the 'overlap extension' reaction. In the initial cycles of this PCR, the two fragments are denatured and annealed to each other in their overlapping regions. The sense strand of fragment *a* binds to the antisense strand of fragment *b* and the overlapping region primes polymerisation of missing 5' to 3' sequence at both ends of parent fragments. The primers included in the reaction (MVCER5' and 3') are then able to prime polymerisation of this long fragment in subsequent cycles. The long fragment of the reactions that initially used the EMSA oligonucleotides as primers was then cloned in to the pDrive cloning vector by TA cloning and the insert was verified by sequencing. The flanking primers used (MVCER5' and 3') had been designed to overlap EcoRI restriction endonuclease recognition elements that were used to subclone the digested mutant PCR fragment of approximately 790bp back into NR2F2p4kb. The orientation of the fragment was checked by restriction digest and verified by sequencing yielding NR2F2p4kb-BS2mut.

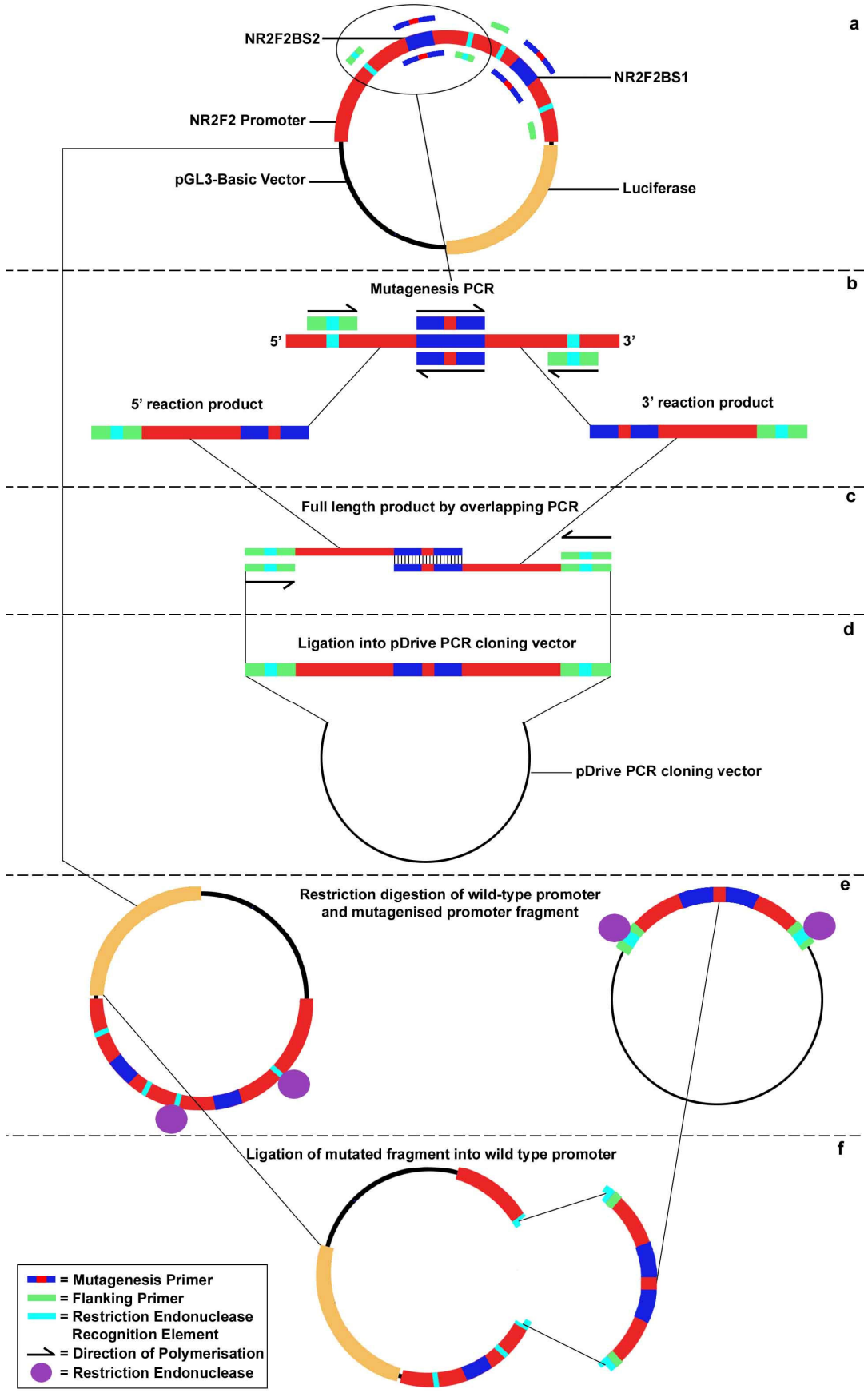

Figure 4.19. Site-directed mutagenesis (SDM) of NR2F2p4kb by overlapping PCR.
a) structure of the NR2F2p4kb promoter construct; *b*) NR2F2BS2 mutagenesis PCR; *c*) full-length insert generation by overlapping PCR; *d*) ligation of full-length insert into the pDrive PCR cloning vector by TA ligation; *e*) restriction digestion of template and full-length insert; *f*) ligation of full-length insert into NR2F2p4kb.

4.10.5 SDM of NR2F2p4kb by overlapping PCR for NR2F2BS1

Having mutated one of the two sites in the *Nr2f2* promoter that bioinformatic prediction and our experiments suggest are responsible for the upregulation of NR2F2p4kb by POU4F3, I attempted to produce a construct in which both POU4F3 binding sites were mutated in order to determine the combined effect of these sites on POU4F3 regulation.

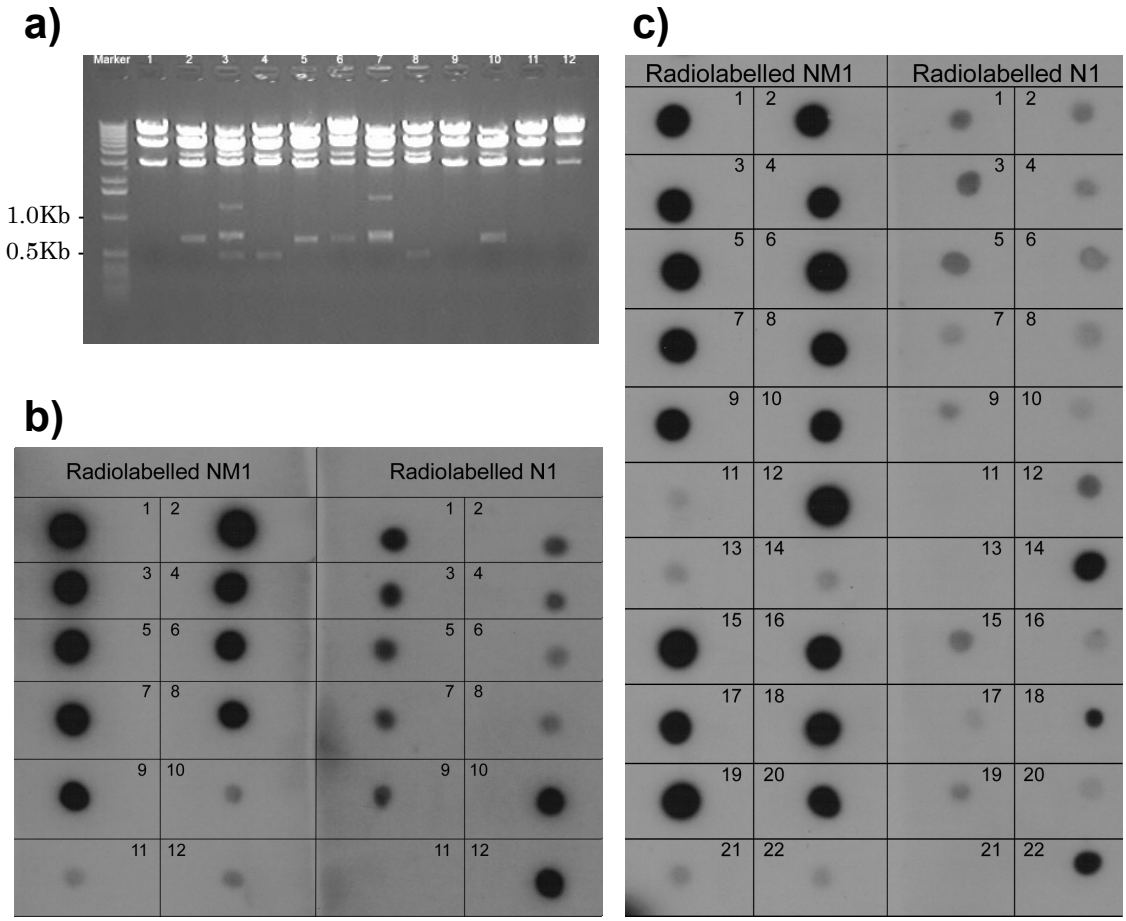

Figure 4.20. Screening of SDM colonies for incorporation of mutation.
a) the orientation of inserts that had been subcloned into the pDrive vector were screened for incorporation of insert and orientation by restriction endonuclease digestion and subsequent electrophoresis. An example of the pattern seen on gel visualisation under UV light is shown. Correctly incorporated and oriented inserts were identified by the presence of a predicted band of 683bp in the absence of any other bands smaller than 1.6Kb (i.e. *lanes 2*, *5*, *6* & *10*). *b*) Miniprep DNA from pDrive clones that had incorporated the insert in the correct orientation were subsequently screened to identify if the desired mutation (NR2F2BS1mut) had been produced by DNA hybridization with radiolabelled EMSA oligonucleotides. Colonies which had incorporated the mutation are identifiable by stronger hybridization with *radiolabelled NM1* than with *radiolabelled N1*. A negative control (NR2F2p4kbBS2mut) that was known to contain wild type NR2F2BS1 was included as a negative control (*box 12*). All clones screened contained the desired mutation apart from *10* (which contained wild type NR2F2BS1) and *11* (which contains an unknown sequence or was of low concentration). NB, *box 2* has been edited for presentation purposes as this clone was spotted out of sequence at the bottom of the NM1 membrane (cropped). *c*) inserts that had been directly subcloned into NR2F2p4kb-BS2 mut were screened for incorporation of the desired mutation in the same way as those cloned into pDrive prior to checking of insert orientation. *Box 22* contains the negative control DNA (NR2F2p4kb-BS2mut). *Boxes 1-10*, *12* and *15-20* are consistent with mutated clones whilst the clone in *box 14* appears unmutated and the remaining boxes appear to contain an unknown sequence or an inadequate amount of DNA.

The strategy used to mutate NR2F2BS2 was also used for NR2F2BS1 with some modification in order to produce a version of NR2F2p4kb in which both NR2F2BS1 and NR2F2BS2 were mutated (named NR2F2p4kb-BS1&2mut). Once the full length mutated PCR fragment had been made (i.e. Figure 4.19c), an aliquot of the purified fragment was digested and ligated directly into the NR2F2p4kb-BS2mut construct using the ApaI restriction endonuclease as well as cloning the remainder of the undigested purified fragment into the pDrive vector by TA cloning. pDrive colonies were screened by Miniprep (Qiagen) and restriction endonuclease digestion in to identify whether the full-length mutant PCR fragment had been incorporated and to determine its orientation (Figure 4.20*a*). pDrive colonies that had been shown to contain the desired insert in the correct orientation were then screened by DNA hybridization to determine whether the mutation had been incorporated or whether the colonies had arisen from wild type NR2F2p4kb i.e. due to incomplete digestion or phosphorylation of this plasmid during earlier cloning stages (Figure 4.20*b*). Colonies yielded by direct ligation of the full-length mutated fragment into NR2F2p4kb-BS2mut were also screened, though their orientation was not determined (Figure 4.20*c*). Having identified colonies that had incorporated the mutation, these clones were sent for sequencing in order to verify that NR2F2BS1 had been mutated and, in the case of colonies that had been directly ligated into NR2F2p4kb-BS2mut, that the insert was in the correct orientation.

4.10.6 Correction of unintended mutations in NR2F2p4kbmut

On sequencing, unintended mutations were noticed to have arisen in the mutated clones, presumably due to PCR errors (different mutations were identified between colonies). A strategy was therefore designed to correct unwanted mutations. The BclI restriction endonuclease was used to excise a region from a clone with a mutation 5' to NR2F2BS1 and replace it with the equivalent region in another clone that did not contain the 5' mutation but did have a mutation within the excised region. Orientation of this fragment was checked by restriction endonuclease digestion and the correction was verified by sequencing of this plasmid (NR2F2p4kb-BS1&2mut). This plasmid had a c to t missense mutation -288bp from the intended mutagenesis site that could not be repaired, however, a c to t missense mutation at +74bp and a three base-pair deletion starting at +301 to the intended mutation were repaired. The remaining mutation is unlikely to have an effect on POU4F3-specific interactions with this promoter due to its distance from POU4F3 binding sites. However, as the remaining mutation might interfere with the binding of other transcription factors to the *Nr2f2* promoter sequence, basal expression of this promoter construct (NR2F2p4kb-BS1&2mut) was not compared to the wild-type construct (NR2F2p4kb) as any difference in luciferase production could not be assigned to POU4F3 alone.

4.10.7 Luciferase assay shows reduced response of NR2F2p4kb-BS1&2mut to POU4F3 compared to wild type NR2F2p4kb

NR2F2p4kb-BS1&2mut was used in cotransfection assays and compared to NR2F2p4kb which was assayed as previously described (see section 4.9.2) in order to assess the contribution of the two binding sites to the upregulation of the *Nr2f2* promoter by POU4F3. However, a lower total amount of DNA (1210ng instead of 3110ng) was used in order to reduce the possibility of cytotoxicity from the transfection confounding the results. If the upregulation is produced by the action of POU4F3 at the identified sites, the mutations should reduce POU4F3 binding and therefore reduce, or abolish the upregulation of luciferase protein production in response to increasing amounts of POU4F3 seen with NR2F2p4kb (Figure 4.14).

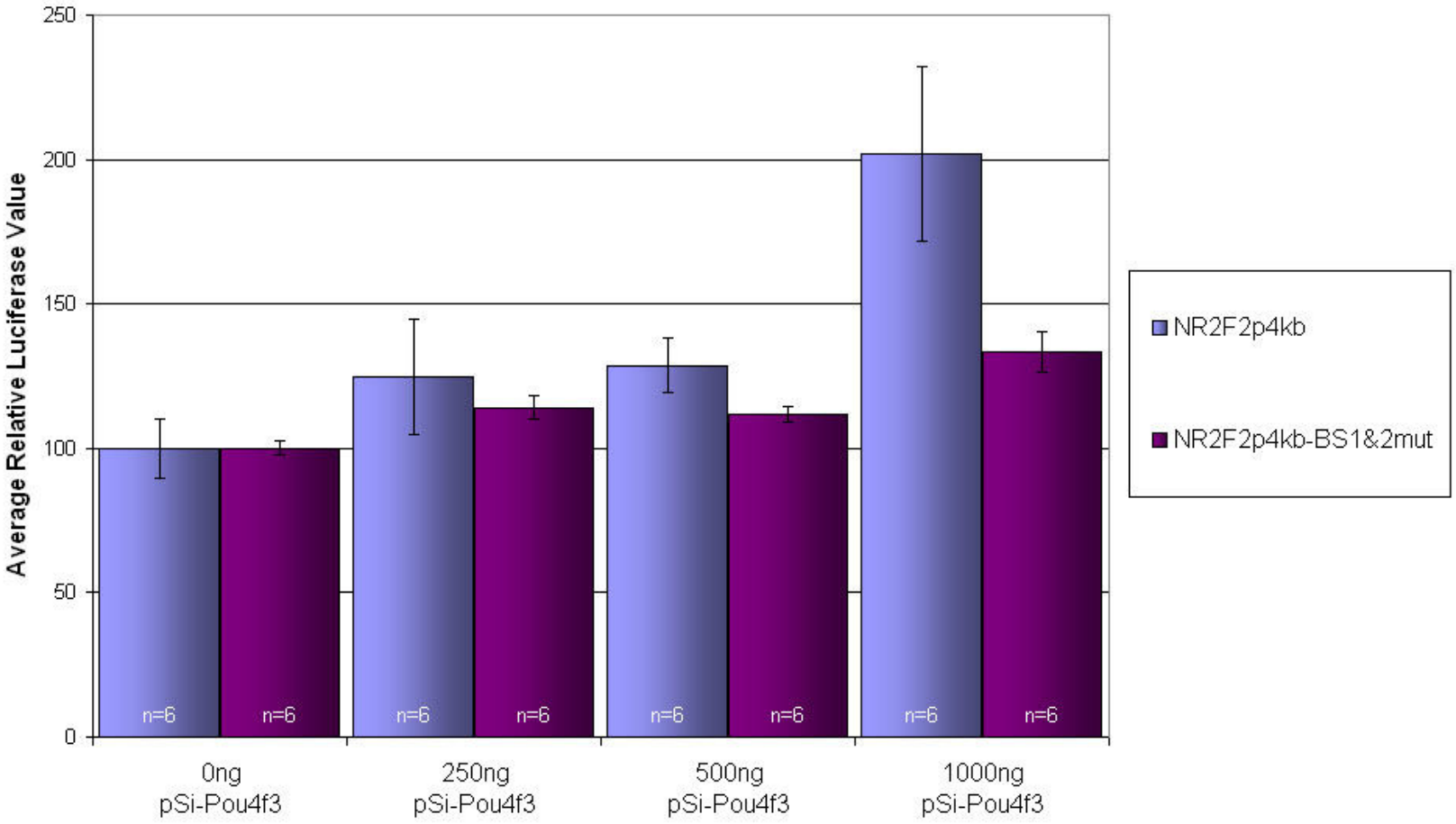

Figure 4.21. POU4F3 binding site mutation reduces *Nr2f2* promoter upregulation.
NR2F2p4kb or NR2F2p4kb-BS1&2mut were cotransfected with increasing amounts of pSi-Pou4f3 and a constant amount of pRL-null. Luciferase production from NR2F2p4kb was increased by pSi-Pou4f3. In contrast, NR2F2p4kb-BS1&2mut demonstrated a much-reduced response, demonstrating the role of NR2F2BS1 and NR2F2BS2 in NR2F2p4kb activation by POU4F3.

Figure 4.21 shows that the mutation of the two POU4F3 binding sites (NR2F2BS1 and NR2F2BS2) reduces the upregulatory effect of POU4F3 on NR2F2p4kb. In this experiment, wild type NR2F2p4kb demonstrated a two-fold upregulation in response to 1000ng of cotransfected pSi-Pou4f3 and the mutated promoter (NR2F2p4kb-BS1&2mut) shows a 1.3-fold upregulation. The response of the wild type promoter (NR2F2p4kb) to POU4F3 in this experiment is lower than the previously identified five-fold upregulation (see Figure 4.14), though this is likely to be due to less POU4F3 expression construct being cotransfected in this experiment to avoid cytotoxicity. Furthermore, the response of NR2F2p4kb to POU4F3 in ND7 cells may vary between passages. This evidence provides further proof that the two POU-family binding sites identified and investigated in the *Nr2f2* promoter are essential for the observed upregulation of this promoter by POU4F3 in this context i.e. NR2F2BS1 and NR2F2BS2 must be intact in order for POU4F3 to be able to upregulate the *Nr2f2* promoter in ND7 cells.

The data in this chapter demonstrate that NR2F2BS1&2 are bound by POU4F3 in NR2F2p4kb and, therefore, are likely to be bound in the *Nr2f2* promoter; POU4F3 is capable of binding these sites in EMSA assay and a reduction in POU4F3 binding to mutant binding sites in EMSA assay is reflected in the reduced response of the mutated *Nr2f2* 5' flanking region (NRF2p4kb-BS1&2mut). These results confirm and extend those of the subtractive hybridization which produced *Nr2f2* as a putative target of POU4F3 as it is also likely that upregulation of *Nr2f2* by POU4F3 is via a direct mechanism with POU4F3 binding the *Nr2f2* promoter at the sites identified (NR2F2BS1 and NR2F2BS2).

4.10.8 Conservation of POU4F3 binding sites in the Nr2f2 promoter

As with coding sequence, regulatory elements are conserved through evolution if their sequence is required for the production of a given phenotype and depending on redundancy i.e. whether a base-pair can be exchanged or deleted without affecting protein binding and upregulation at a *cis*-regulatory element. I therefore investigated the conservation of the identified POU4F3 *cis*-regulatory elements in order to estimate the importance of the interaction that had been identified in the mouse.

The chromosomal locations of the verified mouse *cis*-regulatory elements NR2F2BS1 and NR2F2BS2 were identified and compared with the equivalent regions of the human and rat genomes using precomputed genomic alignments from the Vista project (Loots *et al.* 2004). Once obtained, the sites' conservation was quantified using the BioEdit software package which calculated the percentage sequence similarity between these species.

Nr2f2 promoter POU4F3 binding site 1

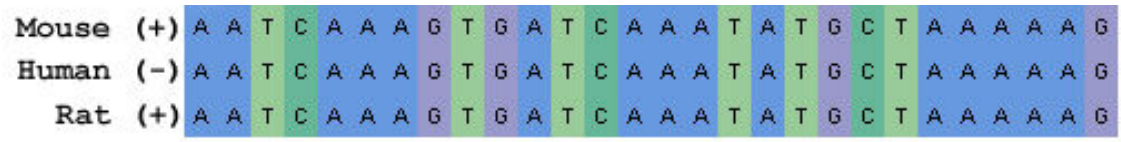

Figure 4.22. Alignment of mouse NR2F2BS1 with equivalent human and rat sequences. Both the human and rat sequences had 100% sequence similarity to the mouse sequence, showing a strong conservation of this site. This figure is modified from the precomputed Vista genomic alignment (Loots *et al.* 2004). + and - indicate sense or antisense strand respectively for each species.

NR2F2BS1 showed 100% conservation between the three species investigated (Figure 4.23). This indicates that this POU4F3 binding site, along with its flanking sequence is well conserved and is therefore likely to play an important role in the regulation of *Nr2f2* expression.

Nr2f2 promoter POU4F3 binding site 2

Figure 4.23. Alignment of mouse NR2F2BS2 with equivalent human and rat sequences. Though this sequence was less well-conserved than NR2F2BS1, the region previously predicted to be the POU4F3 binding site (Figure 4.17), which is shaded in red, has only a single mismatch between mouse and rat sequences (91.7% sequence similarity), showing that this binding site is well-conserved. Figure modified from precomputed Vista genomic alignment (Loots *et al.* 2004). + and - indicate sense or antisense strand respectively for each species.

NR2F2BS2 was less well-conserved than NR2F2BS1. Across the whole sequence, the sequence similarity between species was as follows: mouse:human = 80.5%, mouse:rat = 97.2% and human:rat = 77.7% (Hall 2007). However, in the region that had previously been predicted to be the POU4F3 binding site (Figure 4.17*b*), the conservation was high: mouse:human = 100%, mouse/human:rat = 91.7%. Given the small sample size, it is difficult to compare the conservation of this site to its surrounding sequence, however, it is possible to say that this site, as for NR2F2BS1, is well-conserved. This high level of binding site conservation again indicates that the POU4F3-*Nr2f2* interaction that takes place at NR2F2BS2 is likely to take place *in vivo*.

4.11 Discussion of *Nr2f2* activation by POU4F3

NR2F2 was identified as a putative target of the POU4F3 transcription factor by a subtractive hybridization screen in UB/OC-2 cells. It was selected for further investigation based on its known functions: NR2F2 is known to be required for organogenesis in a range of organs where it has been shown to interact with a number of signalling networks that are known to be involved in inner ear development (sections 4.4 and 4.8). Furthermore, it is expressed in the inner ear where it has been suggested to play a role in inner ear development (section 4.5.2) and many reagents were available for its investigation.

NR2F2 expression in the inner ear was investigated to identify whether it is expressed in hair cells that express POU4F3. The results of these expression studies showed that NR2F2 is widely expressed in the apex of the E18 rat cochlear duct with its expression becoming increasingly restricted to the lesser epithelial ridge towards the base of the cochlear duct (see Figure 4.4). Its expression in the E18 rat inner ear is, therefore, likely to overlap with that of POU4F3 in hair cells (Erkman *et al.* 1996) and is similar to the pattern seen in the developing mouse inner ear at E15.5 (Tang *et al.* 2005;Xiang *et al.* 1998). Immunofluorescence experiments also showed, for the first time, that NR2F2 is expressed in the cochlear hair cells of the postnatal rat inner ear (see Figure 4.5) and the hair cells of the crista in the postnatal mouse inner ear; NR2F2 was only detected in the Hensen cells of the apical organ of Corti in postnatal mice (see Figure 4.6 and Figure 4.7). Furthermore, cytoplasmic NR2F2 expression was detected in basal P8 rat cochlear hair cells (similar to that seen in the rat pituitary gland (Raccurt *et al.* 2006)), suggesting that the function of NR2F2 in hair cells may be controlled by modulation of its subcellular localization. This expression pattern supports the possibility of a physiologically relevant regulatory relationship between POU4F3 and *Nr2f2* in hair cells. Therefore, the putative activation of the *Nr2f2* 5' flanking region by POU4F3 was investigated to verify activation and, if activation was confirmed, to identify the mechanism of regulation.

Two well-conserved POU4F3 binding sites were identified in the *Nr2f2* 5' flanking region by bioinformatic analysis and POU4F3 binding to these sites was verified by EMSA (sections 4.8 and 4.10.8). Having verified that POU4F3 is able to bind to these sites, POU4F3 was shown to activate two reporter constructs containing differing lengths of the *Nr2f2* 5' flanking region by luciferase assay (section 4.9). Furthermore, the POU4F3 binding sites that had previously been identified in the *Nr2f2* 5' flanking region were found to be required for the activation of an *Nr2f2* 5' flanking region reporter construct (NR2F2p4kb) as mutation of these sites reduced its activation from two-fold to 1.3-fold (section 4.10).

Collectively, the data presented provide strong evidence that POU4F3 activates *Nr2f2* and that this may be relevant to hair cell development, though evidence of this regulation would be strengthened by additional experimentation. Firstly, to better-characterise the timing

and variation of NR2F2 expression, a larger number of animals require investigation and investigation of older animals will help explain differences in postnatal NR2F2 expression between mice and rats. Study of NR2F2 expression in relation to markers of hair cell development may aid in this comparison and help determine whether the differences seen are due to the slower development of the rat or true interspecies differences.

To better characterise the effect of POU4F3 on NR2F2p4kb, independent mutations of NR2F2BS1 and NR2F2BS2 require investigation. Though the reduction in the activation of NR2F2pBS1&2mut compared to NR2F2p4kb shows the requirement of these sites for NR2F2p4kb activation, individual mutations of these sites will determine their contribution to this activation. Furthermore, the ability of POU4F3 to bind to these sites in genomic DNA could be investigated by chromatin immunoprecipitation. At a late stage of this investigation, preliminary attempts were made to identify POU4F3 binding to NR2F2BS1 and NR2F2BS2 by this method using a POU4F3 fusion protein (to overcome the lack of a suitable anti-POU4F3 antibody). Though this assay did not identify NR2F2BS1 or NR2F2BS2, the protocol used requires optimization (this was not carried out due to time constraints) and the possibility that the fusion protein used interferes with DNA binding by POU4F3 needs to be excluded.

Finally, the interaction of POU4F3 with the *Nr2f2* promoter in hair cells requires investigation in order to clarify the relevance of this interaction to their development and, if NR2F2 expression in hair cells is maintained throughout life, survival. In order to investigate the effect of POU4F3 expression on *Nr2f2* in hair cells, two models could be used: cochlear cultures and *Pou4f3* mutant mice. Though we intended to manipulate POU4F3 levels in hair cells in culture, we were unable to do so due to extremely low hair cell transfection efficiency despite a number of methods being attempted in our laboratory. Furthermore, we were unable to obtain *Pou4f3* mutant mouse inner ear tissue for investigation of the effect of *Pou4f3* mutation on NR2F2 levels. However, an adenovirus-based transfection protocol is currently being developed in our laboratory for use in cochlear cultures in order to overcome previous transfection problems.

In summary, future work will focus on the *in vivo* relevance of the regulatory relationship identified and clarification of the role of NR2F2 in the developing organ of Corti will aid in our understanding of its role in hair cell development and, potentially, maintenance. As NR2F2 has been shown to be essential for organogenesis and maintenance of a number of organs through signalling networks that are known to be active in the inner ear, future work on the role of NR2F2 in the inner ear is likely to focus on understanding how it interacts with these signalling cascades in this system. Given that its family member, NR2F1, has been shown to be essential for normal inner ear morphogenesis, NR2F2's potentially important role could be investigated using a conditional inner ear knockout to

circumvent the problems of the embryonic lethality of the homozygous *Nr2f2* knockout mouse. Such investigations would shed much light on the role of this multi-faceted transcription factor in the development of hearing and balance.

5

INVESTIGATION OF PUTATIVE *LUZP1*, *RBMS1* AND *ZRANB2* REGULATION BY POU4F3

Having identified putative POU4F3 target genes from a subtractive hybridization screen in UB/OC-2 cells, four candidate genes were prioritised for investigation: *Nr2f2* (chapter 4), *Luzp1*, *Rbms1* and *Zranb2*. These genes were selected based on their potential roles in hair cell development, likelihood of regulation by POU4F3 (estimated by the presence of predicted POU4F binding sites in their 5' flanking regions), and availability of reagents (see section 3.7). The identification and investigation of *Luzp1*, *Rbms1* and *Zranb2* is reported in this chapter.

As for *Nr2f2*, investigation of these genes focused on verification of the ability of POU4F3 to bind sites in their predicted promoter regions and to activate transcription in reporter constructs containing these regions. Furthermore, as an antibody was available for ZRANB2 which was suitable for immunohistochemistry, its inner ear expression profile was characterised to identify whether it is expressed in hair cells and thereby assess the likelihood of its being regulated by POU4F3 *in vivo*.

5.1 Introduction to *Luzp1*, *Rbms1* and *Zranb2*

5.1.1 Luzp1

The *Luzp1* gene is located on mouse chromosome 4 (human chromosome 1) and encodes an mRNA with a long (3940bp) 3' UTR that is suggested to be subject to rapid degeneration due to its AU-rich content. The protein encoded by *Luzp1* (LUZP1, also known as LUZP) was predicted to contain three leucine zipper motifs, numerous putative phosphorylation sites, eight potential glycosylation sites and three putative nuclear localization signals (Sun *et al.* 1996).

Of the predicted protein domains, the three leucine zipper motifs have been the focus of speculation over LUZP function. These domains are commonly seen in transcription factors where they mediate protein-protein interactions. They are often preceded by an adjacent basic region that is involved in sequence-specific DNA binding. Where this basic region is lacking, as is the case for LUZP1, leucine zipper containing proteins can interact with a wide variety of proteins of varying function and subcellular localization. Such proteins are less likely to be involved in transcriptional regulation. However, the predominantly nuclear localization of LUZP1 expression identified by immunohistochemistry in neural tissue suggests that it may have a transcription factor function despite not containing this basic region (Lee *et al.* 2001;Sun *et al.* 1996).

Expression of LUZP1 is strongest in the brain with lower expression levels in the kidney and lung (Sun *et al.* 1996). Immunohistochemical analysis of the perirhinal cortex showed LUZP1 expression in the nuclei of neurons with weaker expression in dendrites (Sun *et al.* 1996). Its expression in neural tissue was further investigated by Lee *et al.* who demonstrated expression in pyramidal neurons in the cerebral cortex and hippocampus as well as neural tissue in teratomas (Lee *et al.* 2001). *Luzp1* knockout mice die perinatally due to cardiac and neural tube defects. Some homozygotes display exencephaly and less severely affected animals show hypomorphic development of the brain and adjacent structures. These defects are due to neural tube closure defects that have been shown to be associated with ectopic sonic hedgehog signalling and elevated apoptosis in the dorso-lateral hindbrain neuroepithelium (Hsu *et al.* 2008).

Based on these data, a working model of LUZP1 function proposes that it acts as a negative transcriptional regulator by binding to transcription factors via its leucine zipper motifs (e.g. bHLH transcription factors which have been shown to be inhibited by leucine zipper containing proteins) and inhibiting their function. Furthermore, phosphorylation of predicted sites in LUZP1 may acts as a means of modulating its function (Sun *et al.* 1996). However, the above model is almost entirely based on computational predictions and the ability of LUZP1 to dimerise and be phosphorylated has not been tested experimentally. The expression and function of LUZP1 in the inner ear has also not been investigated.

5.1.2 Rbms1

RBMS1 (also known as *MSSP gene 2*) is a 16-exon gene with a coding sequence of over 60kb. This sequence gives rise to alternative transcripts to produce the proteins MSSP-1, MSSP-2, SCR2 and human YC1 (Haigermoser *et al.* 1996;Kanaoka *et al.* 1994). MSSP (i.e. either MSSP-1 or MSSP-2) and SCR2 expression was found in all tissues examined though short MSSP transcripts were found to be abundantly expressed in testis tissue (Fujimoto *et al.* 2000).

MSSP has been shown to have versatile functions that are, for the most part, relevant to its interaction with the proto-oncogene c-Myc. The first of its functions to be identified were those of DNA binding and replication. MSSP was found to bind to both the single- and double-stranded forms of a putative DNA replication origin / transcriptional enhancer in the human c-Myc gene (*myc*21) (Negishi *et al.* 1994). The DNA binding properties of MSSP-1 and MSSP-2 were shown to be identical and mediated through two ribonucleoprotein binding domains (RNP-1A and RNP-1B) which are both contained in all MSSP family proteins and are required for DNA binding to an MSSP recognition sequence (TCTCTTA). Furthermore, these proteins were found to promote DNA replication, resulting in G_1 to S phase cell cycle progression and this function was shown to require the integrity of almost the whole MSSP protein (Takai *et al.* 1994). The mechanism by which MSSP produces this effect has been investigated by GST 'pull-down' assays and it was found to bind to the N-terminus of the DNA polymerase alpha catalytic subunit both *in vitro* and in human cells. Furthermore, MSSP was able to stimulate DNA polymerase activity *in vitro*, suggesting that it forms part of the origin of DNA replication complex (tested at the DNA replication origin of the *c-myc* gene) and demonstrating a mechanism through which it can promote G_1 to S phase progression (Niki *et al.* 2000a).

As well as DNA replication, MSSP has been shown to play a role in transcriptional regulation. It is able to bind to cMyc protein (which acts as a transcription factor as well as performing other functions (for review see Eilers *et al.* 2008)) in order to affect its DNA binding ability. cMyc is able to bind to a DNA consensus sequence (the E-box) as a heterodimer with a transcription factor called Max. This heterodimerisation takes place at the cMyc leucine zipper motif which, unlike in LUZP1, has a basic region on its N-proximal side. MSSP-2 was shown to be able to bind to this basic region to form a cMyc/Max/MSSP-2 ternary complex that abrogates the ability of cMyc/Max to bind, and therefore regulate, the E-box DNA sequence (Niki *et al.* 2000b). Therefore, MSSP may be able to modulate transcriptional regulation at other cMyc target genes such as those that promote cellular growth e.g. eIF-2α (Rosenwald 1993). Furthermore, MSSP has been shown to be able to regulate transcription directly e.g. there is strong evidence that it is able to directly transrepress the chicken alpha-smooth actin gene at a site (TATCTTA) in the 5' flanking region of this gene (Kimura *et al.* 1998).

The final experimentally verified functions of *Rbms1* gene products are induction of apoptosis and cell transformation (i.e. induction of neoplasia). Overexpression of MSSP-1 or MSSP-2 in HeLa cells was shown to result in apoptosis in a dose-dependent manner through a Fas-dependent mechanism (Iida *et al.* 1997;Nomura *et al.* 2005) and MSSP was shown to promote cell transformation by *ras*/*myc* in a manner dependent on its RNP domains which have been shown to be necessary for all of its functions (Niki *et al.* 2000b).

Unlike *Luzp1* and *Zranb2*, the regulation of *RBMS1* has been investigated in some detail by investigation of transcriptional activity at its 5' flanking region. Haigermoser *et al.* investigated the basal regulation of *RBMS1* 5' flanking region constructs of differing length. A region from –1709 to +61 (relative to the identified transcriptional start site) was shown to be basally expressed in HeLa cells by luciferase assay. Deletion of the 5' sequence of this construct to as far as -1283 resulted in an approximately two-fold increase in the transcription of the sequence and further deletions resulted in a reduction in transcriptional activation to levels near or below that of the longest sequence tested. This analysis identified that the region from -1709 to -1283 is likely to contain negative regulatory elements with positive regulatory elements present from -1283 to -196 and a region from -488 to -196 being responsible for an approximately four-fold reduction in luciferase production when deleted (Haigermoser *et al.* 1996). This GC rich region was thought to be regulated by SP1 or AP2 due to consensus sequences for these binding sites being present in this region from which the -474 to -440 fragment was shown to be protected from DNAseI by two proteins – one of 38kDa one of 62kDa – that are activated in the G_1 stage of the cell cycle. However, neither SP1 nor AP2 was able to bind this region in a DNA binding assay, and neither of the proteins that bind this region have been identified (Fujimoto *et al.* 1998;Haigermoser *et al.* 1996).

The apparently wide-reaching functions of *Rbms1* are reflected by homozygous knockout mice that demonstrate an approximately 50% embryonic lethality rate, though surviving animals do not display any overt phenotype. This may be due to a similar protein, SCR3 – an MSSP family protein that is produced by a distinct gene – compensating for the lack of *Rbms1* gene products. On closer examination, homozygous knockout mice were shown to have retarded testicular, uterine and ovarian development, with adult females showing disrupted serum progesterone levels in pregnancy (Fujimoto *et al.* 2001). As for *Luzp1* and *Zranb2*, the function, expression and regulation of *Rbms1* and its products has not been studied in the inner ear and the inner ears of *Rbms1* knockout mice have not been investigated. However, given the versatility of its function and potential relevance to inner ear development, the actions of MSSP-1, MSSP-2 and Scr2 in the inner ear could be of particular interest.

5.1.3 Zranb2

Zranb2 (formerly known as *Zis* and *Znf265*) is the most recently discovered of the four genes prioritised in this investigation and encodes ZRANB2, which has been shown to be able to induce alternate splicing of RNA transcripts (Adams *et al.* 2001;Karginova *et al.* 1997). ZRANB2 is an extremely well conserved protein with human and rat ZRANB2 having identical protein sequences and the mouse protein differing by a single residue (Karginova *et al.* 1997). There are two splice variants of human and mouse ZRANB2 which

differ by ten amino acids with ZRANB2-1 (the longer form that contains exon 11 instead of exon 10) appearing to be more predominantly expressed than ZRANB2-2 (the shorter form that contains exons one to ten) (Li *et al.* 2008;Mangs *et al.* 2006;Nakano *et al.* 1998).

The expression of *Zranb2* mRNA has been widely investigated by Northern blot analysis which has shown it to be expressed in the brain, heart, liver, kidney, lung, testis, skin, placenta, muscle and pancreas (Adams *et al.* 2000;Karginova *et al.* 1997;Nakano *et al.* 1998). Its expression appears consistently lower in the lung and liver than in other tissues and the level of expression and detectable transcripts in all organs appears to vary between organisms and ages tested (Adams *et al.* 2000;Karginova *et al.* 1997;Nakano *et al.* 1998). Generally, its expression is stronger and more consistent between organs in foetal tissues, becoming reduced and more specific in adult tissues (Adams *et al.* 2000;Karginova *et al.* 1997;Nakano *et al.* 1998). This pattern of expression suggests that ZRANB2 is widely required for development, progressing to more restricted functions in adult tissues (Adams *et al.* 2000;Karginova *et al.* 1997;Nakano *et al.* 1998). The subcellular localization of ZRANB2 has been investigated in cell lines by western blot and immunofluorescence, showing expression throughout the nucleus or slightly more restricted to nuclear speckles (structures that contain pre-mRNA) (Adams *et al.* 2001;Mangs *et al.* 2006).

The ZRANB2 protein is composed (from N-terminal to C-terminal) of two zinc fingers followed by a predicted nuclear localization signal and an Argine/Serine-rich (RS) domain. The zinc finger motifs are separated by a 24-residue flexible linker (characteristic of an RNA recognition motif) and have been classified as Ran-binding domains based on their homology to this motif (reviewed in Mangs *et al.* 2008). Though the nuclear localization signal was predicted to lie between the zinc finger and RS region, deletion assays with EGFP fusion proteins revealed that this region is not required or sufficient for nuclear ZRANB2 expression in transfected cultured cells and that it is the RS domain that is responsible for nuclear localization in this system. However, the exact location of the nuclear localization signal within the RS region of ZRANB2 remains unknown (Adams *et al.* 2001).

The zinc fingers of ZRANB2 underlie its ability to induce alternative splicing (Adams *et al.* 2001). ZRANB2 is thought to be active at the early spliceosome where it binds to single-stranded RNA containing AGGUAA repeats with micromolar affinity. Through this binding, it is thought to influence splice site selection as it may be able to contact both splice donor and splice acceptor sites to influence splicing (Loughlin *et al.* 2009). Supporting evidence for the role of Zranb2 in alternative splicing is provided by its ability to interact with the spliceosomal constituents SFRS17A, U1-70K and U2AF^{35} in yeast two-hybrid assays and its colocalisation with these proteins in the nucleus (Adams *et al.* 2001;Mangs *et al.* 2006).

More recently, ZRANB2 has been suggested to play a role in immune responses as its expression changes in response to *Ureaplasma Urealyticum* infection in Sertoli cells (both in cultured cells and *in vivo*) (Li *et al.* 2009) and viral infection (Finsterbusch *et al.* 2009) though the mechanisms of these observations have not been characterised. The regulation of *Zranb2* has also not been characterised (Mangs *et al.* 2008). Though its function and expression are poorly understood, characterisation of the potential role of ZRANB2 in the inner ear through its involvement in alternative splicing may aid in the understanding of alternative splicing in hair cells, which is also poorly understood.

5.2 Identification of *Luzp1*, *Rbms1* and *Zranb2* as potential POU4F3 targets

In the subtractive hybridization screen, *Luzp1*, *Rbms1* and *Zranb2* were identified as putatively upregulated POU4F3 targets from three clones (D3, FB5 and FA8). As previously described (sections 3.3.1), these clones were sequenced and adaptor oligonucleotides from the subtractive hybridization screen were identified and deleted from the resulting sequencing files (Figure 5.1*a*, Figure 5.2*a* and Figure 5.3*a*). The trimmed sequences were submitted to the Ensembl BLASTN software to identify alignments to the Ensembl mouse cDNA library (Figure 5.1*b*, Figure 5.2 *b* and Figure 5.3 *b*) with the most significant match from the BLAST analysis being investigated as the corresponding gene for each clone. Furthermore, for prioritised genes, all matches of a given clone to its corresponding gene were aligned with the corresponding gene sequence as the BLAST software does not return matches that are likely to have arisen due to chance e.g. due to single base-pair repeats (Figure 5.1*c*, Figure 5.2*c* and Figure 5.3*c*).

5.2.1 Clone D3 of the subtractive hybridization screen matches Luzp1

On BLAST analysis, the trimmed 727bp sequence of clone D3 of the subtractive hybridization screen (Figure 5.1*a*) most significantly matched a 727bp region of the *Luzp1* 3'UTR with 99.7% sequence identity (Figure 5.1*b*). The next match was of 23bp with 95.7% sequence identity to another gene and was therefore likely to have arisen by chance. The best match was confirmed by alignment of the trimmed sequence with the Ensembl *Luzp1* sequence which revealed a full alignment apart from a 1bp mismatch and a 1bp insertion (Figure 5.1*c*). *Luzp1* was therefore selected as the corresponding gene for clone D3.

5.2.2 Clone FB5 of the subtractive hybridization matches Rbms1

Similarly, the trimmed 286bp sequence of clone FB5 (Figure 5.2*a*) was found to most significantly match a region in the *Rbms1* gene of 132bp with 100% sequence identity (Figure 5.2*b*). All other matches were also to *Rbms1*. Alignment of the trimmed clone FB5 sequence with the Ensembl *Rbms1* sequence showed a full-length match between clone FB5 and *Rbms1* of 99.7% sequence identity i.e. a 286bp match with a 1bp mismatch (Figure 5.2*c*). Furthermore, the position of this alignment to *Rbms1* (Figure 5.2*b*) suggested that clone FB5 corresponded to the shortest *Rbms1* transcript in the Ensembl library.

5.2.3 Clone FA8 of the subtractive hybridization matches Zranb2

Finally, clone FA8 fully matched 108bp of the *Zranb2* 3' UTR (Figure 5.3*b*), the next best match being 19bp long (100% sequence identity) and therefore likely to be due to chance. Alignment of the trimmed clone sequence (Figure 5.3*a*) with *Zranb2* revealed that all 548bp of this sequence fully matched the corresponding region in the *Zranb2* 3' UTR (Figure 5.3*c*). Zranb2 was therefore selected as the corresponding gene for clone FA8.

a)

TCGAGCGGCCGCCCGGGCAGGTACCAATTGGCAGCCCTGAGAGTTAAAAGGAAACAGGCCCC
CTGTGGTGGTCCACTGAAGAGTATAGGAAATTAAGTCTGTGGCTCTTCTCTGCTGATAAAAAC
AGAGGGGCACCAAGCCCTGCCTCAAAATATCTCGTCAATAATTTTTGTCTTTGGGTGTTGAGC
CCTGGATTCTTCTGGTGCTGTAGCTCCTGGTGCCAAAGTCTGGATCTTTCCACATTTTAGCAGC
ACCAACACCTGCTGCTATTTGAAATGTTCTGTGGAAAAGGGACAGCTGTGGGATGCCATTTTG
AAAATCTGAGTGCAATAGCATTTGATTGTAACAATTATTTCAGGATATTTTGTTTCTTTAGTCT
GCACACTTTGTAGTCCTGCCATAAAGTAGATTTTATTTTTAAATACCTTCAGCATTGCAAATGT
TTATACCAAGCAAATGGAGGCTAGAGGGTTCAAGTCCCCTTGGGCCTCATATGGATGGCTAGA
CTGACTCTGATTTCAAGGTCGAAAGACATATCACTTCTGAAAACACCAAGATGTAACCTTTGG
GCCCAAGCCAGAAGCTGCAGGAAGCCTCCACATAGAAGGGAGACTGGTATTCAAACCATTGT
CTAATCAAGCCAAATATTCCCCACTAAAAGACCCACTTTCCTGACAGTGCTTCTCTAAAGTTTG
GGTAGGTGGCTAAATTGAGCCAGCAGGTCAGGAGTCTATGAGAGTTCTGAGTNCCTCGGCCG
CGAGCACGCT

b)

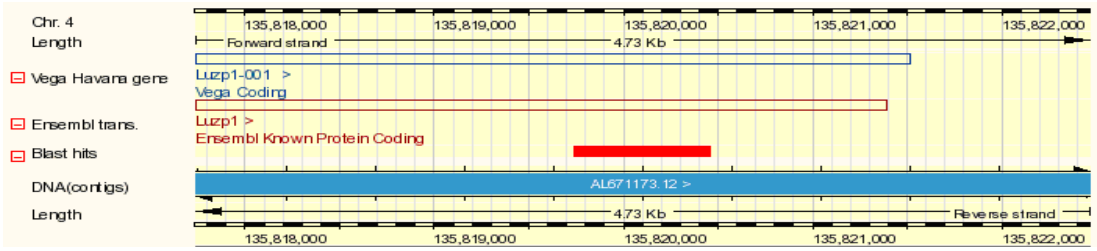

c)

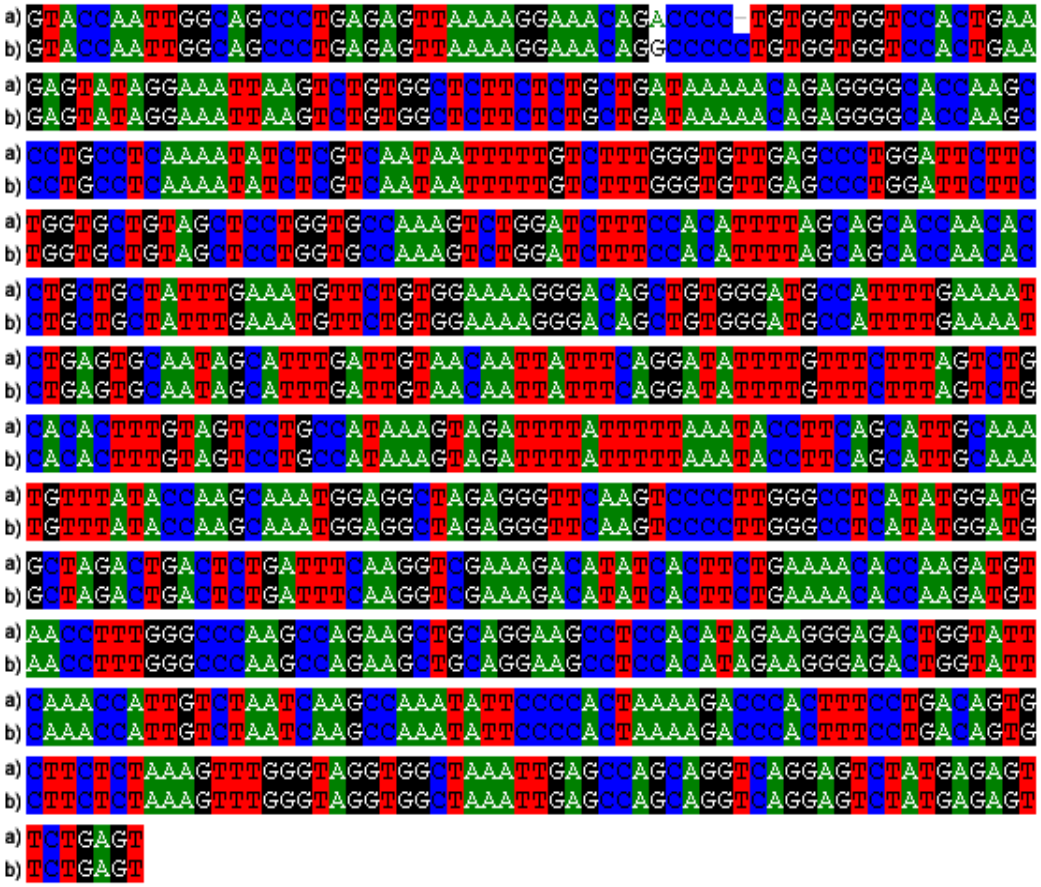

Figure 5.1. Clone D3 of the subtractive hybridization screen matches *Luzp1*.
a) adaptor sequences from the subtractive hybridization screen (*red type*) and non-specified bases (*N*) were deleted from the clone D3 sequence. (*b*) the full length of the trimmed clone matched a region in the *Luzp1* 3' UTR with 99.7% sequence identity. This alignment is shown at the nucleotide level in (*c*). *c.a*, Ensembl sequence; *c.b*, trimmed clone D3.

a)

NNNNNNNNNANGCTGCAGACGCGTTACGTATCGGATCCAGAATTCGTGATT
AGCGTGGTCGCGGCCGAGGTACTTGTTTGGGTTCTGTCTCTTTTTCTGTCCTCC
ATCCGCAAACTTGCACAGTAAAGGTTCTGTAGGAGCAGAAACTCCTGGTGGG
GTCTTGATGAATTTTCCATTAAAATGACCAATTACAGCTTCGCATTTTTCCGTT
GATTCCATCCTGGCAAAGCCAACACCACGGCTGGCACCACTGGAATCACGTA
GGACCCTTGTAGAAATAACTTGTCCAAAGGGTTTGAGCATATTTTCAAGTTCC
TGCTCATCCATGGACAGCGGCAGGTTAGAAATGTACCTGCCCGGGCGGCCGC
TCGAAATCTGA

b)

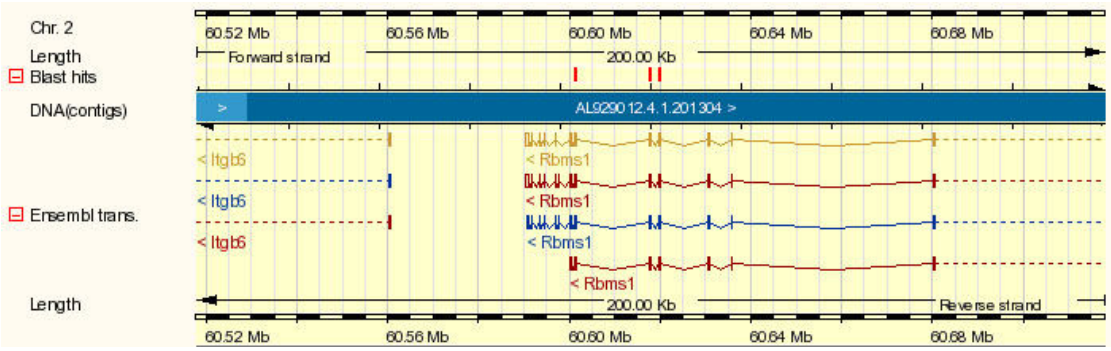

c)

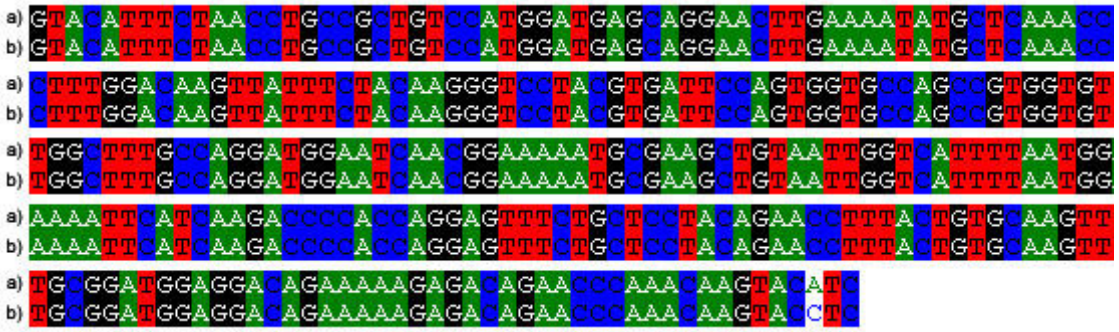

Figure 5.2. Clone FB5 of the subtractive hybridization screen matches *Rbms1*.
a) Full sequencing of clone FB5 was verified by identification of adaptor sequences and non-specified bases (*red type*) from the subtractive hybridization screen. These were deleted from the sequence prior to BLAST analysis, leaving insert sequence alone (*black type*). *b*) Ensembl 'ContigView' of the match of the trimmed insert sequence to the *Rbms1* gene. *Red boxes* on the '*Blast hits*' row represent matches to the *Rbms1* transcripts below. *c*) the trimmed clone FB5 sequence (*c.b*) matches the Ensembl *Rbms1* sequence (*c.a*) with a one base-pair mismatch.

a)

NNNNNNNANNNNNANGCNGCAGACGCGTTACGTATCGGATCCAGAATTCGT
GATTAGCGTGGTCGCGGCCGAGGTACGATACTTTGTTTTCATCTTTAGATCAG
TTGAGAAGAGAAACACTCACTTTAAAATAAAAACATTTTGTTTGATCTGTCTA
CTAAACATCTTAGAAGGCTTTACTTATTTAAACTGCAGCAGACAAATACTAA
AGGAGAAACAGGAAAAATAATTCCCTCACAAGGAGCCCCAGCACAACTGTT
GTCCCTTATATACTTACCTTGCTTTTGCTGCTGAAGAGACTGTTAAAGAGAAA
CCTTTTAACTTTTAAACCAGAGAACAAAATGGATCTCAAGTGACCAGATTTTA
ATTTGAGAAATAAAACTCCAAAAGCATTTTAAGCCATATGGTTTTCTTTTTCA
GATGTGGAGAAAAATGATTTTGCTTAAATTGTGCAGAAATAAGAATTCTTCT
GTTACTTAGGTATCTGCAATGTTCAAAATCAGACATCACAAGGCAAATGTTC
ACTTAAATTCATGTCCCTGTCAGCCTGCCACTGAGAAACAGGTTTCAAAAGCT
TTCTTCAATTTGCTCATTAACTATGATTTAGCCTTTTTTAAAAATCCACCTGCC
CGGGCGGCCGCTCGAATCTG

b)

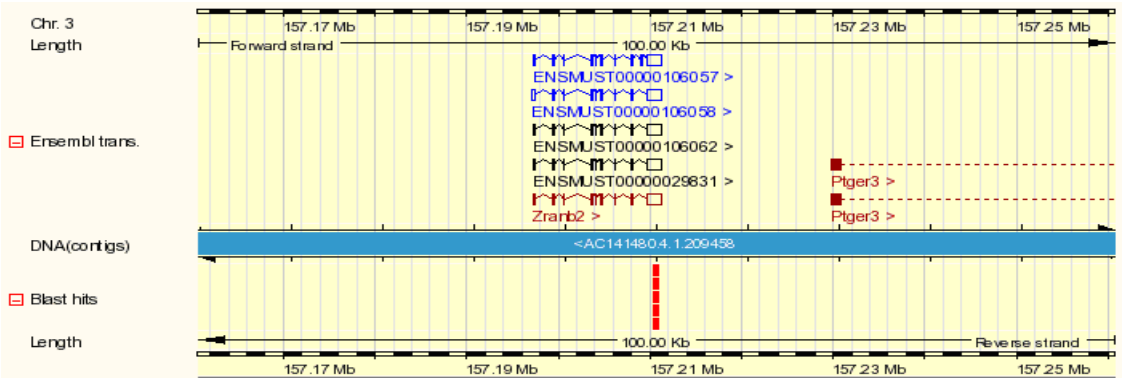

c)

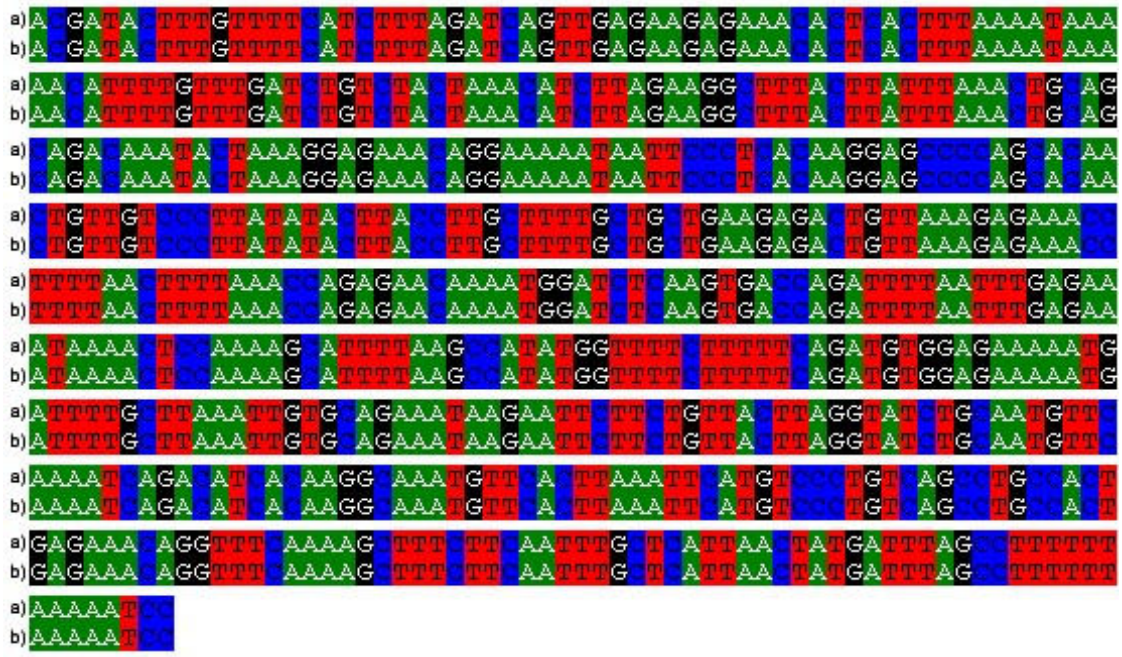

Figure 5.3. Clone FA8 of the subtractive hybridization screen matches *Zranb2*.
a) Adapter oligonucleotide sequences and non-specified bases (*red type*) were trimmed from the clone FA8 sequence prior to BLAST analysis. This analysis (*b*) revealed that part of the clone FA8 sequence (*red*) matched *Zranb2* known protein coding sequence (*maroon*). *c*) shows the alignment of the trimmed FD8 sequence (*c.a*) with the matching region in the Ensembl *Zranb2* sequence (c.b).

5.3 Initial prioritisation of *Luzp1*, *Rbms1* and *Zranb2* for investigation

As previously described (section 3.8), *Luzp1*, *Rbms1* and *Zranb2* were prioritised for investigation over other putative POU4F3 target genes in part due to their known function and availability of reagents for their study. The investigation of the known function of candidate genes was based on the GO units identified for these genes (see section 3.3.2) that were judged with additional information on their supporting evidence from the literature. The availability of reagents was also investigated in the literature and in company catalogues. These analyses are reported here in detail.

5.3.1 Selection of Luzp1 for investigation

Unlike *Nr2f2*, *Luzp1* was (and remains) an uncharacterised gene with only three GO units reported through the Ensembl genome browser (Table 5.1). The lack of GO units reflected the lack of published data for *Luzp1* at the time of the analysis (2006) with only two papers reporting the predominantly nuclear expression of LUZP1 in neural tissue (some expression was seen in dendritic profiles) (Lee *et al.* 2001;Sun *et al.* 1996). Of the GO units identified, *GO:0005634* refers to the nuclear LUZP1 expression pattern that is found in neurons and neural tissue in teratomas (Lee *et al.* 2001;Sun *et al.* 1996). The two other GO units (*GO:0003674* and *GO:0008150*) refer to the predicted leucine zipper motifs in LUZP1 that may mediate protein-protein interactions and allow it to act as a transcription factor (Sun *et al.* 1996).

Though the expression pattern of LUZP1 in the inner ear has not been investigated and its expression in the inner ear was not identified in the online databases investigated (see section 3.6), the predominantly nuclear expression of this protein coupled with its predicted transcription factor function suggest that it may play an interesting role in hair cell development and maintenance if expressed in these cells (Lee *et al.* 2001;Sun *et al.* 1996). Furthermore, the presence of two binding sites in the *Luzp1* 5' flanking region with high similarity to known POU family binding sites (see sections 3.5 and 5.5.1), supported the possibility that *Luzp1* is a directly regulated POU4F3 target. Therefore, despite not being able to obtain an anti-LUZP1 antibody at the time of these analyses, *Luzp1* was selected for further investigation due to its potentially interesting role in the inner ear.

Table 5.1. *Luzp1* GO units.
ND, no biological data available, *IDA*, inferred from direct assay.

GO ID	*GO Term*	*Evidence Code*
GO:0003674	Molecular function	ND
GO:0005634	Nucleus	IDA
GO:0008150	Biological process	ND

5.3.2 Selection of Rbms1 for investigation

NB *For clarity, Rbms1 gene products are collectively referred to as RBMS1 though, in the literature, different isoforms are often referred to as MSSP (for MSSP-1 and/or MSSP-2) and Scr2.*

In contrast to *Luzp1*, RBMS1 has experimentally verified DNA binding ability and is known to play a role in DNA replication (Negishi *et al.* 1994). The GO units identified for this gene reflected this as well as proposed, unproven roles in RNA processing and translation (Table 5.2). However, they fail to identify the ability of RBMS1 to act as a transcription factor (e.g. Kimura *et al.* 1998). These results demonstrate that, though this method provides a useful means by which to rapidly assess gene function, a literature search is required for more sensitive and specific identification of target gene functions.

As for *Luzp1*, the inner ear expression pattern for RBMS1 is unknown, though it has been found to be expressed in all organs examined by Northern blot (Fujimoto *et al.* 2000). Given that the processes in which RBMS1 has been implicated are relevant to hair cell development and maintenance, and as reagents were available for its study (an antibody, expression construct and 5' flanking region luciferase reporter construct), *Rbms1* was selected for further investigation.

Table 5.2. *Rbms1* GO units.
IEA, inferred from electronic annotation; *TAS*, traceable author statement; *NAS*, Non-traceable author statement; *ND*, no biological data available.

GO ID	*GO Term*	*Evidence Code*
GO:0000166	Nucleotide binding	IEA
GO:0003690	Double-stranded DNA binding	TAS
GO:0003697	Single-stranded DNA binding	TAS
GO:0003723	RNA binding	NAS
GO:0005634	Nucleus	IEA
GO:0006260	DNA replication	TAS
GO:0006396	RNA processing	TAS
GO:0006445	Regulation of translation	TAS
GO:0008372	Cellular component unknown	ND

5.3.3 Selection of Zranb2 for investigation

As for other candidate genes, *Zranb2* GO units were obtained, examined and compared to those of other candidate genes in order to decide whether to pursue its putative regulation by POU4F3 in hair cells. *Zranb2* had six identified GO units, four of which were supported by author statements and two of which were predicted based on a zinc finger domain in its sequence (Table 5.3). It was thought to be capable of binding DNA or RNA with the two zinc fingers in this domain (Karginova *et al.* 1997), though subsequent analysis of this region in ZRANB2 showed it to be an RNA-binding protein (Plambeck *et al.* 2003).

Though this candidate gene was not as thoroughly characterised as others, its ability to influence splicing made it an interesting candidate for further investigation (Morris *et al.* 2001), i.e. if ZRANB2 is expressed in hair cells, it might contribute to the hair cell phenotype through this process. Furthermore, it was possible to obtain a sample of an anti-ZRANB2 antibody from a company, making it possible to rapidly assess its expression in the inner ear if found to be suitable for immunohistochemistry (as for LUZP1 and RBMS1, the inner ear expression pattern of ZRANB2 was unknown). Therefore, *Zranb2* was selected for further investigation.

Table 5.3. *Zranb2* GO units.
TAS, traceable author statement; *IEA*, inferred from electronic annotation.

GO ID	*GO Term*	*Evidence Code*
GO:0003700	Transcription factor activity	TAS
GO:0003723	RNA binding	TAS
GO:0005634	Nucleus	TAS
GO:0008270	Zinc ion binding	IEA
GO:0008380	RNA splicing	TAS
GO:0046872	Metal ion binding	IEA

5.4 Investigation of the inner ear expression patterns of selected genes

Following candidate gene prioritisation, I aimed to identify whether the selected genes are expressed in the POU4F3-expressing hair cells of the inner ear. Such coexpression of POU4F3 with candidate genes would aid in the decision to continue the investigation of these genes as it would support the putative upregulatory relationships between POU4F3 and these genes suggested by the subtractive hybridization screen. Two methods, RNA *in situ* hybridization and immunohistochemistry, are best suited to the assessment of target gene expression *in situ*. If a suitable antibody is available for the target gene of interest, immunohistochemistry is the most rapid and robust of these methods. Therefore, I searched the literature and antibody company catalogues to identify suitable reagents for the intended analysis.

Antibodies were found to be available for LUZP1, RBMS1 and ZRANB2. Therefore, I attempted to obtain gifts or samples of these antibodies with which to investigate the inner ear expression patterns of these proteins. By this method, I was able to obtain an anti-RBMS1 antibody from a collaborator (Dr H Ariga) which has been shown to recognise two *Rbms1* alternative transcripts (MSSP-1 and MSSP-2). An anti-ZRANB2 antibody sample was also obtained from a company (Abnova 2008a). I was, however, unable to obtain an anti-LUZP1 antibody at this stage.

5.4.1 Western immunoblot to investigate RBMS1 and ZRANB2 expression in UB/OC-1 and UB/OC-2 cells

Prior to use in immunohistochemistry, the anti-RBMS1 and anti-ZRANB2 antibodies were used in western immunoblots. Though both of these antibodies had previously been shown to be suitable for use in western immunoblotting (see Abnova 2008a for anti ZRANB2;Takai *et al.* 1994 for anti-RBMS1) this analysis was conducted to verify the specificity of these antibodies and to identify which RBMS1 and ZRANB2 isoforms might be expressed in the cells investigated. UB/OC-2 cells were selected for this analysis as they were shown to express *Rbms1* and *Zranb2* mRNAs and were therefore likely to express the corresponding proteins (Figure 3.1). As for a similar investigation of the anti-NR2F2 antibody (section 4.6.1), UB/OC-1 cell protein extract was included for comparison. UB/OC-1 and UB/OC-2 whole cell protein extract was electrophoresed with a molecular weight marker on a 10% polyacrylamide gel and electroblotted onto a PVDF membrane for immunodetection. The transfer of sufficient protein to the membrane for immunodetection was confirmed by Ponceau S staining.

Figure 5.4 shows the results of immunoblots with the anti-RBMS1 (Figure 5.4*a*) and anti-ZRANB2 (Figure 5.4*b*) antibodies. For anti-RBMS1, a single band of approximately 45kDa was identified which was consistent with its previously reported molecular weight of approximately 50kDa (Figure 5.4*a*) (Kimura *et al.* 1998). This demonstrated the specificity of the anti-RBMS1 antibody, though it was not possible to identify to which RBMS1 isoform this band might correspond based on the available literature. Having verified its specificity, this antibody was used in immunohistochemical investigations of the inner ear expression pattern of RBMS1.

In the anti-ZRANB2 immunoblot (Figure 5.4*b*), three bands were identifiable in the UB/OC-1 cell lane and two bands were seen in the UB/OC-2 cell lane. The most dense of these bands is approximately 55kDa and matches the previously reported size of human ZRANB2 identified by polyclonal rabbit antibodies (Adams *et al.* 2001;Li *et al.* 2008), though this is heavier than the predicted 38kDa of both the predicted protein size and the recombinant protein against which it was raised (Abnova 2008a). Two less dense bands were also seen in UB/OC-1 whole cell protein extract. One was lighter and one was heavier than the most dense (55kDa) band. Only the 55kDa band and the lighter band were identified in UB/OC-2 cell protein extract, though both of these bands were less dense in these cells. The latter difference may have been due to unevenness of protein loading onto the SDS-PAGE gel or uneven transfer to the PVDF membrane as Ponceau staining of the membrane revealed that the protein concentration in the UB/OC-2 cell lane was slightly less dense than that in the UB/OC-1 cell lane (data not shown). However, as the assessment of relative levels of protein expression between cell types was not the focus of this experiment, the equality of protein concentration between cell types was not compared by equalising the membrane

with an antibody to a housekeeping gene. This pattern raises the possibility that the expression of different *Zranb2* isoforms may be influenced by differential POU4F3 expression between these two cell types, though the western blot would have to be repeated with confirmation of equal protein loading in order to confirm that the difference seen was not due to a lack of sufficient protein for detection in the UB/OC-2 lane.

Two transcripts of *Zranb2* are known to exist in humans and mice and many alternative transcripts have been identified by Northern blot (Adams *et al.* 2001;Li *et al.* 2008;Mangs *et al.* 2008;Nakano *et al.* 1998). Furthermore, the characterisation of regulation and potential autoregulation of *Zranb2* is poor (Mangs *et al.* 2008). Therefore, these bands were assumed to have arisen due to alternate transcripts of *Zranb2* though it is possible that the antibody used displays some non-specific binding or that different ZRANB2 isoforms exist due to post-translational modification. Given its affinity to a band of equivalent molecular weight to a known ZRANB2 isoform (55kDa), the antibody was judged to be sufficiently specific for immunohistochemical investigation of the ZRANB2 expression.

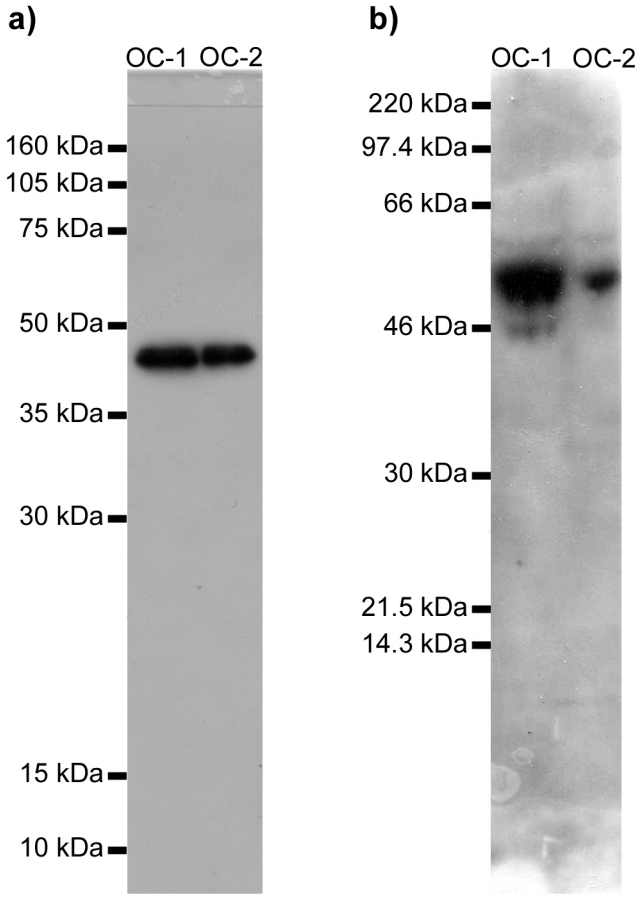

Figure 5.4. RBMS1 and ZRANB2 expression in UB/OC-1 and UB/OC-2 cells.
a) immunoblot analysis of UB/OC-1 and UB/OC-2 whole cell protein extract was carried out with an anti-RBMS1 antibody. This analysis revealed a single band of approximately 45kDa in both UB/OC-1 and UB/OC-2 protein extract lanes. *b*) the same analysis was carried out with an anti-ZRANB2 antibody. This identified a band of approximately 55kDa for both UB/OC-1 and UB/OC-2 cells. A heavier, less dense band of approximately 60kDa was also identified in these two cell types though a lighter band of approximately 46kDa was only identified in UB/OC-1 cell protein extract.

5.4.2 Investigation of RBMS1 expression in the inner ear

Having confirmed the sensitivity of the anti-RBMS1 antibody by western blot, this antibody was used with cryosections of early postnatal rat cochleas, as for NR2F2 (see section 4.7), to characterise RBMS1 expression in this tissue. Several antibody dilutions were attempted and an alternative detection method was used to enhance any signal (ABCelite with DAB/Nickel enhancement (Vector)). However, no specific signal was identified. Therefore, immunofluorescence experiments were attempted in UB/OC-2 cells in which RBMS1 expression had been confirmed by western blot. Again, no specific signal was detected (data not shown) and the antibody was therefore determined not to be suitable for use in immunohistochemistry.

5.4.3 Investigation of ZRANB2 expression in the inner ear

The mouse monoclonal anti-ZRANB2 antibody was also used in immunofluorescence experiments with cryosections of rat inner ears at P0, P4 and P8 to identify any ZRANB2 expression in this tissue and, particularly in hair cells. ZRANB2 expression was detected at P0 (Figure 5.5), though it was not detected at P4 or P8 (data not shown). At P0, all labelling appeared predominantly nuclear with stronger expression noted in cells of the cochlear duct compared to surrounding cells. Its subcellular localization in hair cells was also nuclear (*arrows* Figure 5.5) with no base-to-apex gradient of expression noted within sections. Furthermore, no difference in signal intensity was noted between hair cells and other cells of the cochlear duct (Figure 5.5). These results represent the first description of the cellular and subcellular localization of ZRANB2 in the inner ear and require verification by replication, though they support the hypothesis that POU4F3 may regulate *Zranb2* in hair cells. Given that no ZRANB2 expression was identified by P4 in the rat cochlea, the apparently rapid downregulation of its expression could be further investigated by examining the inner ears of rats at intervening ages to determine the pattern of this downregulation.

5.4.4 Immunohistochemistry as a means of investigating the expression patterns of candidate genes

The results of attempts to characterise the expression of candidate POU4F3 target genes presented in this section illustrate the strengths and weaknesses of the strategy used. The dependence of this strategy on the availability of a suitable antibody for immunohistochemical investigation of candidate gene expression resulted in it not being possible to investigate LUZP1 and RBMS1 expression in the inner ear. However, the specificity of the anti-RBMS1 antibody seen in western blot suggested that it could be valuable for future investigations e.g. supershift or chromatin immunoprecipitation (Nomura *et al.* 2005). In contrast, this strategy was suitable for investigation of ZRANB2 expression (as it had been for NR2F2). Furthermore, the cost and duration of this investigation was much lower and shorter than that of alternative strategies.

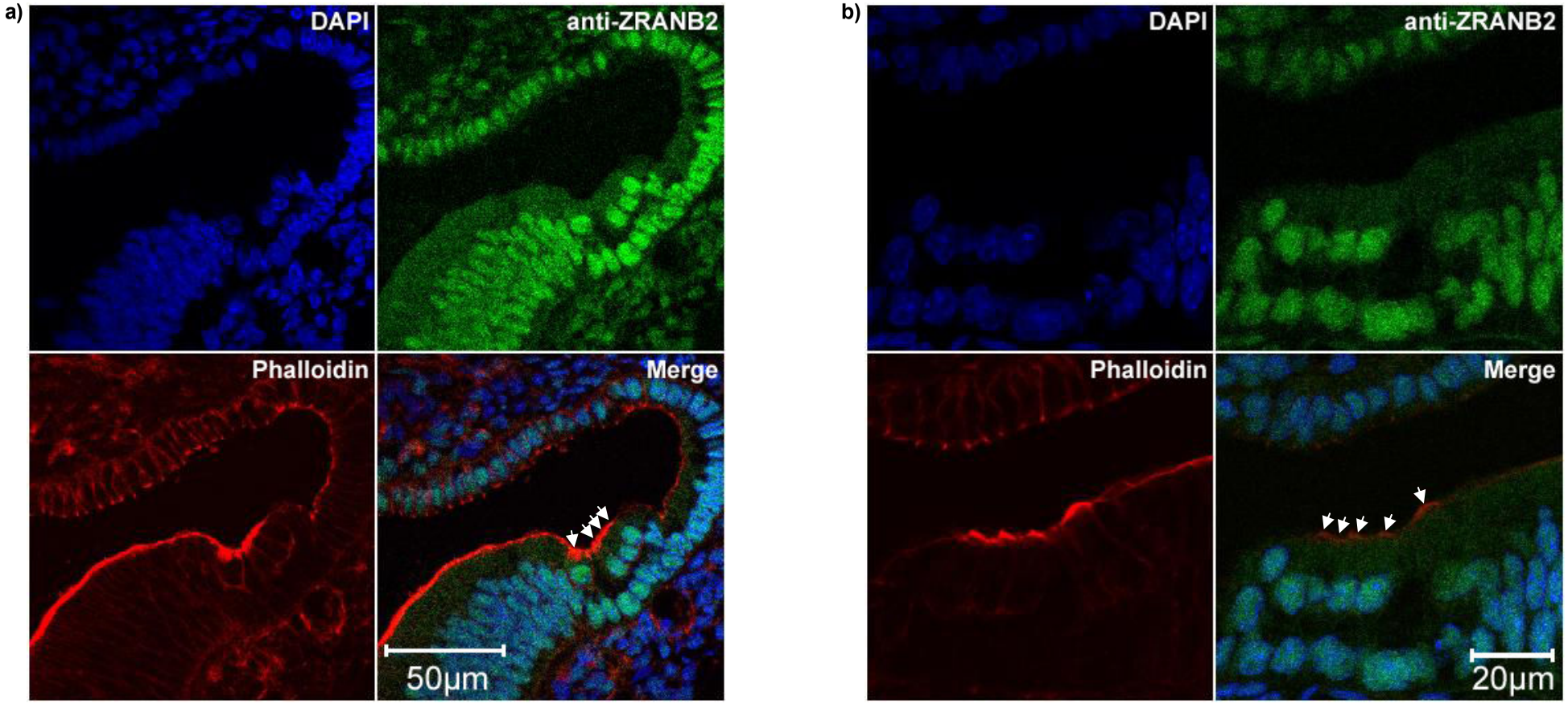

Figure 5.5. ZRANB2 expression in the P0 rat cochlea.
a) Apical turn of P0 rat cochlea labelled with anti-ZRANB2 antibody, DAPI and Phalloidin. *b*) Middle turn of P0 rat cochlea labelled with anti-ZRANB2 antibody, DAPI and Phalloidin. ZRANB2 expression is seen in the nuclei of cells throughout the cochlear duct with weaker expression seen outside the cochlear duct (*a*). Its subcellular localization was nuclear and no base-to-apex expression gradient was seen between turns of the cochlear duct. *Arrows*, hair cells. These results are representative of three examined cochleas.

5.5 Design of oligonucleotides for EMSA analysis of *Luzp1*, *Rbms1* and *Zranb2*

Having selected candidate genes for investigation and attempted to characterise their inner ear expression patterns, the putative activation of all three remaining candidate genes by POU4F3 was investigated. As previously described in section 1.5.5, it is thought that POU4F3 is only able to transactivate target gene promoters once bound to DNA (Sud *et al.* 2005) i.e. POU4F3 binding to target gene promoters is likely to be required if these genes are POU4F3 targets. Therefore, the identification of POU4F3 binding sites in target gene promoters would support the possibility that these genes are direct POU4F3 targets.

As for *Nr2f2* (section 4.8.1), remaining candidate gene promoters were predicted using the Genomatix Gene2Promoter software (see section 3.5.1) and binding sites were predicted within these regions using the Genomatix MatInspector and ModelInspector programs (see section 3.5.2). Oligonucleotides were designed against these putative binding sites and used in EMSA analyses to determine whether POU4F3 is able to bind these regions in candidate gene 5' flanking regions.

5.5.1 Luzp1 promoter prediction, binding site identification and EMSA oligonucleotide design

In the original BLAST analysis that identified *Luzp1* as the corresponding gene for clone D3 of the subtractive hybridization screen (section 5.2.1), the clone sequence matched that of the *Luzp* 3' UTR (Figure 5.1*b*). On subsequent analysis of the *Luzp1* locus in the Ensembl genome browser, only two of the annotated *Luzp1* transcripts contained the 3' UTR to which the original BLAST match for LUZP1 was found (Figure 5.6*a*). Of these two transcripts, one was a Havana protein coding transcript and one was an Ensembl protein coding transcript (Figure 5.6*a*). As Havana protein coding transcripts are manually annotated and therefore based on greater evidence than automatically annotated Ensembl protein coding transcripts, the Havana protein coding transcript was selected as the transcript that most likely corresponded to that identified by the subtractive hybridization screen (Figure 5.6a, *arrowhead*) (Ensembl 2009).

This transcript comprised four exons, and two promoters corresponding to four-exon transcripts were identified by the Gene2Promoter promoter prediction program (Figure 5.6*a*, *GXP_287887* and *GXP_287889*). Only one of these transcripts had confirmed 5' sequencing and was, therefore, selected as the best-matching promoter for MatInspector and ModelInspector analysis (Figure 5.6*b*, *GXP_287887* (*arrowhead*)).

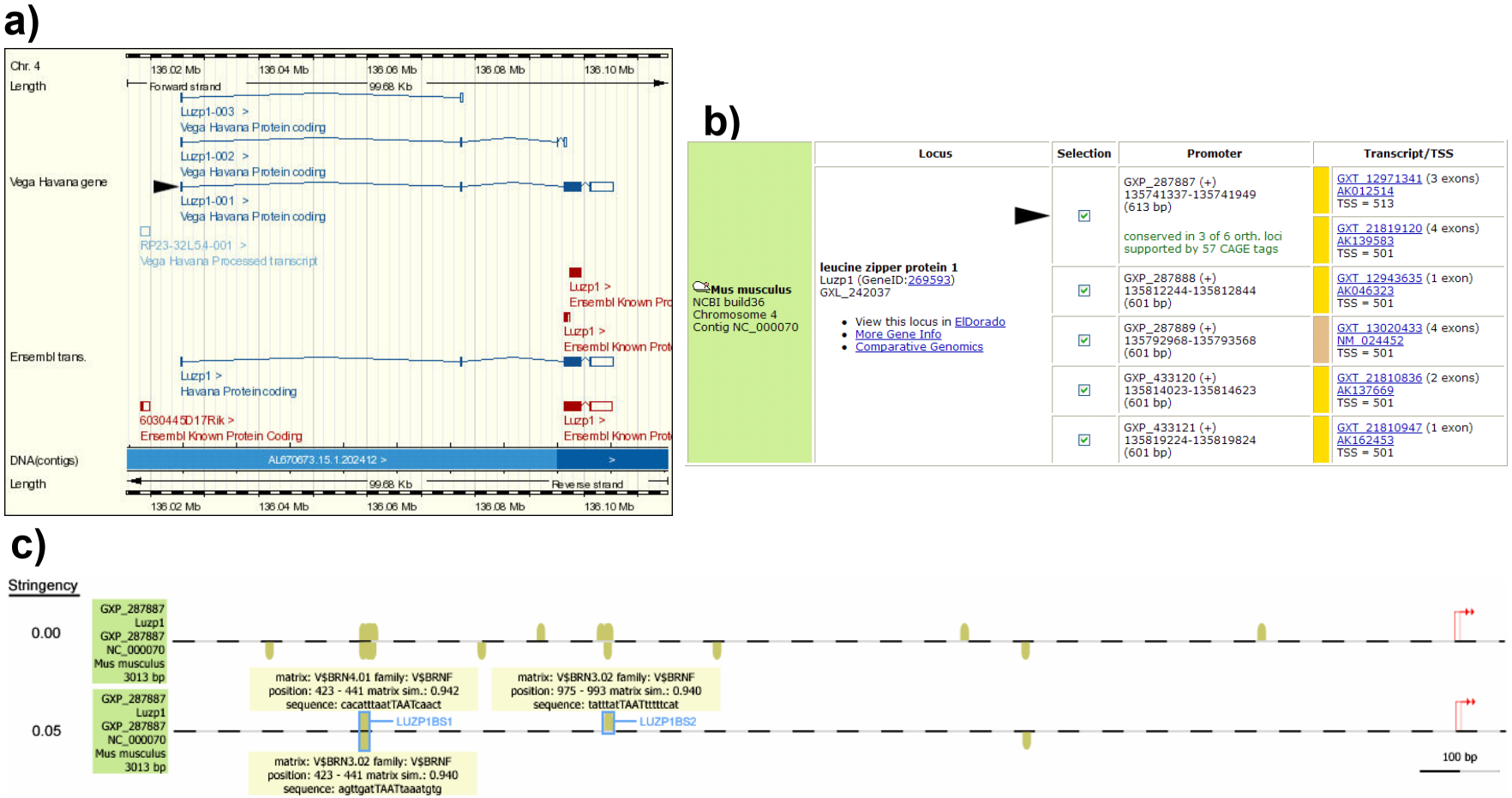

Figure 5.6. Prediction of potential POU4F3 binding sites in the *Luzp1* promoter.
a) the *Luzp1* gene locus viewed in the Ensembl genome browser. A Vega-Havana transcript (*arrowhead*) corresponded to the *Luzp1* transcript identified by subtractive hybridization. *b*) The Genomatix promoter (*GXP_287887*, *arrowhead*) that best matched this transcript was selected for further analysis. *c*) POU4F binding sites of highest stringency that were identified by MatInspector analysis were selected for EMSA analysis.

The selected promoter was submitted for both MatInspector and ModelInspector analysis. Though an OCT1-PBXC module was identified by the ModelInspector program (data not shown), this was more distal to the TSS than two predicted high stringency POU4F3 binding sites (*V$3.02* in Figure 5.6*c*). These two sites were selected for EMSA analysis and another site was not selected for analysis because of its lower matrix similarity to its corresponding POU binding site.

LUZP1BS1 was designed against a region that, on the sense strand, contained a predicted Brn-4 (POU3F) binding site of 0.942 matrix similarity and, on the antisense strand, contained a POU4F3 binding site of 0.940 matrix similarity. To this sequence, additional bases were included in the 5' region so that the end of the oligonucleotide did not interfere with POU4F3 binding and to the 3' region to include POU_{HD} binding motifs (TAAT) and to ensure that this end of the oligonucleotide did not interfere with POU4F3 binding either (Table 5.4).

LUZP1BS2 was designed against a predicted POU4 (Brn-3) binding site of 0.940 matrix similarity. This was the second highest stringency match identified and was more proximal to the TSS than LUZP1BS1. As for LUZP1BS1, additional sequence was included both 5' and 3' to the predicted binding site in order to avoid interference with POU4F3 binding in EMSA analysis (Table 5.4).

Table 5.4. *Luzp1* EMSA oligonucleotides.
Two EMSA oligonucleotides were designed using the MatInspector software to identify putative POU4F3 binding sites in a predicted *Luzp1* promoter region (GXP_287887). Bases were included both 3' and 5' to the sites identified (*underlined*) to ensure that the ends of the oligonucleotides would not interfere with POU4F3 binding.

Name	*Sequence*
LUZP1BS1	GGATTATCACATTTAATTAATCAACTAATTAACTAATTAAC
LUZP1BS1RC	GTTAATTAGTTAATTAGTTGATTAATTAAATGTGATAATCC
LUZP1BS2	ATTTTTATTTATTAATTTTTTCATGTGGATG
LUZP1BS2RC	CATCCACATGAAAAAATTAATAAATAAAAAT

5.5.2 Rbms1 promoter prediction, binding site identification and EMSA oligonucleotide design

Though putative mouse *Rbms1* 5' flanking region POU4F3 binding sites were originally predicted by the same method used for *Nr2f2* (section 4.8.1), *Luzp1* (section 5.5.1) and *Zranb2* (section 5.5.3), this analysis was repeated for the human *RBMS1* gene as the luciferase reporter constructs obtained and cloned for this gene contained segments of the human *RBMS1* 5' flanking region (see section 5.7.1).

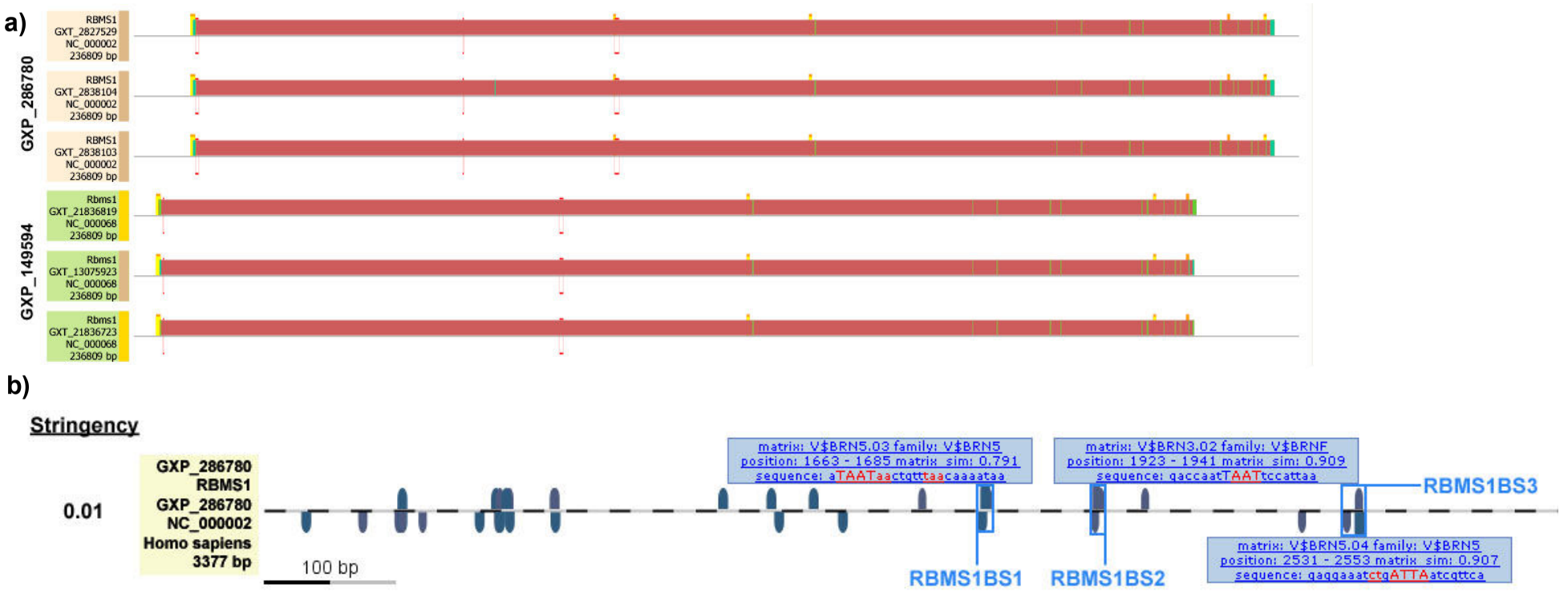

Figure 5.7. Prediction of potential POU4F3 binding sites in the *RBMS1* promoter.
a) The *Rbms1* transcripts corresponding to the predicted promoter *GXP_149594* were compared to human transcripts. The human transcripts that best-matched the mouse transcripts selected corresponded to the human predicted *RBMS1* promoter *GXP_286780* and this promoter was, therefore, selected for prediction of POU4F3 binding sites. *b*) POU4 binding sites identified by MatInspector analysis were selected for EMSA analysis. Three sites were selected for the design of three EMSA oligonucleotides (*RBMS1BS1*, *RBMS1BS2* and *RBMS1BS3*). These sites were selected due to there being clusters of putative POU4F3 binding sites at these loci and due to their proximity to the *RBMS1* transcriptional start site.

In the original *Rbms1* (mouse) promoter prediction, the Genomatix promoter GXP_149594 (Figure 5.7*a*) was found to best match a 14 exon Rbms1 transcript in the Ensembl database. Comparative genomic analysis between the transcripts corresponding to this promoter (Figure 5.7*a*, *green boxes*) and human transcripts in the Genomatix transcript database revealed that the human transcripts (Figure 5.7*a*, *salmon boxes*) that most closely matched the GXP_149594 transcripts corresponded to the human promoter GXP_286780.

This promoter was subjected to MatInspector and ModelInspector analysis in order to identify putative POU4F3 binding sites and modules. As for *Luzp1*, suitable modules were identified in the *RBMS1* 5' flanking region by the ModelInspector software, though these were further 5' than predicted (MatInspector) POU binding sites and were therefore thought to not be contained in an available *RBMS1* 5' flanking region reporter construct. Though many MatInspector predicted POU binding sites were later shown to not be contained in this reporter construct either, they were thought to be included at the time of this analysis. Therefore, EMSA probes were designed against the binding sites identified by the MatInspector software.

RBMS1BS1 was designed against a cluster of POU factor binding sites which contained a V$BRN5.03 binding site of 0.791 matrix similarity (Brn-5 (POU6) binding sites have been shown to be similar to POU4F binding sites (Rhee *et al.* 1998)) and two V$BRNF binding sites of 0.898 and 0.910 matrix similarity (Figure 5.7*b*). As before, additional bases were included both 5' and 3' to these predicted binding sites in EMSA oligonucleotides to prevent the ends of the oligonucleotide from interfering with POU4F3 binding (Table 5.5).

RBMS1BS2 was designed against a cluster of predicted POU4F binding sites which contained a high stringency (0.909 matrix similarity) predicted POU4F3 binding site (Figure 5.7*b*) and a lower stringency (0.793) POU4F binding site, plus additional flanking bases (Table 5.5). As a third cluster of POU family binding sites of comparable stringency to the two described was identified in GXP_286780, a third EMSA probe (RBMS1BS3) was designed for *RBMS1*. This probe encompassed a V$BRN5.04 binding site of 0.907 matrix similarity (i.e. of higher stringency than the V$BRN5 binding site in RBMS1BS1) (Figure 5.7*b*) as well as two POU4F3 binding sites of high stringency (0.923 and 0.927) plus flanking bases (Table 5.5).

Table 5.5. *RBMS1* EMSA oligonucleotides.
Three EMSA oligonucleotides were designed using the MatInspector software to identify putative POU4F3 binding sites in a predicted *RBMS1* promoter region (GXP_286780). As for other EMSA oligonucleotides, bases were included both 3' and 5' to the sites identified (*underlined*) to ensure that the ends of the oligonucleotides would not interfere with POU4F3 binding.

Name	*Sequence*
RBMS1BS1	TTATCATATAAAAATAATAACTGTTTAACAAAATAATGCATTCCAG
RBMS1BS1RC	CTGGAATGCATTATTTTGTTAAACAGTTATTATTTTTATATGATAA
RBMS1BS2	CGGGGACCAATTAATTCCATTAAATTATATCTAGTTA
RBMS1BS2RC	TAACTAGATATAATTTAATGGAATTAATTGGTCCCCG
RBMS1BS3	TTGTGAAAAAAAATTACTGGGCGGTGGGAAGTGAACGATTAATCAGATTTCCTCT
RBMS1BS3RC	AGAGGAAATCTGATTAATCGTTCACTTCCCACCGCCCAGTAATTTTTTTTCACAA

5.5.3 Zranb2 promoter prediction, binding site identification and EMSA oligonucleotide design

The mechanism of the putative upregulation of *Zranb2* by POU4F3 was first investigated, as for other candidate genes, by the identification of putative POU4F3 binding sites in its promoter. On searching the Gene2Promoter software for predicted *Zranb2* promoters, five options were returned. Of these, three were eliminated as they were solely based on computational prediction (Figure 5.8*a*) and two promoters remained in the analysis: GXP_132934 and GXP_430971. The supporting evidence for the former was a single one-exon transcript of gold standard (i.e. this transcript had verified full 5' sequencing, showing that its transcriptional start site had been identified), whereas the latter had 14 gold standard transcripts of ten exons i.e. the same exon number as the Ensembl transcript identified by the BLAST analysis (Figure 5.3*a* and Figure 5.8*b*). Therefore, GXP_430971 was selected for further analysis.

The MatInspector and ModelInspector programs were used to analyse the Zranb2 promoter in order to identify putative POU4F3 transcription factor binding sites. The ModelInspector analysis yielded an OCT1-PIT1 module, a HOXF-HOXF-OCT1 module and a PIT1 GATA module within the region examined. Of these, the OCT1-PIT1 module was selected for further investigation as, unlike the other modules identified, both of the transcription factors that relate to this module are POU domain transcription factors. Therefore, an EMSA oligonucleotide, ZRANB2BS1 (Table 5.6), was designed to a region within this module that had a POU4F (Brn-3) binding site on the sense strand and a POU6 (Brn-5) binding site on the opposite strand (Figure 5.8*c*). Furthermore, the POU4F binding site had the second highest matrix similarity of the sites identified by the MatInspector software for this promoter.

Of the three remaining putative binding sites at the highest level of stringency, ZRANB2BS2 was designed against the middle site (Table 5.6). This site was selected as it had a higher matrix similarity to its corresponding (POU6/Brn-5) sequence than the most 3' site (0.818 compared to 0.807) and was closer to the *Zranb2* transcriptional start site than the most 5' site, though it had slightly lower matrix similarity to its corresponding transcription factor's DNA sequence matrix (0.818 compared to 0.832) (Figure 5.8*c*).

As for other EMSA oligonucleotides, additional sequence was included at both ends of both *Zranb2* EMSA oligonucleotides to ensure that the ends of the oligonucleotide did not interfere with POU4F3 binding. Furthermore, the 3' region of both oligonucleotides was extended to encompass a additional homeodomain binding motifs (TAAT) (Table 5.6).

a)

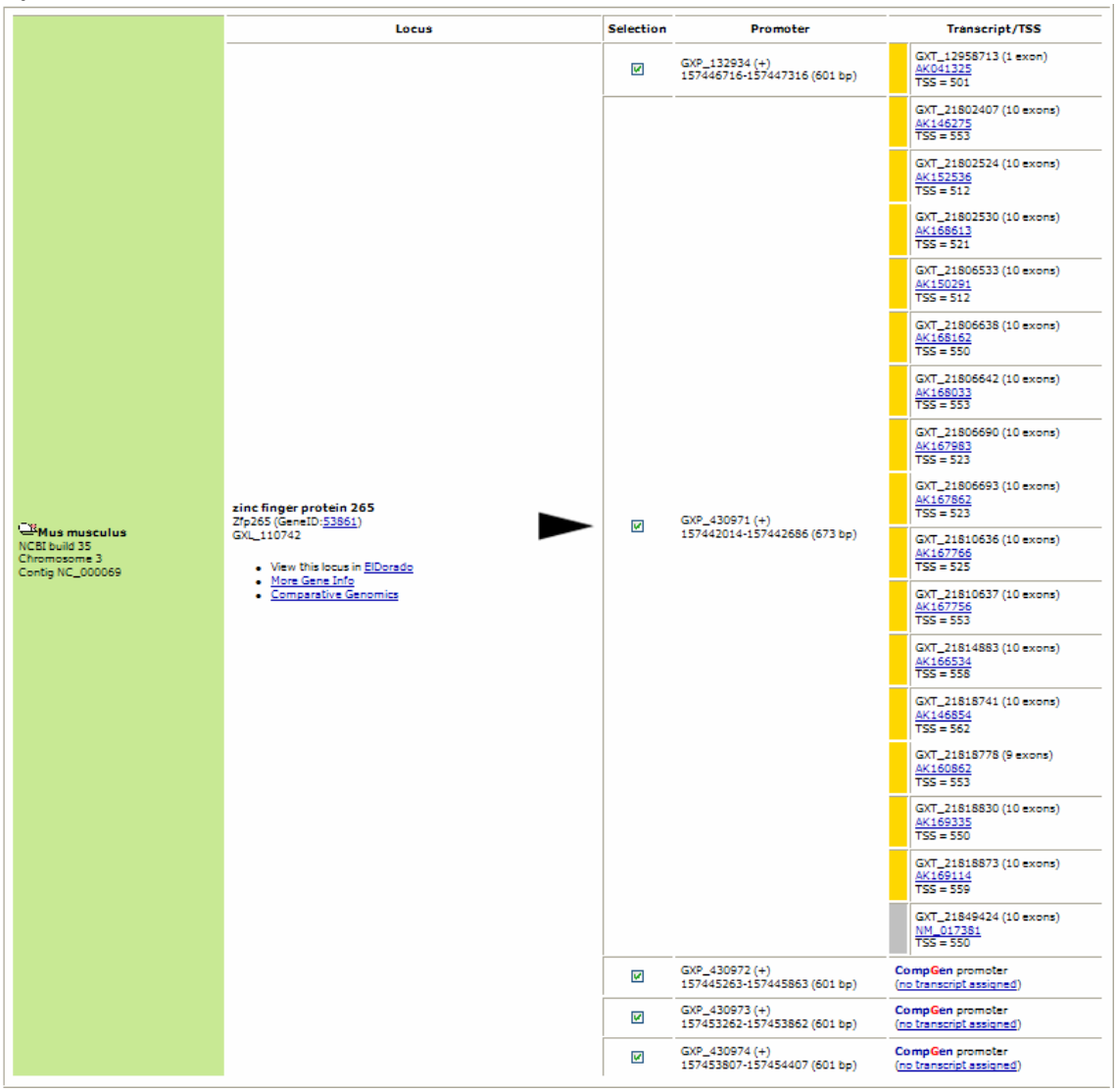

Figure 5.8. Prediction of potential POU4F3 binding sites in the *Zranb2* promoter.
(Legend on page 200)

b)

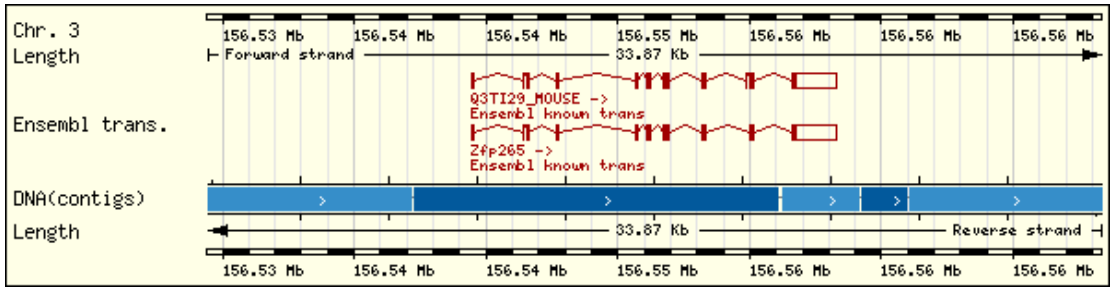

c)

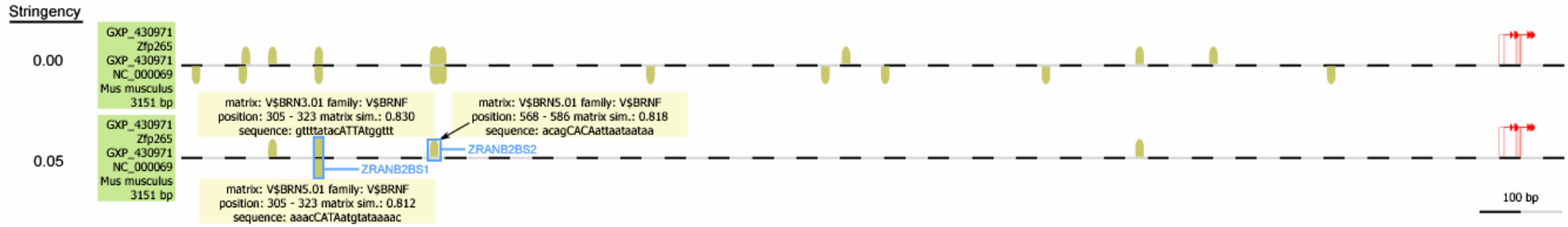

Figure 5.8. Prediction of potential POU4F3 binding sites in the *Zranb2* promoter (continued).
a) The promoter corresponding to gold standard transcripts in the Genomatix database that had ten exons was selected for further analysis (*arrowhead*) as this best matched the transcript identified in Ensembl (*b*). *b*) Graphical representation of the *Zranb2* gene in the Ensembl genome browser (the MGI name for *Zranb2* was ZFP265 at the time of this analysis). *c*) POU-family transcription factor binding sites were identified in MatInspector for *Zranb2*. The two sites that were selected for EMSA analysis are shown in blue.

Table 5.6. *Zranb2* EMSA oligonucleotides.
Zranb2 EMSA oligonucleotides designed against the Genomatix predicted promoter GXP_430971. Additional bases included at both ends are *underlined*.

Name	*Sequence*
ZRANB2BS1	TCATAGTTTTATACATTATGGTTTTAATTTTAC
ZRANB2BS1RC	GTAAAATTAAAACCATAATGTATAAAACTATGA
ZRANB2BS2	TAGTAACAGCACAATTAATAATAATTGAATTAA
ZRANB2BS2RC	TTAATTCAATTATTATTAATTGTGCTGTTACTA

5.6 EMSA analysis of POU4F3 binding sites in candidate gene 5' flanking regions

Having designed EMSA oligonucleotides to predicted POU4F3 binding sites in the *Luzp1*, *Rbms1* and *Zranb2* 5' flanking regions, these oligonucleotides were used in EMSA analysis to identify whether *in vitro* translated POU4F3 and POU4F3 from UB/OC-2 cell nuclear protein extract is able to bind to them.

5.6.1 In vitro translated POU4F3 is able to bind sites in the Luzp1 and Zranb2 promoter

The ability of POU4F3 to bind LUZP1BS1, LUZP1BS2, ZRANB2BS1 and ZRANB2BS2 was tested by EMSA analysis with *in vitro* translated protein. As for *Nr2f2* (section 4.8.2), the radiolabelled EMSA oligonucleotides were incubated either alone, with *in vitro* translated POU4F3 or with *in vitro* translated luciferase protein that had been produced using a rabbit reticulocyte lysate *in vitro* transcription / translation system. Samples were electrophoresed on a 4% polyacrylamide gel that was then dried and autoradiographed. If the oligonucleotide is bound by the *in vitro* translated POU4F3, then a bandshift is seen in the *in vitro* translated POU4F3 lane that is of higher molecular weight than bands seen in the lane containing probe alone. If this bandshift is not due to non-specific binding by other proteins in the *in vitro* translation mixture, it should not be present in the lane containing *in vitro* translated luciferase protein.

On EMSA analysis (see Figure 5.9), LUZP1BS1 (Figure 5.9*a*), LUZP1BS2 (Figure 5.9*b*), ZRANB2BS1 (Figure 5.9*c*) and ZRANB2BS2 (Figure 5.9*d*) all show bandshifts produced by *in vitro* translated POU4F3. These bandshifts are shown to be due to POU4F3 by their absence or marked reduction in *in vitro* translated luciferase protein-containing lanes and lanes that do not contain *in vitro* translated protein (Figure 5.9, *arrowheads*). These results show that *in vitro* translated POU4F3 is able to bind to the four EMSA oligonucleotides tested in this analysis, though they do not show whether this binding is sequence-specific. Therefore, the sequence-specificity of these interactions was tested by competition with a POU4F3 consensus sequence (see section 5.6.3). As for *Nr2f2* binding sites previously tested, this analysis was carried out with UB/OC-2 cell nuclear protein extract as POU4F3 in UB/OC-2 cells is more likely to have the post-translational modifications required for native DNA binding that *in vitro* translated protein may lack (see section 4.8.3).

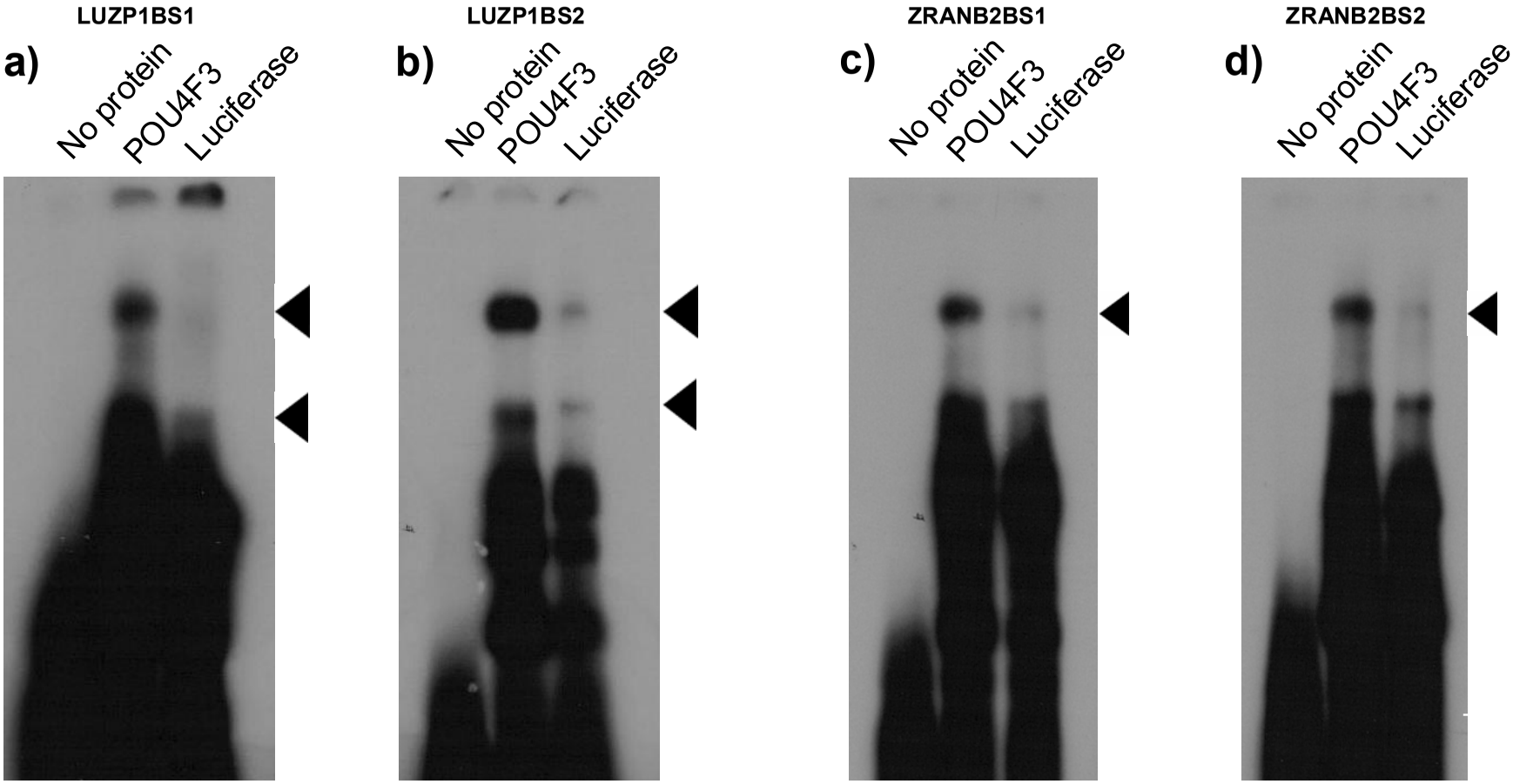

Figure 5.9. Binding of *in vitro* translated POU4F3 to predicted binding sites.
The ability of *in vitro* translated POU4F3 to bind to predicted binding sites in the *Luzp1* and *Zranb2* gene 5' flanking regions was tested by EMSA analysis. Oligonucleotides that had been designed against predicted POU4F3 binding sites were radiolabelled with [γ-32P]ATP and incubated with *in vitro* translated POU4F3 or luciferase protein. LUZP1BS1 (*a*), LUZP1BS2 (*b*), ZRANB2BS1 (*c*) and ZRANB2BS2 (*d*) all show *in vitro* translated POU4F3-specific bandshifts (*arrowheads*), i.e. bands that are present in POU4F3-containing lanes and absent or markedly attenuated in *in* vitro translated luciferase protein containing lanes. This indicates that *in vitro* translated POU4F3 is able to bind to all four of the oligonucleotides tested. NB, the autoradiograph images presented in this figure are cropped for presentation purposes.

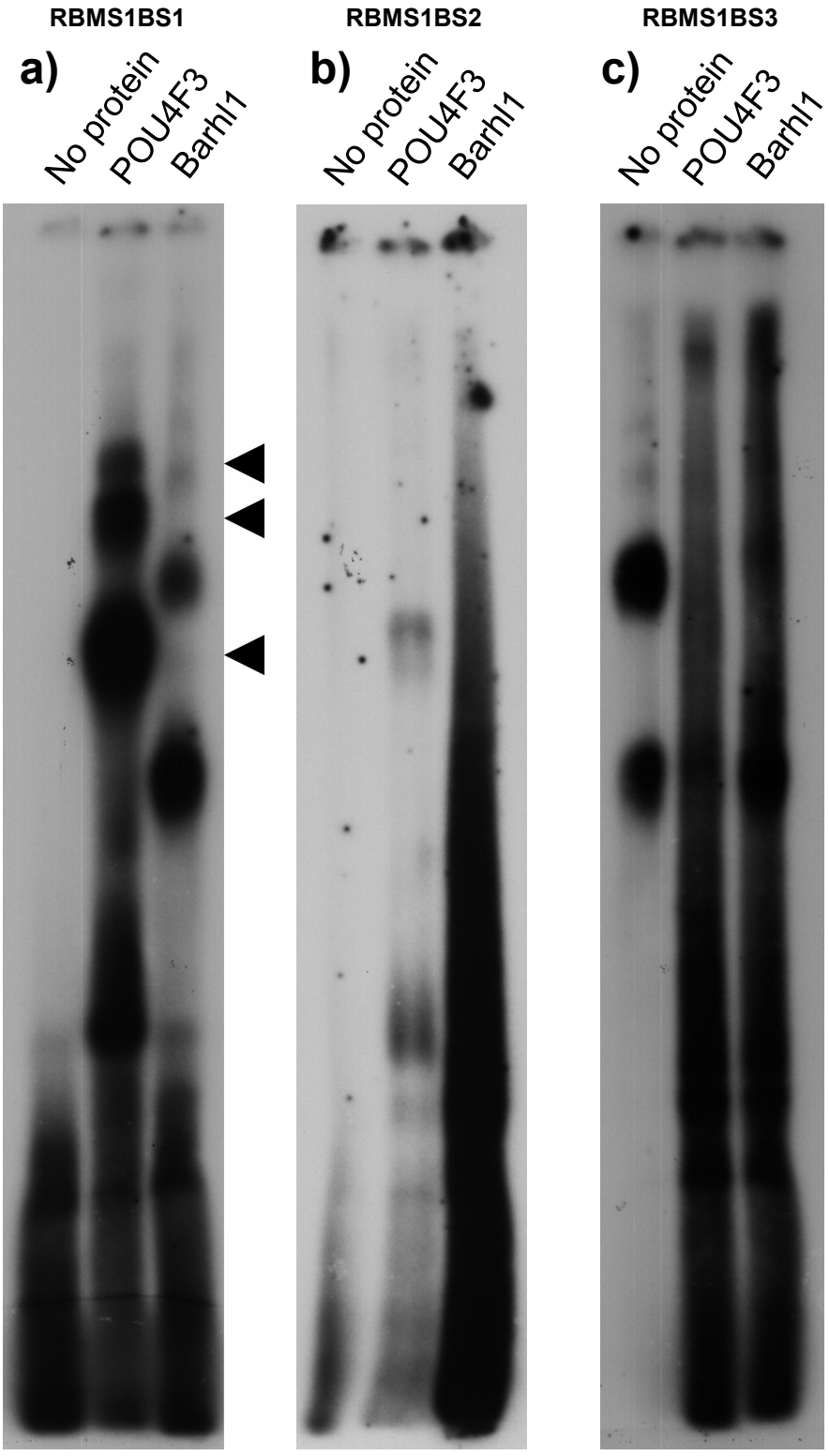

Figure 5.10. Binding of *in vitro* translated POU4F3 to RBMS1BS1-3.
EMSA analysis of *in vitro* translated POU4F3 binding to oligonucleotides designed against predicted binding sites in the *RBMS1* 5' flanking region. This analysis revealed POU4F3-specific bandshifts for RBMS1BS1 (*a*, *arrowheads*). However, a streaky appearance was noted in protein-containing lanes in the analysis of RBMS1BS2 (*b*) and RBMS1BS3 (*c*), most likely due to protein-DNA complex degradation. During attempts to improve the resolution of bands for RBMS1BS2 and RBMS1BS3, POU4F3 binding to these oligonucleotides was identified by an alternative method and this method was, therefore, not pursued further.

5.6.2 EMSA analysis of in vitro translated POU4F3 binding to predicted binding sites in the RBMS1 promoter

The ability of *in vitro* translated POU4F3 to bind *RBMS1* EMSA oligonucleotides was investigated in the same way as for other candidate genes. Though POU4F3-specific binding to RBMS1BS1 was seen (Figure 5.10*a*), autoradiographs for RBMS1BS2 (Figure 5.10*b*) and RBMS1BS3 (Figure 5.10*c*) appeared streaky in protein-containing lanes. This appearance can be caused by protein-DNA complex dissociation or inappropriate salt concentrations (Hellman *et al.* 2007). It was not thought to be due to the *in vitro* translated Barhl1 or POU4F3 used, as these proteins were able to bind to RBMS1BS1 (Figure 5.10*a*).

Another abnormality noted in these experiments was the appearance of RBMS1BS3 on autoradiography in the absence of protein (Figure 5.10*c*). This oligonucleotide appears have migrated much slower than RBMS1BS1 or RBMS1BS2 through the polyacrylamide gel in similar conditions, though this difference may have been due to its greater length (55bp) compared to RBMS1BS1 (46bp) and RBMS1BS2 (37bp) or concatamerisation of the probe. As attempts were being made to optimise EMSA conditions to improve the resolution of bandshifts and thereby determine whether POU4F3 is able to bind to RBMS1BS2 and RBMS1BS3, POU4F3 binding to these oligonucleotides was identified using UB/OC-2 cell nuclear protein extract (see section 5.6.3). Given that the question posed in the *in vitro* translate experiment had been answered by this alternative method, it was not pursued further. The limitations of not having identified POU4F3 binding to RBMS1BS1 and RBMS1BS2 by this method are discussed below.

5.6.3 POU4F3 extracted from UB/OC-2 cell nuclei is able to bind to all oligonucleotides tested

The EMSAs conducted with *in vitro* translated proteins demonstrated that POU4F3 is able to bind to LUZP1BS1 & 2, RBMSBS1 and ZRANB2BS1 & 2. However, they do not show whether this binding is sequence-specific i.e. that POU4F3 is binding to these binding sites because of their sequence and not through an abnormal protein-DNA interaction produced by the conditions of the assay despite these conditions being kept as physiological as possible. Therefore, to verify that the binding seen is sequence-specific, a competition gradient experiment was carried out (as for NR2F2BS1 & 2; reported in section 4.8.3).

In this experiment an increasing amount of non-radiolabelled POU4F3 consensus oligonucleotide was added to EMSA reactions. An oligonucleotide that is known to be bound by POU4F3 (POU4F3 consensus) was used for LUZP1BS1 & 2 and ZRANB2BS1 & 2 with an oligonucleotide called 'Prox6 consensus' – a new POU4F3 consensus sequence designed by SD – used for RBMS1BS1-3. In separate EMSA reactions, a non-radiolabelled non-POU4F3-binding sequence ('AP4 consensus' for LUZP1BS1&2 and ZRANB2BS1&2; 'Prox6 mutant' for RBMS1BS1-2) was included (see Table 5.7). Sequence-specific binding was

identifiable on autoradiographs as a bandshift that that was attenuated or abolished by sufficient POU4F3 consensus sequence competition but not as strongly attenuated by an equivalent amount of non-specific competitor. Though the non-specific competitor should not attenuate POU4F3 bandshifts as much as specific competition, any competing oligonucleotide can reduce specific binding when present at great excess, causing some attenuation of these bandshifts (Hellman *et al.* 2007). The competitor oligonucleotides also serve to identify which of the bandshifts produced by the UB/OC-2 cell nuclear extract is due to POU4F3 and (within experiments) demonstrates the relative POU4F3-binding affinity of test oligonucleotides.

Autoradiographs of experiments with LUZP1BS1 & 2 (Figure 5.11), RBMS1BS1-3 (Figure 5.12) and ZRANB2BS1 & 2 (Figure 5.13) revealed POU4F3 sequence-specific banding patterns for all oligonucleotides tested (*arrowheads* in Figure 5.11, Figure 5.12 and Figure 5.13). For LUZP1BS1 (Figure 5.11*a*), three such bandshifts were seen with the highest affinity bandshift being greatly attenuated by 1000x POU4F3 consensus competition and restored by AP4 consensus competition. Similar bandshifts were seen for LUZP1BS2 (Figure 5.11*b*), with four POU4F3-specific bandshifts seen, the highest affinity of which was abolished by 1000x POU4F3 consensus competition. In contrast, only one POU4F3-specific bandshift was identified for RBMS1BS1 (Figure 5.12*a*), RBMS1BS2 (Figure 5.12*b*), RBMS1BS3 (Figure 5.12*c*), ZRANB2BS1 (Figure 5.13*a*) and ZRANB2BS2 (Figure 5.13*b*). For the *RBMS1* 5' flanking region binding sites, RBMS1BS2 and RBMS1BS3 appeared to be of approximately equal affinity, requiring 1000x Prox 6 consensus competition to greatly attenuate the POU4F3-specific bandshift; RBMS1BS1 required only 500x Prox 6 consensus competition to abolish its equivalent bandshift suggesting a lower POU4F3 binding affinity for this site. Of the *Zranb2* 5' flanking region binding sites, ZRANB2BS1 appeared to have slightly higher affinity for POU4F3 than ZRANB2BS2, requiring 500x POU4F3 consensus competition instead of 100x POU4F3 consensus competition to abolish its POU4F3-specific bandshift. Therefore, the relative affinity of the binding sites tested correlates with the Genomatix predictions of their matrix similarity to known binding sites (see section 5.5).

These bandshifts can be attributed to POU4F3 as it is expressed in UB/OC-2 cells (where POU4F1 and POU4F2 are not expressed); all oligonucleotides except RBMS1BS2 and RBMS1BS3 were shown to be bound by *in vitro* translated POU4F3; and POU4F3 sequence-specific bandshift patterns were seen for all oligonucleotides tested. Further evidence of these bands being produced by POU4F3 would be provided by a 'supershift' analysis, though no suitable antibody exists for this analysis. For RBMS1BS2 and RBMS1BS3, greater evidence of POU4F3 binding could be obtained by optimisation of the EMSA with *in vitro* translated POU4F3 to reduce the streakiness seen in previous attempts of this assay as, in the absence of a supershift analysis, this would support the evidence that the POU4F3 sequence-specific bands identified in Figure 5.12*b* and *c* are produced by POU4F3.

The evidence provided by the EMSA analyses described above shows that POU4F3 is able to bind sites in the *Luzp1*, *RBMS1* and *Zranb2* 5' flanking regions. As POU4F3 sequence-specific binding was seen at all the binding sites identified by analysis of predicted candidate gene promoters (nine binding sites in total), the strategy used to identify these sites appears highly sensitive (see section 5.5). If POU4F3 is able to bind these sites *in vivo*, and if candidate gene upregulation is verified, it may be able to transactivate the candidate genes identified by the subtractive hybridization at the sites identified. Such binding could be investigated by chromatin immunoprecipitation experiments. However, despite preliminary attempts to investigate the binding of a POU4F3 fusion protein to these sites by this method (in cell lines) at a very late stage of this investigation, such binding was not seen. Furthermore, the practical limitations of antibody and tissue availability made the investigation of native POU4F3 binding to these sites in hair cells impractical at this stage (see Chapter 6).

Table 5.7. Consensus sequence oligonucleotides for competition assays.
POU4F3 consensus 1 and AP4 are reproduced from Table 4.2 for ease of reference. Prox 6 consensus and Prox 6 mutant oligonucleotides were designed by SD. Mutant bases in Prox 6 mutant are *underlined*.

Name	*Sequence*
POU4F3 consensus 1	CACGCATAATTAATCGC
AP4 consensus	CTAGCCCAGCTGTGGCAGCCC
Prox 6 consensus	TCGATCTCCTGCATAATTAATTACGCCG
Prox 6 mutant	TCGATCTCCTGCATAAGCAAGCACGCCG

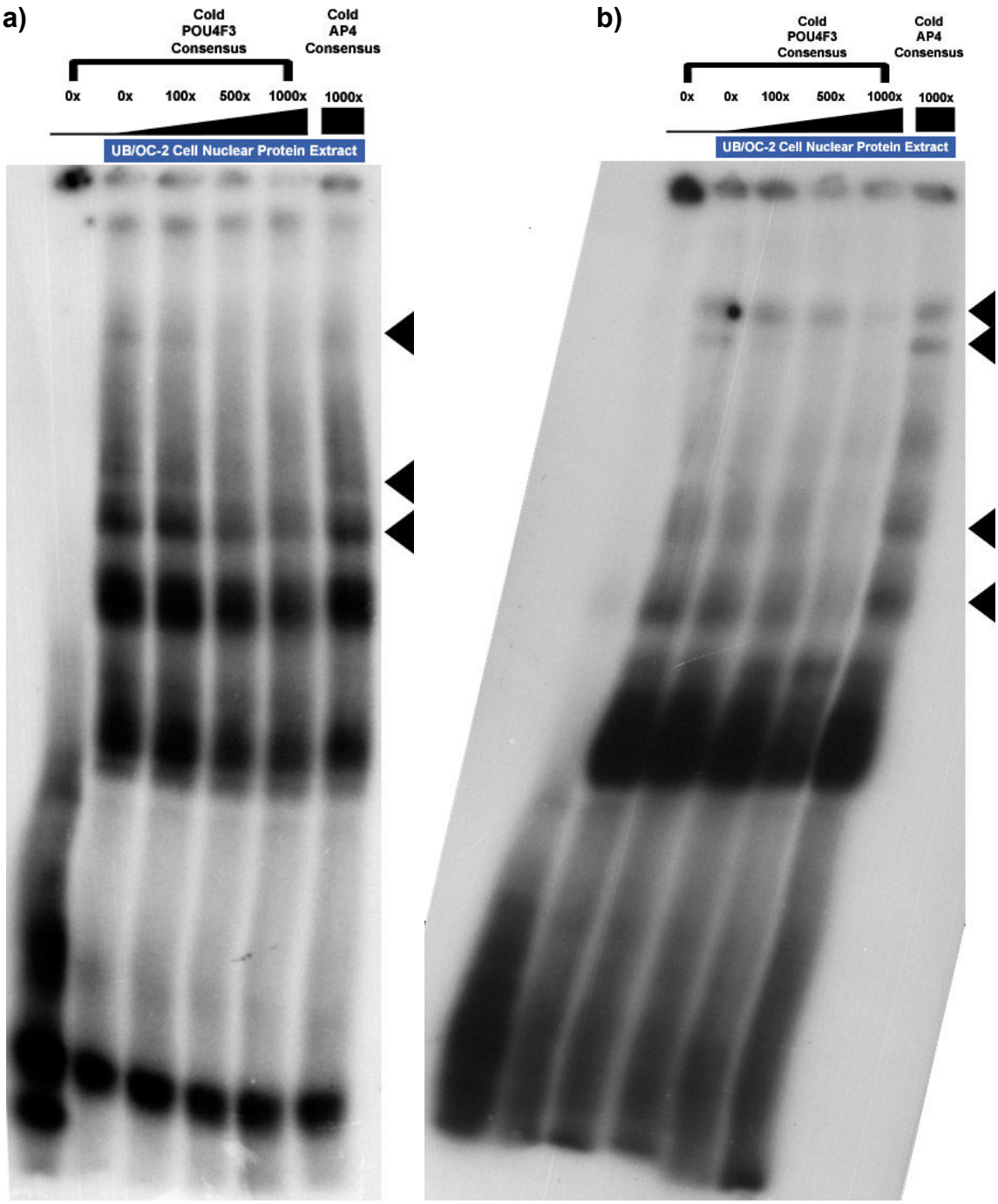

Figure 5.11. Binding of UB/OC-2 cell nuclear protein extract to LUZP1BS1 & 2.
EMSAs were performed using [γ-32P]ATP labelled DNA oligonucleotides which corresponded to two predicted high-stringency POU binding sites in the *Luzp1* gene promoter (LUZP1BS1 and LUZP1BS2). Oligonucleotides were incubated with non-radiolabelled POU4F3 or AP4 consensus binding site to determine bandshifts due to sequence-specific POU4F3 binding. This analysis revealed POU4F3-specific banding patterns for both LUZP1BS1 (*a*, *arrowheads*) and LUZP1BS2 (*b*, *arrowheads*), indicating that POU4F3 from UB/OC-2 cell nuclear extract is able to bind both oligonucleotides.

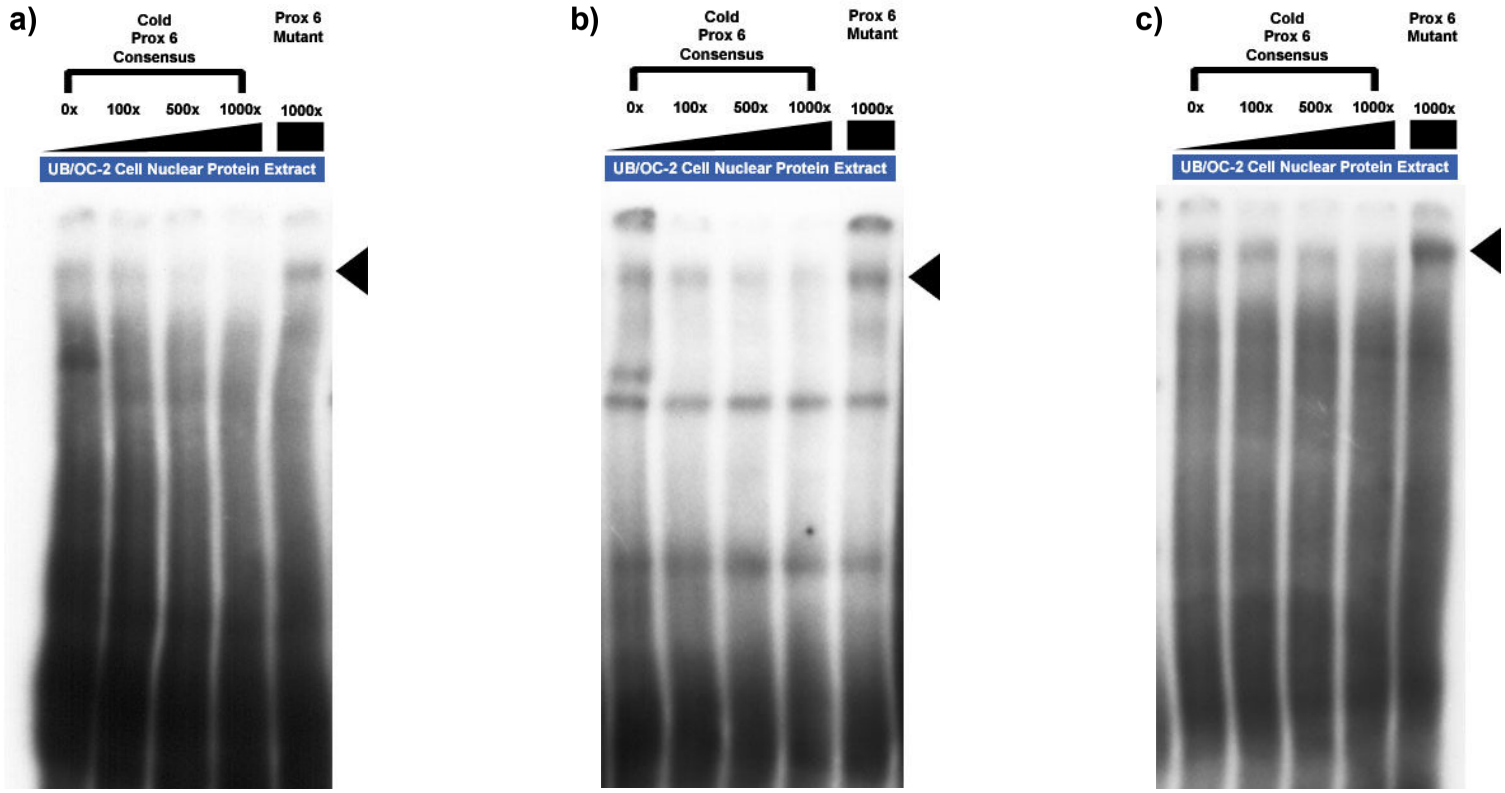

Figure 5.12. Binding of UB/OC-2 cell nuclear protein extract to RBMS1BS1-3.
EMSAs were carried out as for *RBMS1* EMSA oligonucleotides. However, non-radiolabelled Prox6 consensus and Prox6 mutant oligonucleotides was used instead of non-radiolabelled POU4F3 and AP4 consensus oligonucleotides to determine sequence-specific POU4F3 binding to RBMS1-3. POU4F3-specific bandshifts (*arrowheads*) were identified for RBMS1BS1 (*a*), RBMS1BS2 (*b*) and RBMS1BS3 (*c*). NB, the autoradiograph images presented in this figure are cropped for presentation purposes.

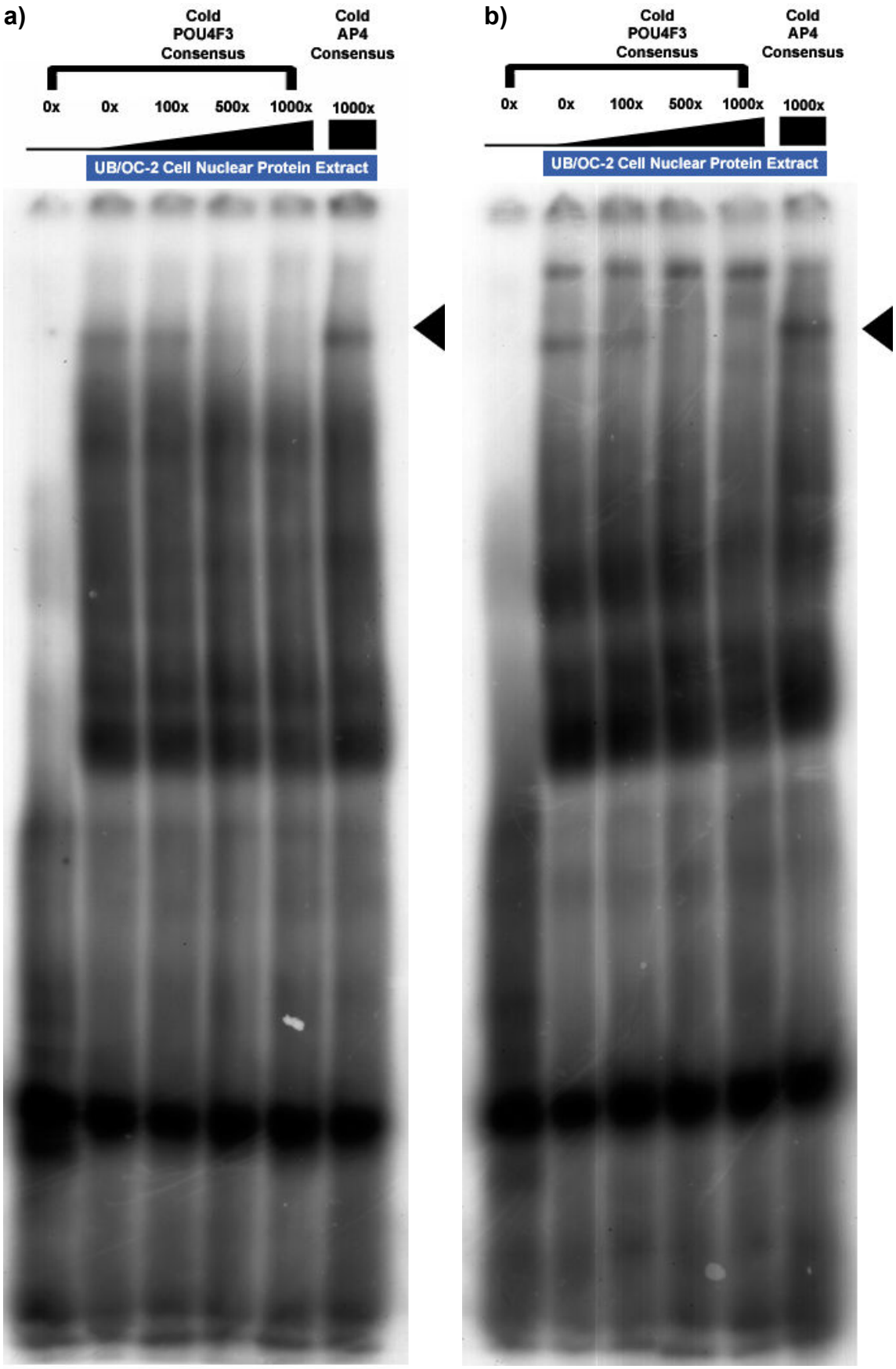

Figure 5.13. Binding of UB/OC-2 cell nuclear protein extract to ZRANB2BS1 & 2.
a) radiolabelled binding site one (ZRANB2BS1) was incubated with / without UB/OC-2 cell nuclear extract and with varying amounts of non-radiolabelled POU4F3 or AP4 consensus binding site. The same assay was conducted using ZRANB2BS2 (b). Both experiments demonstrate a banding pattern that is likely to be due to POU4F3 contained in the UB/OC-2 cell nuclear protein extract used (*arrowheads*).

5.7 Activation of candidate gene 5' flanking regions by POU4F3

The results of the subtractive hybridization suggest that all three of the remaining prioritised candidate genes (*Luzp1*, *Rbms1* and *Zranb2*) are activated by POU4F3 (Table 3.1). In order to verify and characterise this regulation, the ability of POU4F3 to activate the 5' flanking regions of candidate genes (which are likely to form part of the gene promoter) was tested by luciferase reporter gene assays. In order to carry out these experiments, plasmid constructs containing the 5' flanking region of a candidate gene upstream of luciferase cDNA were obtained from collaborators or cloned. Such constructs are occasionally referred to as promoter constructs for convenience though the ability of the candidate gene 5' flanking regions used to act as full length promoters has not been demonstrated. These constructs were cotransfected with a POU4F3 expression construct in ND7 cells and their response was assessed by luminometry. ND7 cells were selected for these assays as they had been shown to be suitable for this application in previous experiments with *Nr2f2* promoter reporter constructs.

5.7.1 Cloning of candidate gene 5'flanking region reporter constructs

Luzp1

As no luciferase reporter promoter construct existed for *Luzp1*, a construct containing 2.8kb of the *Luzp1* 5' flanking region was cloned and named LUZP1p2.8kb. Primers were designed to amplify the 2.8kb sequence from mouse genomic DNA and this was cloned into the pDrive cloning vector prior to subcloning into the pGL4.10 luciferase reporter construct (which contains a luciferase gene that is codon optimised for expression in mammalian cells) and sequencing to verify insert orientation. The sequence cloned encompassed both LUZP1BS1 and LUZP1BS2.

RBMS1

A vector containing 1.3kb of the *RBMS1* 5' flanking region was kindly provided by Dr H Ariga (RBMS1p1.3kb). In this reporter construct, the *RBMS1* 5' flanking region had been cloned into the promoterless pGV-B luciferase reporter vector (Haigermoser *et al.* 1996). The regulation of this vector by POU4F3 had not been assessed. Therefore, an empty pGV-B vector (i.e. pGV-B without the RBMS1 5' flanking region) was created by excision of the *RBMS1* 5' flanking region to assess regulation of the vector by POU4F3 in luciferase assay.

Notably, RBMS1p1.3kb only contains RBMS1BS3 and does not contain RBMS1BS1 or RBMS1BS2 which lie upstream of this *RBMS1* 5' flanking sequence. Therefore, to encompass these binding sites, an *RBMS1* 5' flanking region reporter construct was cloned

in our laboratory (by SD) by excising 5.1kb of the *RBMS1* 5' flanking sequence from a plasmid containing 21kb of the *RBMS1* 5' flanking sequence in the pUC19 vector (also kindly provided by Dr H Ariga) and inserting the 5.1kb sequence into the pGL4.10 vector.

Zranb2

As for *Luzp1*, no luciferase reporter constructs existed for the *Zranb2* promoter. Therefore, a 3.2kb region of the *Zranb2* 5' flanking region that includes ZRANB2BS1 & 2 was amplified from mouse genomic DNA and cloned into the pDrive cloning vector prior to subcloning into the pGL4.10 vector. As the GC content of the region immediately 5' to the Zranb2 transcriptional start site (TSS) was too high for suitable primer design and, given that designing a primer 5' to this region might exclude the core promoter from the cloned sequence, I designed the 3' PCR primer to a region immediately downstream of the TSS. As the cloned promoter would contain the *Zranb2* TSS, the primer was designed to be in frame with the *luc2* TSS in the pGL-4.10 vector to avoid interference with luciferase transcription. The fragment amplified with these primers was ligated into pDrive and the KpnI-XbaI fragment of this construct was subsequently inserted into the KpnI-NheI site of pGL4.10[*luc2*]. Correct insertion of the amplified sequence was verified by sequencing. This reporter construct was named ZRANB2p3.2kb.

5.7.2 Regulation of LUZP1p2.8kb by POU4F3

The ability of POU4F3 to regulate a *Luzp1* promoter construct (LUZP1p2.8kb) was investigated by luciferase assay. LUZP1p2.8kb was cotransfected with increasing amounts of a POU4F3 expression construct (pSi-Pou4f3) and pRL-null for normalization of luciferase values to transfection efficiency. The total amount of DNA transfected was maintained at a constant level with empty pSi vector. An identical assay was carried out with the dreidel expression construct (pSi-Dreidel) in place of pSi-Pou4f3 to ensure that any response seen was due to the specific action of POU4F3. The empty pGL4.10 vector has previously been show to show modest (1.4-fold) regulation by POU4F3 in ND7 cells in experiments in our laboratory (by JK).

The results of this experiment show that the LUZP1p2.8kb responds to 1µg of cotransfected pSi-Pou4f3 with a two-fold upregulation (Figure 5.14). This response is likely to be due to specific regulation by POU4F3 as the response of the promoter construct to the same amount of pSi-Dreidel revealed a smaller (1.4-fold) upregulation. However, the difference in regulation by POU4F3 and dreidel mutant protein is modest. The results presented in Figure 5.14 represent the results of two separate experiments with each condition assayed in triplicate i.e. six samples per data point. In order to verify the small difference in regulation between POU4F3 and dreidel mutant POU4F3, a greater number of repeats would be required to ensure that the difference seen is not due to chance and thereby provide stronger evidence that the LUZP1p2.8kb regulation seen is POU4F3-specific.

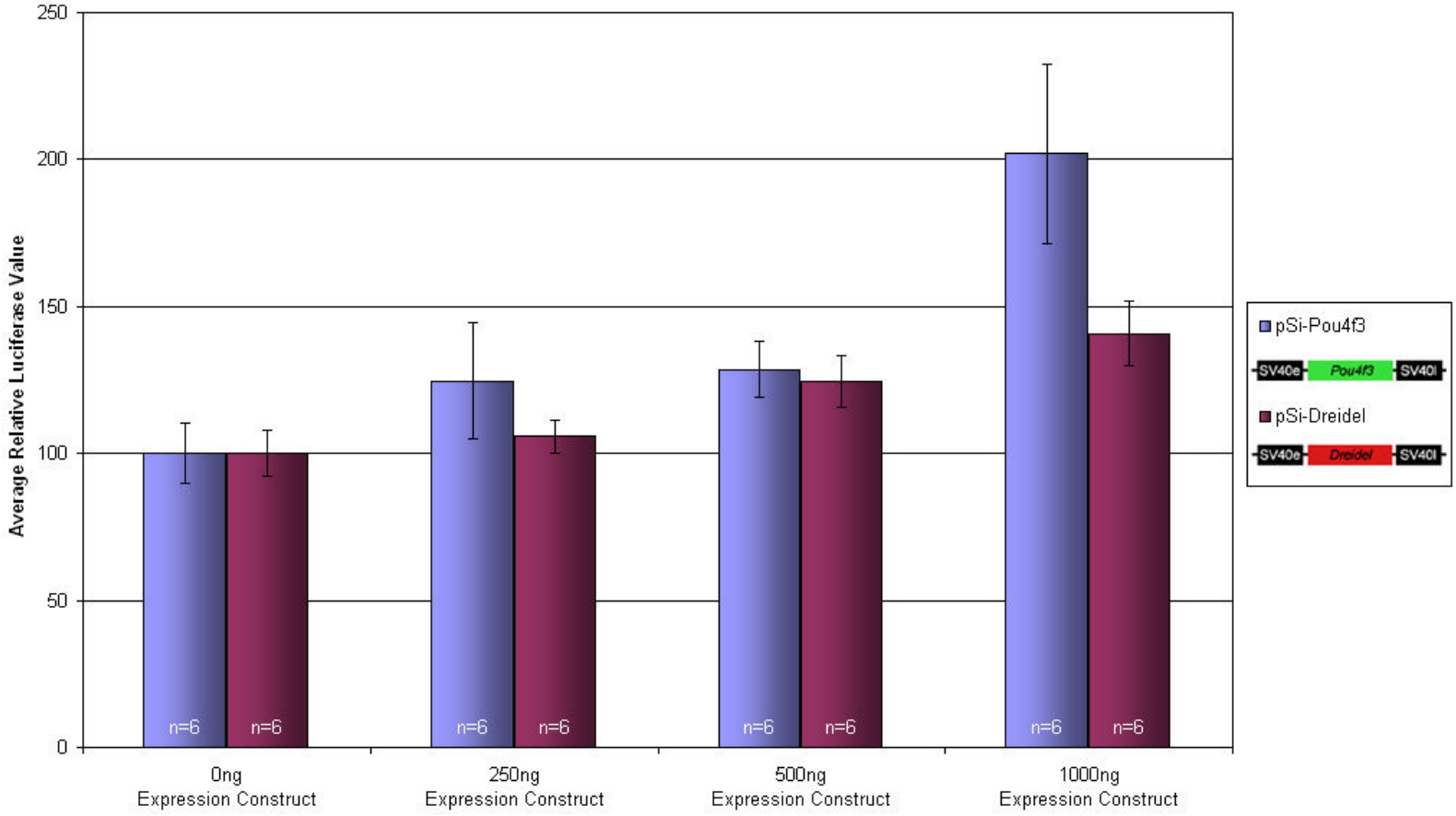

Figure 5.14. Response of LUZP1p2.8kb to POU4F3.
ND7 cells were cotransfected with 200ng LUZP1p2.8kb, 10ng pRL-null and increasing amounts of expression construct (pSi-Pou4f3 or pSi-Dreidel). The total amount of DNA in each cotransfection was maintained at 1210ng using the empty pSi vector. Increasing the amount of POU4F3 results in an increase in LUZP1p2.8kb activation of two-fold at the maximal level transfected (1000ng pSi-Pou4f3) and cotransfections of LUZP1p2.8kb with an equivalent amount of the mutant *Pou4f3* expression vector pSi-Dreidel results in a smaller upregulation (1.4-fold). *SV40e*, SV40 enhancer / early promoter; *SV40l*, SV40 late poly(A).

5.7.3 Regulation of RBMS1p1.3kb and RBMS1p5.1kb by POU4F3

The ability of POU4F3 to regulate the RBMS1p1.3kb promoter construct was tested similarly to LUZP1p2.8kb (section 5.7.2) though assays were repeated a different number of times. Furthermore, due to problems with low transfection efficiency, the amount of pRL-null included in experiments where RBMS1p1.3kb and pSi-Dreidel or pGV-B and pSi-Pou4f3 were cotransfected was increased to 50ng to ensure sufficient sea pansy luciferase production for detection on luminometry.

These experiments showed that RBMS1p1.3kb is activated by increasing amounts of POU4F3. At the largest amount of pSi-Pou4f3 (1µg) RBMS1p1.3kb is activated 2.7-fold compared to transfections with an equivalent amount of empty pSi vector. This effect was shown to be POU4F3-specific and not caused by regulation of the pGV-B plasmid into which the 1.3kb *Rbms1* promoter is cloned as control experiments demonstrated that RBMS1p1.3kb activity is repressed by 1µg pSi-Dreidel and pGV-B is repressed by 1µg pSi-Pou4f3 (Figure 5.15).

Given that POU4F3 has been shown to bind the RBMS1BS3 binding site contained in RBMS1p1.3kb by EMSA analysis (Figure 5.12*c*), it is likely that the upregulation of this reporter construct by POU4F3 is produced at this site. As well as RBMS1BS3, two other sites (RBMS1BS1 and RBMSBS2) were shown to be bound by POU4F3 in EMSA analysis. A construct containing a longer fragment (5.1kb) of the *RBMS1* 5' flanking sequence that encompassed these sites as well as RBMS1BS1 was cloned in order to identify whether their inclusion affected *RBMS1* 5' flanking region activation by POU4F3 (see section 5.7.1).

The activation of 200ng RBMS1p5.1kb cotransfected with 0ng or 1µg pSi-Pou4f3 and 50ng pRL-null was compared to RBMS1p5.1kb cotransfected with 0ng or 1µg pSi-Dreidel and 10ng pRL-null. Figure 5.16 shows that RBMS1p5.1kb is upregulated 2.6-fold by 1µg pSi-Pou4f3 – an activation which is similar to that of RBMS1p1.3kb when cotransfected with equivalent amounts of pSi-Pou4f3. As for RBMS1p1.3kb, this response was shown to be POU4F3-specific as pSi-Dreidel is unable to activate RBMS1p5.1kb. Furthermore, the response seen is not due to regulation of the pGL4.10 vector which only shows a 1.4-fold response to POU4F3 in these conditions as determined by JK in our laboratory.

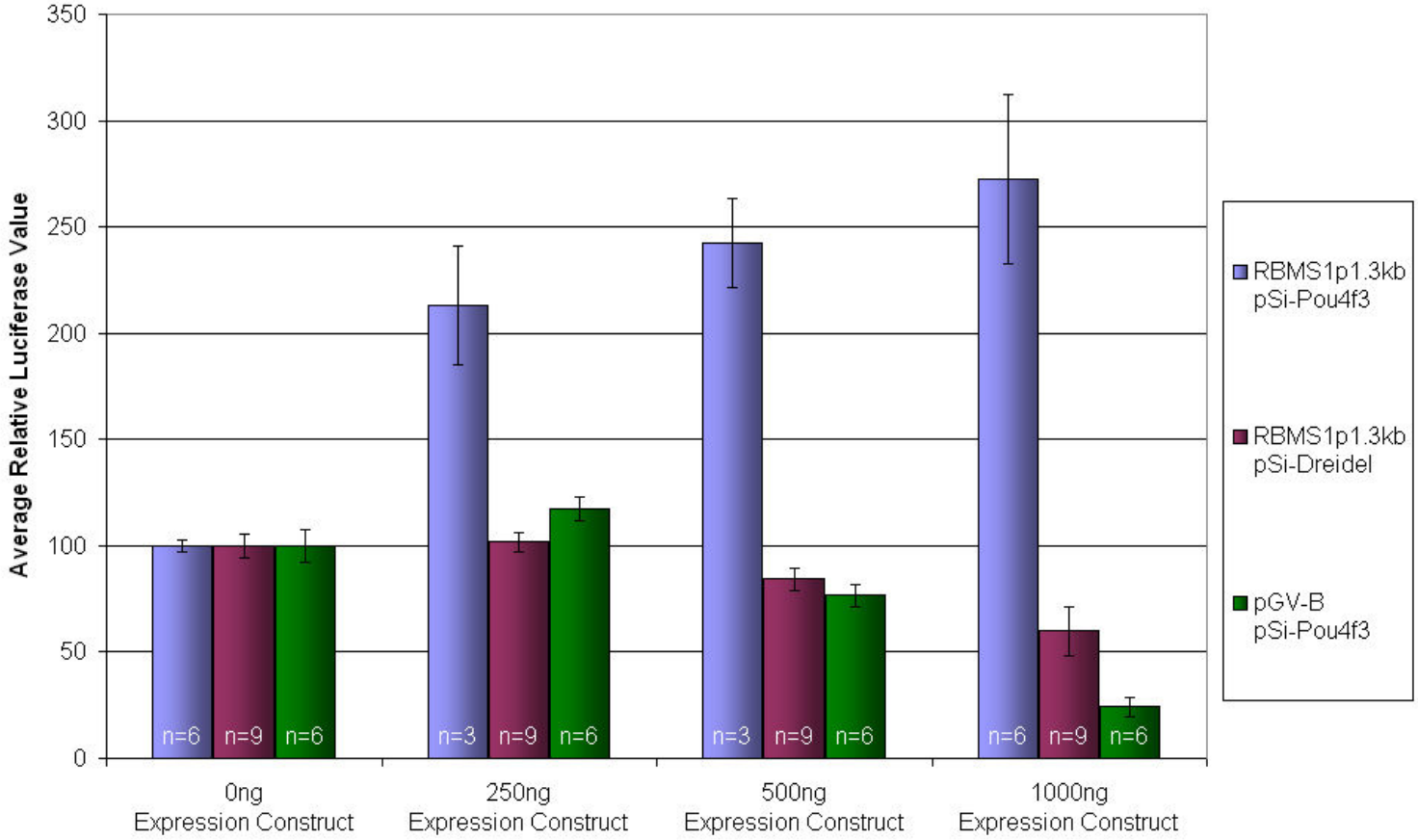

Figure 5.15. Regulation of RBMS1p1.3kb by POU4F3.
ND7 cells were cotransfected with 200ng RBMS1p1.3kb or pGV-B and increasing amounts of expression construct (pSi-Pou4f3 or pSi-Dreidel).The amount of pRL-null used was 10ng for RBMS1p1.3kb cotransfections with pSi-Pou4f3 and 50ng for all other assays. The total amount of DNA in each cotransfection was maintained at a constant level using the empty pSi vector. Increasing POU4F3 expression increases RBMS1p1.3kb activation 2.7-fold at the maximal level transfected (1000ng pSi-Pou4f3). This regulation is not due to regulation of the pGV-B vector into which the *Rbms1* promoter was cloned as this vector is not activated by POU4F3. Furthermore, this activation is POU4F3-specific as an equivalent amount of pSi-Dreidel results in a reduction in RBMS1p1.3kb activation.

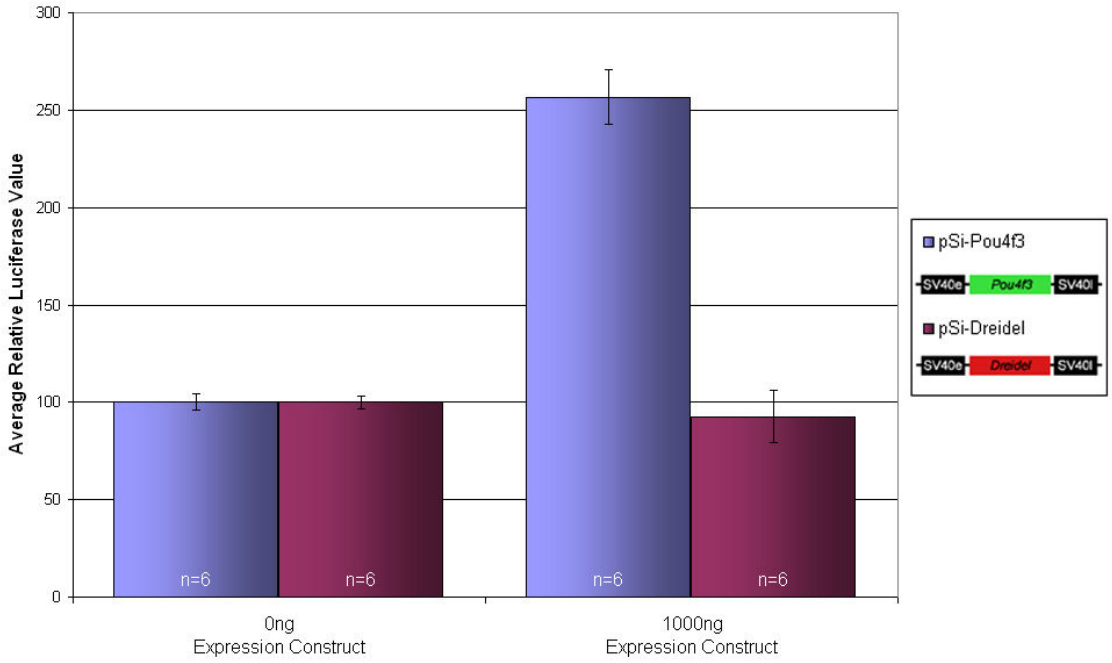

Figure 5.16. Regulation of RBMS1p5.1kb by POU4F3.
200ng RBMS1p5.1kb was cotransfected with either pSi-Pou4f3 and 50ng pRL-null or pSi-Dreidel with 10ng pRL-null in ND7 cells. The total amount of DNA transfected was kept constant using the empty pSi expression vector. RBMS1p5.1kb showed a 2.6-fold response to 1µg pSi-Pou4f3 and this response was shown to be POU4F3-specific as dreidel mutant POU4F3 did not activate RBMS1p5.1kb. *SV40e*, SV40 enhancer / early promoter; *SV40l*, SV40 late poly(A).

Taken together, the POU4F3-specific activation of two different *RBMS1* promoter constructs in two different reporter vectors (pGV-B for RBMS1p1.3kb and pGL4.10 for RBMS1p5.1kb) clearly demonstrates the ability of POU4F3 to activate the *RBMS1* 5' flanking region *in vitro*. Furthermore, these results and EMSA data that demonstrate POU4F3 binding to three sites in the *RBMS1* 5' flanking region strongly suggest that this activation is produced by a direct mechanism i.e. that POU4F3 binds to the *RBMS1* 5' flanking region to produce this activation in this cellular context.

Though it is tempting to speculate that RBMS1BS1 and RBMS1BS2 are unlikely to influence POU4F3 regulation of the *RBMS1* promoter because RBMS1p5.1kb does not show a larger response than the construct that only contains RBMS1BS3 (RBMS1p1.3kb), this is not necessarily the case as RBMS1p5.1kb may contain binding sites for transcription factors that mediate repression of *RBMS1*. Furthermore, it is known to contain the -1283 to -1709 region (which contains RBMSBS1 and RBMS1BS2) that reduces basal *RBMS1* 5' flanking region activation in HeLa cells (Haigermoser *et al.* 1996). Therefore, the preferred method for assessment of the putative contribution of each binding to site to POU4F3 activation of *RBMS1* promoter reporter constructs remains site-directed mutagenesis.

5.7.4 Assessment of ZRANB2p3.2kb regulation by POU4F3

A luciferase assay was carried out with the ZRANB2p3.2kb luciferase reporter construct as for RBMS1p5.1kb. As before, the reporter construct was cotransfected with pRL-null (to control for variation in transfection efficiency and cell number) and either pSi-Pou4f3 or pSi-Dreidel. The results of this assay (Figure 5.17) show that ZRANB2p3.2kb is upregulated 1.6-fold by 1µg pSi-Pou4f3 and 2.1-fold by 1µg pSi-Dreidel. This shows that the *Zranb2* 5' flanking region cloned is not specifically activated by POU3F3.

The unusually large response of ZRANB2p3.2kb to dreidel mutant POU4F3 and high levels of basal luciferase production seen with this construct suggest that any protein-specific activation may be masked in the conditions used to investigate its regulation. Due to the inclusion of the *Zranb2* transcriptional start site in ZRANB2p3.2kb, basal regulation of this promoter in ND7 cells, which have been shown to express ZRANB2 (data not shown), may be sufficient to mask any POU4F3-specific effect. This hypothesis could be tested by subcloning a promoter construct that does not include the *Zranb2* transcriptional start site or by assaying ZRANB2p3.2kb activation in cells that do not constitutively express ZRANB2 to reduce the suggested background regulation, though the transcriptional environment in such cells may not be suitable for the assessment of POU4F3 function. However, based on current evidence (Figure 5.17), ZRANB2p3.2kb does not appear to be activated by POU4F3 and, therefore, *Zranb2* is unlikely to be a true target of POU4F3.

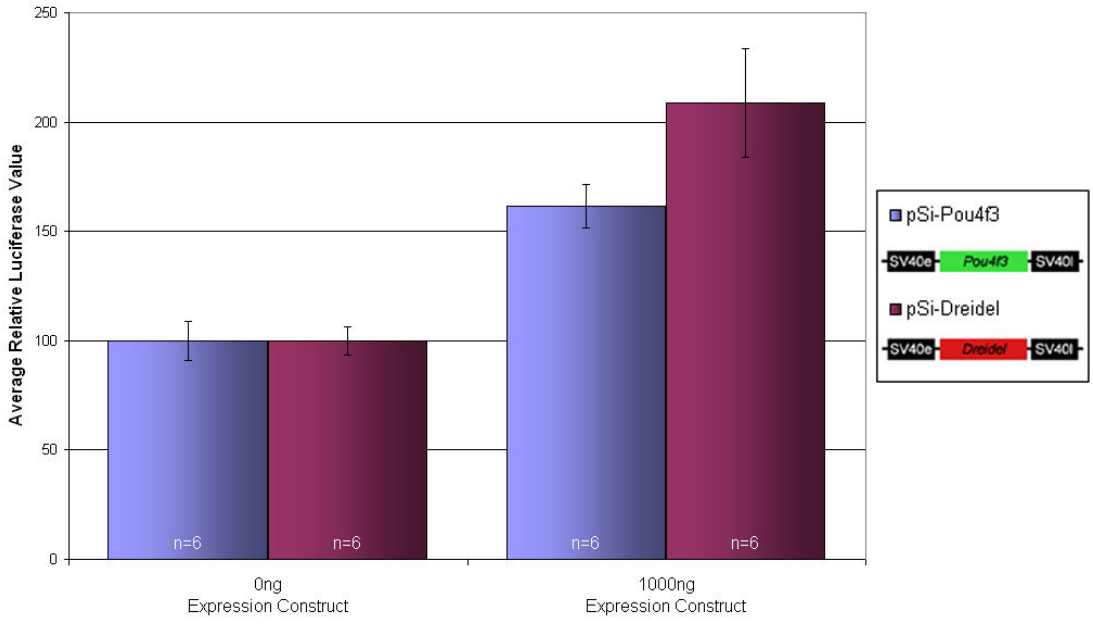

Figure 5.17. ZRANB2p3.2kb is not regulated by POU4F3.
Cotransfections were carried out for ZRANB2p3.2kb as for other promoter constructs tested. In this experiment 200ng of the reporter construct was cotransfected with differing amounts of pSi-Pou4f3 (with 50ng pRL-null) or pSi-Dreidel (with 10ng pRL-null) in ND7 cells. Though the promoter demonstrated a 1.6-fold increase in luciferase production in the presence of 1000ng pSi-Pou4f3, a 2.1-fold response was seen with an equivalent amount of pSi-Dreidel. Therefore, ZRANB2p3.2 does not appear to be specifically activated by POU4F3. *SV40e*, SV40 enhancer / early promoter; *SV40l*, SV40 late poly(A).

5.8 Summary and discussion of candidate gene activation by POU4F3

Luzp1, *Rbms1* and *Zranb2* were suggested to be POU4F3 target genes by a subtractive hybridization screen in UB/OC-2 cells. These genes were prioritised for further investigation on the basis of their potential roles in hair cell development and survival; the availability of reagents for their study; and the identification of putative POU4F3 binding sites in their predicted promoter regions.

I first attempted to determine the inner ear expression patterns of these candidate genes by immunohistochemistry. As *Zranb2* was the only candidate gene (apart from *Nr2f2*) for which I was able to obtain an antibody that was suitable for immunohistochemistry, its inner ear expression pattern was characterised. This revealed widespread ZRANB2 expression in the P0 cochlea that declined to undetectable levels by P4. It was noted to be expressed in hair cells at P0, suggesting that it is coexpressed with POU4F3, which is known to be expressed in hair cells at this stage. This coexpression supported the possibility that POU4F3 might regulate *Zranb2* in hair cells. Given that it was not possible to obtain suitable antibodies to investigate LUZP1 and RBMS1 expression in the inner ear, RNA *in situ* hybridization could be used in future work to investigate their expression.

Following the investigation of candidate gene inner ear expression, putative regulation of target genes by POU4F3 was investigated at the transcriptional level. Bioinformatic software was used to identify POU4F3 binding sites in predicted target gene promoters and putative POU4F3 binding sites were identified in these regions. The identification of high stringency predicted POU4F3 binding sites aided in the selection of these candidate genes for further investigation and oligonucleotides designed against predicted binding sites were used in a protein-DNA binding assay (EMSA) to determine whether POU4F3 can bind oligonucleotides that correspond to these sites in candidate gene promoters.

This analysis revealed that POU4F3 is able to bind to two sites in the *Luzp1* 5' flanking region, three sites in the *RBMS1* 5' flanking region and two sites in the *Zranb2* 5' flanking region. These binding sites therefore represent potential locations for POU4F3 regulation of candidate target genes. Having demonstrated that POU4F3 is able to bind sites in candidate gene 5' flanking regions, its ability to activate candidate gene 5' flanking region luciferase reporter constructs that contain these binding sites was assessed.

Candidate gene 5' flanking regions were cloned for *Luzp1*, *Rbms1* and *Zranb2* and a luciferase reporter construct was obtained for *Rbms1*. The *Luzp1* promoter construct (LUZP1p2.8kb) and two *RBMS1* promoter constructs (RBMS1p1.3kb and RBMS1p5.1kb) were shown to be activated by POU4F3, supporting the hypothesis that POU4F3 is able to

regulate the 5' flanking regions of these genes in the context of genomic DNA. However, POU4F3 was shown not to be able to specifically upregulate the *Zranb2* promoter construct ZRANB2p3.2kb.

Based on the above evidence, *Luzp1* is suggested to be modestly regulated by POU4F3. Therefore, the upregulation of LUZP1p2.8kb should be confirmed by repetition of luciferase assays (section Figure 5.14) and putative sites at which POU4F3 might produce upregulation of this reporter construct (i.e. LUZP1BS1 and LUZP1BS2) should by mutated (as for NR2F2BS1 and NR2F2BS2) in order to identify whether these are the sites of activation and, therefore, whether POU4F3 is likely to directly activate LUZP1p2.8kb. Results from these experiments will, furthermore, provide stronger evidence that POU4F3 might upregulate *Luzp1 in vivo*. In order to investigate the relevance of any interaction in the inner ear, LUZP1 expression requires investigation. Since the conclusion of the studies reported in this chapter, an anti-LUZP1 antibody has been obtained and is currently being used to attempt to identify whether LUZP1 is expressed in the inner ear.

Unlike *Luzp1*, the evidence for POU4F3 upregulation of the *Rbms1* 5' flanking region reporter constructs, RBMS1p1.3kb and RBMS1p5.1kb is strong. Therefore, RBMS1BS1-3 should be mutated in these constructs to identify which, if any, of these is responsible for the activations seen at these promoters. As for LUZP1, the expression pattern of RBMS1 in the inner ear remains to be characterised and would require an antibody that is suitable for immunohistochemistry to be obtained or RNA *in situ* hybridizations to be conducted. Such experiments would identify whether *Rbms1* is expressed in hair cells and, therefore, whether *Rbms1* activation by POU4F3 is likely to be relevant to hair cell development and maintenance. Alternatively, reverse transcriptase PCR strategies or investigation of *Rbms1* knockout mouse inner ears may identify whether it plays a role in hair cell development or survival.

ZRANB2 has been shown to be expressed in the inner ear and two sites in its promoter have been shown to be bound by POU43 by EMSA analysis. However, the ability of POU4F3 to activate the *Zranb2* 5' flanking region has not been characterised as the reporter construct cloned (ZRANB2p3.2kb) displays strong basal regulation in ND7 cells that may mask any transcriptional effect of POU4F3. Therefore, a *Zranb2* promoter construct should be cloned that omits the transcriptional start site to attempt to abolish this basal regulation. Alternatively the response of ZRANB2p3.2kb to POU4F3 could be assayed in a cell type that does not exhibit high basal regulation of this construct. However, given that POU4F3 has been shown to activate some target gene promoters in a cell-specific manner, attempts should be made to ensure that the transcriptional environment in the cell type chosen is likely to reflect that of neuronal or sensory epithelial cells.

The varying levels of evidence for the expression and POU4F3 regulation of candidate genes reported above demonstrates the difficulty of investigating a large number of genes following a screen such as a subtractive hybridization (discussed further in Chapter 6). However, they also demonstrate the value of obtaining clear evidence of candidate gene expression and regulation in order to prioritise these genes for further investigation, thereby allowing more effective allocation of limited resources. Therefore, based on the current evidence available for *Luzp1*, *Rbms1* and *Zranb2*, the interaction between POU4F3 and *Rbms1* appears to be the best candidate for further investigation. This is because, the *RBMS1* 5' flanking region reporter constructs tested demonstrate the most robust activation in response to POU4F3 and RBMS1 is known to be involved in many roles relevant to hair cell maintenance and survival (see section 5.1.2). However, a priority in such an investigation would be to identify whether RBMS1 is expressed in hair cells in order to determine whether the regulatory relationship seen in ND7 cells and the known functions of RBMS1 are relevant to the development and maintenance of these cells.

6

GENERAL DISCUSSION

The investigation reported in this thesis represents an attempt to better understand the mechanism by which POU4F3 mediates hair cell differentiation and survival. We aimed to clarify why hair cells fail to terminally differentiate and survive in homozygous *Pou4f3* knockout mice and how the human deafness caused by *POU4F3* mutation (DFNA15) occurs (Collin *et al.* 2008;Vahava *et al.* 1998;Xiang *et al.* 1998). As POU4F3 is a transcription factor with no other identified function, these phenotypes are almost certainly caused by dysregulation of POU4F3 target genes.

At the time that this investigation was commenced in our laboratory, subtractive hybridization was selected to identify POU4F3 target genes, as it was the most appropriate strategy available. The selection of this strategy, as well as other methodologies applied in this investigation, reflects ongoing difficulties in the analysis of inner ear biology. In particular, the investigation of hair cells presents unique challenges as these cells are relatively inaccessible, making it difficult to obtain sufficient material for molecular analysis. Furthermore, these cells are mitotically quiescent and must therefore be isolated from primary tissue prior to investigation. Finally, it is difficult to use standard methodologies and reagents to investigate gene regulation in these cells, requiring time-consuming and potentially costly methods to be used for their investigation e.g. viral transfection.

As previously discussed (section 3.3), the subtractive hybridization itself presented the challenge of managing, prioritising and investigating a large number of candidate genes. In contrast to a similar experiment conducted in our laboratory for another inner ear transcription factor that only revealed four differentially expressed clones (unpublished data, VG), the present study yielded a large number of differentially expressed clones. This is likely to not only reflect differences in the methodology used (i.e. the stringency by which differentially expressed transcripts were identified) but also the nature of POU4F3 function i.e. POU4F3 is likely to produce its effects by the subtle modulation of a large number of genes which, in turn, mediate hair cell survival and maintenance by a summative action rather than it simply activating the expression of known hair cell structural components to

produce the hair cell phenotype. The results of this subtractive hybridization therefore represented a difficult middle-ground whereby the potentially differentially expressed genes identified are too numerous to all be investigated but too few to submit to bioinformatic software, developed for microarray studies, that might be able to provide information on the systems-level effect of POU4F3 e.g. by extracting common pathways that candidate target genes are involved in by literature mining (Munir *et al.* 2004).

The method by which target genes were prioritised for investigation was, therefore, a difficult and sometimes subjective process, with ongoing experiments revealing potentially interesting results for genes that were not originally prioritised for investigation by this method. Thus, the outcomes seen identify the strengths and weaknesses of the strategy employed. For example, the identification of genes with available (and obtainable) reagents allowed for the rapid verification and characterisation of NR2F2 and ZRANB2 expression in the early postnatal inner ear. However, the lack of available reagents for other candidate genes led to their investigation not being pursued despite subsequent work demonstrating potentially interesting roles for these genes e.g. recent work with RCN1 has shown that it is expressed in hair cells in the P1 mouse inner ear (unpublished data).

The case of *Rcn1* and other genes investigated herein also illustrate a general problem reaffirmed by the present study: that many of the large online databases of gene information, expression etc. are still incomplete and sometimes misleading. For example, clones that were originally not found to significantly match genomic DNA in the mouse genome (through BLAST analysis) can now be seen to match genes in this database. Therefore, such resources cannot be used as a reliable replacement for appropriately reported information in the scientific literature, though they may eventually incorporate this information.

Turning now to the evidence identified for candidate gene expression in the ear and potential regulation by POU4F3. Immunohistochemistry proved to be a rapid and cost-efficient method by which to investigate candidate gene expression in the inner ear. In this study, it was effective for characterising NR2F2 expression (section 4.7) and identifying ZRANB2 expression (section 5.4.3).

Future work for NR2F2 will focus on verifying and explaining differences in its expression in the mouse and rat inner ears; characterising the suggested nuclear to cytoplasmic shift in its expression seen in the basal P8 rat cochlea; and verifying that POU4F3 is able to regulate its expression in this system (see below). Future work for ZRANB2 will focus on verifying and characterising its apparently rapid downregulation between P0 and P4 rat inner ears. It would also be interesting to examine its expression in development i.e. around the time of onset of POU4F3 expression, in order to see what relationship the expression

patterns of the two genes bear (if any). Furthermore, the investigation of the potential for ZRANB2 to induce alternative splicing in the inner ear could be of particular interest.

As previously mentioned, LUZP1 expression is currently being investigated in the inner ear and investigation of *Rbms1* expression is dependant on obtaining a suitable antibody for immunohistochemistry or pursuing RNA *in situ* hybridization (which has been attempted without success) to characterise its expression. Though RNA *in situ* hybridization may be required for future work, its use at earlier stages of the investigation would have been less efficient than immunohistochemistry which was shown to be an efficient means of assessing candidate gene expression in the inner ear in this study. For all of the genes that were found to be expressed in the inner ear, greater information on the potential effect of POU4F3 on their regulation could be provided by quantification of their level of expression (e.g. by quantitative PCR), though the technical impediments to this may be substantial, depending on their expression pattern.

In terms of the investigation of transcriptional regulation reported here, the strategy used (identification of POU4F3 binding to sites in target gene 5' flanking regions and luciferase assay of target gene reporter promoter constructs) appeared to be highly sensitive. The binding sites predicted by the Genomatix programs used (MatInspector and ModelInspector) were all shown to be bound by POU4F3 which, in comparison to previous experiments in our laboratory, is a substantial improvement compared to older versions of this software. Therefore, the existing positional weight matrix and contextual information for POU-factor binding contained in the Genomatix database appears to be extremely accurate though, as the TransFac database is no longer being maintained, it is a shame that no freely available resource for the collation of transcriptional regulatory information now exists. This deficit hindered attempts to investigate the basic mechanisms by which POU4F3 binds and activates target gene promoters.

Luciferase assays of reporter constructs with the luciferase gene under the regulation of candidate gene 5' flanking regions demonstrated that POU4F3 is able to activate these regions for *Nr2f2*, *Luzp1* (pending verification) and *RBMS1* with further work required to identify whether it is able to activate the *Zranb2* 5' flanking region. Furthermore, activation of the *Nr2f2* 5' flanking region tested was shown to occur at identified binding sites by site-directed mutagenesis, though the individual contribution of each of these sites remains to be determined. Future experiments will focus on determining whether the binding sites identified in the *Luzp1* and *RBMS1* 5' flanking regions are the loci for regulation of their reporter constructs. This can be investigated by site-directed mutagenesis, as for *Nr2f2*. Furthermore, demonstration of the ability of POU4F3 to bind these sites in a more physiological context than that of the EMSA analysis will provide evidence as to whether these sites are likely to be bound by POU4F3 *in vivo*. At a very late

stage of this work preliminary attempts were made to investigate POU4F3 binding to these sites by chromatin immunoprecipitation using a fusion protein to overcome the lack of a suitable anti-POU4F3 antibody. However, none of the binding sites were identified by this method. Furthermore, this protocol requires further optimisation and the possibility that the fusion protein affects POU4F3 binding ability has not been excluded.

Taken together, the results of the DNA-binding and promoter regulation experiments conducted (EMSAs and luciferase assays respectively) verify and extend the results of the subtractive hybridization. These results support the hypothesis that the candidate genes investigated (*Nr2f2*, *Luzp1*, *Rbms1* and *Zranb2*) may be targets of POU4F3 regulation in hair cells (though the ability of POU4F3 to regulate the *Zranb2* and *Luzp1* 5' flanking regions particularly requires further investigation).

In order to investigate candidate gene responses to POU4F3 in hair cells, we intended to manipulate *Pou4f3* expression in these cells in cochlear cultures and assay target gene response (to the single cell level) using a cell collection and quantitative (real time) reverse transcriptase PCR strategy devised in our laboratory (unpublished data). As previously discussed, inner ear biology is difficult to investigate by such methods as the required tissue is difficult to obtain and manipulate; hence the use of UB/OC-2 cells to identify POU4F3 target genes by subtractive hybridization. Accordingly, despite many transfection methods being attempted (e.g. cationic agents, electroporation and gene gun), it was not possible to transfect hair cells in cochlear cultures and, thereby, investigate the response and function of POU4F3 target genes in this system. Current attempts to manipulate target gene expression in these cells using viral vectors appear more promising and may therefore aid in the elucidation of the physiological regulation of POU4F3 target genes.

An alternative method to examine candidate gene regulation in response to POU4F3 would be to examine the inner ears of *Pou4f3* mutant mice. However, the abnormalities seen in these mutants (i.e. disruption of the elaborate mosaic structure of the organ of Corti, impaired nascent hair cell terminal differentiation and degeneration of hair cells by apoptosis) may mask the effect of POU4F3 on their regulation (Erkman *et al.* 1996;Hertzano *et al.* 2004;Xiang *et al.* 1998;Xiang *et al.* 1997). Furthermore, the expression patterns of investigated genes show that they are not only expressed in hair cells in the inner ear, demonstrating that POU4F3 is unlikely to be required for their expression and might therefore play a subtle role in their regulation. Therefore, the controlled manipulation of *Pou4f3* expression in cochlear cultures appears to be a more sensitive and versatile means of investigating the proposed regulation of target genes in hair cells and, potentially, elucidating their function in hair cells.

The clones investigated in this study represent approximately half of those obtained from the subtractive hybridization screen. The remainder of these clones were investigated by ET and a discussion of the understanding of POU4F3 function gained from this investigation is, therefore, not complete without the inclusion of these genes. Though some of the candidate genes identified share common functions (e.g. transcription factor activity), the putative POU4F3 target genes identified by the subtractive hybridization appear to have varied function, ranging from transcription factors to ion channels. As some of these putative POU4F3 targets are extremely undercharacterised and others have not been characterised in the inner ear, it has been difficult to relate the regulation of verified POU4F3 target genes to the production of the hair cell phenotype and any such relation remains speculative. However, recent investigations by ET suggest that at least three POU4F3 target genes identified by the subtractive hybridization may be involved in cellular responses to stressful stimuli (e.g. heat shock or, aminoglycoside antibiotics) (unpublished data), thus illustrating how POU4F3 may mediate hair cell responses to stress and suggesting roles for these factors in ensuring hair cell survival in development.

One notable observation of the subtractive hybridization was that it did not identify known direct targets of POU4F3 (*Bdnf* and *Ntf3*) and transcription factors that have been strongly associated with POU4F3 expression and shown to be involved in hair cell development (*Gfi1* and *Lhx3*). Though POU4F3 regulation in hair cells has only been investigated for *Bdnf*, its regulation of *Bdnf* and *Ntf3* was identified in UB/OC-2 cells and they would, therefore, be expected to have been identified by the subtractive hybridization.

There are three likely explanations for this. Firstly, the subtractive hybridization strategy used is biased towards identifying the most differentially regulated transcripts between populations tested. Though the genes linked (*Bdnf* and *Ntf3*) or associated (*Gfi1* and *Lhx3*) with POU4F3 regulation may have been differentially expressed in UB/OC-2 cells in which POU4F3 expression had been manipulated, they would not necessarily have been *more* differentially expressed than candidate genes identified. In fact, clones that appeared less differentially regulated than those sequenced following the qualitative virtual Northern blot analysis of the subtractive hybridization screen may have corresponded to these genes.

The second explanation is that the above candidate genes were identified to be putative POU4F3 target genes by different methods. *Bdnf* and *Ntf3* were identified as POU4F3 target genes by CAT assay and DNAse I footprinting of their 5' flanking regions (Clough *et al.* 2004) and *Gfi1* and *Lhx3* were identified by cDNA microarray that compared whole homozygous dreidel *Pou4f3* mutant mouse inner ears to those of wild type animals (Hertzano *et al.* 2004;Hertzano *et al.* 2007). These differences in methodology may be sufficient to explain the differences seen between these quite different experiments, especially where the effects seen might be transient (Fortunel *et al.* 2003).

The third explanation for this observation centres on the transcriptional environment in UB/OC-2 cells. It would not be possible to carry out a subtractive hybridization in hair cells, and the transcriptional effects of POU4F3 have been shown to be cell type specific (Smith *et al.* 1998;Sud *et al.* 2005). Therefore, these cells were selected for the present study as they were the best available model of the hair cell transcriptional environment that could be manipulated as required and would provide sufficient material for analysis. However, there are clear differences between UB/OC-2 cells and hair cells, i.e. though they express hair cell marker genes, they do not resemble hair cells morphologically and they are not mitotically quiescent in their undifferentiated state (Rivolta *et al.* 1998a). Therefore, the difference in the transcriptional environment between hair cells and UB/OC-2 cells may explain why previously described likely POU4F3 target genes were not identified by the method used in this study.

6.1 Conclusions

Transcriptional regulation in hair cells of the inner ear is poorly understood and this deficit is an impediment to the creation of therapies for hearing loss e.g. gene or stem cell therapy. Therefore, in this project I to aimed identify POU4F3 target genes to aid in the explanation of the mechanism by which this transcription factor appears to produce and maintain hair cells and, therefore, hearing.

14 candidate POU4F3 target genes were identified from 21 clones of transcripts that were shown to be differentially regulated by POU4F3 in a subtractive hybridization screen in UB/OC-2 cells. Seven putative POU4F3 target genes were initially investigated based on their potential role in hair cell development and survival and, of these, four were selected for detailed analysis based on their known expression, potential function, potential for POU4F3 regulation (as determined by the presence of predicted POU4F3 binding sites in their 5' flanking regions) and availability of reagents for their investigation.

Nr2f2 was shown to be a likely direct target of POU4F3; two 5' flanking region reporter constructs for *Rbms1* were shown to be regulated by POU4F3 with potential sites of regulation identified; and POU4F3 was shown to be able to bind to two sites in the *Zranb2 and Luzp1* 5' flanking regions with a likely activation of the *Luzp1* 5' flanking region that requires verification. This represents a substantial contribution to the understanding of the network that POU4F3 regulates. Furthermore, the identification and characterisation of NR2F2 and ZRANB2 expression in the hair cells of the inner ear supports the possibility that POU4F3 is able to regulate *Nr2f2* and *Zranb2* expression in these cells and that these factors, in turn, might play a role in generating and maintaining the hair cell phenotype.

It is hoped that this contribution to the understanding of transcriptional regulation by POU4F3 might aid in future work to elucidate its function in hair cell development and maintenance, thereby contributing to the development of new therapies for the increasing number of people affected by hearing loss.

APPENDIX:

REVERSE TRANSCRIPTASE PCR PRIMERS

Primers used for reverse transcriptase PCR (see Figure 3.1) are shown below. The predicted melting temperature shown (*Tm*) is salt-adjusted and amplicon lengths were calculated based on transcript sequences in the Ensembl database for *mus musculus*. *cDNA*, complementary DNA; *gDNA*, genomic DNA.

Gene	*Primer Name*	*Primer Orientation*	*Primer Sequence (5' to 3')*	*Primer Length (bp)*	*Primer Tm (ºC)*	*cDNA Amplicon (bp)*	*gDNA Amplicon (bp)*
Luzp1	LISPriF	Forward	CCACTCTCCTGTACCAATTGGCAGCC	26	71	1081	1081
	LISPriR	Reverse	GCCTCTGAGTCCCTGTTCCTTTACTGAC	28	72		
Metap2	METAP3GSP1	Forward	GACAGCTGCTTGGAGAACCACAAGTG	26	70	886	10177
	MISPriR	Reverse	GCCCAAGTCACACAGATTCTTCAGAGC	27	70		
Nr2f2	NR2PriF	Forward	AGGAACCTGAGCTACACGTGCCG	23	68	890	5318
	NISHPriR	Reverse	CTGCTGCCGGACAGTAACATATCC	24	67		
Rbms1	RBMPriF	Forward	AGTAGCAGCAGTAGCAACTCAGGATG	26	68	780	88610
	RBISHPriR	Reverse	CTGCTGGCCACTTGCTTCCTCAAC	24	69		

Gene	*Primer Name*	*Primer Orientation*	*Primer Sequence (5' to 3')*	*Primer Length (bp)*	*Primer Tm (°C)*	*cDNA Amplicon (bp)*	*gDNA Amplicon (bp)*
Rcn1	RCNPriF	Forward	CAAGCAGGCCACCTATGGCTACTACC	26	71	1143	7355
	RcISHPriR	Reverse	GTGGGTTTATTGTGCACATTAGCAGGTC	28	68		
Sertad2	SERPriF	Forward	CTATCCATGGCTGGCTGGCTGTATTCC	27	71	1034	105075
	SISHPriR	Reverse	GGACACTGGACTCACTGGAGGTTCC	25	71		
Zranb2	ZNFPriF	Forward	AAGACACTGGCAGAGAAGAGCC	22	64	1195	10576
	ZISPriR	Reverse	CCATGTGTCTGAAGTCCAGGCAAGCC	26	71		

BIBLIOGRAPHY

Abcam. NR2F2 antibody (ab66662) datasheet | Abcam. http://www.abcam.com/index.html?datasheet=66662 . 2008.
Ref Type: Internet Communication

Abello, G. & Alsina, B. 2007, "Establishment of a proneural field in the inner ear", *Int.J.Dev.Biol*, vol. 51, no. 6-7, pp. 483-493.

Abnova. NR2F2 MaxPab polyclonal antibody (B01) - H00007026-B01 - Abnova. http://www.abnova.com/Products/products_detail.asp?Catalog_id=H00007026-B01#p00 . 2008b.
Ref Type: Internet Communication

Abnova. ZNF265 monoclonal antibody (M01), clone 1D10 - H00009406-M01 - Abnova. http://www.abnova.com/Products/products_detail.asp?Catalog_id=H00009406-M01 . 2008a.
Ref Type: Internet Communication

Acevedo-Arozena, A., Wells, S., Potter, P., Kelly, M., Cox, R. D., & Brown, S. D. 2008, "ENU mutagenesis, a way forward to understand gene function", *Annu.Rev Genomics Hum.Genet.*, vol. 9, pp. 49-69.

Adams, D. J., van der, W. L., Kovacic, A., Lovicu, F. J., Copeland, N. G., Gilbert, D. J., Jenkins, N. A., Ioannou, P. A., & Morris, B. J. 2000, "Chromosome localization and characterization of the mouse and human zinc finger protein 265 gene", *Cytogenet.Cell Genet*, vol. 88, no. 1-2, pp. 68-73.

Adams, D. J., van der, W. L., Mayeda, A., Stamm, S., Morris, B. J., & Rasko, J. E. 2001, "ZNF265--a novel spliceosomal protein able to induce alternative splicing", *J.Cell Biol.*, vol. 154, no. 1, pp. 25-32.

Agrawal, Y., Platz, E. A., & Niparko, J. K. 2008, "Prevalence of hearing loss and differences by demographic characteristics among US adults: data from the National Health and Nutrition Examination Survey, 1999-2004", *Arch Intern.Med.*, vol. 168, no. 14, pp. 1522-1530.

Ahmed, Z. M., Kjellstrom, S., Haywood-Watson, R. J., Bush, R. A., Hampton, L. L., Battey, J. F., Riazuddin, S., Frolenkov, G., Sieving, P. A., & Friedman, T. B. 2008, "Double homozygous waltzer and Ames waltzer mice provide no evidence of retinal degeneration", *Mol Vis.*, vol. 14, pp. 2227-2236.

Alberts, B., Johnson, A., Lewis, J., Raff, M., Roberts, K., & Walter, P. 2002, "Control of Gene Expression," in *Molecular Biology of the Cell*, 4 edn, S. Gibbs, ed., Garland Science, New York, pp. 375-466.

Andersen, B. & Rosenfeld, M. G. 2001, "POU Domain Factors in the Neuroendocrine System: Lessons from Developmental Biology Provide Insights into Human Disease", *Endocrine Reviews*, vol. 22, no. 1, pp. 2-35.

Anderson, C. T. & Zheng, J. 2007, "Isolation of outer hair cells from the cochlear sensory epithelium in whole-mount preparation using laser capture microdissection", *Journal of Neuroscience Methods*, vol. 162, no. 1-2, pp. 229-236.

Aurora, R. & Herr, W. 1992, "Segments of the POU domain influence one another's DNA-binding specificity", *Molecular and Cellular Biology*, vol. 12, no. 2, pp. 455-467.

Bajic, V. B., Tan, S. L., Suzuki, Y., & Sugano, S. 2004, "Promoter prediction analysis on the whole human genome", *Nat Biotechnol.*, vol. 22, no. 11, pp. 1467-1473.

Ballachanda, B. B. 1997, "Theoretical and applied external ear acoustics", *J.Am.Acad.Audiol.*, vol. 8, no. 6, pp. 411-420.

Bardoux, P., Zhang, P., Flamez, D., Perilhou, A., Lavin, T. A., Tanti, J. F., Hellemans, K., Gomas, E., Godard, C., Andreelli, F., Buccheri, M. A., Kahn, A., Le Marchand-Brustel, Y., Burcelin, R., Schuit, F., & Vasseur-Cognet, M. 2005, "Essential role of chicken ovalbumin upstream promoter-transcription factor II in insulin secretion and insulin sensitivity revealed by conditional gene knockout", *Diabetes*, vol. 54, no. 5, pp. 1357-1363.

Baroukh, N., Ahituv, N., Chang, J., Shoukry, M., Afzal, V., Rubin, E. M., & Pennacchio, L. A. 2005, "Comparative genomic analysis reveals a distant liver enhancer upstream of the COUP-TFII gene", *Mamm.Genome*, vol. 16, no. 2, pp. 91-95.

Beato, M., Herrlich, P., & Schutz, G. 1995, "Steroid hormone receptors: many actors in search of a plot", *Cell*, vol. 83, no. 6, pp. 851-857.

Benoit, G., Malewicz, M., & Perlmann, T. 2004, "Digging deep into the pockets of orphan nuclear receptors: insights from structural studies", *Trends Cell Biol.*, vol. 14, no. 7, pp. 369-376.

Bermingham-McDonogh, O., Oesterle, E. C., Stone, J. S., Hume, C. R., Huynh, H. M., & Hayashi, T. 2006, "Expression of Prox1 during mouse cochlear development", *J Comp Neurol.*, vol. 496, no. 2, pp. 172-186.

Boeda, B., El-Amraoui, A., Bahloul, A., Goodyear, R., Daviet, L., Blanchard, S., Perfettini, I., Fath, K. R., Shorte, S., Reiners, J., Houdusse, A., Legrain, P., Wolfrum, U., Richardson, G., & Petit, C. 2002, "Myosin VIIa, harmonin and cadherin 23, three Usher I gene products that cooperate to shape the sensory hair cell bundle", *EMBO J*, vol. 21, no. 24, pp. 6689-6699.

Boguski, M. S. & Schuler, G. D. 1995, "ESTablishing a human transcript map", *Nat Genet*, vol. 10, no. 4, pp. 369-371.

Bok, J., Chang, W., & Wu, D. K. 2007, "Patterning and morphogenesis of the vertebrate inner ear", *Int J Dev.Biol.*, vol. 51, no. 6-7, pp. 521-533.

Boley, J. Auditory System. http://www.perceptualentropy.com/wiki/index.php?title=Auditory_system . 2008. Ref Type: Internet Communication

Bryant, J. E., Forge, A., & Richardson, G. P. 2005, "The Differentiation of Hair Cells," in *Development of the Inner Ear*, M. K. Kelley et al., eds., Springer, New York, pp. 158-203.

Budhram-Mahadeo, V., Morris, P. J., Lakin, N. D., Theil, T., Ching, G. Y., Lillycrop, K. A., Moroy, T., Liem, R. K., & Latchman, D. S. 1995, "Activation of the alpha-internexin promoter by the Brn-3a transcription factor is dependent on the N-terminal region of the protein", *J Biol.Chem.*, vol. 270, no. 6, pp. 2853-2858.

Bull, P. & Clarke, R. 2007, "Deafness," in *Diseases of the Ear, Nose and Throat*, 10 edn, V. Noyes, ed., Blackwell Publishing, Oxford, pp. 17-22.

Burgermeister, E. & Seger, R. 2007, "MAPK kinases as nucleo-cytoplasmic shuttles for PPARgamma", *Cell Cycle*, vol. 6, no. 13, pp. 1539-1548.

Cartharius, K., Frech, K., Grote, K., Klocke, B., Haltmeier, M., Klingenhoff, A., Frisch, M., Bayerlein, M., & Werner, T. 2005, "MatInspector and beyond: promoter analysis based on transcription factor binding sites", *Bioinformatics*, vol. 21, no. 13, pp. 2933-2942.

Chen, P., Johnson, J. E., Zoghbi, H. Y., & Segil, N. 2002, "The role of Math1 in inner ear development: Uncoupling the establishment of the sensory primordium from hair cell fate determination", *Development*, vol. 129, no. 10, pp. 2495-2505.

Chen, P. & Segil, N. 1999, "p27(Kip1) links cell proliferation to morphogenesis in the developing organ of Corti", *Development*, vol. 126, no. 8, pp. 1581-1590.

Chen, W., Cacciabue-Rivolta, D. I., Moore, H. D., & Rivolta, M. N. 2007, "The human fetal cochlea can be a source for auditory progenitors/stem cells isolation", *Hear.Res.*, vol. 233, no. 1-2, pp. 23-29.

Cheng, A. G., Cunningham, L. L., & Rubel, E. W. 2005, "Mechanisms of hair cell death and protection", *Curr.Opin.Otolaryngol.Head Neck Surg.*, vol. 13, no. 6, pp. 343-348.

Clack, J. A. & Allin, E. 2004, "The Evolution of Single- and Multiple-Ossicle Ears in Fishes and Tetrapods," in *Evolution of the Vertebrate Auditory System*, G. A. Manley, A. N. Popper, & R. R. Fay, eds., Springer-Verlag, New York, pp. 128-163.

Clontech Laboratories, I. 2008, "PCR-Select™ cDNA Subtraction Kit User Manual", *http://www.clontech.com/images/pt/PT1117-1.pdf*.

Clough, R. L., Sud, R., vis-Silberman, N., Hertzano, R., Avraham, K. B., Holley, M., & Dawson, S. J. 2004, "Brn-3c (POU4F3) regulates BDNF and NT-3 promoter activity", *Biochem.Biophys.Res.Commun.*, vol. 324, no. 1, pp. 372-381.

Cole, L. K., Le, R., I, Nunes, F., Laufer, E., Lewis, J., & Wu, D. K. 2000, "Sensory organ generation in the chicken inner ear: contributions of bone morphogenetic protein 4, serrate1, and lunatic fringe", *J Comp Neurol.*, vol. 424, no. 3, pp. 509-520.

Collin, R. W., Chellappa, R., Pauw, R. J., Vriend, G., Oostrik, J., van, D. W., Huygen, P. L., Admiraal, R., Hoefsloot, L. H., Cremers, F. P., Xiang, M., Cremers, C. W., & Kremer, H. 2008, "Missense mutations in POU4F3 cause autosomal dominant hearing impairment DFNA15 and affect subcellular localization and DNA binding", *Hum.Mutat.*, vol. 29, no. 4, pp. 545-554.

Cotanche, D. A. 2008, "Genetic and pharmacological intervention for treatment/prevention of hearing loss", *J Commun.Disord.*, vol. 41, no. 5, pp. 421-443.

Cristobal, R., Wackym, P. A., Cioffi, J. A., Erbe, C. B., & Popper, P. 2004, "Selective acquisition of individual cell types in the vestibular periphery for molecular biology studies", *Otolaryngology - Head and Neck Surgery*, vol. 131, no. 5, pp. 590-595.

Cristobal, R., Wackym, P. A., Cioffi, J. A., Erbe, C. B., Roche, J. P., & Popper, P. 2005, "Assessment of differential gene expression in vestibular epithelial cell types using microarray analysis", *Molecular Brain Research*, vol. 133, no. 1, pp. 19-36.

Crooks, G. E., Hon, G., Chandonia, J. M., & Brenner, S. E. 2004, "WebLogo: a sequence logo generator", *Genome Research*, vol. 14, no. 6, pp. 1188-1190.

Cureoglu, S., Schachern, P. A., Ferlito, A., Rinaldo, A., Tsuprun, V., & Paparella, M. M. 2009, "Otosclerosis: etiopathogenesis and histopathology", *American Journal of Otolaryngology*, vol. 27, no. 5, pp. 334-340.

Curwen, V., Eyras, E., Andrews, T. D., Clarke, L., Mongin, E., Searle, S. M. J., & Clamp, M. 2004, "The Ensembl Automatic Gene Annotation System", *Genome Research*, vol. 14, no. 5, pp. 942-950.

da Silva, S. L., Cox, J. J., Jonk, L. J. C., Kruijer, W., & Burbach, J. P. 1995, "Localization of transcripts of the related nuclear orphan receptors COUP-TF I and ARP-1 in the adult mouse brain", *Molecular Brain Research*, vol. 30, no. 1, pp. 131-136.

Dabdoub, A., Puligilla, C., Jones, J. M., Fritzsch, B., Cheah, K. S. E., Pevny, L. H., & Kelley, M. W. 2008, "Sox2 signaling in prosensory domain specification and subsequent hair cell differentiation in the developing cochlea", *Proceedings of the National Academy of Sciences*, vol. 105, no. 47, pp. 18396-18401.

Dallos, P. 1992, "The active cochlea", *J Neurosci.*, vol. 12, no. 12, pp. 4575-4585.

Daniel, E. 2007, "Noise and hearing loss: a review", *J.Sch Health*, vol. 77, no. 5, pp. 225-231.

Darrat, I., Ahmad, N., Seidman, K., & Seidman, M. D. 2007, "Auditory research involving antioxidants", *Curr.Opin.Otolaryngol.Head Neck Surg.*, vol. 15, no. 5, pp. 358-363.

Daudet, N., Ariza-McNaughton, L., & Lewis, J. 2007, "Notch signalling is needed to maintain, but not to initiate, the formation of prosensory patches in the chick inner ear", *Development*, vol. 134, no. 12, pp. 2369-2378.

Dawson, S. J., Liu, Y. Z., Rodel, B., Moroy, T., & Latchman, D. S. 1996, "The ability of POU family transcription factors to activate or repress gene expression is dependent on the spacing and context of their specific response elements", *Biochem.J*, vol. 314 (Pt 2), pp. 439-443.

de Heer, A. M., Huygen, P. L., Collin, R. W., Kremer, H., & Cremers, C. W. 2009, "Mild and variable audiometric and vestibular features in a third DFNA15 family with a novel mutation in POU4F3", *Ann.Otol.Rhinol.Laryngol.*, vol. 118, no. 4, pp. 313-320.

de Kok, Y. J., van der Maarel, S. M., Bitner-Glindzicz, M., Huber, I., Monaco, A. P., Malcolm, S., Pembrey, M. E., Ropers, H. H., & Cremers, F. P. 1995, "Association between X-linked mixed deafness and mutations in the POU domain gene POU3F4", *Science*, vol. 267, no. 5198, pp. 685-688.

De Preter, K., Vandesompele, J., Heimann, P., Kockx, M. M., Van Gele, M., Hoebeeck, J., De Smet, E., Demarche, M., Laureys, G., Van Roy, N., De Paepe, A., & Speleman, F. 2003, "Application of laser capture microdissection in genetic analysis of neuroblastoma and neuroblastoma precursor cells", *Cancer Letters*, vol. 197, no. 1-2, pp. 53-61.

Dean, C. & Pegington, J. 1996, "The Ear," in *The Head and Neck*, W.B. Saunders Company Ltd., London, pp. 27-35.

DeFranco, D. B., Ramakrishnan, C., & Tang, Y. 1998, "Molecular chaperones and subcellular trafficking of steroid receptors", *J.Steroid Biochem.Mol.Biol.*, vol. 65, no. 1-6, pp. 51-58.

Diez, H., Fischer, A., Winkler, A., Hu, C. J., Hatzopoulos, A. K., Breier, G., & Gessler, M. 2007, "Hypoxia-mediated activation of Dll4-Notch-Hey2 signaling in endothelial progenitor cells and adoption of arterial cell fate", *Exp.Cell Res.*, vol. 313, no. 1, pp. 1-9.

Edge, A. S. & Chen, Z. Y. 2008, "Hair cell regeneration", *Curr.Opin.Neurobiol.*, vol. 18, no. 4, pp. 377-382.

Eilers, M. & Eisenman, R. N. 2008, "Myc's broad reach", *Genes and Development*, vol. 22, no. 20, pp. 2755-2766.

Ensembl. M.musculus - Gene summary - Gene: Nr2f2 (ENSMUSG00000030551). http://www.ensembl.org/Mus_musculus/Gene/Summary?g=ENSMUSG00000030551 . 2008b. Ref Type: Internet Communication

Ensembl. Frequently asked questions. http://www.ensembl.org/Help/Results?_referer=;result=faq_152;result=glossary_85;result=faq_129;result=glossary_78;result=view_143;result=view_162;result=view_144;result=view_151;result=view_140 . 2009.
Ref Type: Internet Communication

Ensembl. BlastView. http://www.ensembl.org/Multi/blastview . 2008a.
Ref Type: Electronic Citation

Enzmann, V., Yolcu, E., Kaplan, H. J., & Ildstad, S. T. 2009, "Stem cells as tools in regenerative therapy for retinal degeneration", *Arch Ophthalmol.*, vol. 127, no. 4, pp. 563-571.

Erkman, L., McEvilly, R. J., Luo, L., Ryan, A. K., Hooshmand, F., O'Connell, S. M., Keithley, E. M., Rapaport, D. H., Ryan, A. F., & Rosenfeld, M. G. 1996, "Role of transcription factors a Brn-3.1 and Brn-3.2 in auditory and visual system development", *Nature*, vol. 381, no. 6583, pp. 603-606.

Eshraghi, A. A. & Van de Water, T. R. 2006, "Cochlear implantation trauma and noise-induced hearing loss: Apoptosis and therapeutic strategies", *Anat.Rec.A Discov.Mol Cell Evol.Biol.*, vol. 288, no. 4, pp. 473-481.

Fekete, D. M., Homburger, S. A., Waring, M. T., Riedl, A. E., & Garcia, L. F. 1997, "Involvement of programmed cell death in morphogenesis of the vertebrate inner ear", *Development*, vol. 124, no. 12, pp. 2451-2461.

Fekete, D. M., Muthukumar, S., & Karagogeos, D. 1998, "Hair cells and supporting cells share a common progenitor in the avian inner ear", *J Neurosci.*, vol. 18, no. 19, pp. 7811-7821.

Fekete, D. M. & Wu, D. K. 2002, "Revisiting cell fate specification in the inner ear", *Current Opinion in Neurobiology*, vol. 12, no. 1, pp. 35-42.

Fettiplace, R. & Ricci, A. J. 2006, "Mechanoelectrical Transduction in Auditory Hair Cells," in *Vertebrate Hair Cells*, R. A. Eatock, R. R. Fay, & A. N. Popper, eds., Springer, New York, pp. 154-203.

Finsterbusch, T., Steinfeldt, T., Doberstein, K., Rodner, C., & Mankertz, A. 2009, "Interaction of the replication proteins and the capsid protein of porcine circovirus type 1 and 2 with host proteins", *Virology*, vol. 386, no. 1, pp. 122-131.

Forge, A. & Richardson, G. 1993, "Freeze fracture analysis of apical membranes in cochlear cultures: differences between basal and apical-coil outer hair cells and effects of neomycin", *J Neurocytol.*, vol. 22, no. 10, pp. 854-867.

Fortnum, H. M., Summerfield, A. Q., Marshall, D. H., Davis, A. C., Bamford, J. M., Davis, A., Yoshinaga-Itano, C., & Hind, S. 2001, "Prevalence of permanent childhood hearing impairment in the United Kingdom and implications for universal neonatal hearing screening: questionnaire based ascertainment study Commentary: Universal newborn hearing screening: implications for coordinating and developing services for deaf and hearing impaired children", *BMJ*, vol. 323, no. 7312, p. 536.

Fortunel, N. O., Otu, H. H., Ng, H. H., Chen, J., Mu, X., Chevassut, T., Li, X., Joseph, M., Bailey, C., Hatzfeld, J. A., Hatzfeld, A., Usta, F., Vega, V. B., Long, P. M., Libermann, T. A., & Lim, B. 2003, "Comment on " 'Stemness': Transcriptional Profiling of Embryonic and Adult Stem Cells" and "A Stem Cell Molecular Signature" (I)", *Science*, vol. 302, no. 5644, p. 393b.

Fransen, E., Topsakal, V., Hendrickx, J. J., Van, L. L., Huyghe, J. R., Van, E. E., Lemkens, N., Hannula, S., Maki-Torkko, E., Jensen, M., Demeester, K., Tropitzsch, A., Bonaconsa, A.,

Mazzoli, M., Espeso, A., Verbruggen, K., Huyghe, J., Huygen, P. L., Kunst, S., Manninen, M., az-Lacava, A., Steffens, M., Wienker, T. F., Pyykko, I., Cremers, C. W., Kremer, H., Dhooge, I., Stephens, D., Orzan, E., Pfister, M., Bille, M., Parving, A., Sorri, M., Van de, H. P., & Van, C. G. 2008, "Occupational noise, smoking, and a high body mass index are risk factors for age-related hearing impairment and moderate alcohol consumption is protective: a European population-based multicenter study", *J Assoc.Res.Otolaryngol.*, vol. 9, no. 3, pp. 264-276.

Frech, K. & Werner, T. "Specific modelling of regulatory units in DNA sequences", in *Pacific Symposium on Biocomputing 1997*, R. B. Altman et al., eds., World Scientific, pp. 151-162.

Friedman, L. M., Dror, A. A., & Avraham, K. B. 2007, "Mouse models to study inner ear development and hereditary hearing loss", *Int J Dev.Biol.*, vol. 51, no. 6-7, pp. 609-631.

Friedman, L. M., Dror, A. A., Mor, E., Tenne, T., Toren, G., Satoh, T., Biesemeier, D. J., Shomron, N., Fekete, D. M., Hornstein, E., & Avraham, K. B. 2009a, "MicroRNAs are essential for development and function of inner ear hair cells in vertebrates", *Proc.Natl.Acad.Sci U.S.A*, vol. 106, no. 19, pp. 7915-7920.

Friedman, R. A., Van, L. L., Huentelman, M. J., Sheth, S. S., Van, E. E., Corneveaux, J. J., Tembe, W. D., Halperin, R. F., Thorburn, A. Q., Thys, S., Bonneux, S., Fransen, E., Huyghe, J., Pyykko, I., Cremers, C. W., Kremer, H., Dhooge, I., Stephens, D., Orzan, E., Pfister, M., Bille, M., Parving, A., Sorri, M., Van de Heyning, P. H., Makmura, L., Ohmen, J. D., Linthicum, F. H., Jr., Fayad, J. N., Pearson, J. V., Craig, D. W., Stephan, D. A., & Van, C. G. 2009b, "GRM7 variants confer susceptibility to age-related hearing impairment", *Hum.Mol Genet.*, vol. 18, no. 4, pp. 785-796.

Fritzsch, B., Barald, K. F., & Lomax, M. I. 1998, "Early Embryology of the Vertebrate Ear," in *Development of the Auditory System*, E. W. Rubel, A. N. Popper, & R. R. Fay, eds., Springer-Verlag, New York, pp. 80-145.

Frydman, M., Vreugde, S., Nageris, B. I., Weiss, S., Vahava, O., & Avraham, K. B. 2000, "Clinical characterization of genetic hearing loss caused by a mutation in the POU4F3 transcription factor", *Arch Otolaryngol.Head Neck Surg.*, vol. 126, no. 5, pp. 633-637.

Fujimoto, M., Iguchi-Ariga, S. M., & Ariga, H. 1998, "Characterization of an element positively regulating the transcription of MSSP gene-2 which encodes C-MYC binding proteins", *Gene*, vol. 214, no. 1-2, pp. 113-120.

Fujimoto, M., Matsumoto, K., Iguchi-Ariga, S. M., & Ariga, H. 2001, "Disruption of MSSP, c-myc single-strand binding protein, leads to embryonic lethality in some homozygous mice", *Genes Cells*, vol. 6, no. 12, pp. 1067-1075.

Fujimoto, M., Matsumoto, K. I., Iguchi-Ariga, S. M., & Ariga, H. 2000, "Structures and comparison of genomic and complementary DNAs of mouse MSSP, a c-Myc binding protein", *Int.J.Oncol.*, vol. 16, no. 2, pp. 245-251.

Gale, J. E., Marcotti, W., Kennedy, H. J., Kros, C. J., & Richardson, G. P. 2001, "FM1-43 dye behaves as a permeant blocker of the hair-cell mechanotransducer channel", *J Neurosci.*, vol. 21, no. 18, pp. 7013-7025.

Gale, J. E., Piazza, V., Ciubotaru, C. D., & Mammano, F. 2004, "A mechanism for sensing noise damage in the inner ear", *Curr.Biol.*, vol. 14, no. 6, pp. 526-529.

Gao, J., Maison, S. F., Wu, X., Hirose, K., Jones, S. M., Bayazitov, I., Tian, Y., Mittleman, G., Matthews, D. B., Zakharenko, S. S., Liberman, M. C., & Zuo, J. 2007, "Orphan Glutamate Receptor {delta}1 Subunit Required for High-Frequency Hearing", *Molecular and Cellular Biology*, vol. 27, no. 12, pp. 4500-4512.

Gates, G. A. & Mills, J. H. 2005, "Presbycusis", *Lancet*, vol. 366, no. 9491, pp. 1111-1120.

Gene Ontology Consortium, T. 2008, "The Gene Ontology project in 2008", *Nucleic Acids Res.*, vol. 36, no. Database issue, p. D440-D444.

Genomatix. Gene2Promoter.
http://www.genomatix.de/online_help/help_eldorado/Gene2Promoter_Intro.html . 2008.
Ref Type: Internet Communication

Gerrero, M. R., McEvilly, R. J., Turner, E., Lin, C. R., O'Connell, S., Jenne, K. J., Hobbs, M. V., & Rosenfeld, M. G. 1993, "Brn-3.0: a POU-domain protein expressed in the sensory, immune, and endocrine systems that functions on elements distinct from known octamer motifs", *Proc.Natl.Acad.Sci U.S.A*, vol. 90, no. 22, pp. 10841-10845.

Gish, W. WU BLAST 2.0. http://blast.wustl.edu . 2004.
Ref Type: Internet Communication

Gold, T. 1948, "Hearing. II. The Physical Basis of the Action of the Cochlea", *Proc.R.Soc.Lond.B.*, vol. 135, no. 881, pp. 492-498.

Gong, S., Zheng, C., Doughty, M. L., Losos, K., Didkovsky, N., Schambra, U. B., Nowak, N. J., Joyner, A., Leblanc, G., Hatten, M. E., & Heintz, N. 2003, "A gene expression atlas of the central nervous system based on bacterial artificial chromosomes", *Nature*, vol. 425, no. 6961, pp. 917-925.

Goodyear, R. J., Kros, C. J., & Richardson, G. P. 2006, "The Development of Hair Cells in the Inner Ear," in *Vertebrate Hair Cells*, R. A. Eatock, R. R. Fay, & A. N. Popper, eds., Springer, New York, pp. 20-94.

Gopinath, B., Rochtchina, E., Wang, J. J., Schneider, J., Leeder, S. R., & Mitchell, P. 2009, "Prevalence of age-related hearing loss in older adults: Blue Mountains Study", *Arch Intern.Med.*, vol. 169, no. 4, pp. 415-416.

Grillet, N., Xiong, W., Reynolds, A., Kazmierczak, P., Sato, T., Lillo, C., Dumont, R. A., Hintermann, E., Sczaniecka, A., Schwander, M., Williams, D., Kachar, B., Gillespie, P. G., & Müller, U. 2009, "Harmonin Mutations Cause Mechanotransduction Defects in Cochlear Hair Cells", *Neuron*, vol. 62, no. 3, pp. 375-387.

Gronemeyer, H., Gustafsson, J. A., & Laudet, V. 2004, "Principles for modulation of the nuclear receptor superfamily", *Nat Rev.Drug Discov.*, vol. 3, no. 11, pp. 950-964.

Groves, A. K. 2005, "The Induction of the Otic Placode," in *Development of the Inner Ear*, M. K. Kelley et al., eds., Springer, New York, pp. 10-42.

Gruber, C. A., Rhee, J. M., Gleiberman, A., & Turner, E. E. 1997, "POU domain factors of the Brn-3 class recognize functional DNA elements which are distinctive, symmetrical, and highly conserved in evolution", *Molecular and Cellular Biology*, vol. 17, no. 5, pp. 2391-2400.

Haigermoser, C., Fujimoto, M., Iguchi-Ariga, S. M., & Ariga, H. 1996, "Cloning and characterization of the genomic DNA of the human MSSP genes", *Nucleic Acids Res.*, vol. 24, no. 19, pp. 3846-3857.

Hall, T. A. BioEdit sequence alignment editor for Windows 95/98/NT/XP.
http://www.mbio.ncsu.edu/BioEdit/BioEdit.html . 27-6-2007.
Ref Type: Internet Communication

Hall, T. A. 1999, "BioEdit: a user-friendly biological sequence alignment editor and analysis program for Windows 95/98/NT", *Nucl.Acids.Symp.Ser.*, vol. 41, pp. 95-98.

He, D. Z., Zheng, J., Edge, R., & Dallos, P. 2000, "Isolation of cochlear inner hair cells", *Hear.Res.*, vol. 145, no. 1-2, pp. 156-160.

He, X., Treacy, M. N., Simmons, D. M., Ingraham, H. A., Swanson, L. W., & Rosenfeld, M. G. 1989, "Expression of a large family of POU-domain regulatory genes in mammalian brain development", *Nature*, vol. 340, no. 6228, pp. 35-41.

Heine, C. & Browning, C. J. 2002, "Communication and psychosocial consequences of sensory loss in older adults: overview and rehabilitation directions", *Disabil.Rehabil.*, vol. 24, no. 15, pp. 763-773.

Heintzman, N. D. & Ren, B. 2007, "The gateway to transcription: identifying, characterizing and understanding promoters in the eukaryotic genome", *Cell Mol Life Sci*, vol. 64, no. 4, pp. 386-400.

Hellman, L. M. & Fried, M. G. 2007, "Electrophoretic mobility shift assay (EMSA) for detecting protein-nucleic acid interactions", *Nat.Protoc.*, vol. 2, no. 8, pp. 1849-1861.

Henderson, D., Bielefeld, E. C., Harris, K. C., & Hu, B. H. 2006, "The role of oxidative stress in noise-induced hearing loss", *Ear Hear.*, vol. 27, no. 1, pp. 1-19.

Hertzano, R., Dror, A. A., Montcouquiol, M., Ahmed, Z. M., Ellsworth, B., Camper, S., Friedman, T. B., Kelley, M. W., & Avraham, K. B. 2007, "Lhx3, a LIM domain transcription factor, is regulated by Pou4f3 in the auditory but not in the vestibular system", *Eur.J.Neurosci.*, vol. 25, no. 4, pp. 999-1005.

Hertzano, R., Montcouquiol, M., Rashi-Elkeles, S., Elkon, R., Yucel, R., Frankel, W. N., Rechavi, G., Moroy, T., Friedman, T. B., Kelley, M. W., & Avraham, K. B. 2004, "Transcription profiling of inner ears from Pou4f3(ddl/ddl) identifies Gfi1 as a target of the Pou4f3 deafness gene", *Hum.Mol.Genet*, vol. 13, no. 18, pp. 2143-2153.

Holley, M. C. 2005, "Keynote review: The auditory system, hearing loss and potential targets for drug development", *Drug Discov.Today*, vol. 10, no. 19, pp. 1269-1282.

Holt, J. R. & Corey, D. P. 2000, "Two mechanisms for transducer adaptation in vertebrate hair cells", *Proc.Natl.Acad.Sci U.S.A*, vol. 97, no. 22, pp. 11730-11735.

Horton, R. M. 1993, "In Vitro Recombination and Mutagenesis of DNA," in *Methods in Molecular Biology*, vol. 15 PCR Protocols: Current Methods and Applications. B. A. White, ed., Humana Press Inc., Totowa, NJ, USA, pp. 251-261.

Housley, G. D., Marcotti, W., Navaratnam, D., & Yamoah, E. N. 2006, "Hair cells--beyond the transducer", *J Membr.Biol.*, vol. 209, no. 2-3, pp. 89-118.

Howarth, A. & Shone, G. R. 2006, "Ageing and the auditory system", *Postgrad.Med.J.*, vol. 82, no. 965, pp. 166-171.

Hsu, C. Y., Chang, N. C., Lee, M. W., Lee, K. H., Sun, D. S., Lai, C., & Chang, A. C. 2008, "LUZP deficiency affects neural tube closure during brain development", *Biochem.Biophys.Res.Commun.*, vol. 376, no. 3, pp. 466-471.

Hudspeth, A. J. 2000, "Hearing," in *Principles of Neural Science*, 4 edn, E. R. Kandel, J. H. Schwartz, & T. M. Jessell, eds., McGraw-Hill, New York, pp. 590-613.

Hultcrantz, M., Simonoska, R., & Stenberg, A. E. 2006, "Estrogen and hearing: a summary of recent investigations", *Acta Otolaryngol.*, vol. 126, no. 1, pp. 10-14.

Iida, M., Taira, T., Ariga, H., & Iguchi-Ariga, S. M. 1997, "Induction of apoptosis in HeLa cells by MSSP, c-myc binding proteins", *Biol.Pharm.Bull.*, vol. 20, no. 1, pp. 10-14.

Izumikawa, M., Minoda, R., Kawamoto, K., Abrashkin, K. A., Swiderski, D. L., Dolan, D. F., Brough, D. E., & Raphael, Y. 2005, "Auditory hair cell replacement and hearing improvement by Atoh1 gene therapy in deaf mammals", *Nat.Med.*, vol. 11, no. 3, pp. 271-276.

Jacobson, E. M., Li, P., Leon-del-Rio, A., Rosenfeld, M. G., & Aggarwal, A. K. 1997, "Structure of Pit-1 POU domain bound to DNA as a dimer: unexpected arrangement and flexibility", *Genes and Development*, vol. 11, no. 2, pp. 198-212.

Jenny, A. & Mlodzik, M. 2006, "Planar cell polarity signaling: a common mechanism for cellular polarization", *Mt.Sinai J.Med.*, vol. 73, no. 5, pp. 738-750.

Jensen-Smith, H. & Hallworth, R. 2007, "Lateral wall protein content mediates alterations in cochlear outer hair cell mechanics before and after hearing onset", *Cell Motil.Cytoskeleton*, vol. 64, no. 9, pp. 705-717.

Jones, C. & Chen, P. 2007, "Planar cell polarity signaling in vertebrates", *Bioessays*, vol. 29, no. 2, pp. 120-132.

Jonk, L. J., de Jonge, M. E., Pals, C. E., Wissink, S., Vervaart, J. M., Schoorlemmer, J., & Kruijer, W. 1994, "Cloning and expression during development of three murine members of the COUP family of nuclear orphan receptors", *Mech.Dev.*, vol. 47, no. 1, pp. 81-97.

Kanaoka, Y. & Nojima, H. 1994, "SCR: novel human suppressors of cdc2/cdc13 mutants of Schizosaccharomyces pombe harbour motifs for RNA binding proteins", *Nucleic Acids Res.*, vol. 22, no. 13, pp. 2687-2693.

Karginova, E. A., Pentz, E. S., Kazakova, I. G., Norwood, V. F., Carey, R. M., & Gomez, R. A. 1997, "Zis: a developmentally regulated gene expressed in juxtaglomerular cells", *Am.J.Physiol*, vol. 273, no. 5 Pt 2, p. F731-F738.

Karis, A., Pata, I., van Doorninck, J. H., Grosveld, F., de Zeeuw, C. I., de, C. D., & Fritzsch, B. 2001, "Transcription factor GATA-3 alters pathway selection of olivocochlear neurons and affects morphogenesis of the ear", *J Comp Neurol.*, vol. 429, no. 4, pp. 615-630.

Katayama, S., Ashizawa, K., Gohma, H., Fukuhara, T., Narumi, K., Tsuzuki, Y., Tatemoto, H., Nakada, T., & Nagai, K. 2006, "The expression of Hedgehog genes (Ihh, Dhh) and Hedgehog target genes (Ptc1, Gli1, Coup-TfII) is affected by estrogenic stimuli in the uterus of immature female rats", *Toxicol.Appl.Pharmacol.*, vol. 217, no. 3, pp. 375-383.

Kazmierczak, P., Sakaguchi, H., Tokita, J., Wilson-Kubalek, E. M., Milligan, R. A., Muller, U., & Kachar, B. 2007, "Cadherin 23 and protocadherin 15 interact to form tip-link filaments in sensory hair cells", *Nature*, vol. 449, no. 7158, pp. 87-91.

Keithley, E. M., Erkman, L., Bennett, T., Lou, L., & Ryan, A. F. 1999, "Effects of a hair cell transcription factor, Brn-3.1, gene deletion on homozygous and heterozygous mouse cochleas in adulthood and aging", *Hear.Res.*, vol. 134, no. 1-2, pp. 71-76.

Kelley, M. W. 2006, "Regulation of cell fate in the sensory epithelia of the inner ear", *Nat Rev Neurosci.*, vol. 7, no. 11, pp. 837-849.

Kelley, M. W. 2007, "Cellular commitment and differentiation in the organ of Corti", *Int.J.Dev.Biol*, vol. 51, no. 6-7, pp. 571-583.

Kelley, M. W. & Wu, D. K. 2005, "Developmental Neurobiology of the Ear: Current Status and Future Directions," in *Development of the Inner Ear*, M. K. Kelley et al., eds., Springer, New York, pp. 1-9.

Kelly, M. & Chen, P. 2007, "Shaping the mammalian auditory sensory organ by the planar cell polarity pathway", *Int J Dev.Biol.*, vol. 51, no. 6-7, pp. 535-547.

Kemp, D. T. 1978, "Stimulated acoustic emissions from within the human auditory system", *J Acoust.Soc.Am.*, vol. 64, no. 5, pp. 1386-1391.

Kesser, B. W., Hashisaki, G. T., & Holt, J. R. 2008, "Gene transfer in human vestibular epithelia and the prospects for inner ear gene therapy", *Laryngoscope*, vol. 118, no. 5, pp. 821-831.

Kharkovets, T., Dedek, K., Maier, H., Schweizer, M., Khimich, D., Nouvian, R., Vardanyan, V., Leuwer, R., Moser, T., & Jentsch, T. J. 2006, "Mice with altered KCNQ4 K+ channels implicate sensory outer hair cells in human progressive deafness", *EMBO J*, vol. 25, no. 3, pp. 642-652.

Kiernan, A. E., Cordes, R., Kopan, R., Gossler, A., & Gridley, T. 2005a, "The Notch ligands DLL1 and JAG2 act synergistically to regulate hair cell development in the mammalian inner ear", *Development*, vol. 132, no. 19, pp. 4353-4362.

Kiernan, A. E., Pelling, A. L., Leung, K. K., Tang, A. S., Bell, D. M., Tease, C., Lovell-Badge, R., Steel, K. P., & Cheah, K. S. 2005b, "Sox2 is required for sensory organ development in the mammalian inner ear", *Nature*, vol. 434, no. 7036, pp. 1031-1035.

Kimura, K., Saga, H., Hayashi, K., Obata, H., Chimori, Y., Ariga, H., & Sobue, K. 1998, "c-Myc gene single-strand binding protein-1, MSSP-1, suppresses transcription of alpha-smooth muscle actin gene in chicken visceral smooth muscle cells", *Nucleic Acids Res.*, vol. 26, no. 10, pp. 2420-2425.

Kimura, Y., Suzuki, T., Kaneko, C., Darnel, A. D., Moriya, T., Suzuki, S., Handa, M., Ebina, M., Nukiwa, T., & Sasano, H. 2002, "Retinoid receptors in the developing human lung", *Clin.Sci.(Lond)*, vol. 103, no. 6, pp. 613-621.

Kingsley, R. E. 1999b, "The Auditory System," in *Concise Text of Neuroscience*, 2 edn, Lippincott Williams & Wilkins, Baltimore, pp. 393-432.

Kingsley, R. E. 1999a, "The Cranial Nerves," in *Concise Text of Neuroscience*, 2 edn, Lippincott Williams & Wilkins, Baltimore, pp. 337-392.

Kingston, R. E., Chen, C. A., & Okayama, H. 2001, "Calcium phosphate transfection", *Curr.Protoc.Immunol.*, vol. Chapter 10, p. Unit 10.13.

Kishimoto, M., Fujiki, R., Takezawa, S., Sasaki, Y., Nakamura, T., Yamaoka, K., Kitagawa, H., & Kato, S. 2006, "Nuclear receptor mediated gene regulation through chromatin remodeling and histone modifications", *Endocr.J.*, vol. 53, no. 2, pp. 157-172.

Klein, M., Koedel, U., Kastenbauer, S., & Pfister, H. W. 2008, "Nitrogen and oxygen molecules in meningitis-associated labyrinthitis and hearing impairment", *Infection*, vol. 36, no. 1, pp. 2-14.

Klemm, J. D., Rould, M. A., Aurora, R., Herr, W., & Pabo, C. O. 1994, "Crystal structure of the Oct-1 POU domain bound to an octamer site: DNA recognition with tethered DNA-binding modules", *Cell*, vol. 77, no. 1, pp. 21-32.

Krishnamurthy, S. & Hampsey, M. 2009, "Eukaryotic transcription initiation", *Curr.Biol.*, vol. 19, no. 4, p. R153-R156.

Krishnan, V., Elberg, G., Tsai, M. J., & Tsai, S. Y. 1997, "Identification of a Novel Sonic Hedgehog Response Element in the Chicken Ovalbumin Upstream Promoter-Transcription Factor II Promoter", *Molecular Endocrinology*, vol. 11, no. 10, pp. 1458-1466.

Kros, C. J. 1996, "Hair Cell Physiology," in *The Cochlea*, P. Dallos, A. N. Popper, & R. R. Fay, eds., Springer-Verlag, New York, pp. 318-385.

Kruse, S. W., Suino-Powell, K., Zhou, X. E., Kretschman, J. E., Reynolds, R., Vonrhein, C., Xu, Y., Wang, L., Tsai, S. Y., Tsai, M. J., & Xu, H. E. 2008, "Identification of COUP-TFII orphan nuclear receptor as a retinoic acid-activated receptor", *PLoS.Biol.*, vol. 6, no. 9, p. e227.

Kulkarni, K. & Hartley, D. E. 2008, "Recent advances in hearing restoration", *J R.Soc.Med.*, vol. 101, no. 3, pp. 116-124.

Kurihara, I., Lee, D. K., Petit, F. G., Jeong, J., Lee, K., Lydon, J. P., DeMayo, F. J., Tsai, M. J., & Tsai, S. Y. 2007, "COUP-TFII mediates progesterone regulation of uterine implantation by controlling ER activity", *PLoS.Genet.*, vol. 3, no. 6, p. e102.

Kurokawa, H. & Goode, R. L. 1995, "Sound pressure gain produced by the human middle ear", *Otolaryngol Head Neck Surg*, vol. 113, no. 4, pp. 349-355.

Ladias, J. A. & Karathanasis, S. K. 1991, "Regulation of the apolipoprotein AI gene by ARP-1, a novel member of the steroid receptor superfamily", *Science*, vol. 251, no. 4993, pp. 561-565.

Laine, H., Doetzlhofer, A., Mantela, J., Ylikoski, J., Laiho, M., Roussel, M. F., Segil, N., & Pirvola, U. 2007, "p19Ink4d and p21Cip1 Collaborate to Maintain the Postmitotic State of Auditory Hair Cells, Their Codeletion Leading to DNA Damage and p53-Mediated Apoptosis", *Journal of Neuroscience*, vol. 27, no. 6, pp. 1434-1444.

Ledakis, P., Tanimura, H., & Fojo, T. 1998, "Limitations of differential display", *Biochem.Biophys.Res.Commun.*, vol. 251, no. 2, pp. 653-656.

Lee, C. T., Li, L., Takamoto, N., Martin, J. F., DeMayo, F. J., Tsai, M. J., & Tsai, S. Y. 2004, "The nuclear orphan receptor COUP-TFII is required for limb and skeletal muscle development", *Mol Cell Biol.*, vol. 24, no. 24, pp. 10835-10843.

Lee, M. W., Chang, A. C., Sun, D. S., Hsu, C. Y., & Chang, N. C. 2001, "Restricted expression of LUZP in neural lineage cells: a study in embryonic stem cells", *J.Biomed.Sci.*, vol. 8, no. 6, pp. 504-511.

Lelli, A., Asai, Y., Forge, A., Holt, J. R., & Geleoc, G. S. G. 2009, "Tonotopic Gradient in the Developmental Acquisition of Sensory Transduction in Outer Hair Cells of the Mouse Cochlea", *Journal of Neurophysiology*, vol. 101, no. 6, pp. 2961-2973.

Lenoir, M. Organ of Corti. http://www.cochlea.org . 1999.
Ref Type: Internet Communication

Leon, Y., Sanchez-Galiano, S., & Gorospe, I. 2004, "Programmed cell death in the development of the vertebrate inner ear", *Apoptosis.*, vol. 9, no. 3, pp. 255-264.

Lewis, M. A., Quint, E., Glazier, A. M., Fuchs, H., De Angelis, M. H., Langford, C., van, D. S., breu-Goodger, C., Piipari, M., Redshaw, N., Dalmay, T., Moreno-Pelayo, M. A., Enright, A. J., & Steel, K. P. 2009, "An ENU-induced mutation of miR-96 associated with progressive hearing loss in mice", *Nat.Genet.*, vol. 41, no. 5, pp. 614-618.

Li, J., Chen, X. H., Xiao, P. J., Li, L., Lin, W. M., Huang, J., & Xu, P. 2008, "Expression pattern and splicing function of mouse ZNF265", *Neurochem.Res.*, vol. 33, no. 3, pp. 483-489.

Li, P., He, X., Gerrero, M. R., Mok, M., Aggarwal, A., & Rosenfeld, M. G. 1993, "Spacing and orientation of bipartite DNA-binding motifs as potential functional determinants for POU domain factors", *Genes and Development*, vol. 7, no. 12b, pp. 2483-2496.

Li, R., Xi, Y., Liu, X., Chen, G., Wang, B., Jiang, L., & Li, W. 2009, "Expression of IL-1alpha, IL-6, TGF-beta, FasL and ZNF265 during sertoli cell infection by ureaplasma urealyticum", *Cell Mol Immunol.*, vol. 6, no. 3, pp. 215-221.

Liang, Y., Wang, A., Probst, F. J., Arhya, I. N., Barber, T. D., Chen, K. S., Deshmukh, D., Dolan, D. F., Hinnant, J. T., Carter, L. E., Jain, P. K., Lalwani, A. K., Li, X. C., Lupski, J. R., Moeljopawiro, S., Morell, R., Negrini, C., Wilcox, E. R., Winata, S., Camper, S. A., & Friedman, T. B. 1998, "Genetic Mapping Refines DFNB3 to 17p11.2, Suggests Multiple Alleles of DFNB3, and Supports Homology to the Mouse Model shaker-2", *The American Journal of Human Genetics*, vol. 62, no. 4, pp. 904-915.

Lillycrop, K. A., Budrahan, V. S., Lakin, N. D., Terrenghi, G., Wood, J. N., Polak, J. M., & Latchman, D. S. 1992, "A novel POU family transcription factor is closely related to Brn-3 but has a distinct expression pattern in neuronal cells", *Nucleic Acids Res.*, vol. 20, no. 19, pp. 5093-5096.

Lim, D. J. & Anniko, M. 1985, "Developmental morphology of the mouse inner ear. A scanning electron microscopic observation", *Acta Otolaryngol.Suppl*, vol. 422, pp. 1-69.

Ling, M. M. & Robinson, B. H. 1997, "Approaches to DNA Mutagenesis: An Overview", *Analytical Biochemistry*, vol. 254, no. 2, pp. 157-178.

Liu, W., Khare, S. L., Liang, X., Peters, M. A., Liu, X., Cepko, C. L., & Xiang, M. 2000, "All Brn3 genes can promote retinal ganglion cell differentiation in the chick", *Development*, vol. 127, no. 15, pp. 3237-3247.

Liu, W., Mo, Z., & Xiang, M. 2001, "The Ath5 proneural genes function upstream of Brn3 POU domain transcription factor genes to promote retinal ganglion cell development", *Proc.Natl.Acad.Sci U.S.A*, vol. 98, no. 4, pp. 1649-1654.

Liu, X. Z., Ouyang, X. M., Xia, X. J., Zheng, J., Pandya, A., Li, F., Du, L. L., Welch, K. O., Petit, C., Smith, R. J. H., Webb, B. T., Yan, D., Arnos, K. S., Corey, D., Dallos, P., Nance, W. E., & Chen, Z. Y. 2003, "Prestin, a cochlear motor protein, is defective in non-syndromic hearing loss", *Human Molecular Genetics*, vol. 12, no. 10, pp. 1155-1162.

Liu, Z. & Zuo, J. 2008, "Cell cycle regulation in hair cell development and regeneration in the mouse cochlea", *Cell Cycle*, vol. 7, no. 14, pp. 2129-2133.

Loots, G. G. & Ovcharenko, I. 2004, "rVISTA 2.0: evolutionary analysis of transcription factor binding sites", *Nucleic Acids Res.*, vol. 32, no. Web Server issue, p. W217-W221.

Loughlin, F. E., Mansfield, R. E., Vaz, P. M., McGrath, A. P., Setiyaputra, S., Gamsjaeger, R., Chen, E. S., Morris, B. J., Guss, J. M., & Mackay, J. P. 2009, "The zinc fingers of the SR-like protein ZRANB2 are single-stranded RNA-binding domains that recognize 5' splice site-like sequences", *Proc.Natl.Acad.Sci U.S.A*, vol. 106, no. 14, pp. 5581-5586.

Lowenheim, H., Furness, D. N., Kil, J., Zinn, C., Gultig, K., Fero, M. L., Frost, D., Gummer, A. W., Roberts, J. M., Rubel, E. W., Hackney, C. M., & Zenner, H. P. 1999, "Gene disruption of p27(Kip1) allows cell proliferation in the postnatal and adult organ of corti", *Proc.Natl.Acad.Sci U.S.A*, vol. 96, no. 7, pp. 4084-4088.

Ludman, H. & Kemp, D. T. 1998, "Basic Acoustics and Hearing Tests," in *Diseases of the Ear*, 6 edn, H. Ludman & T. Wright, eds., Arnold, London, pp. 58-86.

Lutz, B., Kuratani, S., Cooney, A. J., Wawersik, S., Tsai, S. Y., Eichele, G., & Tsai, M. J. 1994, "Developmental regulation of the orphan receptor COUP-TF II gene in spinal motor neurons", *Development*, vol. 120, no. 1, pp. 25-36.

Mangs, A. H. & Morris, B. J. 2008, "ZRANB2: structural and functional insights into a novel splicing protein", *Int.J.Biochem.Cell Biol.*, vol. 40, no. 11, pp. 2353-2357.

Mangs, A. H., Speirs, H. J., Goy, C., Adams, D. J., Markus, M. A., & Morris, B. J. 2006, "XE7: a novel splicing factor that interacts with ASF/SF2 and ZNF265", *Nucleic Acids Res.*, vol. 34, no. 17, pp. 4976-4986.

Mansour, S. L. & Schoenwolf, G. C. 2005, "Morphogenesis of the Inner Ear," in *Development of the Inner Ear*, M. K. Kelley et al., eds., Springer, New York, pp. 43-84.

Mantela, J., Jiang, Z., Ylikoski, J., Fritzsch, B., Zacksenhaus, E., & Pirvola, U. 2005, "The retinoblastoma gene pathway regulates the postmitotic state of hair cells of the mouse inner ear", *Development*, vol. 132, no. 10, pp. 2377-2388.

Marcotti, W. & Kros, C. J. 1999, "Developmental expression of the potassium current IK,n contributes to maturation of mouse outer hair cells", *J Physiol*, vol. 520 Pt 3, pp. 653-660.

Matsui, J. I. & Cotanche, D. A. 2004a, "Sensory hair cell death and regeneration: two halves of the same equation", *Curr.Opin.Otolaryngol.Head Neck Surg.*, vol. 12, no. 5, pp. 418-425.

Matsui, J. I., Gale, J. E., & Warchol, M. E. 2004b, "Critical signaling events during the aminoglycoside-induced death of sensory hair cells in vitro", *J Neurobiol.*, vol. 61, no. 2, pp. 250-266.

Matsui, J. I., Parker, M. A., Ryals, B. M., & Cotanche, D. A. 2005, "Regeneration and replacement in the vertebrate inner ear", *Drug Discovery Today*, vol. 10, no. 19, pp. 1307-1312.

McCaffery, P., Wagner, E., O'Neil, J., Petkovich, M., & Drager, U. C. 1999, "Dorsal and ventral retinal territories defined by retinoic acid synthesis, break-down and nuclear receptor expression", *Mech.Dev.*, vol. 82, no. 1-2, pp. 119-130.

McGhee, J. D. & Krause, M. W. 1997, "Transcription Factors and Transcriptional Regulation," in *C.Elegans II Online Edition*, 2nd edn, D. L. Riddle et al., eds., COLD SPRING HARBOR LABORATORY PRESS, New York.

Mencia, A., Modamio-Hoybjor, S., Redshaw, N., Morin, M., Mayo-Merino, F., Olavarrieta, L., Aguirre, L. A., del, C., I, Steel, K. P., Dalmay, T., Moreno, F., & Moreno-Pelayo, M. A. 2009, "Mutations in the seed region of human miR-96 are responsible for nonsyndromic progressive hearing loss", *Nat.Genet.*, vol. 41, no. 5, pp. 609-613.

Meyer, A. C., Frank, T., Khimich, D., Hoch, G., Riedel, D., Chapochnikov, N. M., Yarin, Y. M., Harke, B., Hell, S. W., Egner, A., & Moser, T. 2009, "Tuning of synapse number, structure and function in the cochlea", *Nat.Neurosci.*, vol. 12, no. 4, pp. 444-453.

Middlebrooks, J. C. & Green, D. M. 1991, "Sound localization by human listeners", *Annu.Rev Psychol.*, vol. 42, pp. 135-159.

Milton, N. G., Bessis, A., Changeux, J. P., & Latchman, D. S. 1996, "Differential regulation of neuronal nicotinic acetylcholine receptor subunit gene promoters by Brn-3 POU family transcription factors", *Biochem.J*, vol. 317 (Pt 2), pp. 419-423.

Mockler, T. C., Chan, S., Sundaresan, A., Chen, H., Jacobsen, S. E., & Ecker, J. R. 2005, "Applications of DNA tiling arrays for whole-genome analysis", *Genomics*, vol. 85, no. 1, pp. 1-15.

Moeller, M. P. 2007, "Current state of knowledge: psychosocial development in children with hearing impairment", *Ear Hear.*, vol. 28, no. 6, pp. 729-739.

Moore, K. L. & Dalley, A. F. 1999, "Head," in *Clinically Oriented Anatomy*, 4 edn, P. J. Kelly, ed., Lippincott Williams & Wilkins, Baltimore, pp. 831-993.

More, E., Fellner, T., Doppelmayr, H., Hauser-Kronberger, C., Dandachi, N., Obrist, P., Sandhofer, F., & Paulweber, B. 2003, "Activation of the MAP kinase pathway induces chicken ovalbumin upstream promoter-transcription factor II (COUP-TFII) expression in human breast cancer cell lines", *J Endocrinol*, vol. 176, no. 1, pp. 83-94.

Morris, B. J., Adams, D. J., & van der, W. L. 2001, "Renin gene expression: the switch and the fingers", *Clin.Exp.Pharmacol.Physiol*, vol. 28, no. 12, pp. 1044-1047.

Morris, P. J., Lakin, N. D., Dawson, S. J., Ryabinin, A. E., Kilimann, M. W., Wilson, M. C., & Latchman, D. S. 1996, "Differential regulation of genes encoding synaptic proteins by members of the Brn-3 subfamily of POU transcription factors", *Brain Res.Mol Brain Res.*, vol. 43, no. 1-2, pp. 279-285.

MRC Hearing & Communication Group. NHS Newborn Hearing Screening Programme. http://hearing.screening.nhs.uk/ . 2008.
Ref Type: Internet Communication

Munir, S., Singh, S., Kaur, K., & Kapur, V. 2004, "Suppression subtractive hybridization coupled with microarray analysis to examine differential expression of genes in virus infected cells", *Biol.Proced.Online.*, vol. 6, pp. 94-104.

Murakami, D. M., Erkman, L., Hermanson, O., Rosenfeld, M. G., & Fuller, C. A. 2002, "Evidence for vestibular regulation of autonomic functions in a mouse genetic model", *Proc.Natl.Acad.Sci U.S.A*, vol. 99, no. 26, pp. 17078-17082.

Murayama, C., Miyazaki, H., Miyamoto, A., & Shimizu, T. 2008, "Involvement of Ad4BP/SF-1, DAX-1, and COUP-TFII transcription factor on steroid production and luteinization in ovarian theca cells", *Mol Cell Biochem.*, vol. 314, no. 1-2, pp. 51-58.

Naka, H., Nakamura, S., Shimazaki, T., & Okano, H. 2008, "Requirement for COUP-TFI and II in the temporal specification of neural stem cells in CNS development", *Nat Neurosci.*

Nakano, M., Yoshiura, K. i., Oikawa, M., Miyoshi, O., Yamada, K., Kondo, S., Miwa, N., Soeda, E., Jinno, Y., Fujii, T., & Niikawa, N. 1998, "Identification, characterization and mapping of the human ZIS (zinc-finger, splicing) gene", *Gene*, vol. 225, no. 1-2, pp. 59-65.

Nayak, G. D., Ratnayaka, H. S., Goodyear, R. J., & Richardson, G. P. 2007, "Development of the hair bundle and mechanotransduction", *Int J Dev.Biol.*, vol. 51, no. 6-7, pp. 597-608.

Negishi, Y., Nishita, Y., Saegusa, Y., Kakizaki, I., Galli, I., Kihara, F., Tamai, K., Miyajima, N., Iguchi-Ariga, S. M., & Ariga, H. 1994, "Identification and cDNA cloning of single-stranded DNA binding proteins that interact with the region upstream of the human c-myc gene", *Oncogene*, vol. 9, no. 4, pp. 1133-1143.

Niki, T., Galli, I., Ariga, H., & Iguchi-Ariga, S. M. 2000a, "MSSP, a protein binding to an origin of replication in the c-myc gene, interacts with a catalytic subunit of DNA polymerase alpha and stimulates its polymerase activity", *FEBS Lett.*, vol. 475, no. 3, pp. 209-212.

Niki, T., Izumi, S., Saegusa, Y., Taira, T., Takai, T., Iguchi-Ariga, S. M., & Ariga, H. 2000b, "MSSP promotes ras/myc cooperative cell transforming activity by binding to c-Myc", *Genes Cells*, vol. 5, no. 2, pp. 127-141.

Ninkina, N. N., Stevens, G. E. M., Wood, J. N., & Richardson, W. D. 1993, "A novel Brn3-like POU transcription factor expressed in subsets of rat sensory and spinal cord neurons", *Nucleic Acids Research*, vol. 21, no. 14, pp. 3175-3182.

Nishida, Y., Rivolta, M. N., & Holley, M. C. 1998, "Timed markers for the differentiation of the cuticular plate and stereocilia in hair cells from the mouse inner ear", *J Comp Neurol.*, vol. 395, no. 1, pp. 18-28.

Nishikori, T., Hatta, T., Kawauchi, H., & Otani, H. 1999, "Apoptosis during inner ear development in human and mouse embryos: an analysis by computer-assisted three-dimensional reconstruction", *Anat.Embryol.(Berl)*, vol. 200, no. 1, pp. 19-26.

Nolan, L. S., Jagutpal, S. S., Cadge, B. A., Woo, P., & Dawson, S. J. 2007, "Identification and functional analysis of common sequence variants in the DFNA15 gene, Brn-3c", *Gene*, vol. 400, no. 1-2, pp. 89-97.

Nomura, J., Matsumoto, K., Iguchi-Ariga, S. M., & Ariga, H. 2005, "Positive regulation of Fas gene expression by MSSP and abrogation of Fas-mediated apoptosis induction in MSSP-deficient mice", *Exp.Cell Res.*, vol. 305, no. 2, pp. 324-332.

Noy, N. 2007, "Ligand specificity of nuclear hormone receptors: sifting through promiscuity", *Biochemistry*, vol. 46, no. 47, pp. 13461-13467.

Nuclear Receptors Nomenclature Committee. 1999, "A unified nomenclature system for the nuclear receptor superfamily", *Cell*, vol. 97, no. 2, pp. 161-163.

Ohlemiller, K. K. 2004, "Age-related hearing loss: the status of Schuknecht's typology", *Curr.Opin.Otolaryngol Head Neck Surg*, vol. 12, no. 5, pp. 439-443.

Olusanya, B. O. & Newton, V. E. 2007, "Global burden of childhood hearing impairment and disease control priorities for developing countries", *Lancet*, vol. 369, no. 9569, pp. 1314-1317.

Omahoney, C. F. & Davies, R. A. 1998, "Vestibular Investigations," in *Diseases of the Ear*, 6 edn, H. Ludman & T. Wright, eds., Arnold, London, pp. 87-104.

OMIM. OMIM Home. www.ncbi.nlm.nih.gov/sites/entrez?db=omim . 2009.
Ref Type: Internet Communication

Panin, V. M., Shao, L., Lei, L., Moloney, D. J., Irvine, K. D., & Haltiwanger, R. S. 2002, "Notch ligands are substrates for protein O-fucosyltransferase-1 and Fringe", *J Biol.Chem.*, vol. 277, no. 33, pp. 29945-29952.

Park, J. I., Tsai, S. Y., & Tsai, M. J. 2003, "Molecular mechanism of chicken ovalbumin upstream promoter-transcription factor (COUP-TF) actions", *Keio J.Med.*, vol. 52, no. 3, pp. 174-181.

Patuzzi, R. 1996, "Cochlear Micromechanics and Macromechanics," in *The Cochlea*, P. Dallos, A. N. Popper, & R. R. Fay, eds., Springer-Verlag, New York, pp. 186-257.

Pauw, R. J., van Drunen, F. J., Collin, R. W., Huygen, P. L., Kremer, H., & Cremers, C. W. 2008, "Audiometric characteristics of a Dutch family linked to DFNA15 with a novel mutation (p.L289F) in POU4F3", *Arch.Otolaryngol.Head Neck Surg.*, vol. 134, no. 3, pp. 294-300.

Pereira, F. A., Qiu, Y., Tsai, M. J., & Tsai, S. Y. 1995, "Chicken ovalbumin upstream promoter transcription factor (COUP-TF): expression during mouse embryogenesis", *J.Steroid Biochem.Mol Biol.*, vol. 53, no. 1-6, pp. 503-508.

Pereira, F. A., Qiu, Y., Zhou, G., Tsai, M. J., & Tsai, S. Y. 1999, "The orphan nuclear receptor COUP-TFII is required for angiogenesis and heart development", *Genes and Development*, vol. 13, no. 8, pp. 1037-1049.

Pereira, F. A., Tsai, M. J., & Tsai, S. Y. 2000, "COUP-TF orphan nuclear receptors in development and differentiation", *Cell Mol Life Sci.*, vol. 57, no. 10, pp. 1388-1398.

Petit, C., Levilliers, J., & Hardelin, J. P. 2001, "Molecular genetics of hearing loss", *Annu.Rev Genet.*, vol. 35, pp. 589-646.

Petit, F. G., Salas, R., Tsai, M. J., & Tsai, S. Y. 2004, "The regulation of COUP-TFII gene expression by Ets-1 is enhanced by the steroid receptor co-activators", *Mech.Ageing Dev.*, vol. 125, no. 10-11, pp. 719-732.

Pfister, M. & Lalwani, A. K. 2007, "Gene Therapy of the Inner Ear," in *Genes, Hearing and Deafness*, A. Martini, D. Stephens, & A. P. Read, eds., Informa UK Ltd., London, pp. 299-304.

Phelps, P. D. 1998, "Diagnostic Imaging of the Ear (Normal and Congenital)," in *Diseases of the Ear*, 6 edn, H. Ludman & T. Wright, eds., Arnold, London, pp. 105-124.

Pickles, J. O. 1988, "The Outer and Middle Ears," in *An Introduction to the Physiology of Hearing*, 2 edn, Academic Press Limited, London, pp. 12-25.

Plambeck, C. A., Kwan, A. H., Adams, D. J., Westman, B. J., van der, W. L., Medcalf, R. L., Morris, B. J., & Mackay, J. P. 2003, "The structure of the zinc finger domain from human splicing factor ZNF265 fold", *Journal of Biological Chemistry*, vol. 278, no. 25, pp. 22805-22811.

Prosser, S. & Martini, A. 2007, "Understanding the Phenotype: Basic Concepts in Audiology," in *Genes, Hearing and Deafness*, A. Martini, D. Stephens, & A. P. Read, eds., Informa UK Ltd., London, pp. 19-38.

Pujades, C., Kamaid, A., Alsina, B., & Giraldez, F. 2006, "BMP-signaling regulates the generation of hair-cells", *Dev.Biol.*, vol. 292, no. 1, pp. 55-67.

Qiu, Y., Cooney, A. J., Kuratani, S., DeMayo, F. J., Tsai, S. Y., & Tsai, M. J. 1994a, "Spatiotemporal expression patterns of chicken ovalbumin upstream promoter-transcription factors in the developing mouse central nervous system: evidence for a role in segmental patterning of the diencephalon", *Proc.Natl.Acad.Sci.U.S.A*, vol. 91, no. 10, pp. 4451-4455.

Qiu, Y., Krishnan, V., Pereira, F. A., Tsai, S. Y., & Tsai, M.-J. 1996, "Chicken ovalbumin upstream promoter-transcription factors and their regulation", *The Journal of Steroid Biochemistry and Molecular Biology*, vol. 56, no. 1-6, pp. 81-85.

Qiu, Y., Tsai, S. Y., & Tsai, M. J. 1994b, "COUP-TF an orphan member of the steroid/thyroid hormone receptor superfamily", *Trends in Endocrinology and Metabolism*, vol. 5, no. 6, pp. 234-239.

Quandt, K., Frech, K., Karas, H., Wingender, E., & Werner, T. 1995, "MatInd and MatInspector: new fast and versatile tools for detection of consensus matches in nucleotide sequence data", *Nucleic Acids Res.*, vol. 23, no. 23, pp. 4878-4884.

Raccurt, M., Smallwood, S., Mertani, H. C., Devost, D., Abbaci, K., Boutin, J. M., & Morel, G. 2006, "Cloning, Expression and Regulation of Chicken Ovalbumin Upstream Promoter Transcription Factors (COUP-TFII and EAR-2) in the Rat Anterior Pituitary Gland", *Neuroendocrinology*, vol. 82, no. 5-6, pp. 233-244.

Radde-Gallwitz, K., Pan, L., Gan, L., Lin, X., Segil, N., & Chen, P. 2004, "Expression of Islet1 marks the sensory and neuronal lineages in the mammalian inner ear", *J Comp Neurol.*, vol. 477, no. 4, pp. 412-421.

Raft, S., Nowotschin, S., Liao, J., & Morrow, B. E. 2004, "Suppression of neural fate and control of inner ear morphogenesis by Tbx1", *Development*, vol. 131, no. 8, pp. 1801-1812.

Ramsden, R., Saeed, S., & Aggarwal, R. 2007, "Cochlear Implantation in Genetic Deafness," in *Genes, Hearing and Deafness*, A. Martini, D. Stephens, & A. P. Read, eds., Informa UK Ltd., London, pp. 253-262.

Raphael, Y. & Altschuler, R. A. 2003, "Structure and innervation of the cochlea", *Brain Res.Bull.*, vol. 60, no. 5-6, pp. 397-422.

Raz, Y. & Kelley, M. W. 1999, "Retinoic Acid Signaling Is Necessary for the Development of the Organ of Corti", *Developmental Biology*, vol. 213, no. 1, pp. 180-193.

Reiners, J., Nagel-Wolfrum, K., Jurgens, K., Marker, T., & Wolfrum, U. 2006, "Molecular basis of human Usher syndrome: Deciphering the meshes of the Usher protein network provides insights into the pathomechanisms of the Usher disease", *Experimental Eye Research*, vol. 83, no. 1, pp. 97-119.

Rhee, J. M., Gruber, C. A., Brodie, T. B., Trieu, M., & Turner, E. E. 1998, "Highly Cooperative Homodimerization Is a Conserved Property of Neural POU Proteins", *Journal of Biological Chemistry*, vol. 273, no. 51, pp. 34196-34205.

Richardson, G. P., Lukashkin, A. N., & Russell, I. J. 2008, "The tectorial membrane: one slice of a complex cochlear sandwich", *Curr.Opin.Otolaryngol Head Neck Surg*, vol. 16, no. 5, pp. 458-464.

Rinkwitz, S., Bober, E., & Baker, R. 2001, "Development of the vertebrate inner ear", *Ann.N.Y.Acad.Sci.*, vol. 942, pp. 1-14.

Ritchie, H. H., Wang, L. H., Tsai, S., O'Malley, B. W., & Tsai, M. J. 1990, "COUP-TF gene: a structure unique for the steroid/thyroid receptor superfamily", *Nucleic Acids Res.*, vol. 18, no. 23, pp. 6857-6862.

Rivolta, M. N. 2007, "Stem Cells in the Inner Ear: Advancing Towards a New Therapy for Hearing Impairment," in *Genes, Hearing and Deafness*, A. Martini, D. Stephens, & A. P. Read, eds., Informa UK Ltd., London, pp. 279-288.

Rivolta, M. N., Grix, N., Lawlor, P., Ashmore, J. F., Jagger, D. J., & Holley, M. C. 1998a, "Auditory hair cell precursors immortalized from the mammalian inner ear", *Proc.Biol.Sci.*, vol. 265, no. 1406, pp. 1595-1603.

Rivolta, M. N. & Holley, M. C. 1998b, "GATA3 is downregulated during hair cell differentiation in the mouse cochlea", *J Neurocytol.*, vol. 27, no. 9, pp. 637-647.

Rizzi, M. D. & Hirose, K. 2007, "Aminoglycoside ototoxicity", *Curr.Opin.Otolaryngol.Head Neck Surg.*, vol. 15, no. 5, pp. 352-357.

RNID. Royal National Institute for Deaf People. www.rnid.org.uk . 2009.
Ref Type: Internet Communication

Robertson, M. 1988, "Homoeo boxes, POU proteins and the limits to promiscuity", *Nature*, vol. 336, no. 6199, pp. 522-524.

Robin, N. H., Prucka, S. K., Woolley, A. L., & Smith, R. J. 2005, "The use of genetic testing in the evaluation of hearing impairment in a child", *Curr.Opin.Pediatr.*, vol. 17, no. 6, pp. 709-712.

Robles, L. & Ruggero, M. A. 2001, "Mechanics of the mammalian cochlea", *Physiol Rev*, vol. 81, no. 3, pp. 1305-1352.

Romand, R., Dolle, P., & Hashino, E. 2006, "Retinoid signaling in inner ear development", *J.Neurobiol.*, vol. 66, no. 7, pp. 687-704.

Ruben, R. J. 1967, "Development of the inner ear of the mouse: a radioautographic study of terminal mitoses", *Acta Otolaryngol.* p. Suppl-44.

Ryan, A. F. 1997, "Transcription factors and the control of inner ear development", *Semin.Cell Dev.Biol.*, vol. 8, no. 3, pp. 249-256.

Rybak, L. P. & Ramkumar, V. 2007, "Ototoxicity", *Kidney Int*, vol. 72, no. 8, pp. 931-935.

Sage, C., Huang, M., Karimi, K., Gutierrez, G., Vollrath, M. A., Zhang, D. S., Garcia-Anoveros, J., Hinds, P. W., Corwin, J. T., Corey, D. P., & Chen, Z. Y. 2005, "Proliferation of functional hair cells in vivo in the absence of the retinoblastoma protein", *Science*, vol. 307, no. 5712, pp. 1114-1118.

Sage, C., Huang, M., Vollrath, M. A., Brown, M. C., Hinds, P. W., Corey, D. P., Vetter, D. E., & Chen, Z. Y. 2006, "Essential role of retinoblastoma protein in mammalian hair cell development and hearing", vol. 103, no. 19, pp. 7345-7350.

Sataloff, R. T. & Sataloff, J. 1993, "Classification and Measurement of Hearing Loss," in *Occupational Hearing Loss*, 2 edn, Marcel Dekker, New York, pp. 49-72.

Sato, Y., Suzuki, T., Hidaka, K., Sato, H., Ito, K., Ito, S., & Sasano, H. 2003, "Immunolocalization of nuclear transcription factors, DAX-1 and COUP-TF II, in the normal human ovary: correlation with adrenal 4 binding protein/steroidogenic factor-1 immunolocalization during the menstrual cycle", *J.Clin.Endocrinol Metab*, vol. 88, no. 7, pp. 3415-3420.

Scherf, M., Klingenhoff, A., & Werner, T. 2000, "Highly specific localization of promoter regions in large genomic sequences by PromoterInspector: a novel context analysis approach", *J.Mol.Biol.*, vol. 297, no. 3, pp. 599-606.

Scott, M. P., Tamkun, J. W., & Hartzell, G. W., III 1989, "The structure and function of the homeodomain", *Biochim.Biophys.Acta*, vol. 989, no. 1, pp. 25-48.

Siemens, J., Lillo, C., Dumont, R. A., Reynolds, A., Williams, D. S., Gillespie, P. G., & Muller, U. 2004, "Cadherin 23 is a component of the tip link in hair-cell stereocilia", *Nature*, vol. 428, no. 6986, pp. 950-955.

Slepecky, N. B. 1996, "Cochlear Structure," in *The Cochlea*, P. Dallos, A. N. Popper, & R. R. Fay, eds., Springer-Verlag, New York, pp. 44-129.

Smith, A. & Mathers, C. 2006, "Epidemiology of Infection as a Cause of Hearing Loss," in *Infection and Hearing Impairment*, V. E. Newton & P. J. Vallely, eds., Whurr Publishers Limited (a subsidiary of John Wiley & Sons Ltd), Chichester, pp. 31-66.

Smith, M. D., Morris, P. J., & Latchman, D. S. 1998, "The Brn-3c transcription factor contains a neuronal-specific activation domain", *Neuroreport*, vol. 9, no. 5, pp. 851-856.

Smith, R. J., Bale, J. F., Jr., & White, K. R. 2005, "Sensorineural hearing loss in children", *Lancet*, vol. 365, no. 9462, pp. 879-890.

Spongr, V. P., Flood, D. G., Frisina, R. D., & Salvi, R. J. 1997, "Quantitative measures of hair cell loss in CBA and C57BL/6 mice throughout their life spans", *J Acoust.Soc.Am.*, vol. 101, no. 6, pp. 3546-3553.

Stratagene. QuikChange® Primer Design Program.
http://www.stratagene.com/sdmdesigner/default.aspx . 2006.
Ref Type: Internet Communication

Sud, R., Jones, C. M., Banfi, S., & Dawson, S. J. 2005, "Transcriptional regulation by Barhl1 and Brn-3c in organ-of-Corti-derived cell lines", *Brain Res.Mol Brain Res.*, vol. 141, no. 2, pp. 174-180.

Sun, D. S., Chang, A. C., Jenkins, N. A., Gilbert, D. J., Copeland, N. G., & Chang, N. C. 1996, "Identification, molecular characterization, and chromosomal localization of the cDNA encoding a novel leucine zipper motif-containing protein", *Genomics*, vol. 36, no. 1, pp. 54-62.

Suzuki, T., Moriya, T., Darnel, A. D., Takeyama, J., & Sasano, H. 2000, "Immunohistochemical distribution of chicken ovalbumin upstream promoter transcription factor II in human tissues", *Mol.Cell Endocrinol.*, vol. 164, no. 1-2, pp. 69-75.

Takai, T., Nishita, Y., Iguchi-Ariga, S. M., & Ariga, H. 1994, "Molecular cloning of MSSP-2, a c-myc gene single-strand binding protein: characterization of binding specificity and DNA replication activity", *Nucleic Acids Res.*, vol. 22, no. 25, pp. 5576-5581.

Takamoto, N., Kurihara, I., Lee, K., Demayo, F. J., Tsai, M. J., & Tsai, S. Y. 2005a, "Haploinsufficiency of chicken ovalbumin upstream promoter transcription factor II in female reproduction", *Molecular Endocrinology*, vol. 19, no. 9, pp. 2299-2308.

Takamoto, N., You, L. R., Moses, K., Chiang, C., Zimmer, W. E., Schwartz, R. J., DeMayo, F. J., Tsai, M. J., & Tsai, S. Y. 2005b, "COUP-TFII is essential for radial and anteroposterior patterning of the stomach", *Development*, vol. 132, no. 9, pp. 2179-2189.

Tang, L. S., Alger, H. M., Lin, F., & Pereira, F. A. 2005, "Dynamic expression of COUP-TFI and COUP-TFII during development and functional maturation of the mouse inner ear", *Gene Expr.Patterns.*, vol. 5, no. 5, pp. 587-592.

Tang, L. S., Alger, H. M., & Pereira, F. A. 2006, "COUP-TFI controls Notch regulation of hair cell and support cell differentiation", *Development*, vol. 133, no. 18, pp. 3683-3693.

Tarabichi, M. B., Todd, C., Khan, Z., Yang, X., Shehzad, B., & Tarabichi, M. M. 2008, "Deafness in the developing world: the place of cochlear implantation", *J Laryngol.Otol.*, vol. 122, no. 9, pp. 877-880.

Theil, T., Lean-Hunter, S., Zornig, M., & Moroy, T. 1993, "Mouse Brn-3 family of POU transcription factors: a new aminoterminal domain is crucial for the oncogenic activity of Brn-3a", *Nucleic Acids Res.*, vol. 21, no. 25, pp. 5921-5929.

Theil, T., Rodel, B., Spiegelhalter, F., & Moroy, T. 1995, "Short isoform of POU factor Brn-3b can form a heterodimer with Brn-3a that is inactive for octamer motif binding", *J Biol.Chem.*, vol. 270, no. 52, pp. 30958-30964.

Thelen, N., Breuskin, I., Malgrange, B., & Thiry, M. 2009, "Early identification of inner pillar cells during rat cochlear development", *Cell Tissue Res.*

Trieu, M., Rhee, J. M., Fedtsova, N., & Turner, E. E. 1999, "Autoregulatory Sequences are Revealed by Complex Stability Screening of the Mouse brn-3.0 Locus", *Journal of Neuroscience*, vol. 19, no. 15, pp. 6549-6558.

Tripodi, M., Filosa, A., Armentano, M., & Studer, M. 2004, "The COUP-TF nuclear receptors regulate cell migration in the mammalian basal forebrain", *Development*, vol. 131, no. 24, pp. 6119-6129.

Tritsch, N. X., Yi, E., Gale, J. E., Glowatzki, E., & Bergles, D. E. 2007, "The origin of spontaneous activity in the developing auditory system", *Nature*, vol. 450, no. 7166, pp. 50-55.

Ulfendahl, M. 2007, "Tissue Transplantation into the Inner Ear," in *Genes, Hearing and Deafness*, A. Martini, D. Stephens, & A. P. Read, eds., Informa UK Ltd., London, pp. 289-298.

Vahava, O., Morell, R., Lynch, E. D., Weiss, S., Kagan, M. E., Ahituv, N., Morrow, J. E., Lee, M. K., Skvorak, A. B., Morton, C. C., Blumenfeld, A., Frydman, M., Friedman, T. B., King, M. C., & Avraham, K. B. 1998, "Mutation in Transcription Factor POU4F3 Associated with Inherited Progressive Hearing Loss in Humans", *Science*, vol. 279, no. 5358, pp. 1950-1954.

Van Camp, G. & Smith, R. Hereditary Hearing Loss Homepage.
http://webh01.ua.ac.be/hhh . 2008.
Ref Type: Internet Communication

van Drunen, F. J., Pauw, R. J., Collin, R. W., Kremer, H., Huygen, P. L., & Cremers, C. W. 2009, "Vestibular impairment in a Dutch DFNA15 family with an L289F mutation in POU4F3", *Audiol Neurootol*, vol. 14, no. 5, pp. 303-307.

Van Laer, L. & Van Camp, G. 2007, "Age-related hearing impairment: ensemble playing of environmental and genetic factors," in *Genes, Hearing, and Deafness*, A. Martini, D. Stephens, & A. P. Read, eds., Informa Healthcare, London, pp. 79-90.

Van Laer, L., Van Eyken, E., Fransen, E., Huyghe, J. R., Topsakal, V., Hendrickx, J. J., Hannula, S., Maki-Torkko, E., Jensen, M., Demeester, K., Baur, M., Bonaconsa, A., Mazzoli, M., Espeso, A., Verbruggen, K., Huyghe, J., Huygen, P., Kunst, S., Manninen, M., Konings, A., az-Lacava, A. N., Steffens, M., Wienker, T. F., Pyykko, I., Cremers, C. W., Kremer, H., Dhooge, I., Stephens, D., Orzan, E., Pfister, M., Bille, M., Parving, A., Sorri, M., Van de Heyning, P. H., & Van, C. G. 2008, "The grainyhead like 2 gene (GRHL2), alias TFCP2L3, is associated with age-related hearing impairment", *Hum.Mol Genet.*, vol. 17, no. 2, pp. 159-169.

Vander, A., Sherman, J., & Luciano, D. 2001, "The Sensory Systems," in *Human Physiology*, 8 edn, McGraw-Hill, New York, pp. 227-262.

Veenstra, G. J., van, d., V, & Destree, O. H. 1997, "POU domain transcription factors in embryonic development", *Mol Biol.Rep.*, vol. 24, no. 3, pp. 139-155.

Verrijzer, C. P. & van, d., V 1993, "POU domain transcription factors", *Biochim.Biophys.Acta*, vol. 1173, no. 1, pp. 1-21.

Waguespack, J., Salles, F. T., Kachar, B., & Ricci, A. J. 2007, "Stepwise morphological and functional maturation of mechanotransduction in rat outer hair cells", *J Neurosci.*, vol. 27, no. 50, pp. 13890-13902.

Wallis, D., Hamblen, M., Zhou, Y., Venken, K. J., Schumacher, A., Grimes, H. L., Zoghbi, H. Y., Orkin, S. H., & Bellen, H. J. 2003, "The zinc finger transcription factor Gfi1, implicated in lymphomagenesis, is required for inner ear hair cell differentiation and survival", *Development*, vol. 130, no. 1, pp. 221-232.

Wang, J., Mark, S., Zhang, X., Qian, D., Yoo, S. J., Radde-Gallwitz, K., Zhang, Y., Lin, X., Collazo, A., Wynshaw-Boris, A., & Chen, P. 2005, "Regulation of polarized extension and planar cell polarity in the cochlea by the vertebrate PCP pathway", *Nat Genet*, vol. 37, no. 9, pp. 980-985.

Wang, L. H., Ing, N. H., Tsai, S. Y., O'Malley, B. W., & Tsai, M. J. 1991, "The COUP-TFs compose a family of functionally related transcription factors", *Gene Expr.*, vol. 1, no. 3, pp. 207-216.

Wang, S. W., Mu, X., Bowers, W. J., Kim, D. S., Plas, D. J., Crair, M. C., Federoff, H. J., Gan, L., & Klein, W. H. 2002, "Brn3b/Brn3c double knockout mice reveal an unsuspected role for Brn3c in retinal ganglion cell axon outgrowth", *Development*, vol. 129, no. 2, pp. 467-477.

Wangemann, P. 2006, "Supporting sensory transduction: cochlear fluid homeostasis and the endocochlear potential", *J Physiol*, vol. 576, no. Pt 1, pp. 11-21.

Wangemann, P. & Schacht, J. 1996, "Homeostatic Mechanisms in the Cochlea," in *The Cochlea*, P. Dallos, A. N. Popper, & R. R. Fay, eds., Springer-Verlag, New York, pp. 130-185.

Weigel, N. L. 1996, "Steroid hormone receptors and their regulation by phosphorylation", *Biochem.J.*, vol. 319 (Pt 3), pp. 657-667.

Weiss, S., Gottfried, I., Mayrose, I., Khare, S. L., Xiang, M., Dawson, S. J., & Avraham, K. B. 2003, "The DFNA15 deafness mutation affects POU4F3 protein stability, localization, and transcriptional activity", *Mol Cell Biol.*, vol. 23, no. 22, pp. 7957-7964.

Weston, M. D. & Soukup, G. A. 2009, "MicroRNAs sound off", *Genome Med.*, vol. 1, no. 6, p. 59.

Wheeler, D. L., Church, D. M., Federhen, S., Lash, A. E., Madden, T. L., Pontius, J. U., Schuler, G. D., Schriml, L. M., Sequeira, E., Tatusova, T. A., & Wagner, L. 2003, "Database resources of the National Center for Biotechnology", *Nucleic Acids Research*, vol. 31, no. 1, pp. 28-33.

Whitfield, T. T. & Hammond, K. L. 2007, "Axial patterning in the developing vertebrate inner ear", *Int J Dev.Biol.*, vol. 51, no. 6-7, pp. 507-520.

Willson, T. M. & Moore, J. T. 2002, "Minireview: Genomics Versus Orphan Nuclear Receptors--A Half-Time Report", *Molecular Endocrinology*, vol. 16, no. 6, pp. 1135-1144.

Wood, J. N., Bevan, S. J., Coote, P. R., Dunn, P. M., Harmar, A., Hogan, P., Latchman, D. S., Morrison, C., Rougon, G., Theveniau, M., & . 1990, "Novel cell lines display properties of nociceptive sensory neurons", *Proc.Biol.Sci.*, vol. 241, no. 1302, pp. 187-194.

World Health Organization. Fact sheet N°300.
http://www.who.int/mediacentre/factsheets/fs300/en/print.html . 2006.
Ref Type: Internet Communication

Wright, T. J., Hatch, E. P., Karabagli, H., Karabagli, P., Schoenwolf, G. C., & Mansour, S. L. 2003, "Expression of mouse fibroblast growth factor and fibroblast growth factor receptor genes during early inner ear development", *Dev.Dyn.*, vol. 228, no. 2, pp. 267-272.

Wu, X., Wang, X., Gao, J., Yu, Y., Jia, S., Zheng, J., Dallos, P., He, D. Z. Z., Cheatham, M., & Zuo, J. 2008, "Glucose transporter 5 is undetectable in outer hair cells and does not contribute to cochlear amplification", *Brain Research*, vol. 1210, pp. 20-28.

Xia, Y. R., Andersen, B., Mehrabian, M., Diep, A. T., Warden, C. H., Mohandas, T., McEvilly, R. J., Rosenfeld, M. G., & Lusis, A. J. 1993, "Chromosomal organization of mammalian POU domain factors", *Genomics*, vol. 18, no. 1, pp. 126-130.

Xiang, M., Gao, W. Q., Hasson, T., & Shin, J. J. 1998, "Requirement for Brn-3c in maturation and survival, but not in fate determination of inner ear hair cells", *Development*, vol. 125, no. 20, pp. 3935-3946.

Xiang, M., Maklad, A., Pirvola, U., & Fritzsch, B. 2003, "Brn3c null mutant mice show long-term, incomplete retention of some afferent inner ear innervation", *BMC.Neurosci.*, vol. 4, p. 2.

Xiang, M., Zhou, L., Macke, J. P., Yoshioka, T., Hendry, S. H., Eddy, R. L., Shows, T. B., & Nathans, J. 1995, "The Brn-3 family of POU-domain factors: primary structure, binding specificity, and expression in subsets of retinal ganglion cells and somatosensory neurons", *Journal of Neuroscience*, vol. 15, no. 7, pp. 4762-4785.

Xiang, M., Zhou, L., Peng, Y. W., Eddy, R. L., Shows, T. B., & Nathans, J. 1993, "Brn-3b: a POU domain gene expressed in a subset of retinal ganglion cells", *Neuron*, vol. 11, no. 4, pp. 689-701.

Xiang, M., Gan, L., Li, D., Chen, Z. Y., Zhou, L., O'Malley, B. W., Klein, W., & Nathans, J. 1997, "Essential role of POU-domain factor Brn-3c in auditory and vestibular hair cell

development", *Proceedings of the National Academy of Sciences of the United States of America*, vol. 94, no. 17, pp. 9445-9450.

Xu, L., Glass, C. K., & Rosenfeld, M. G. 1999, "Coactivator and corepressor complexes in nuclear receptor function", *Curr.Opin.Genet Dev.*, vol. 9, no. 2, pp. 140-147.

Xu, Z., Ricci, A. J., & Heller, S. 2009, "Rethinking how hearing happens", *Neuron*, vol. 62, no. 3, pp. 305-307.

Yamamoto, M., Fujinuma, M., Tanaka, M., Drager, U. C., & McCaffery, P. 1999, "Sagittal band expression of COUP-TF2 gene in the developing cerebellum", *Mech.Dev.*, vol. 84, no. 1-2, pp. 143-146.

Yang, T. T. & Chow, C. W. 2003, "Transcription cooperation by NFAT.C/EBP composite enhancer complex", *J Biol.Chem.*, vol. 278, no. 18, pp. 15874-15885.

You, L. R., Lin, F. J., Lee, C. T., DeMayo, F. J., Tsai, M. J., & Tsai, S. Y. 2005a, "Suppression of Notch signalling by the COUP-TFII transcription factor regulates vein identity", *Nature*, vol. 435, no. 7038, pp. 98-104.

You, L. R., Takamoto, N., Yu, C. T., Tanaka, T., Kodama, T., DeMayo, F. J., Tsai, S. Y., & Tsai, M. J. 2005b, "Mouse lacking COUP-TFII as an animal model of Bochdalek-type congenital diaphragmatic hernia", *Proc.Natl.Acad.Sci.U.S.A*, vol. 102, no. 45, pp. 16351-16356.

Zajac, M., Jones, G. L., & Glazier, J. A. 2000, "Model of convergent extension in animal morphogenesis", *Phys.Rev Lett.*, vol. 85, no. 9, pp. 2022-2025.

Zelarayan, L. C., Vendrell, V., Alvarez, Y., Dominguez-Frutos, E., Theil, T., Alonso, M. T., Maconochie, M., & Schimmang, T. 2007, "Differential requirements for FGF3, FGF8 and FGF10 during inner ear development", *Dev.Biol.*, vol. 308, no. 2, pp. 379-391.

Zhang, H. J., Xu, C. H., Zhan, Y. J., Zhao, S. Y., Shan, Y. F., Geng, X. X., & Shan, X. N. 2005, "Sequence analysis of the mitochondrial genome from a large family with maternally inherited nonsyndromic deafness", *Zhonghua Yi.Xue.Yi.Chuan Xue.Za Zhi.*, vol. 22, no. 4, pp. 368-371.

Zhang, P., Bennoun, M., Gogard, C., Bossard, P., Leclerc, I., Kahn, A., & Vasseur-Cognet, M. 2002, "Expression of COUP-TFII in metabolic tissues during development", *Mech.Dev.*, vol. 119, no. 1, pp. 109-114.

Zheng, J., Madison, L. D., Oliver, D., Fakler, B., & Dallos, P. 2002, "Prestin, the motor protein of outer hair cells", *Audiol.Neurootol.*, vol. 7, no. 1, pp. 9-12.

Zheng, J., Shen, W., He, D. Z., Long, K. B., Madison, L. D., & Dallos, P. 2000, "Prestin is the motor protein of cochlear outer hair cells", *Nature*, vol. 405, no. 6783, pp. 149-155.

Zine, A. & Romand, R. 1996, "Development of the auditory receptors of the rat: a SEM study", *Brain Res.*, vol. 721, no. 1-2, pp. 49-58.